The Petrogenesis of the Volcanic Rocks of the Witwatersrand Triad in the Klerksdorp area, Transvaal

by

Michael Peter Bowen
B.Sc. (Hons.)

Thesis submitted in fulfilment of the requirements for the degree of Master of Science

Department of Geology
Rhodes University
Grahamstown

December 1984

THIS THESIS REPRESENTS THE ORIGINAL WORK
OF THE AUTHOR EXCEPT WHERE SPECIFIC
ACKNOWLEDGEMENT IS MADE TO
THE WORK OF OTHERS

DECEMBER 1984

ABSTRACT

Several hundred chemical analyses of early Proterozoic lavas of the Witwatersrand triad (incorporating the Dominion Group, Witwatersrand Supergroup and Ventersdorp Supergroup) in the Klerksdorp area, have revealed the presence of various distinct magma types. These essentially correspond to formally defined lithostratigraphic units, but several inconsistencies have necessitated the use of informal nomenclature.

The lavas have been regionally metamorphosed to low-grade, greenschist facies assemblages. Original igneous textures are preserved, despite a metamorphic overprint. Metamorphism has resulted in a certain degree of random chemical remobilization. Ba, Sr, Rb, K_2O, Na_2O and CaO have been highly mobile, and their usefulness in petrogenetic modelling is extremely limited. In contrast, Zr, Nb, Y, LREE's, Cr, Ni, TiO_2, P_2O_5 and Al_2O_3 have remained immobile. Ti/Zr and Ti/P ratios together constitute efficient discriminating variables for characterizing the different magma types.

Lava compositions range from primitive Mg-rich tholeiites to rhyolites, the bulk being tholeiitic andesites. Al_2O_3 contents do not exceed 15%, a feature which reflects the tholeiitic, as opposed to calc-alkaline, character of these lavas.

Two magma-types are present within the Dominion Group, which is a typical example of bimodal volcanism. The Dominion basic lavas are overlain by the Dominion acid porphyries, with a limited amount of interfingering. The basic lava suite is highly fractionated, with compositions ranging from Mg-, Cr- and Ni-rich tholeiites (close to primary mantle melts) to evolved tholeiitic andesites. The most primitive liquids evolved by 45% fractional crystallization of hornblende, followed by a further 70% crystallization of an orthopyroxene-plagioclase assemblage containing up to 3% sulphides.

The Dominion porphyries are rhyolitic, display very limited compositional variation, and probably represent a crustal melt related to the same magmatic event which produced the basic lavas.

The only lavas from the Witwatersrand Supergroup present in the Klerksdorp area are those of the Crown Formation (Jeppestown amygdaloid). These are tholeiitic dacites which display extremely limited compositional variation, and are unrelated to any of the other magmas of the Witwatersrand triad.

The Ventersdorp Supergroup comprises 4 magma-types:

The Klipriviersberg Group lavas at the base are subdivisible into 3 sub-types on the basis of Zr contents. The lowermost Alberton lavas (Zr>110ppm) are the most evolved. They are tholeiitic andesites which display fairly limited compositional variation. It is likely that more evolved compositions are present in other areas where the porphyritic lavas which characterize this unit are better developed. The overlying Orkney lavas are characterized by 110ppm>Zr>90ppm. They are tholeiitic andesites of similar composition to the Alberton lavas, but have lower incompatible element levels, higher siderophile element levels, and are of extremely uniform composition. The uppermost Loraine/Edenville lavas range from magnesian tholeiites to tholeiitic andesites. They are distinguished by Zr< 90ppm, and contain the most primitive magmas of the Witwatersrand triad, with up to 17,5% MgO, 2600ppm Cr, 600ppm Ni and M-values up to 77. The most primitive liquids evolved by 38% fractional crystallization of orthopyroxene $\pm$ chromite, followed by 35% fractional crystallization of an extract containing clinopyroxene and plagioclase. The absence of olivine precipitation is a result of the inherently high SiO_2 content of the magma. The Loraine/Edenville, Orkney and Alberton lavas do not lie on a common liquid line of descent, but are probably consanguinous.

The Platberg Group overlies the Klipriviersberg Group, and has a coarse-clastic sedimentary unit, the Kameeldoorns Formation, at the base. Three petrographically distinct porphyritic lava sequences overlie the Kameeldoorns Formation, namely the informal "Goedgenoeg formation", the Makwassie quartz-feldspar porphyries and the Rietgat Formation. Despite petrographic differences, the Goedgenoeg and Rietgat lavas are chemically indistinguishable and thus form a single magma-type. The Makwassie porphyries are dacitic in composition with a high proportion of feldspar and quartz phenocrysts. Rational variation trends are attributed to a nett loss of SiO_2 during secondary alteration. The

porphyries are probably of crustal origin. The Goedgenoeg/Rietgat lavas display unusual chemistry and a broad, irrational compositional spectrum. They contain very high incompatible element levels, high normative quartz, as well as high MgO, M-values, Cr and Ni relative to the other tholeiitic andesites of the Witwatersrand triad. It is tentatively suggested that they are hybrid magmas containing both crust and mantle components, the former possibly represented by the Makwassie porphyries. Field evidence suggests that Platberg volcanism commenced directly after Klipriviersberg volcanism ceased, and was accompanied by a period of enhanced tectonic activity. The Platberg lavas thus probably reflect a crustal melting cycle associated with the Klipriviersberg magmatic event.

The Allanridge lavas are the youngest rocks of the Witwatersrand triad. They are separated from the Platberg Group by a unit of flat-lying sediments, the Bothaville Formation, which was deposited after an extended period of peneplanation. The Allanridge lavas form a separate magma-type. They are tholeiitic andesites of similar composition to the Alberton lavas, but have higher incompatible element levels and are not consanguinous.

The compositional similarities amongst the basic magma-types of the Witwatersrand triad suggests that all were generated in an hydrous mantle. Interelement ratio differences between the various magma-types nevertheless support the concept that the mantle was chemically heterogeneous during the early Proterozoic.

CONTENTS

FIGURES

PLATES

TABLES

I INTRODUCTION

The "Witwatersrand triad" is an informal name which refers to the rocks of the Dominion Group, Witwatersrand Supergroup and Ventersdorp Supergroup, which respectively represent the three earliest cover sequences to be laid down during the early Proterozoic, following the stabilization of the Kaapvaal Craton at about 3000 Ma. The relative position of these rocks within the Southern African stratigraphic column is illustrated in Figure 1. Figure 2 shows the approximate areal location of the Witwatersrand triad rocks within the Southern African sub-continent.

The predominantly volcanic Dominion and Ventersdorp rocks respectively underlie and overlie the gold-bearing sediments of the Witwatersrand Supergroup. The lava sequences are thick and monotonous, with few reliable marker horizons. Consequently, interpretation of the often complex structural problems existing around the edges of the Witwatersrand basin is hampered by the inability to determine stratigraphic position within the lava sequences. For this reason the Anglo American Corporation financed the present study, which is aimed at determining whether geochemistry might provide a more reliable alternative to visual identification of stratigraphic position within the Witwatersrand triad lavas.

The study entailed the collection of 500 samples from 17 representative boreholes from the Klerksdorp area (see Figure 7). Of these samples, 326 were analysed for major elements and 15 trace elements. The sampling and analytical phases of the investigation were performed jointly by the writer and T.B. Bowen (1984). Further investigations were conducted separately. In this thesis, the petrography, chemistry and petrogenetic aspects of the various lava groups are described and evaluated. In a parallel thesis, T.B. Bowen (op. cit.) has undertaken a statistical assessment of the geochemical data and compiled a literature review of the Witwatersrand triad rocks.

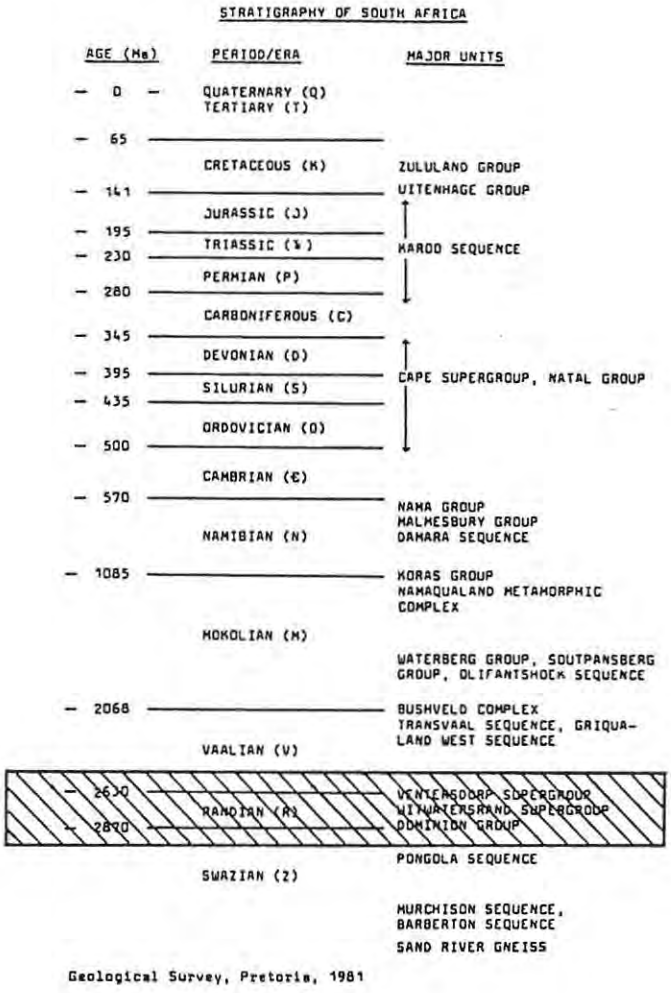

Figure 1: Stratigraphy of Southern Africa, illustrating the position of the Witwatersrand triad (Compiled by the Geological Survey, Pretoria, 1981).

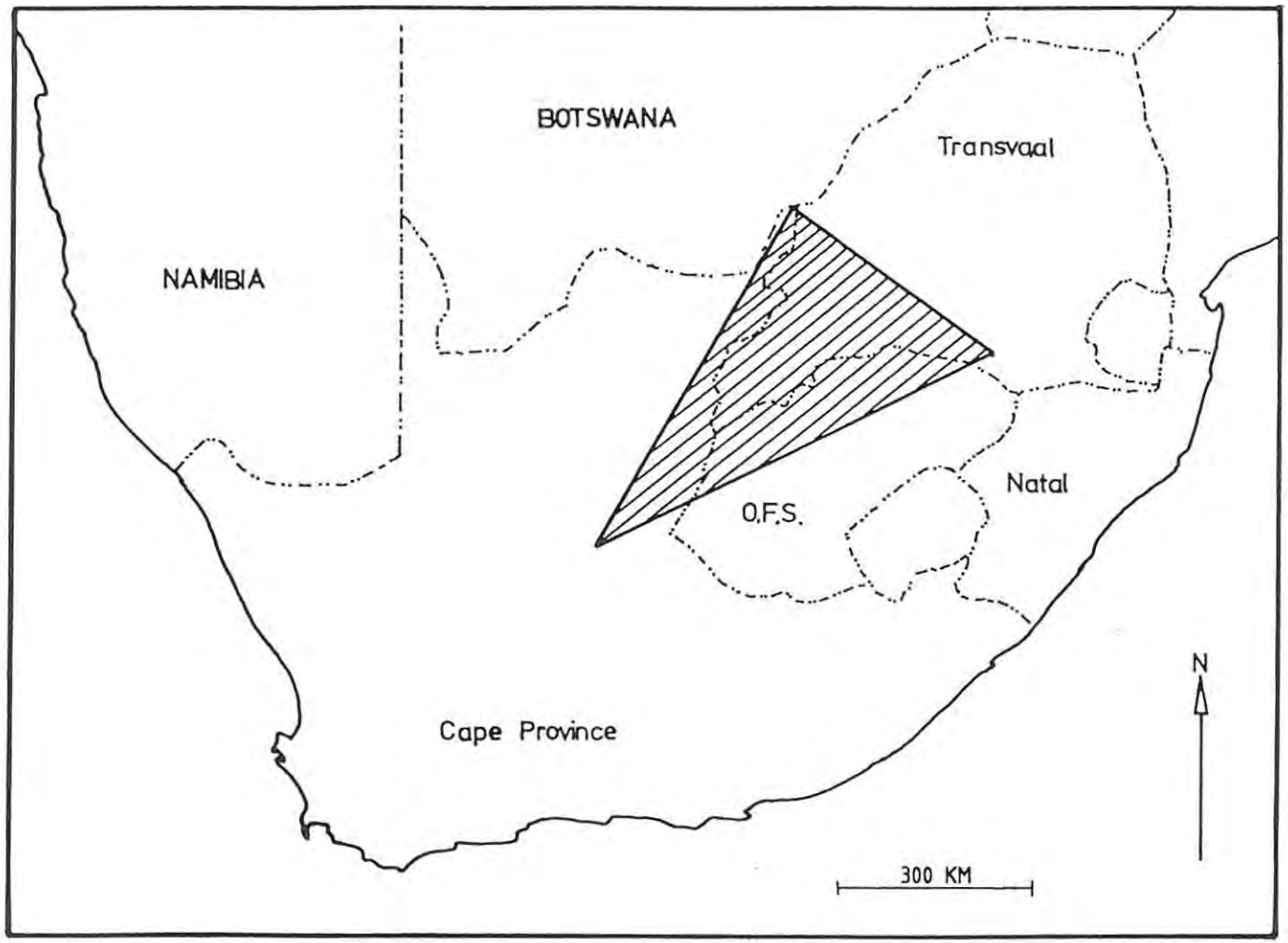

Figure 2: Approximate areal distribution of the Witwatersrand triad rocks.

II GENERAL STRATIGRAPHY OF THE WITWATERSRAND TRIAD

A. Introduction

Lavas of the Witwatersrand triad were first described by Stow (1874), who referred to lavas outcropping along the Vaal River near Barkly West which are now correlated with the Ventersdorp Supergroup . Molengraaff (1905) first recognised rocks of the Dominion Group in the Western Transvaal, naming them the Dominion Reef Series. Largely due to their association with the Witwatersrand goldfields, these lavas subsequently received much attention in the literature, with most workers dwelling mainly on aspects of description, outcrop areas, correlation and stratigraphic nomenclature. This chapter contains a brief description of the general stratigraphy and tectonic setting of the Witwatersrand triad as it has currently been defined by the South African Committee for Stratigraphy (SACS, 1980). The historical developments leading up to the current lithostratigraphic classification will not be described in this thesis as T.B. Bowen (1984) has compiled an in-depth literature review to which the reader is referred, in addition to publications such as SACS (1980), Winter (1976), Whiteside (1970), Wyatt (1976) and Simpson (1964).

B. Dominion Group

The Dominion Group, previously termed the Dominion Reef System (Truswell, 1970), forms the oldest sequence of the Proterozoic in South Africa and it unconformably overlies the Archaean granite-greenstone basement of the Kaapvaal Craton. The stratigraphy is well established and has been extensively described by numerous workers. The following resumé has been extracted chiefly from Whiteside (1970), Watchorn (1980) and SACS (1980).

Despite lithological similarities with several other volcanic sequences in Southern Africa, the Dominion Group appears to be restricted primarily to the Western Transvaal. Although largely overlain by younger rocks, the sequence is exposed to the west of Klerksdorp and in the area surrounding Ottosdal (Figure 3), where it is preserved within three broad

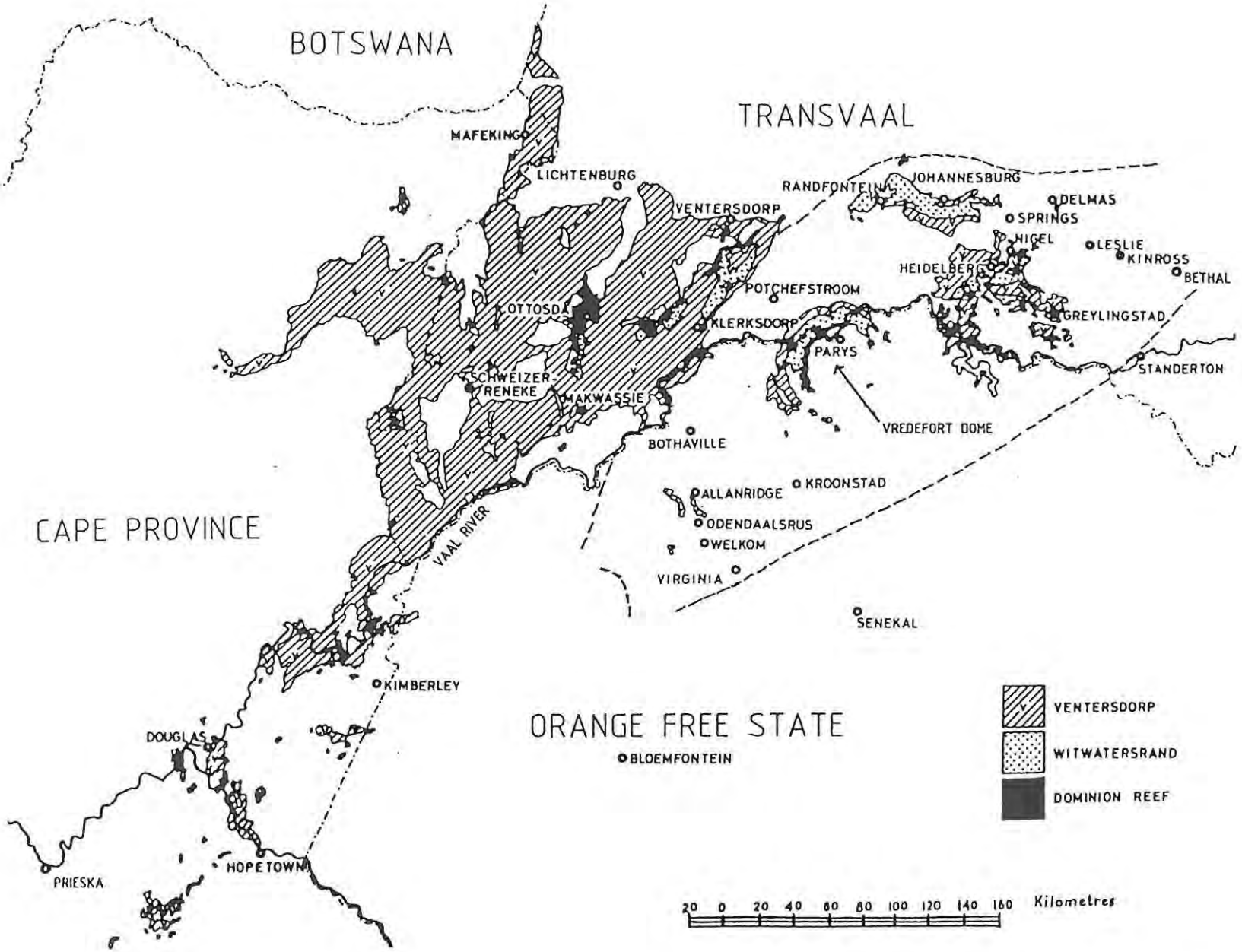

Figure 3: Outcrop distribution of the Witwatersrand triad rocks. Dashed line indicates the approximate limits of the Witwatersrand basin (After Truswell, 1970).

synformal structures plunging towards the south and southwest (Watchorn, 1980). To the north of Klerksdorp, Dominion rocks are exposed along the southeastern limb of the Varkenskraal anticline which plunges to the northeast, and to the east they outcrop around the northwestern rim of the Vredefort dome (Figure 3).

The Dominion Group has been subdivided into three formations (SACS, 1980), namely the Rhenosterspruit Quartzite Formation, the Rhenosterhoek Andesite Formation and the Syferfontein Porphyry Formation (Figure 4). In the type area to the west of Klerksdorp around the old Dominion Reef mine, the Rhenosterspruit Quartzite Formation comprises grey quartzite and yellow sericitic quartzite up to 60m in thickness. Several conglomerate bands occur within the quartzite, two of which, the "Upper" and "Lower Dominion Reefs", are persistent and have been extensively exploited for uranium and gold respectively. In the Ottosdal area the sequence is up to 120m thick with lensoid intercalations of lava and tuff. The lavas are generally andesitic, although more felsic varieties may occur.

The Rhenosterhoek Andesite Formation comprises predominantly basic to intermediate fine-grained grey to green lavas with occasional bands of felsic porphyries. Subordinate tuffs are present mainly in the upper part of the formation, while intercalated bands of sediments up to 40m in thickness may be present in the lower part. Individual flows are characterized by amygdaloidal bases and amygdaloidal, flow-brecciated and/or tuffaceous tops. According to Whiteside (1970), three distinctive horizons occur in the type area, namely a bed of quartzite up to 30m thick near the base, a quartz-feldspar porphyry up to 50m thick and a contorted, tuffaceous flow breccia, 15m thick, occurring about 150m above the base. The lavas are often slightly schistose and metamorphosed by low grade regional metamorphism to greenschist facies assemblages. The maximum thickness attained is 1100m.

The Syferfontein Porphyry Formation consists essentially of quartz-feldspar porphyries and attains a thickness of 1500m. Numerous intercalations of tuff and up to five units of basic to intermediate amygdaloidal lavas have been recognised (Whiteside, 1970). SACS (1980) made a distinction between a lower 750m of medium-grained porphyry, a middle 500m of silicified porphyry and an upper 300m of medium-grained

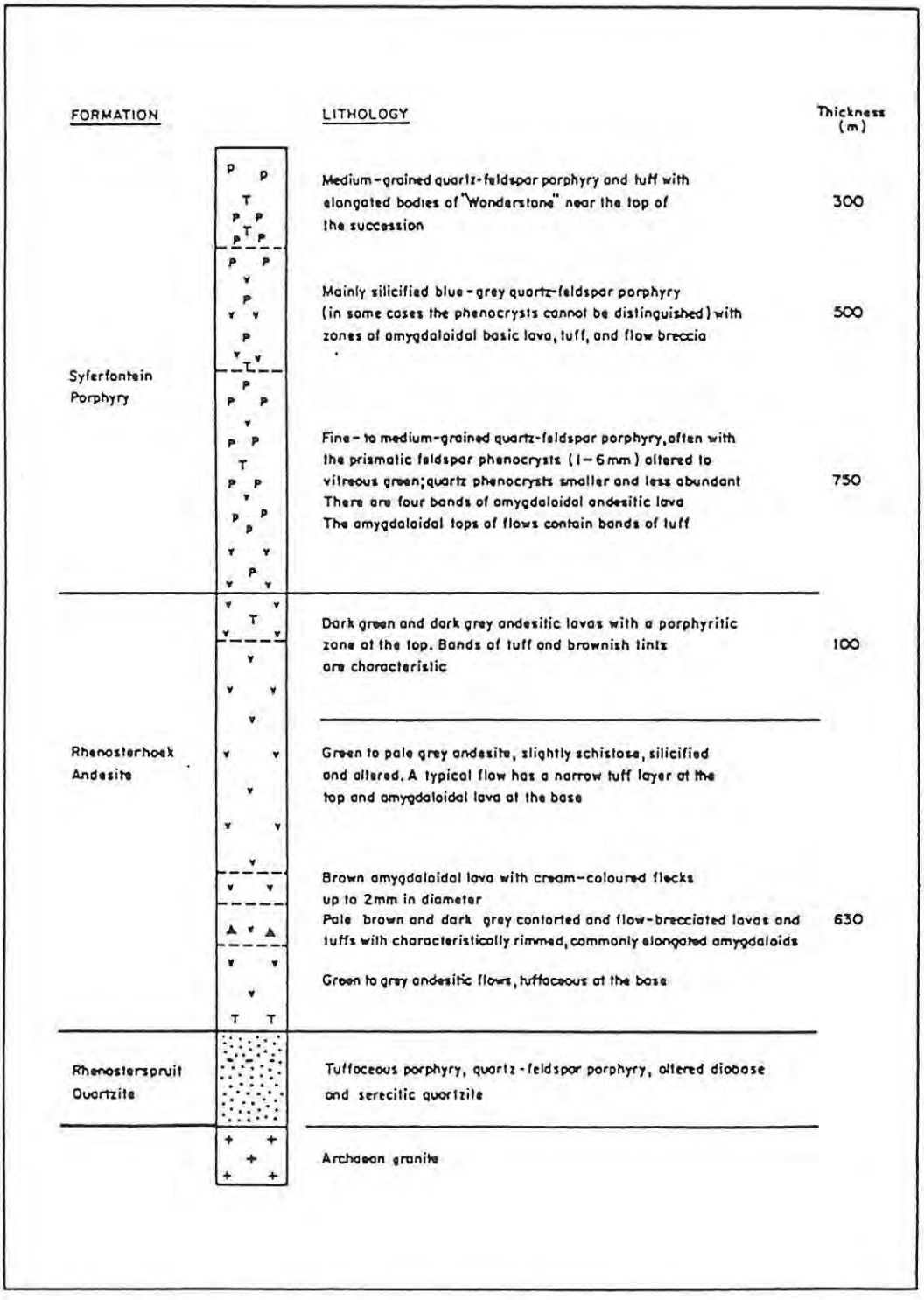

Figure 4: Formal lithostratigraphy of the Dominion Group (From SACS, 1980).

porphyry again in which a series of lenticular bodies of "Wonderstone", up to 70m thick, occur. These bodies comprise about 90% pyrophyllite and are considered by Nel et al. (1937) to be representative of regionally metamorphosed, water-lain volcanic ash.

C. Witwatersrand Supergroup

In contrast to the Dominion and Ventersdorp sequences, volcanics are poorly represented in the Witwatersrand Supergroup, which consists essentially of quartzites, shales and conglomerates and hosts the famous Witwatersrand gold mineralization. The outline of the Witwatersrand depositional basin is shown in Figure 3. Figure 5 summarises the major stratigraphic subdivisions of the Witwatersrand Supergroup.

The subdivision into the West Rand and Central Rand Groups (previously the "Lower" and "Upper Division" respectively) represents a lithological transition from the predominantly argillaceous sediments of the West Rand Group to the almost entirely quartzitic and conglomeratic sediments of the Central Rand Group. Only two volcanic units occur within the Witwatersrand Supergroup, namely the Crown Formation and the Bird Amygdaloid Marker. The latter is restricted to the East Rand and is thus not considered in this study. The Crown Formation, originally known as the Jeppestown Amygdaloid, is more widespread and has been intersected in boreholes and mine workings over the whole of the Witwatersrand basin with the exception of the Central Rand and Evander goldfields to the east. It occurs stratigraphically towards the top of the West Rand Group within the Jeppestown Subgroup (Figure 5), and comprises dense andesitic lavas, pale grey to dark green in colour, containing abundant amygdales of quartz and chlorite. Short stubby dark green phenocrysts are occasionally present, as well as tuffaceous and agglomeratic material (Whiteside, 1970). The thickness varies, usually between 30m and 100m.

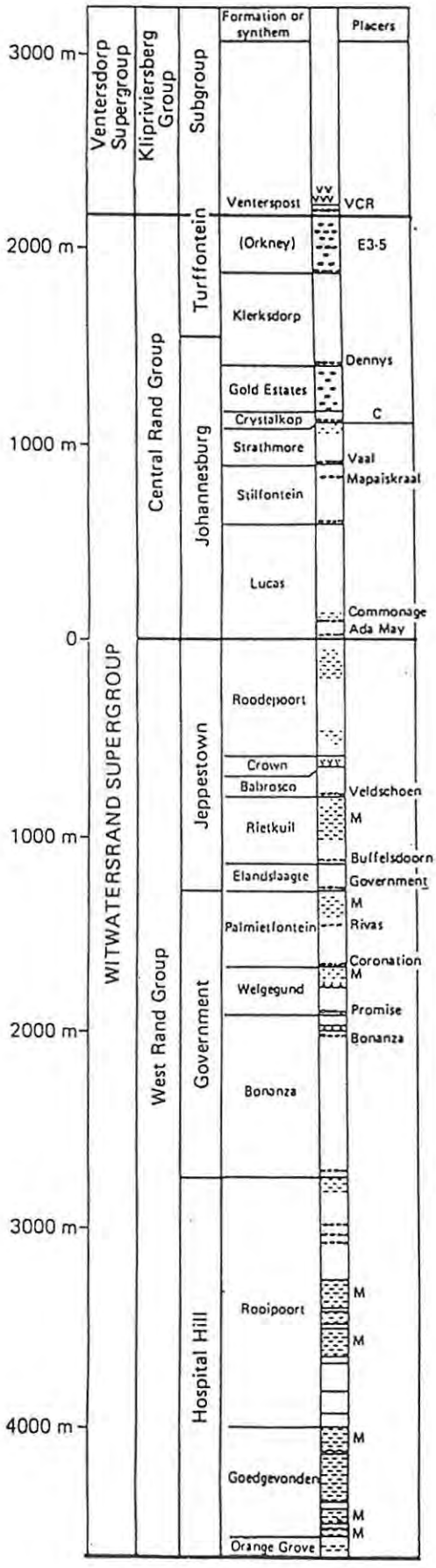

Figure 5: Lithostratigraphy of the Witwatersrand Supergroup in the Klerksdorp area (After Tankard et. al., 1982).

D. Ventersdorp Supergroup

1 Introduction

The most comprehensive work on the stratigraphy of the Ventersdorp Supergroup is that of Winter (1965) in a Ph.D. thesis, subsequently summarised in revised form (Winter, 1976). This work forms the basis, along with unpublished work by P.M. Strydom (see Whiteside, 1970), of the current formal lithostratigraphic subdivision which has been adopted by SACS (1980). The summary below is drawn from these publications.

The Ventersdorp Supergroup occurs stratigraphically between the Witwatersrand and Transvaal Supergroups. Ventersdorp rocks are exposed mainly in the Western Transvaal (Figure 3), extending south-westwards along the Vaal River where they can be traced as far as Prieska, and north-eastwards into Botswana. Further outcrops occur around and to the south of Johannesburg in the Central Rand, and along the north-western rim of the Vredefort Dome in the northern Orange Free State. In the Transvaal, the possible northern limits of the sequence are obscured by Transvaal Supergroup cover and the Bushveld Complex, while southwards, extensive diamond drilling through Transvaal and Karoo Supergroup cover has traced the sequence roughly as far as a line extending from Bethal in the east, south-westwards through Virginia in the Orange Free State towards Hopetown in the northern Cape Province. Thus Ventersdorp rocks extend beyond the limits of the Witwatersrand basin, (delineated on Figure 3) and in the Western Transvaal rest unconformably on the West Rand Group of the Witwatersrand Supergroup and progressively step on to Dominion and Archaean basement rocks.

The Ventersdorp Supergroup comprises a thick, predominantly volcanic pile within which two prominent sedimentary formations occur. These rest on major unconformities which provide the basis for the primary subdivision of the Ventersdorp into a lower Klipriviersberg Group, a middle Platberg Group and an upper unit of two formations, the Bothaville and Allanridge Formations. The combined maximum thickness of the volcanics and sediments intersected by boreholes in the type

area around Bothaville are 5100m and 2900m respectively. Thicknesses vary considerably, however, and in certain areas not all of the formations are represented. Figure 6 summarises the stratigraphic breakdown of the Ventersdorp Supergroup, the lithologies of which are described briefly below.

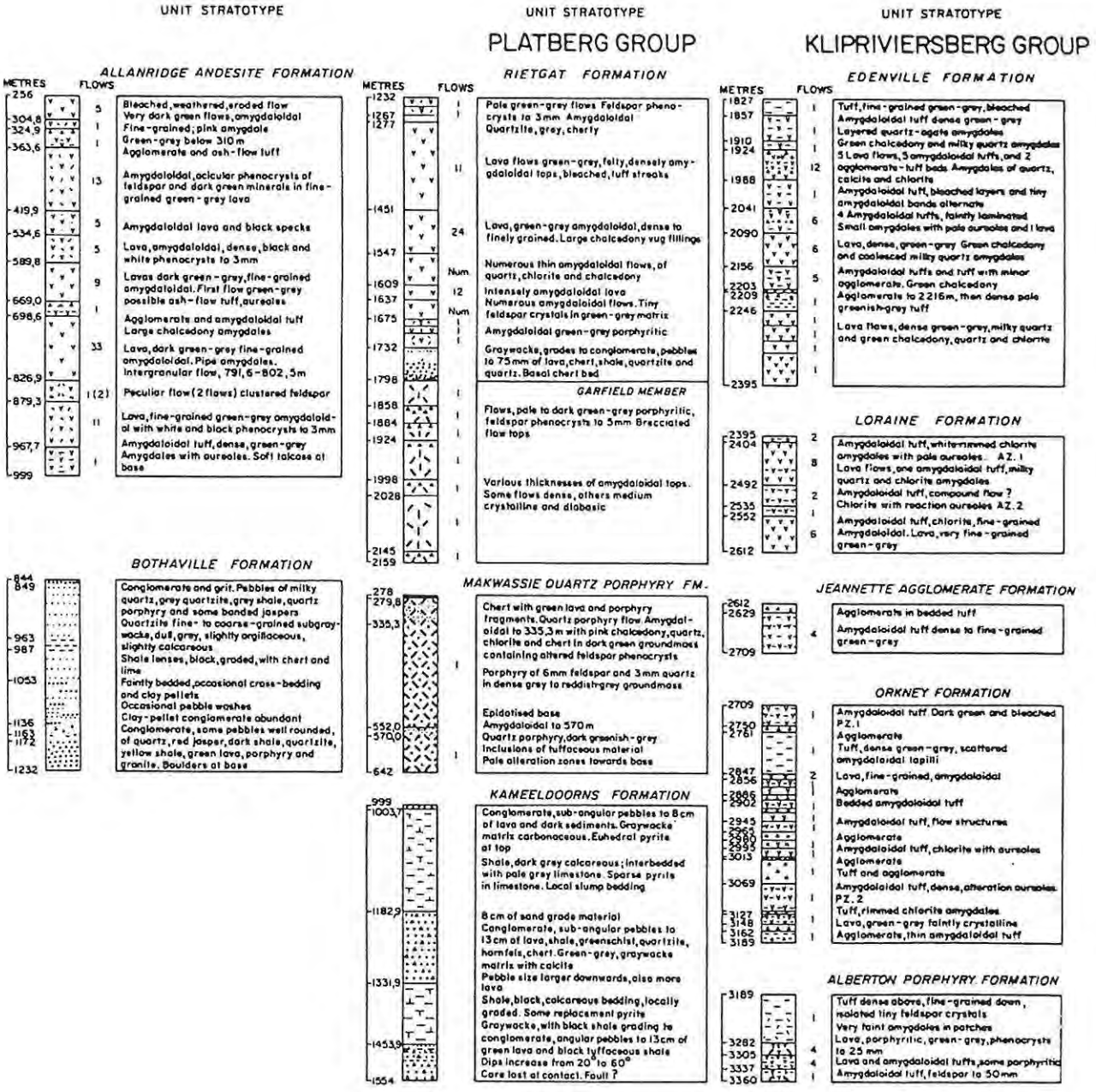

Figure 6: Type lithostratigraphic section of the Ventersdorp Supergroup (From SACS, 1980).

2 Klipriviersberg Group

The Klipriviersberg Group consists of six formations, namely, from the base upwards, the Westonaria, Alberton, Orkney, Jeanette Agglomerate, Loraine and Edenville Formations. According to Winter (1976), the Group as a whole consists almost exclusively of andesitic material comprising lavas, tuffs and agglomerates. The Westonaria Formation is confined to the deepest parts of the basin, and is characterized in the Bothaville type area by a series of dark green "talcose tuffs". The overlying Alberton Formation is characterized by a number of porphyritic zones, one of which contains scattered feldspar phenocrysts longer than 50mm and forms a distinctive marker horizon at the base, locally termed the "Porphyritic Marker". The Orkney Formation is distinguished by the presence of several zones described by Winter (1976) as "purple-topped ash-flow tuffs", or "purple zones". Pienaar (1956) recognized two of these purple zones as forming distinctive marker horizons by virtue of their characteristic purple colour and round amygdales of epidote and chlorite, 2 to 4mm in diameter, which are surrounded by sharply defined alteration haloes. These are termed PZ 1 and PZ 2, or "upper" and "lower purple zones" respectively. The latter occurs a short but variable distance above the base of the formation, while the former is taken to mark the top of the formation. The Jeanette Agglomerate Formation consists of agglomerates and tuffs, where a prominent thick agglomerate at the top of this formation forms a distinctive mappable unit. The overlying Loraine Formation contains a number of distinctive "altered zones" formed by a concentration of "variolitic and spherulitic structures surrounded by whitish groundmass" (Winter, 1976). Pienaar (1956) recognised two of these zones as representing prominent "altered zone" markers, an upper one, AZ 1 and a lower one, AZ 2, the former marking the top of the Loraine Formation (Winter, 1976). The Edenville Formation forms the top of the Klipriviersberg Group and is characterized by the presence of "green chalcedony and clusters of milky quartz amygdales" (Winter, 1976).

Apart from the distinctive features mentioned above, the bulk of the Klipriviersberg Group consists of monotonous, fine-grained to aphanitic and occasionally finely porphyritic green to grey

amygdaloidal and non-amygdaloidal lavas, as well as tuffs and agglomerates. In outcrop and borehole core the lavas are often indistinguishable from those of the Dominion Group, and have also been metamorphosed to low-grade, greenschist-facies assemblages.

3 Platberg Group

The Platberg Group comprises the Kameeldoorns Formation, the Makwassie Quartz Porphyry Formation and the Rietgat Formation. The Kameeldoorns Formation, originally termed the New Kameeldoorns Formation (Truswell, 1970), is a sedimentary sequence comprising coarse, first-cycle clastics which rapidly grade into finer sands, muds and carbonates. It indicates the presence of a major unconformity in that it is developed as coarse clastic wedges adjacent to fault scarps, with the thickest sections comprising massive boulder conglomerates and talus breccias. Clasts derived from the adjacent horsts are predominantly of Klipriviersberg and Witwatersrand strata. As the sequence thins out away from the fault scarps, the sediments become finer and better sorted. In places, sands, muds and carbonates interfinger with conglomerates, while the proportion of conglomerate often decreases to less than 10% within 10km of the fault (Winter, 1976). Sediments were not developed in upfaulted areas, and overlying volcanic units may rest directly on Klipriviersberg lavas, a feature which suggests the presence of an extensive unconformity.

The Makwassie Quartz Porphyry Formation overlies the Kameeldoorns sediments with no evidence of an hiatus prior to extrusion, and oversteps on to the Klipriviersberg lavas where Kameeldoorns sediments are absent. To the west, Makwassie porphyries overstep on to lower Witwatersrand and basement rocks. While the presence of quartz-feldspar porphyries characterizes this formation, a large proportion comprises quartz-free porphyritic and non-porphyritic lavas in addition to minor layers of sediments. Quartz porphyries predominate only where the thickest development of this formation occurs, and here they contain the largest and most abundant quartz phenocrysts. The formation terminates, by definition, at the top of the uppermost quartz porphyry.

The overlying Rietgat Formation comprises "green-grey porphyritic and non-porphyritic lavas" in which Winter (1976) notes an upward diminishing ratio of lavas to sediments, which he interprets as being indicative of "a waning phase of andesitic-to-dacitic volcanicity." Within the lower portion of this formation, a group of pale, green-grey porphyritic lavas containing minor intercalations of sediment and non-porphyritic lavas has been identified. This unit has been formally termed the Garfield Member (SACS, 1980) and may be allocated to either the Makwassie or Rietgat Formation, depending on its stratigraphic position relative to the uppermost quartz-feldspar porphyry, which varies from place to place. Winter (1976) notes that while no extensive erosional loss prior to the extrusion of Rietgat lavas is evident, "weathering of the upper portion of the Makwassie formation and in places the absence of amygdaloidal flow tops do indicate that there was a period of non-activity, and that the environment was terrestrial". This is further evidenced by the occurrence of bleached and intensely altered flow tops towards the top of the formation, which in places contain pink and red chalcedony amygdales, a combination of features which Winter (1976) cites as being indicative of a period of exposure and which are unique to the Rietgat Formation.

4 Bothaville and Allanridge Formations

Prospecting boreholes have intersected the Bothaville Formation extensively in the type area around Bothaville. It is a sedimentary formation, and typically displays a sedimentation cycle commencing with conglomerates, fining upwards into quartzites and shales, then coarsening again to culminate as conglomerates. It overlies a large expanse of the Rietgat Formation, with which it is conformable in places, but laps across older Ventersdorp formations onto Witwatersrand sediments and Archaean granites. Conglomerate pebbles are characteristically varied in origin, and include material derived from the Makwassie Formation. The Bothaville sediments differ from those of the Kameeldoorns in that the sand grade sediments are more mature and the conglomerate pebbles are more rounded, indicative of a widespread transportation of clastic material prior to deposition (Winter, 1976). The interpretation of the existence of a major unconformity at the base of the Bothaville Formation thus appears to be justified.

The Allanridge Formation, forming the uppermost sequence of the Ventersdorp Supergroup, consists essentially of green-grey to dark green-grey amygdaloidal andesitic lavas, in which zones containing small acicular feldspar phenocrysts alternate with non-porphyritic zones. In more phaneritic flows, small dark green phenocrysts are common (Winter, 1965). This formation conformably overlies the Bothaville Formation and isopach maps (Winter, 1965) demonstrate the coincidence of their respective depocentres. It does, however, extend beyond the established limits of occurrence of the Bothaville Formation and steps onto various older sequences. Characteristic features of the Allanridge Formation are the relative scarcity of tuffs and agglomerates, the lack of intercalated sediments and the occurrence, mainly in the uppermost flows, of red chalcedony amygdales. The Allanridge Formation is overlain by sediments of the Transvaal Supergroup, the relationship of which, according to Winter (1976), "could be conformable in basins, with marginal unconformities occurring on the arches".

5 Vaal Bend Unit

The presence of an additional unit within the Ventersdorp Supergroup, the Vaal Bend unit, has been suggested by Strydom and Whiteside (Whiteside, 1970.) This unit comprises a sequence of "shales, tuffs, quartzites, conglomerates, andesitic lavas, pyroclastics and feldspar and quartz-feldspar porphyries" and has been intersected in deep prospecting boreholes below the Klipriviersberg Group west and south-west of Klerksdorp. It appears, however, that the SACS working group (SACS, 1980) failed to reach agreement on the stratigraphic position of this sequence, and have thus recommended that it be regarded as an informal unit.

E. Age of the Witwatersrand Triad Volcanics

Basement granite underlying the Dominion Group at the Dominion Reef mine has yielded a Rb-Sr age of 2900 $\pm$ 150 Ma (Nicolaysen et al., 1962). Van Niekerk and Burger (1969) obtained a U-Pb age of 2800 $\pm$ 60 on sulphide concentrates from the Dominion Group lavas surrounding the Dominion Reef

mine, while Burger and Coertze (1973-1974) obtained a preliminary Rb-Sr age of 2730 Ma based on only two samples of "felsite" from the Ottosdal area. The most probable age of the Dominion Group thus appears to be around 2800 Ma.

A Makwassie quartz-feldspar porphyry from the Klerksdorp area yielded a U-Pb age of 2300 $\pm$ 100 Ma (van Niekerk and Burger, 1964) while Burger and Coertze (1973, p.13) obtained U-Pb ages of 2238 $\pm$ 110 Ma and 2245 $\pm$ 90 Ma on other Ventersdorp lavas. Subsequently van Niekerk and Burger (1978), using more refined techniques on zircons from the Makwassie porphyries, obtained a U-Pb age 2620 $\pm$ 50 Ma, while Burger and Walraven (1980) quote Rb-Sr isochron ages of 1960 Ma and 2180 Ma obtained at the Bernard Price Institute on two respective suites of Ventersdorp lavas, each comprising 4 samples. Thus while no concensus has been reached, it seems prudent to accept a provisional age of around 2300 Ma for the Ventersdorp Supergroup.

As no radiometric dating has been performed on Witwatersrand Supergroup volcanics, their age can only be inferred to be somewhere between 2300 and 2800 Ma, by virtue of their position within the stratigraphic column.

III STRATIGRAPHY OF THE STUDY AREA

A. Introduction

The purpose of the following section is to elucidate the stratigraphy of the study area, which differs slightly from the type stratigraphy, and to introduce a number of corruptions to the formal stratigraphic nomenclature which have been applied in this work for the sake of convenience. The study is based on samples from seventeen boreholes made available by the Anglo American Corporation, and selected by Mr P.M. Strydom, of Anglo American, to be representative of the stratigraphic sequences occurring in the Klerksdorp area. In addition to the original borehole logs which were made available to us, Strydom has recently relogged these holes in terms of the latest SACS stratigraphic nomenclature (SACS, 1980). These new logs thus form the basis of the succeeding descriptions, although the positioning of boundaries has in some cases been altered in the light of geochemical data obtained during this study. Although these modifications, which are restricted to the Ventersdorp Supergroup, are generally trivial and usually occur where the absence of a marker horizon has made precise positioning of the boundary difficult, a major modification has been made in one borehole which will be discussed in Section E of this chapter.

B. Locality of Boreholes

Figure 7 shows the distribution of the boreholes sampled. Seven of these boreholes, namely, DSF-7, DSF-10, DRS-6, DRH-14, DRH-15, DHF-8 and DRL-13, are located in an area roughly 40km to the west of Klerksdorp, and are representative of the Dominion Group. These holes were drilled directly into Dominion Group exposures. Of the remaining holes located to the south of Klerksdorp, WS-4, WS-5, VHD-1, JHA-1, JBF-1, SH-1, PK-10 and W-20 are representative of the Ventersdorp Supergroup, and were drilled either directly into outcropping Ventersdorp lavas, or through Transvaal and Karoo Supergroup cover. Boreholes R-1 and JY-8 were sampled exclusively for lavas of the Crown Formation. Boreholes DSF-7

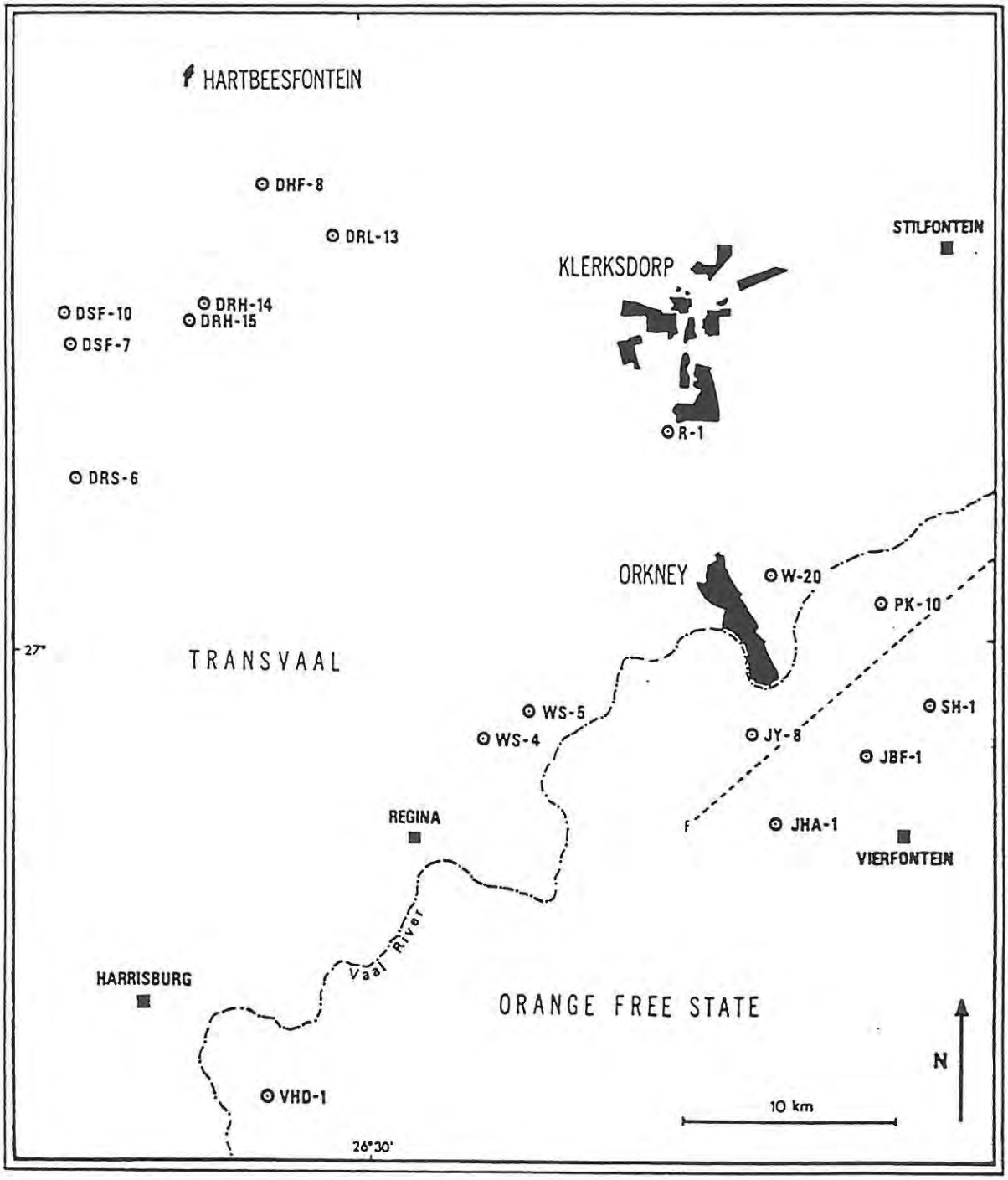

Figure 7: Localities of boreholes sampled. (Drawn by T.B. Bowen, 1984).

and WS-5 were selected by P.M. Strydom of the Anglo American Corporation to represent type sections through the Dominion Group and Ventersdorp Supergroup respectively, and consequently more attention has been given to the core from these holes in this study.

C. Dominion Group

Figure 8 represents a condensed version of the logs drawn up by Mr Strydom for the Dominion boreholes. As these boreholes are located within the type area, the stratigraphy is essentially the same as that described in Section B of the previous chapter. A notable feature, however, is the presence of a prominent 75m thick quartz-feldspar porphyry unit towards the top of the Rhenosterspruit Formation in boreholes DSF-7 and DSF-10. This unit, according to P.M. Strydom (pers. comm., March 1980) is possibly intrusive, since it has been observed elsewhere to transgress sedimentary horizons. Near the top of borehole DSF-7, a 27m thick basic intrusive occurs, and samples of this along with samples of similar intrusives from other holes, have been analysed and appear to have chemical characteristics similar to lavas of the Klipriviersberg Group of the Ventersdorp Supergroup.

It should be noted that, as the top of the sequence in the Dominion holes is determined by the present level of erosion, the complete sequence has been truncated at the top, where the uppermost porphyries, containing the "Wonderstone" bands described in the previous chapter, are not represented. Borehole DRS-6 contains an anomalous succession towards the base of the Rhenosterhoek Formation which displays peculiar segregation textures which are suggestive of liquid immiscibility. These will be described in Chapter V.

Finally, as will be shown in Chapter VI, the fine-grained to aphanitic basic to intermediate lavas of the Dominion Group as a whole, regardless of the formation in which they occur, represent a continuous differentiation sequence, while the acid porphyries form a geochemically discrete group within which very limited compositional variation occurs. For this reason, except where stratigraphic position may be relevant, Dominion lavas will be considered in the succeeding chapters as belonging to either of two strictly informal groups, namely the "Dominion basic lavas" and the "Dominion porphyries". In this way it is hoped to avoid

Figure 8: Condensed logs of the Dominion boreholes, showing sample positions. (Drawn by T.B. Bowen, 1984).

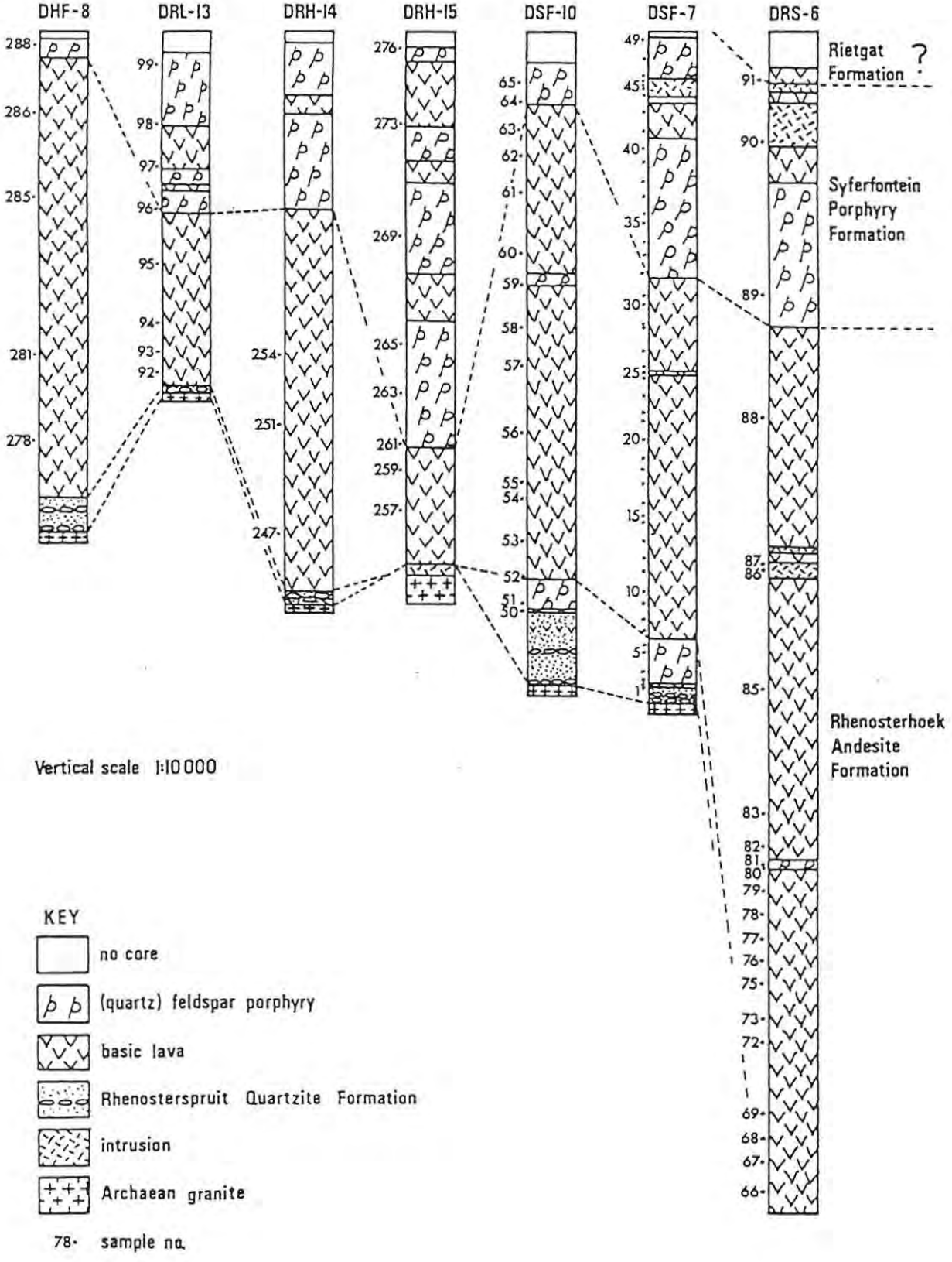

confusion, were the formal nomenclature to be used, resulting from the transgression of these discrete magma types across formational boundaries.

D. Crown Formation

Partial logs of boreholes JY-8 and R-1 are presented in Figure 9, where the Crown Formation attains thicknesses of 55m and 43m respectively. While in both cases the formation comprises essentially highly amygdaloidal lavas, in borehole R-1 it is capped by a thin band of agglomerate. Because of the entrenchment in the literature of the old term, "Jeppestown amygdaloid" for the Crown Formation, these lavas will in the following chapters be referred to by their old name on an informal basis, as recommended by SACS (1980).

E. Ventersdorp Supergroup

The stratigraphy of the Ventersdorp boreholes, as logged by P.M. Strydom (pers. comm.) is presented in Figure 10. A number of features, applicable to the Ventersdorp study area as a whole, are at variance with the stratigraphy of the type area around Bothaville.

At the base of the Klipriviersberg Group, the Westonaria Formation is not represented, being confined to the deepest parts of the Witwatersrand basin. The Alberton Formation thus rests directly on pre-Ventersdorp rocks and is distinguished from the overlying formations in that the lavas are generally coarser grained and finely porphyritic towards the top. The basal zone characterized by the Porphyritic Marker is not always present. The overlying Orkney Formation is readily recognised by the presence of "purple zones", although the boundaries are not easily established, especially in the case of borehole WS-5, where the upper purple zone is absent. The Jeanette Agglomerate Formation has not been recognized in the study area, while the Loraine Formation is again easily recognized by the presence of "altered zones", although the boundaries are poorly defined, especially where the upper altered zone is absent.

The Edenville Formation is generally inferred to occur above the upper altered zone of the Loraine Formation and as a result the lower boundary

Figure 9: Partial logs of boreholes R-1 and JY-8, showing sample positions. (Drawn by T.B. Bowen, 1984).

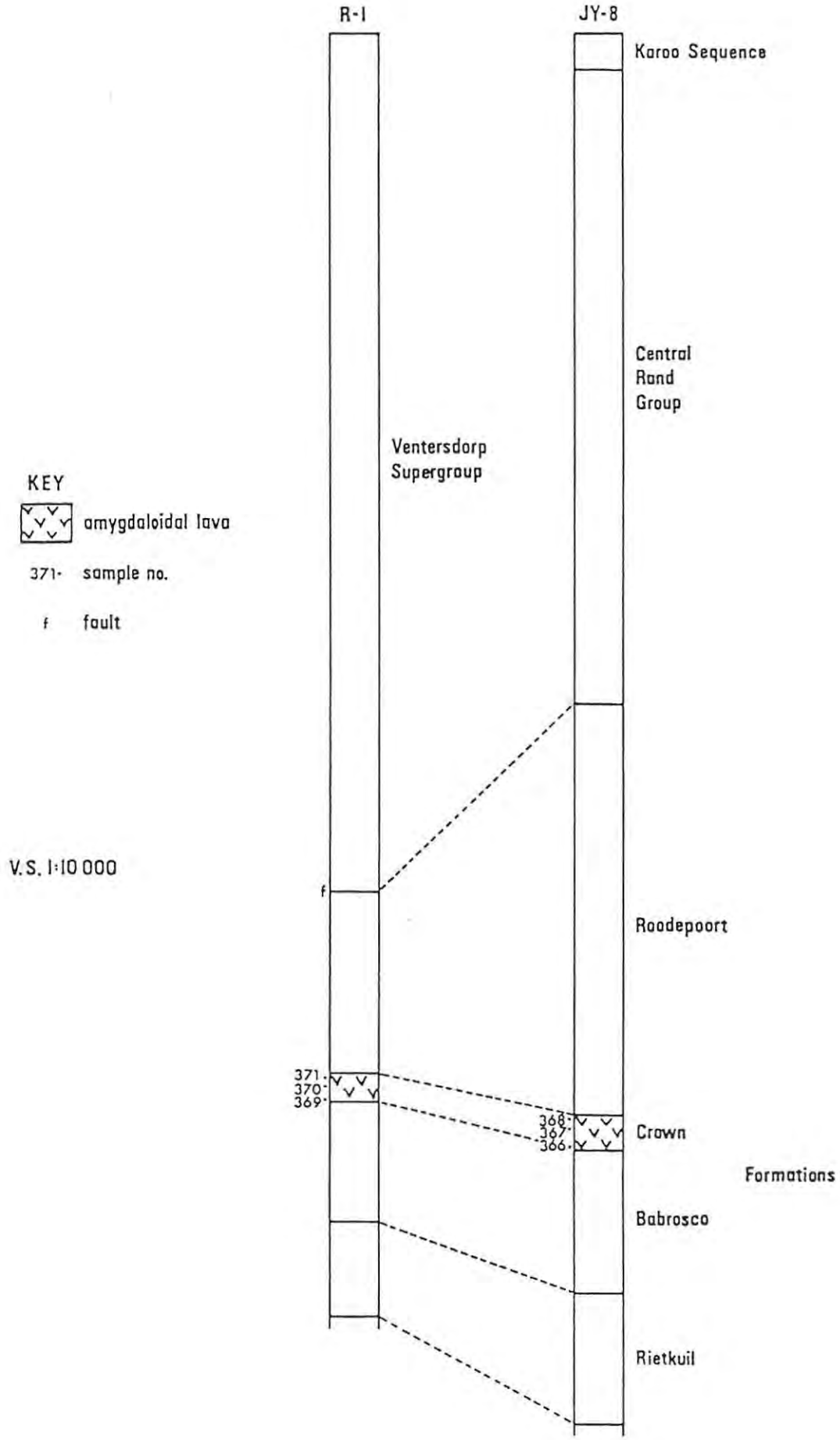

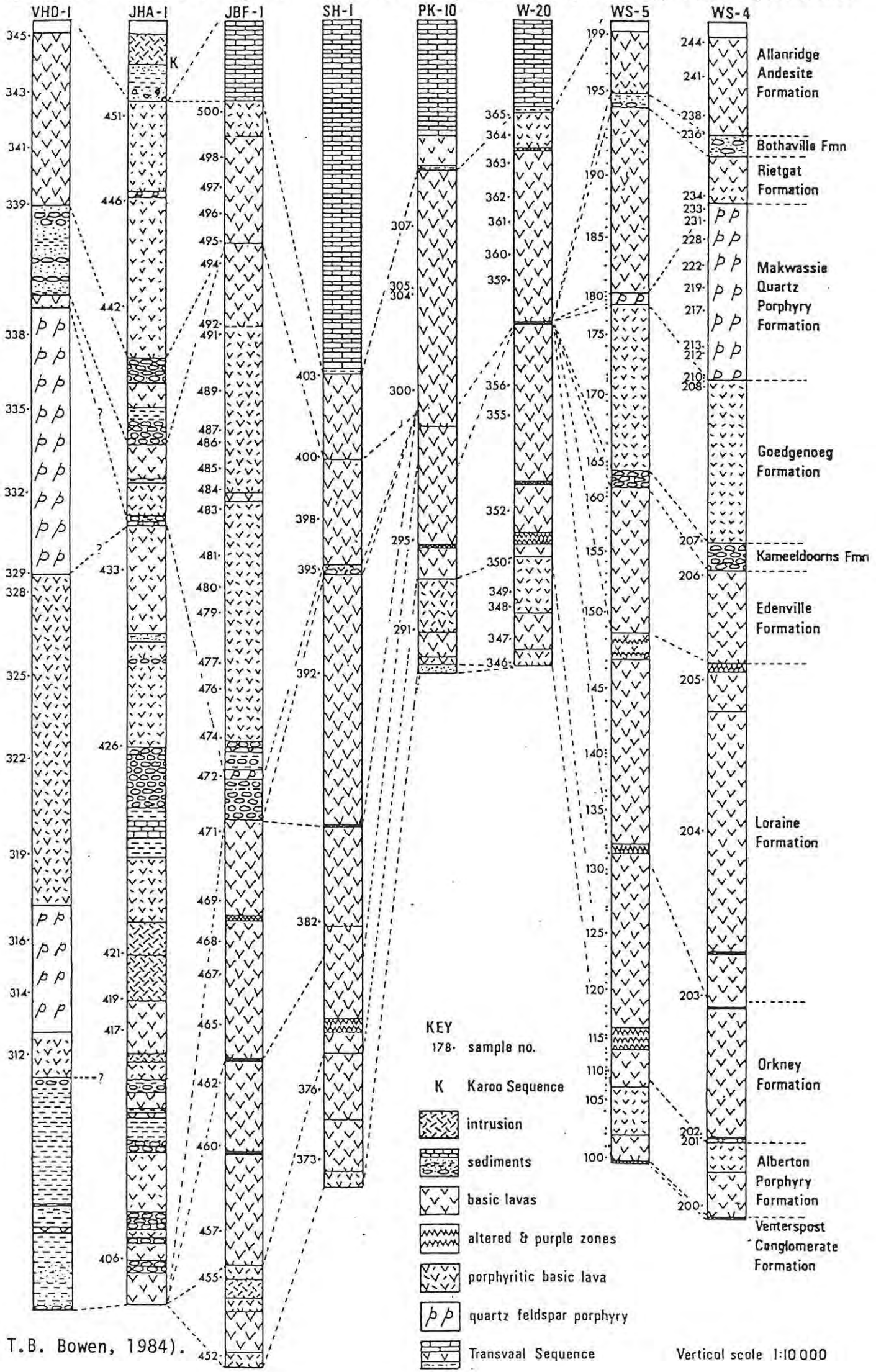

(Drawn by T.B. Bowen, 1984).

is difficult to establish. The presence of the Edenville Formation has not been acknowledged on the logs where the upper altered zone is absent, and although it is uncertain whether this is due to the absence of this formation or the inability to distinguish between the Loraine and Edenville Formations where the upper altered zone is not developed, it is not problematical to this study as these two formations are chemically indistinguishable. Zones of porphyritic lava containing small black phenocrysts occur within the Edenville Formation and may serve to characterise it to a certain extent, but as these make up only a small proportion of the formation, and are also present, although more rarely, in the Loraine Formation, their presence is inadequate to serve as a criterion for discriminating between these formations.

Lithological grounds for the stratigraphic subdivision of the Klipriviersberg Group in the Klerksdorp area thus appear to be somewhat obscure in the absence of marker horizons. It will be demonstrated in Chapter VI, however, that the Alberton, Orkney and combined Loraine/Edenville Formations are individually distinguishable on a geochemical basis after accommodating some minor boundary adjustments, and the original nomenclature will thus be retained in this study although on an informal basis.

In the Klerksdorp area, the stratigraphy of the Platberg Group is essentially as has been described in Chapter II, although the Makwassie Formation is amenable to further subdivision on both lithological and geochemical grounds as has been suggested by Winter (1976) and SACS (1980). While this formation is formally defined as occurring between the Kameeldoorns Formation and the top of the uppermost quartz-feldspar porphyry, in the study area it is typified by two discrete units. A single quartz-feldspar porphyry unit is separated from the Kameeldoorns sediments by a unit of greenish-grey, crystalline porphyritic lavas characterized by small dark green and scattered larger feldspar phenocrysts, the latter serving to distinguish this unit from other porphyritic lavas. P.M. Strydom (pers. comm.) has named this unit the Goedgenoeg formation, while the term "Makwassie formation" is strictly reserved for the actual quartz-feldspar porphyry unit. This nomenclature will be used for this study, although geochemically the Goedgenoeg and Rietgat formations are indistinguishable despite the characteristic feldspar phenocrysts of the former, and will thus be treated together, while the intervening Makwassie porphyries are geochemically distinctive.

The lithological successions of the Bothaville and Allanridge Formations are essentially the same as described for the type area, although P.M. Strydom (pers. comm.) has noted in his logs that the porphyritic lavas of the Allanridge Formation are concentrated in the upper part of the sequence. This distinction is not considered significant, however, as the formation as a whole displays very limited geochemical variation.

Features illustrative of the general stratigraphic relationships described in the previous chapter are, among others, the large variations in thickness of individual formations from borehole to borehole, and the absence of certain formations in some boreholes. In borehole JHA-1, the Platberg Group directly overlies pre-Ventersdorp rocks with a fault contact . The same borehole contains a thick, anomalous sequence of Goedgenoeg volcanics intercalated with Kameeldoorns-type sediments. Furthermore, the uppermost three samples of the Klipriviersberg Group in borehole WS-5, as well as the uppermost Klipriviersberg sample in borehole WS-4, are chemically equivalent to the Goedgenoeg/Rietgat lavas. Thus, considering the tectonic control of Kameeldoorns sediment deposition described in the previous chapter, these features suggest a certain amount of contemporaneous faulting and volcanicity, with a limited time lapse between the extrusion of Klipriviersberg and Platberg Group lavas. Other holes show no evidence of faulting and the absence of certain formations may be attributable to non-deposition due to topographic influences and overlap of younger formations beyond the areal limits of the older formations, as has been described in the previous chapter. Thus in borehole VHD-1, the Klipriviersberg Group is not represented, while the Goedgenoeg and Makwassie formations are absent from borehole SH-1, and boreholes PK-10 and W-20 consist of Allanridge lavas directly overlying those of the Klipriviersberg.

The stratigraphy of borehole W-20 has been inferred from geochemical data obtained during the course of this study, and is still subject to confirmation by P.M. Strydom, who has logged this hole as predominantly Klipriviersberg lavas, with a 4,5m sedimentary horizon at 267m depth (Figure 10) representing the Kameeldoorns Formation overlain by 55m of Goedgenoeg lavas. The chemistry of the Klipriviersberg, Goedgenoeg and Allanridge lavas is, however, considered to be sufficiently diagnostic to permit such a drastic modification, and the chemically inferred stratigraphy as shown in Figure 10 will thus be assumed. This, in

addition, appears to be more in accordance with the stratigraphy of borehole PK-10, situated 5km to the west of W-20 (Figure 7).

Finally, in borehole JBF-1, P.M. Strydom (pers. comm.) has identified the Garfield Member, which substitutes for the Goedgenoeg and Makwassie formations. While the lavas are predominantly of Goedgenoeg/Rietgat type, several thin zones are present which are lithologically and chemically similar to the Makwassie porphyries. A similar, relatively thick (260m) unit occurs near the base of the Goedgenoeg formation in borehole VHD-1.

IV. SAMPLING PROCEDURES

Over a period of four weeks spent at a number of Anglo American's core yards in the Klerksdorp area, approximately 500 samples of Witwatersrand triad volcanics were taken from the boreholes described in the preceding chapter, of which 326 were selected for analysis.

All samples selected from the type boreholes DSF-7 and WS-5 were analysed, making up 49 and 100 samples respectively and representing an average sampling interval of 22 metres. The remaining boreholes were sampled at approximately 40 to 50m intervals (although not all samples were analysed), the primary aims here being to ensure an effective lateral component in the sample population and to establish a more comprehensive sampling profile through units which are poorly represented in the type boreholes. For example, the Makwassie formation in type borehole WS-5 attains a thickness of only 22m, and the number of samples of this formation was thus bolstered by more detailed sampling of the Makwassie porphyries in borehole WS-4, where a thickness of 367m is attained.

Criteria used for sample selection were as follows: In the type boreholes, samples were taken where possible at a regular interval in order to avoid imposing any sampling bias which might affect the applicability of chemical discrimination techniques. Superimposed on this criterion, samples were taken as close as possible to the base of individual flows, but above the amygdaloidal zone. Justification for this procedure may be found in Pemberton (1978, p. 8) who ascertained, in a study on Karoo basalt flows, that samples taken from the base and tops of flows, after the removal of amygdales, were most representative of the original magma composition of the flow. Within-flow compositional variation has been attributed by Watkins et al. (1970) to the non-random distribution of phenocrysts, while large variation in alkalies has been attributed by Hart et al. (1971) to the upward migration of the last 1% of the liquid, which is alkali-enriched, before final solidification of the flow. Where flows attained thicknesses much greater than the sampling interval, samples were taken within the flows at a regular interval. In all cases, amygdaloidal, fractured, veined and brecciated samples were avoided as far as possible, while any included extraneous

material was removed prior to analysis. Marker horizons such as the "purple zones" were specifically sampled in order to ascertain whether they exhibit any distinctive geochemical features.

The sample positions are included on the logs in Figures 8, 9 and 10. Only the analysed samples are shown. Sample numbers are numerical and have no locative connotations. Prefixes have been added to the sample numbers where the analytical data is presented in Chapter VI to indicate their stratigraphic affinities which are primarily based on chemical criteria. The reader is thus requested to refer to the relevant logs should it be necessary to establish to which borehole any particular sample may belong.

V PETROGRAPHY

A. Introduction

The following chapter summarises the petrography of the analysed lavas, emphasis being placed on those aspects which are of direct significance to the petrogenesis of these lavas and thus complement the geochemical interpretations presented in succeeding chapters. The objectives of this chapter are thus as follows :

Many igneous differentiation models are based on the premise that the samples involved are representative of liquids. Since a major proportion of the volcanics of the Witwatersrand triad have been referred to in the literature as representing tuffaceous material (Winter, 1976), it is necessary to establish petrographically whether the analysed samples do in fact represent lavas. The recognition of igneous textures and the absence of pyroclastic features in thin section are required to confirm the liquid nature of the samples. Moreover, having established texturally that the sample, in its pristine state, does represent a liquid, an assessment of the degree of secondary alteration and metamorphism is required to aid in establishing whether the chemistry of the sample is representative of the original liquid, and whether any systematic chemical variations are associated with the type and intensity of the alteration. Further discussion on this topic will be deferred to the succeeding chapter. Finally, the presence and identification of relict phenocryst phases is important from a petrogenetic viewpoint in establishing whether the original magma composition has been modified by crystal accumulation and for providing some constraints on the elucidation of any fractional crystallization mechanisms which may account for the observed chemical variation within and between magma suites.

With the above aims in mind, the ensuing commentary has been subdivided such that individual lava groups defined in the previous chapter are treated separately, and each group further subdivided where this is warranted by geochemical diversity within individual suites.

B. Dominion Group

1. Dominion Basic Lavas

In general, these lavas appear to have suffered more intense metamorphism than the younger lavas of the Witwatersrand triad, although this may be an illusion resulting from the predominance of extremely fine-grained lavas within this suite, which hampers the recognition of original igneous textures. In hand specimen, these lavas are aphanitic to fine-grained, varying from green to grey in colour. While the weathered outer surface of the core is generally lighter, the more evolved samples weather to a brown colour. The few "tuffaceous" samples which were analysed characteristically appear non-homogeneous in hand specimen, showing a finely mottled alternation of dark green or brown and lighter green colours which often give the impression of turbid flow structures. However, no shard relicts, crystal or lithic fragments were discernable in thin section and the chemistry of these samples conforms to that of the group as a whole, thus attesting to their liquid character.

Microscopically, the original textures of this suite have largely been obliterated by the effects of alteration and metamorphism. The lavas are generally microcrystalline and allotriomorphic, comprising varying proportions of plagioclase, chlorite, calcite, epidote, clinozoisite, quartz and amorphous sphene, interspersed with fibrous flakes of amphibole. Plagioclase compositions are in the low-calcium range and appear to be albitic in composition, although maximum symmetrical extinction angles on albite twins in this range are ambiguous and dependent on relative refractive index determinations. These are difficult to perform as a result of the small grain size and ubiquitous presence of alteration products surrounding the grains. The presence of andesine reported by Malan (1959) can thus not be discounted. Chlorite is more concentrated in areas once occupied by interstitial glass. Here it occurs in conjunction with epidote and clinozoisite, both of which are often euhedral. Quartz generally occurs as irregular segregations of cryptocrystalline mosaics, and probably has resulted from small-scale remobilization of silica expelled during the formation of chlorite and epidote.

Secondary sphene occurs as tiny amorphous segregations scattered throughout the rock, while in a few samples the octahedral form of relict skeletal titaniferous magnetite grains is still discernible.

Mg-rich samples are distinguished from the more evolved samples in that they characteristically comprise an extremely fine-grained, turbid groundmass peppered with altered opaques, and a relatively large proportion of colourless to faintly pleochroic flakes of amphibole, which is probably tremolitic to actinolitic in composition. In contrast, the more evolved lavas are often not as fine-grained and the presence of relict skeletal magnetite crystals in the groundmass is more common. Amphibole occurs in lesser amounts, and as fine pleochroic needles or tiny spherulitic growths, the optically estimated composition being in the actinolite to hornblende range. Some samples contain occasional plagioclase phenocrysts, often embayed and extensively carbonated towards the core. Three samples, DB-1,2 and 3 from the Rhenosterspruit Formation in borehole DSF-7 are coarser than usual and in addition to the minerals already mentioned, contain abundant grains of stilpnomelane in association with actinolite and chlorite.

The anomalous section of borehole DRS-6 mentioned in Chapter III, occurs between 1594.6 and 1777.4 metres depth. A large proportion of these lavas is variolitic, containing peculiar aphanitic segregation structures which are pale green in colour and set in an aphanitic dark green matrix. The segregations are generally of flattened ovoid shape, ranging from .5 to 2cm in diameter, with the outline becoming irregular with increase in size. They generally occur in zones less than 1m thick which are often banded due to coalescence of the segregations on a variety of scales, and the darker material may be completely displaced to yield an homogeneous, brown-weathering lava. In thin section, both components are cryptocrystalline with a secondary felted mass of amphibole needles. In some specimens, the darker matrix displays quench textures in the form of long radiating sheaves of what appears to be a silica mineral intergrown with a pyroxene or amphibole, giving rise to a "micro-spinifex" texture. While none of the segregation-bearing samples were analysed, the homogeneous, brown-weathering samples within this unit, viz. DB-69,72

and 73, represent some of the most evolved lavas of the Dominion basic lava sequence.

To summarise, the analysed Dominion basic lava samples display no evidence to suggest that they were not originally of a liquid nature, and although original textures and mineralogy have largely been obliterated by secondary processes, or obscured by the microcrystalline nature of the majority of samples, the suite represents a sequence of essentially hypocrystalline lavas in which the only observable liquidus phase present is plagioclase in some of the more evolved samples. An assesssment as to whether secondary processes have caused a substantial modification of the original chemistry of these lavas will be made in the succeeding chapter.

2. Dominion Porphyries

The Dominion acid porphyries generally occur as massive, well-defined flows, the bases of which are characterised by a thin dark band of sheared material probably representing the original tuffaceous or scoriacious top of the previous flow. In hand specimen the samples comprise a dark grey to lighter green-grey matrix containing lighter feldspar and less abundant quartz phenocrysts. Feldspar phenocrysts are seldom larger than 5mm in length, and the total phenocryst content is visually estimated as less than 10% with an average of about 5%. In hand specimen the proportion of phenocrysts often appears to be much larger, but thin section examination of these samples reveals that this is due to the presence of spherulitic structures consisting of fine radial intergrowths of quartz and feldspar (Plate I). Where best developed, spherulites make up a major proportion of the groundmass and are separated from each other by a network of secondary mafic stringers consisting mainly of chlorite, stilpnomelane and amphibole as well as finely disseminated altered opaques. Phenocrysts are often surrounded by spherulitic structures which appear to have nucleated on them (Plate I). In areas where spherulites are not developed, as well as in non-spherulitic samples, the groundmass is often slightly coarser, comprising an allotriomorphic mixture of quartz and feldspar, with minor amounts of chlorite, epidote, amphibole and sphene. Epidote sometimes occurs as small radial growths of euhedral, elongated

grains, while plagioclase may form subhedral twinned laths. Amphibole is ubiquitous in the groundmass of the non-spherulitic samples, occurring as brownish flakes or fine, microcrystalline needles. More altered samples show a patchy development of calcite, while local silica remobilization is indicated by irregular, finely-crystalline, mosaic quartz segregations. In sample DP-33, the groundmass consists almost entirely of sericite. This feature is unusual and is reflected in the chemistry of this sample.

The phenocrysts are often surprisingly well-preserved, especially where the groundmass is fine-grained (Plate I). The phenocryst population consists predominantly of euhedral plagioclase of oligoclase composition, with lesser amounts of perthitic or microperthitic alkali feldspar and rounded, resorbed quartz, which may sometimes be absent. The feldspars occur individually or as glomeroporphyritic aggregates. Secondary carbonation and sericitization is common. In many cases the feldspars may be embayed and show sieve textures.

In conclusion, the recognition of individual flows in borehole sections and the intrusive nature of the porphyry unit at the base of the type borehole, DSF-7, attests to the liquid nature of these lavas which is supported by textural evidence such as the lack of pyroclastic features and the presence of spherulites which, according to Williams et al., (1958), commonly occur in siliceous lavas and generally result during the rapid crystallization of a viscous magma or from the devitrification of glass. Furthermore, Cox et al. (1979, p.194), suggest that the presence of spherulites indicates the former presence of glass and hence a rapidly quenched liquid. As these lavas form a relatively tight chemical cluster, the original chemistry is not considered to have been significantly affected by secondary processes, although this will be assessed in Chapter VI. Finally, the presence of plagioclase, K-feldspar and quartz phenocrysts must be considered in forthcoming petrogenetic interpretation.

C. Jeppestown Amygdaloid

The altered nature of the Jeppestown amygdaloid lavas has already been mentioned in Chapter III. Apart from the highly amygdaloidal nature of these lavas, they are riddled with fine veinlets of calcite and quartz, which often form a network interconnecting the amygdales, which have altered rims of the same material. Due to the limited stratigraphic thickness and veined and amygdaloidal nature of these lavas, only six samples were taken from the two boreholes, R-1 and JY-8. Each borehole was sampled near the base, middle and top of the formation, and all samples were comparatively homogeneous and free of veins and amygdales.

In hand specimen the samples are weathered to colours ranging from dark brown to lighter green-grey. They are fine-grained to aphanitic, the latter showing a pronounced tendency for rapid weathering, with a dark brown outer surface grading inwards over a distance of 5mm to a light green inner core, reflecting an original high proportion of glass. Although, with the exception of sample JA-371, these samples show a remarkable consistency in chemistry, they exhibit a variety of textures, probably resulting from differential cooling rates.

A common feature of all the samples is the scattered occurrence of comparatively large, relict plagioclase grains, which represent the only recognizable phenocryst phase. The samples are pervaded by a secondary, finely-felted mass of acicular actinolite laths. The finest-grained sample, JA-370, appears originally to have been almost holohyaline, and recognizable in the dirty brown, devitrified groundmass are tiny, scattered feldspar microlites and stumpy, microcrystalline lath-shaped ghost structures after a ferromagnesian phase, identified by virtue of a fine peppering of opaques which renders them slightly darker than the surrounding groundmass. Sample JA-368 displays an unusual texture made up largely of high-relief, golden-brown, often-coalescing globules (Plate II). On closer inspection these appear to represent relict spherulitic structures, the high relief being imparted by the presence, in addition to quartz and feldspar, of finely-granular epidote, the optical properties of which are largely obscured by the dark brown staining, possibly caused by the presence of hematite impurities. Areas interstitial to the spherulites comprise an allotriomorphous

Plate I: Sample DP-39 (Dominion porphyry). Well-preserved phenocrystal plagioclase intergrowth (centre right) surrounded by a spherulitic overgrowth. Another spherulite is present in the lower left part of the photomicrograph. Crossed nicols. Width of photomicrograph is 4mm.

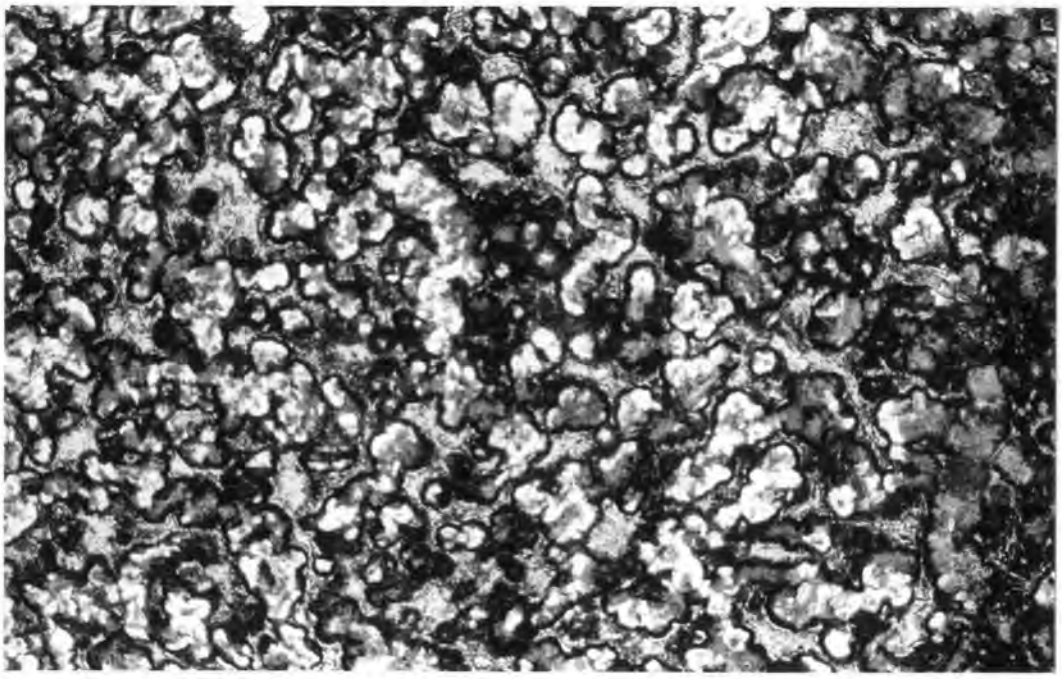

Plate II: Well-preserved spherulitic texture in sample JA-368, Jeppestown amygdaloid. Plane polarized light. Width of photomicrograph is 4mm.

brown-stained mass of chlorite, quartz and epidote as well as comparatively large platy laths of impure calcite of obscure origin. Actinolite is present as scattered flaky needles and spherulitic bundles.

The remaining samples are hypocrystalline and characterized by a well-developed network of fine plagioclase laths set in a dirty allotriomorphic groundmass of secondary chlorite, epidote, quartz, amphibole, altered opaques and patches of calcite. Sample JA-371 differs both texturally and chemically, in that the plagioclase laths are arranged in a subparallel orientation, thus imparting a trachytic texture to the rock, while the interstices comprise a uniformly green chloritic mass containing regular, discrete segregations of amorphous sphene. In addition to the ubiquitous altered feldspar phenocrysts, this sample contains occasional, strongly resorbed, quartz grains. It is uncertain whether these are phenocrysts or xenocrysts.

On the whole, the Jeppestown lavas display textures commensurate with rapid solidification from a liquid phase, with plagioclase being the only recognizable phenocryst phase. The validity of the chemistry of these lavas will be discussed in the succeeding chapter, although it may be noted that they form a relatively small volume within a large proportion of sediments, and would thus be readily susceptible to metasomatic chemical modification.

D. Ventersdorp Supergroup

1. Klipriviersberg Group

(a) Alberton Formation : The Alberton lavas are grey to green-grey in colour, with grainsize ranging from medium-grained phaneritic to aphanitic. Zones of finely-porphyritic lavas are present in the upper part of the formation. Samples from near the base of the formation are generally aphanitic and highly carbonated (e.g. KA-100) with no preservation of original textures.

Microscopically, textures are variable and dependent on grain size. The coarser samples have a distinct doleritic appearance. They are hypocrystalline and fine- to medium-grained, with a well-developed plagioclase network which in fresher samples can be seen to have been formerly intergrown with relatively large, ophitic plates of augite, the remnants of which are still preserved. The interstices comprise a fine mass of secondary minerals, mainly chlorite, clinozoisite, quartz and sphene, as well as relatively large, clear grains of epidote and clinozoisite. A large proportion of this interstitial material appears to have been glass, while a minor amount of micropegmatite is preserved in places.

Actinolite occurs as large bladed laths displaying a reaction relationship with pyroxene. Actinolite initially forms a reaction rim around the pyroxene grains, while cracks within grains are altered to chlorite (Plate III). The actinolite subsequently extends through the original pyroxene grain as well as into the groundmass until finally the pyroxene has been completely replaced, with chlorite remaining subordinate. With decreasing grainsize, the pyroxenes adopt a lath-shaped habit, with the proportion of mesostasis increasing and the texture becoming intersertal, while the mineralogy remains essentially the same. The size of actinolite grains becomes subordinate and they occur, along with feldspar, as a felted mass in the finest-grained samples.

A feature of all the samples from the Alberton formation is the presence of two generations of plagioclase. An older generation occurs as scattered, embayed and generally highly altered phenocrysts of variable size (usually between 1mm and 3mm in length, but up to 50mm in the Porphyritic Marker). The second generation is represented by the network of finer, less-altered laths already described.

(b) Orkney Formation : In contrast to the relatively well-preserved textures of the Alberton formation, those of the Orkney formation bear closer resemblance to the Dominion basic lavas. This is because the Orkney lavas are predominantly aphanitic.

The original textures appear to have been intersertal to hyalopilitic, and the presence of varying proportions of dirty brown devitrified glass imparts to the samples a clouded appearance in thin section resulting in poor resolution of the mineral constituents.

In general, small anhedral plagioclase laths form a felted network on which is superimposed a felt of fine, flaky, microcrystalline tremolite/actinolite laths of metamorphic origin. Small, anhedral, elongated, ill-defined grains of augite are ubiquitous. These commonly display yellow-brown tints. Discrete grains of epidote and clinozoisite often form the coarsest constituents of these samples. They are usually euhedral and occur in association with secondary chlorite, calcite, tiny quartz mosaics and altered opaques. Again the presence of an older generation of plagioclase is evident as scattered, embayed phenocrysts, as in the Alberton formation, but the phenocrysts are generally less than 2mm in length.

The "purple zones" which characterize this formation display a purple tinge in hand specimen, although they are not microscopically distinctive. The actual purple marker horizons are characterized by round amygdales, 2mm to 4mm in diameter, with sharply-defined alteration haloes. The amygdales are filled with chlorite interstitial to euhedral laths of clinozoisite and more granular epidote. This is surrounded by a narrow, sharply-defined rim of fine altered opaque material followed by a broader area which is relatively free of the usual clouded appearance of the groundmass, thus giving rise to the distinctive alteration haloes. Textures and mineralogy are otherwise identical to those of other samples from this formation. Pienaar (1956) noted that the purple zones are not chemically different from the other lavas, a feature confirmed by this study. He attributes their presence to the reaction of oxygen in ascending vapour bubbles with iron-bearing minerals to form haematite, which imparts the purple colouration to the rock. He suggested that conditions favourable for this process were only present in the horizons where the purple zones are developed. While no attempt has been made to verify this

proposal, both studies confirm the liquid nature of these lavas, and there is no evidence to suggest that the purple zones represent "purple-topped ash flow tuffs" as described by Winter (1976).

Sample KO-121 contains a high density of small chloritic amygdales with broad, pale alteration aureoles, giving the sample an appearance similar to the "altered zones" that characterize the Loraine Formation. In thin section the tiny amygdales consist mainly of crystalline calcite in an amorphous, chloritic base surrounded by a halo of dirty brown material, comprising mainly impure epidote, which extends with decreasing concentration into a chloritic groundmass in which no original minerals, including plagioclase, are preserved. It is noteworthy that despite the presence of amygdales, and the extreme degree of alteration which this sample has undergone, the immobile minor element concentrations have remained characteristic of the Orkney formation, although the major element chemistry has been extensively modified.

(c) Loraine/Edenville Formations : These two formations are considered together for reasons discussed in Chapter III. The lavas exhibit a relatively large chemical variation relative to the underlying formations and also display a wide range in well-preserved textures. Microscopically these lavas are texturally and mineralogically similar to those of the lower formations, with several subtle but significant differences. In describing these lavas, it is convenient to subdivide them into two groups, namely porphyritic and non-porphyritic types.

The non-porphyritic lavas make up the bulk of the sequence, and are indistinguishable in hand specimen from those of the lower formations. Included in this group are samples which appear in hand specimen to contain tiny phenocrysts which, under the microscope, are revealed to be tiny chlorite amygdales generally smaller than 0.5mm in diameter. Texturally these lavas are similar to those of the Orkney formation, although they have a lower proportion of glassy mesostasis and a larger proportion of augite. The latter occurs as non-ophitic, usually lath-shaped

grains, occasionally twinned and with a yellow-brown tint. They sometimes occur as microphenocrysts, although a large size variation within samples is present. In exceptional cases a length of up to 1mm is attained. A second feature of these lavas is a dearth of older-generation plagioclase phenocrysts which are characteristic of the lower formations. Thus augite appears to represent one of the first liquidus phases, along with, and in some cases, possibly prior to, plagioclase. The predominance of fine-grained lavas suggests that crystallization commenced during the extrusive or post-extrusive phase, or that earlier-formed crystals were entirely extracted from or resorbed by the magma prior to extrusion.

The porphyritic group is characterized by the presence of chlorite pseudomorphs after one or more primary mafic phenocryst phases (Plate IV). These pseudomorphs (0.1mm to 2mm in length) make up a maximum of 5% of the rock. Groundmass textures of these lavas are variable and indistinguishable from those of the non-porphyritic group. Grain size varies from microcrystalline to medium-grained. The degree of crystallinity of these lavas varies independently of the size variation of the chlorite pseudomorphs. This size relationship is considered to be indicative of the association of the phenocrysts with an intratelluric stage of crystallization, while grain size of the groundmass was determined essentially by cooling rates. Since this group of lavas represents the most primitive magma of the Witwatersrand triad, as mentioned in Chapter III, the original composition of these phenocrysts is of major significance to the petrogenetic interpretation of these lavas, and they warrant further discussion.

The present composition of these phenocrysts is mainly chlorite of penninitic composition, usually showing well-defined (001) cleavage and slight pleochroism (Plate V). The cleavage is orientated parallel to the original crystallographic axes of the primary mineral, so that the grains now appear to have parallel extinction. Amorphous chloritic material generally occurs in smaller phenocrysts in association with a microcrystalline mosaic of quartz. In all cases a small amount of epidote/

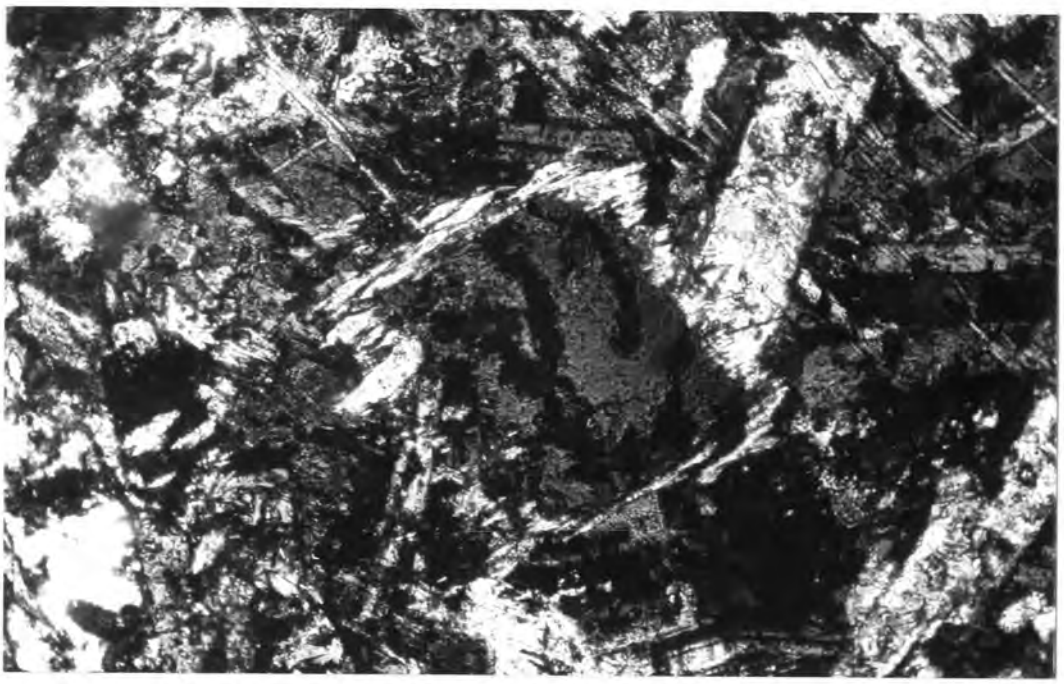

Plate III: Early stages of augite breakdown illustrated in sample KA-105, Alberton formation. Augite (centre of photo) is replaced by chlorite (dark grey) along internal cracks, while a reaction rim of actinolite (light grey) develops, subsequently replacing the augite, with chlorite remaining subordinate. Crossed nicols. Width of photomicrograph is 1mm.

Plate IV: Chlorite pseudomorphs after a primary mafic phenocryst phase, in this case in an aphanitic matrix. Sample KL-146, Loraine/Edenville formation. Plane polarized light. Width of photomicrograph is 4mm.

clinozoisite is present, usually as small euhedral grains within the phenocrysts. Electron microprobe analyses of the constituent minerals of these phenocryst pseudomorphs are presented in Appendix II. The phenocrysts are sometimes penetrated by amphibole needles. In some cases, especially where the groundmass is comparatively coarse, the phenocrysts are partially surrounded by an overgrowth of augite. No remnant of the original phenocryst phase could be located and the only clue to its identity is the often well-preserved euhedral shape, which is generally typical of augite, and has been identified as such by workers such as Jacobsen (1943) and Pienaar (1956).

According to Cox et al. (1979), low temperature alteration features of olivine include a concentration of fine opaque material around the rim and along internal cracks, while the bulk of the olivine is converted to a mass of low-relief micaceous material. Hornblende commonly alters to a fine-grained mass impregnated with disseminated opaques. As none of these features is exhibited, and the mode of occurrence is considered to indicate a high temperature alteration of a phenocryst phase, pyroxene appears to be the favoured candidate. Augite, however, is often well-preserved in the groundmass of these lavas, and occasionally mantles the altered phenocrysts. Furthermore, Garcia (1978) has stated that "clinopyroxene phenocrysts are commonly the only unaltered remnant phase present in metavolcanic rocks". The fact that no remnants of the original phenocrysts were located is somewhat of an anomaly.

A number of electron microprobe analyses (see Appendix II) were obtained of pyroxenes in a non-porphyritic sample, NL-789 (see below), which lies within the compositional range of these lavas. These pyroxenes represent high-calcium, diopsidic augites. It thus appears that no reason exists for augites of similar composition to be totally altered, and the phenocrysts are thus considered to have been low-calcium pyroxenes which, in equilibrium with liquids within the compositional range of these lavas, would be Mg-rich. While the above problem will be discussed further in the light of geochemical evidence, it

should be stated that the conclusions reached above are by no means unequivocal, being based almost entirely on circumstantial evidence. The characteristic crystallographic orientation of the chlorite relative to the original grain appears to be a result of the a unit cell parameter of chlorite coinciding with the c parameter of pyroxene, both being around 5.3A (Deer et al., 1966). This is not diagnostic, however, as amphibole has a similar c parameter.

The "altered zone" markers characterizing the lavas of the Loraine Formation (see Chapters II, D and III, E) are aphanitic, green in colour and contain a high concentration of variolitic structures, often coalescing, of a few millimetres diameter. These are altered to a lighter colour, giving the rock its distinctive appearance. In the samples analysed (e.g. KL-132) the varioles are strongly calcitized and chloritized, the original texture being destroyed, although no significant chemical modification is evident. Pienaar (1956) has reported varioles of up to 30mm in diameter. Sample NL-789, mentioned in the previous paragraph, represents one of a batch of samples which did not form part of the sampling program, but was submitted to us subsequently by the Anglo American Corporation for identification purposes. This particular sample contains orbicular structures, light green in colour and up to 15mm in diameter, set in a darker green matrix. Whether or not this sample is stratigraphically equivalent to an "altered zone" is uncertain, as the latter do not appear to exhibit any distinctive chemistry. This sample nevertheless warrants a brief description. In thin section, the rock is characterized by fairly numerous, well-preserved euhedral to subhedral microphenocrysts of diopsidic augite (see Appendix II) occurring within both the orbicules and the matrix. The orbicules comprise brown glassy material containing abundant sheaves of elongated crystallites representing either a quench or a devitrification texture, while the groundmass contains a high proportion of devitrified glassy material in which abundant secondary epidote, amphibole and chlorite can be identified, in addition to the augite microphenocrysts and smaller sub- to anhedral feldspar grains. Disseminated opaques are scattered

throughout, although a higher proportion is sometimes in evidence around the rims of the orbicules, which are not sharp but grade into the groundmass. On the whole, the textures indicate a rapidly quenched liquid. Plate VI shows the internal texture of an orbicule.

It is probable that this sample is equivalent to the "variolitic lavas" first described by Pienaar (1956) and identified as the "altered zone" marker horizons. The nomenclature is thus misleading, since the sample is not excessively altered, and the crystallites in the orbicules are not arranged in a radial pattern as the term "variole" implies.

(d) Summary: The Klipriviersberg group as a whole displays no features suggestive of a volcaniclastic origin for any of the samples studied. Although the degree of secondary alteration is variable, a large proportion of the lavas exhibits well-preserved primary textures suggesting that no extensive modification of the original chemistry has occurred. Both the Alberton and Orkney formation lavas contain plagioclase phenocrysts or microphenocrysts, the lack of which characterizes the Loraine/Edenville formations. The latter formations contain a relict mafic phenocryst phase which has provisionally been identified as representing a low-calcium pyroxene. The presence of augite has been observed in all cases, sometimes occurring as a phenocryst phase.

2. Platberg Group

(a) Goedgenoeg/Rietgat Formations: In hand specimen, these lavas are aphanitic to medium-grained phaneritic, grey to green-grey in colour, and are usually finely porphyritic. The large, scattered feldspar phenocrysts which characterize the Goedgenoeg formation are generally concentrated towards the middle of the flows, and consequently the samples, having been taken from near the base of each flow, show little distinction from those of the Rietgat formation. The phenocrysts present are plagioclase as well as small mafic laths of similar appearance to those in the Loraine/Edenville formations, attaining lengths of up to 5mm.

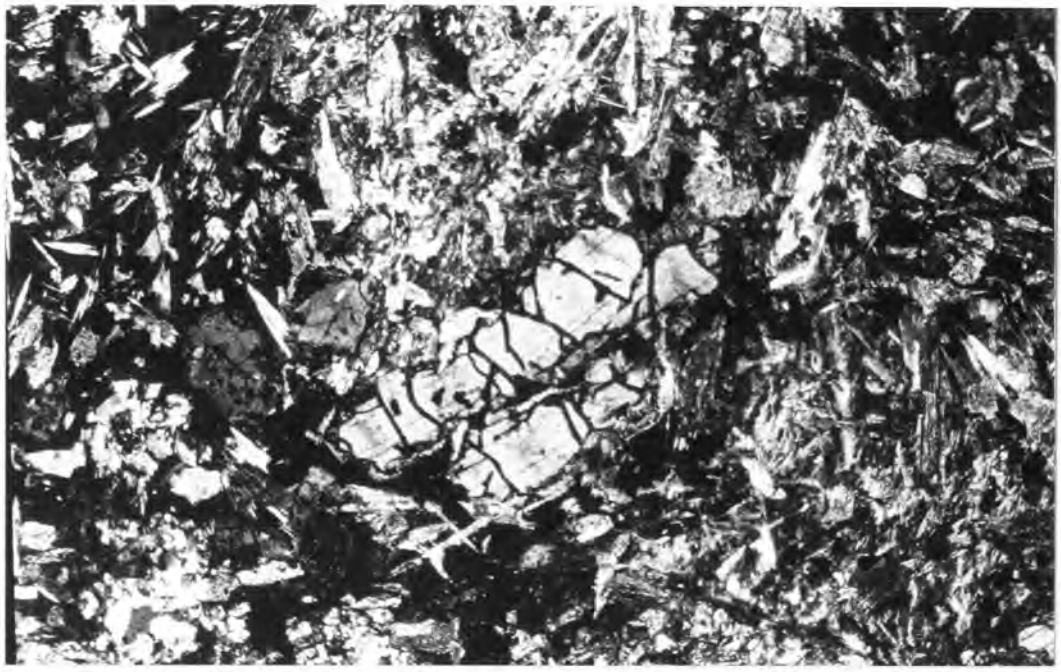

Plate V: Chlorite pseudomorph, as in Plate IV, under crossed nicols to illustrate the characteristic internal morphology. The chlorite basal cleavage is parallel to the original long axis of the crystal. The prominent internal cracks are probably original. Note the augite grains to the left of the phenocryst, and the amphibole flakes in the mesostasis. Sample KL-158, Loraine/Edenville formation. Width of photomicrograph is 1mm.

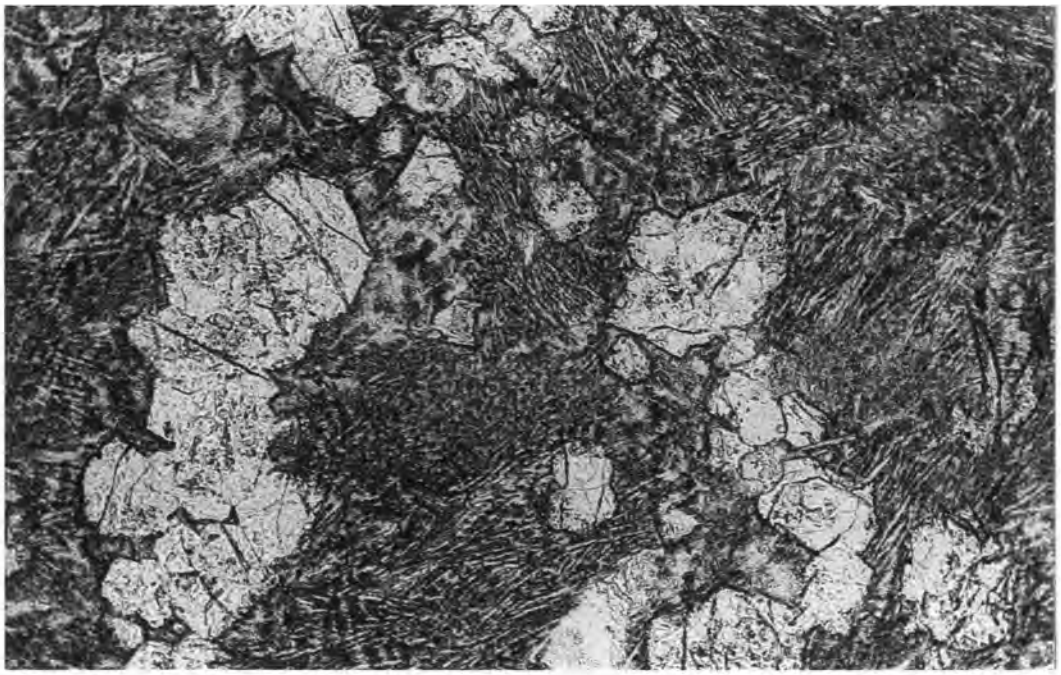

Plate VI: Well-preserved microphenocrysts of diopsidic augite (see Appendix II) within a micro-spinifex textured orbicule from sample NL-789 (see text). Plane polarized light. Width of photomicrograph is 1mm.

Microscopically, groundmass textures have largely been obscured by secondary processes, the major constituents being low-calcic plagioclase which forms a felted mass along with actinolite needles in the finer-grained rocks, while the coarser samples display an intersertal texture made up of a framework of relatively coarse, stubby laths of feldspar. Occasionally, hollow feldspar laths were observed, a habit which, according to Lofgren (1972) is a function of cooling rates. The interstices are filled with secondary material comprising dirty devitrified glass containing a high proportion of amorphous sphene (leucoxene?) and altered disseminated opaques, along with epidote, clinozoisite, amphibole, quartz and chlorite. Quartz sometimes occurs with an unusual skeletal habit in coarser, quenched samples, and may be the high temperature polymorph, tridymite. Small remnants of augite are apparent in some samples. Calcite is common in some samples, often replacing plagioclase and forming irregular patches in the groundmass.

The phenocrysts occur either individually or as stellate clusters, giving the rock a glomeroporphyritic texture. In these clusters plagioclase is often intergrown with, and sometimes enclosed by, the mafic phenocrysts (Plate VII). Again the identity of the mafic phenocrysts is problematical and no remnants of the original phase could be located. They generally occur in shapes characteristic of pyroxenes, and display certain features which distinguish them from those in the Loraine/ Edenville formation. The most common replacement material is chlorite, which sometimes has deep anomalous blue or purple interference colours. The fixed orientation of the chlorite basal cleavage, which was noted in the pseudomorphs of the Loraine/Edenville lavas, is again apparent. The proportion of epidote is high and in some specimens chlorite may be absent and the phenocryst is entirely pseudomorphed by epidote. A common feature within these phenocrysts is the development of an amorphous phase of high relief and birefringence, confirmed by electron microprobe analysis to be sphene (see Appendix II). In some cases it occurs as tiny blebs elongated along the direction of the chlorite cleavage trace, while in others it forms well-developed spindle-shaped lamellae extending the whole

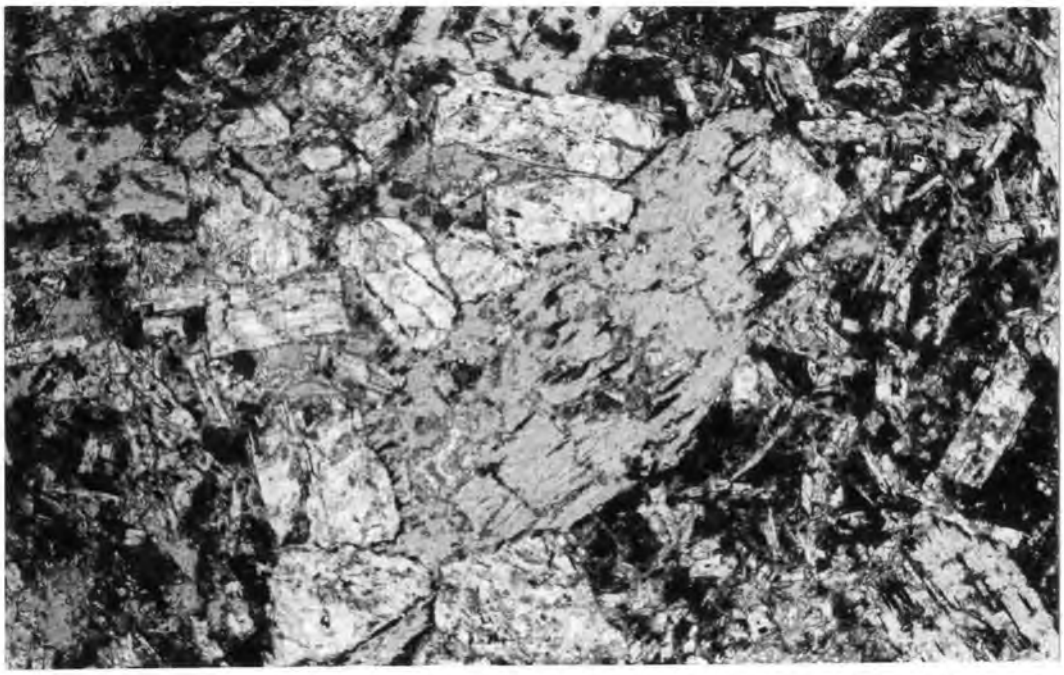

Plate VII: Glomeroporphyritic intergrowth of plagioclase (white) with chlorite pseudomorphs after pyroxene (pale grey). Note the spindle-shaped blebs of sphene (dark grey) within the pseudomorph. Sample PR-191, Rietgat formation. Plane polarized light. Width of photomicrograph is 4mm.

Plate VIII: Chlorite pseudomorphs as in Plate VII, but displaying well-developed, spindle-shaped sphene lamellae along cleavage planes. The smaller (white) laths in the groundmass are plagioclase. Sample PR-186, Rietgat formation. Plane polarized light. Width of photomicrograph is 4mm.

length of the grain along cleavage planes (Plate VIII), and may form up to 10% of the phenocryst. The outlines of these phenocrysts are often blurred by a jagged rim of amphibole, which may extend as tongues into the groundmass.

These phenocrysts have been identified in the earlier literature as augite (e.g. Jacobson, 1943; Pienaar, 1956), although Jacobson (1943) has mentioned the possible presence of pseudomorphs after amphibole in certain areas. The phenocryst shapes are characteristic of pyroxenes (Plate IX). The presence of epidote pseudomorphs, along with sphene in the chlorite pseudomorphs, may suggest an original calcic pyroxene in which the formation of epidote and sphene was necessitated by the inability of chlorite to accommodate Ca. This cannot be quantified, however, because of the relatively high mobility of Ca, which would inevitably result in a certain amount of Ca exchange between phenocryst and groundmass. If the presence of Ca-bearing alteration products within the phenocrysts reflects an original calcic phase, despite the high mobility of Ca, then the TiO_2 component of the sphene has an even greater likelihood of being derived from the original phenocryst, because of its relatively immobile behaviour (see Chapter VI). The TiO_2 content of sphene varies between 35 and 40 wt% (Deer et al., 1966), although it is slightly lower in the specimen analysed (32%). If it is assumed that the visually estimated maximum volume proportion of 10% sphene is roughly equivalent to its weight proportion in the altered phenocryst, the original phenocryst would be required to have accommodated up to 4% TiO_2. This is beyond the range of common augite (.5 to .8% TiO_2) reported by Deer et al. (1966) but does, however, fall within their reported range in titanaugite of between 3% and 6% TiO_2. However, it should be noted that in modern rocks, titanaugites are known to occur only in undersaturated alkaline lavas.

Sample PG-177, from the top of the Goedgenoeg formation in borehole WS-5, has a phaneritic appearance in hand specimen, but under the microscope it comprises an abundance of glass shards, now altered to chlorite, set in a matrix of fine quartz,

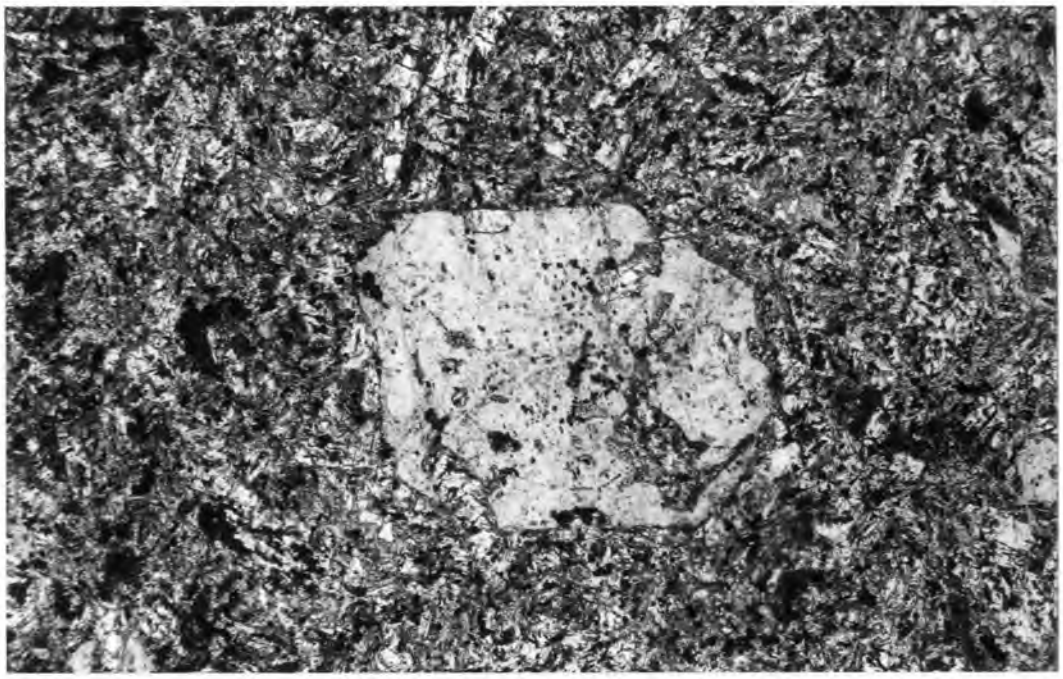

Plate IX: Typical pyroxene morphology displayed by chlorite pseudomorph in basal section. Sample PR-186, Rietgat formation. Plane polarized light. Width of photomicrograph is 4mm.

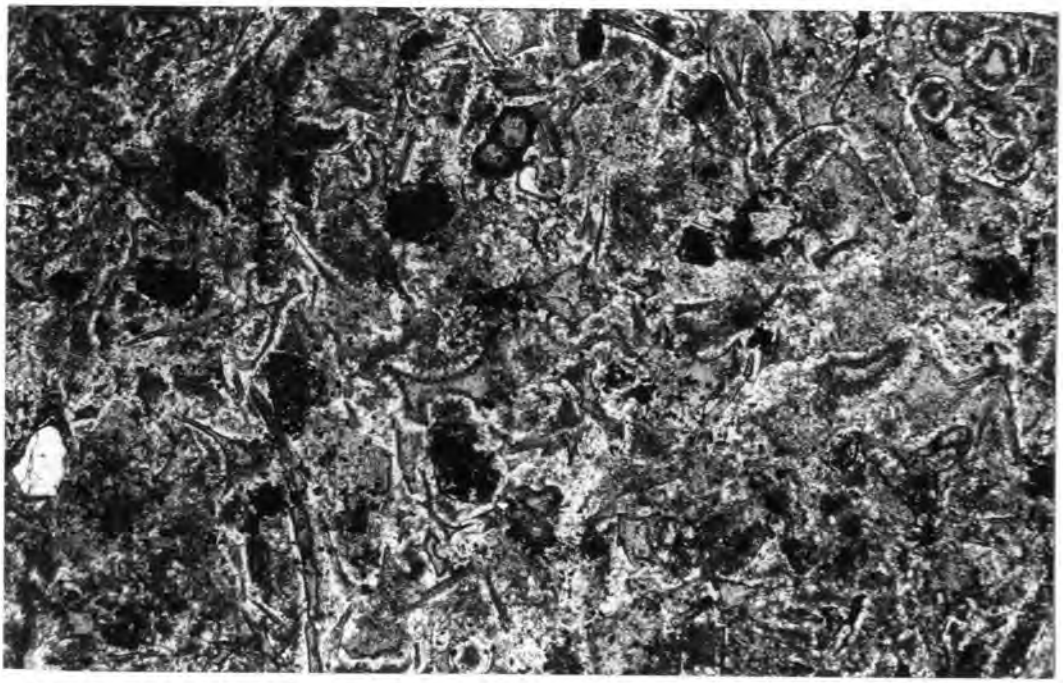

Plate X: Shard structures attesting to the pyroclastic origin of sample PG-177, Goedgenoeg formation. Plane polarized light. Width of photomicrograph is 1mm.

scattered opaques and occasional calcitized plagioclase relicts (Plate X). This represents the only sample of pyroclastic origin identified in the entire sample suite, with the possible exception of the Makwassie porphyries. In addition to its distinctive textures, this sample is compositionally far removed from any of the other samples analysed in this study.

Lavas of the Goedgenoeg/Rietgat formations thus display textures indicative of solidification from a liquid and may therefore be considered to represent magmas. At least two phenocryst phases are present in many samples, and their combined proportion of less than 10% is not considered sufficient to significantly modify the liquid chemistry. The phenocryst phases are low-calcium plagioclase, the composition of which has probably been modified by loss of Ca due to secondary processes, and a mafic phase which has tentatively been identified, by very speculative reasoning, as representing a Ti-rich augite. Intergrowths of these two phases imply that both were liquidus phases prior to extrusion. An assessment as to whether the original chemistry has been significantly modified by secondary processes will be made in the succeeding chapter, although the degree of alteration does not appear to be excessive.

(b) Makwassie Formation : Quartz feldspar porphyries of the Makwassie formation are highly distinctive in hand specimen by virtue of their abundant large feldspar and quartz phenocrysts. Feldspar phenocrysts are characteristically stubby, often rounded, and average around 6mm in length, although composite grains of up to 20mm in diameter are fairly common. Green chloritic inclusions resulting from incipient remelting of the phenocrysts are often observed in hand specimen. Quartz is less abundant and generally occurs as clear, rounded grains between 2mm and 4mm in diameter. The proportions of phenocrysts are variable, but are usually high, so that in extreme cases individual phenocrysts may almost be touching. The groundmass is generally of a grey-green colour, although shades of greens and reds are sometimes present, and is aphanitic with a dense cherty appearance, often impregnated with chlorite and whitish specks of leucoxene.

Microscopically, these lavas exhibit a complex variety of textures which are difficult to interpret. The groundmass is primarily composed of a fine, allotriomorphic aggregate of quartz and feldspar interspersed with equally fine-grained chlorite, epidote/clinozoisite, calcite, altered opaques and sericite. Small vugs filled with chlorite are present in many samples, and are stretched out, often bending around phenocrysts to form schlieren-like structures which possibly resulted from viscous flow. A number of features present in these rocks raise doubts as to whether they are, in fact, lavas. Fragmental quartz and feldspar grains in the groundmass of some samples may suggest either a pyroclastic or a cataclastic origin. In the former context, at least some of the schlieren observed may represent relict shard structures. Furthermore, discrete xenoliths of the same rock-type can be identified in some specimens, and in extreme cases careful inspection reveals that the sample is a composite aggregate of discrete fragments, the rounded, interfusive nature of which suggests that they consolidated while still in a plastic state.

Another feature of these samples is the presence of aggregates of smaller feldspar and quartz grains, along with a relict ferromagnesian mineral (which is now pseudomorphed by chlorite and sometimes epidote), altered titaniferous magnetite, apatite and zircon. It is uncertain whether these aggregates, ranging up to a few millimetres in diameter, represent xenolithic fragments or pockets of the final liquid to crystallize. Less commonly, the constituents do occur individually within the groundmass. The relict ferromagnesian phase is generally sub- to anhedral and probably represents an original pyroxene or amphibole because of its elongated shape. It now comprises an amorphous mass of chloritic material, with a concentration of what is probably red-brown haematite along original cracks and around the edges (thus similar to the description of relict olivine by Cox et al. (1979, p.182)). Relict titaniferous magnetite is represented by subhedral to anhedral grains showing opaque to semi-opaque lamellae of altered magnetite, while the original ilmenite component has been altered to amorphous leucoxene and/or sphene, which in addition forms a major

component of the interstices of the aggregates, and gives rise to the whitish specks observed in hand specimen. Apatite occurs as conspicuous euhedral hexagons and subhedral, often spindle-shaped laths of variable size up to .6mm in length. Zircon, although sometimes anhedral, is usually euhedral and may attain lengths of up to .5mm in exceptional cases.

In the phenocryst assemblage the feldspars are of two types - plagioclase of oligoclase composition and an alkali-feldspar. In addition to exhibiting variable degrees of alteration (mainly to calcite), the feldspars display a variety of textures within individual specimens. Plagioclase exhibits both paired and multilamellar twinning, while both feldspar types may display textures indicative of remelting, giving rise to a honeycomb structure where up to 50% of the grain contains groundmass material, while other grains remain unaffected. Alkali-feldspars are usually subordinate, exhibit perthitic and microperthitic exsolution and appear to be more prone to remelting and alteration (Plate XI). Quartz phenocrysts are strongly resorbed and often cracked, with groundmass material filling the cracks in many instances.

Resorption features displayed by the phenocrysts indicate that they were present prior to extrusion, and along with the agglomeratic nature of some samples, the presence of schlieren structures and broken phenocrysts in places may be a result of the high shear stress involved during viscous flow, as well as faster cooling of some parts of the flow with subsequent fragmentation and reincorporation into less viscous portions. During the sampling operation, flows could not be recognised with certainty. Both Winter (1976) and Jacobsen (1943) have reported that flows are recognizable, and the latter author invoked the presence of thick cooling crusts as indicating that the lava was relatively viscous. Jacobsen (1943) also commented on the "irregular character" of the rock, which may sometimes have a "very turbulent nature" which makes the identification of flows difficult.

A more detailed study would be required to adequately account for the petrographic features observed in the samples studied. A gradational alternation of lighter and darker zones was noted in the succession during sampling operations. There are indications that this may represent a primary mineralogical zonation. However, the variations in composition between individual samples could not be related to total phenocryst content and/or phenocryst proportions, both of which are variable. It is probable that such a relationship would emerge if a larger number of samples was studied in more detail.

Despite inconclusive petrographic evidence, it is considered likely, in view of the highly porphyritic nature and fairly silicic composition of the Makwassie rocks, that they were very viscous at the time of extrusion and that they comprise both pyroclastic and liquid components. They nevertheless bear a unique geochemical signature and display rational compositional trends (see Chapter VI), various possible explanations for which will be considered in Chapter VII.

3. Allanridge Formation :

In hand specimen, lavas of the Allanridge formation are green-grey to dark green in colour, and fine- to medium-grained phaneritic. Finely porphyritic lavas are evident towards the top of the formation.

Under the microscope, Allanridge lavas bear a strong resemblance to the coarse-grained lavas of the Alberton formation and the non-porphyritic lavas of the Goedgenoeg/Rietgat formations. They show a wide range in the type and intensity of alteration, with a large proportion of samples being strongly carbonated, and others show a remarkable preservation of plagioclase grains although the interstices have been chloritized and epidotized. Stubby laths of brownish augite are preserved in a few samples, while several samples from near the top of the formation contain well-preserved euhedral to anhedral augite phenocrysts, often in glomeroporphyritic clusters. Altered opaques and scattered specks of amorphous sphene are common, while small relict skeletal magnetite crystals are preserved in some samples (Plate XII). Chlorite-filled micro-amygdales may be

identified under the microscope in some samples. In hand specimens these may be mistaken for chloritized mafic phenocrysts similar to those which characterize the Goedgenoeg/Rietgat formations. An altered mafic phenocryst phase is nevertheless occasionally present in insignificant quantities. These phenocrysts are similar to those of the Goedgenoeg/Rietgat formation, although their shapes are poorly defined and brown sphene inclusions are not always present. Although it is not possible to ascertain whether they represent the altered equivalents of the augite phenocrysts described above, this should not be discounted in view of the wide range in the intensity of secondary alteration. A microphenocrystal generation of plagioclase is evident in many samples and generally occurs as intensely carbonated relicts.

On the basis of texture there is little doubt about the liquid nature of these samples, with at least two minerals, plagioclase and augite, present as phenocryst phases. Chemically these lavas show very limited variation of immobile element concentrations, and hence provide a useful indicator of the degree of chemical modification which may be expected from samples showing a wide range in intensity and type of secondary alteration.

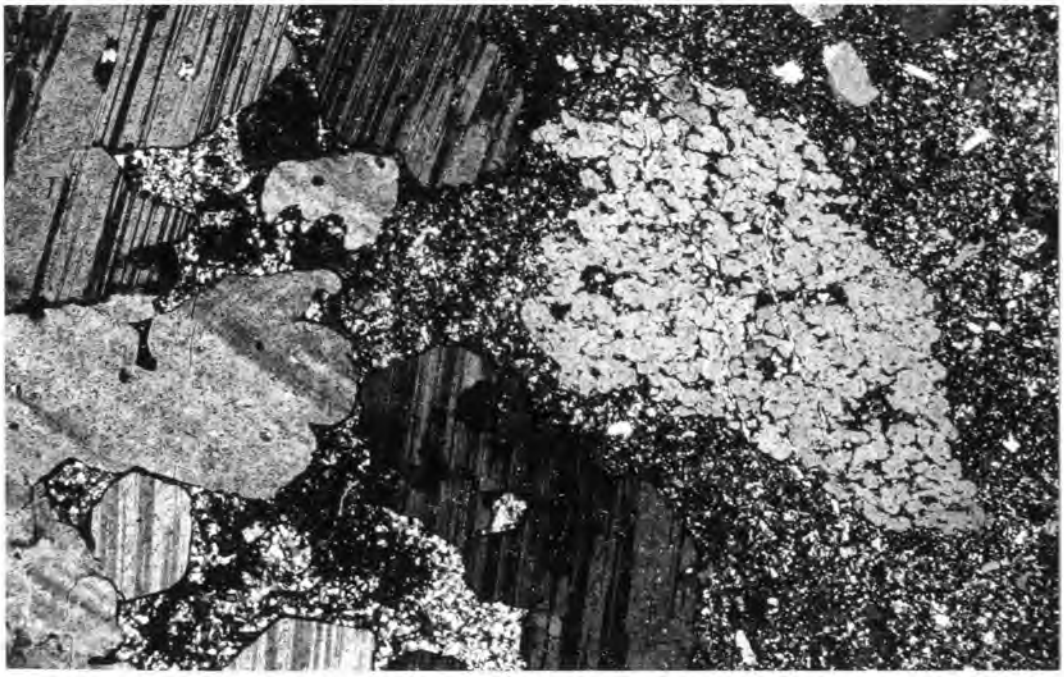

Plate XI: Partially remelted plagioclase and alkali-feldspar phenocrysts. Note the more extensive resorption features displayed by the alkali-feldspar phenocryst (pale-grey, right). Sample PM-212, Makwassie porphyries. Crossed nicols. Width of photomicrograph is 4mm.

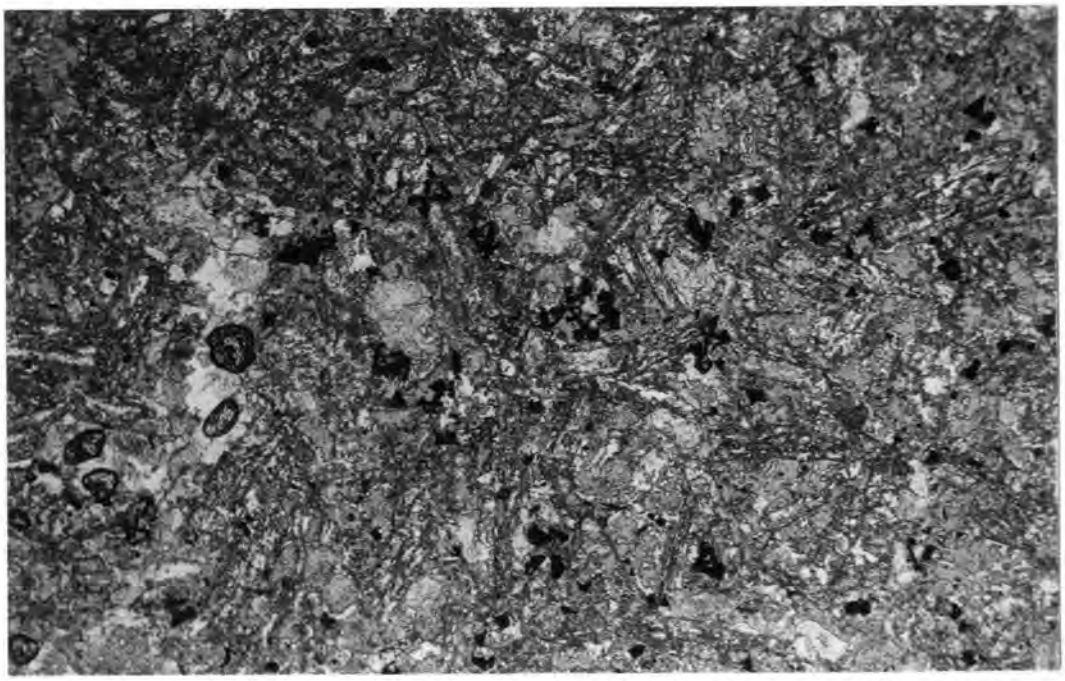

Plate XII: Typical occurrence of skeletal magnetite octahedra in the groundmass of some of the Allanridge formation lavas. Sample AR-400. Plane polarized light. Width of photomicrograph is 4mm.

VI DESCRIPTIVE CHEMISTRY OF THE WITWATERSRAND TRIAD LAVAS

A. Introduction

Chemical analyses of lavas of the Witwatersrand triad are, with a few exceptions, conspicuously absent from the literature. Wyatt (1976) has perhaps provided the most comprehensive collection of geochemical data to date, with major and trace element analyses for about 50 lavas of the Klipriviersberg Group from the area to the south of Johannesburg. A substantial proportion of these analyses represent the Meredale Member, a sequence of high-Mg lavas within the basal Westonaria Formation, which he showed to be unrelated petrogenetically to the younger Klipriviersberg formations, and which display features indicative of liquid immiscibility (Cawthorn et al., 1979; Cawthorn and McCarthy, 1977). Meredale Member lavas are not represented in the present study.

Labuschagne (1974) presented 20 major element analyses of lava samples from the lower 850m of the "Ventersdorp Group" in the East Driefontein gold mine to the west of Johannesburg. These samples represent the Klipriviersberg Group.

Apart from a small number of analyses presented by Cornell (1978) and Tyler (1979) of Ventersdorp correlates in the Prieska district and west-central Transvaal respectively, and isolated numbers of analyses interspersed throughout the earlier literature of Dominion and Ventersdorp volcanics (see T.B. Bowen, 1984) , virtually no data is available on Witwatersrand triad lavas excluding the Klipriviersberg Group. It is thus hoped that the data presented in this study will at least partially fill this void in what must be one of the major volcanic sequences in the South African stratigraphic record.

New analyses for a total of 326 samples are presented in Table I. The number of samples in each compositional group is listed below :

GROUP	NUMBER OF ANALYSES
Dominion basic lavas	72
Dominion porphyries	32
Alberton fm	19
Orkney fm	32
Loraine/Edenville fms	39
Goedgenoeg/Rietgat fms	66
Makwassie fm	17
Allanridge fm	34
Jeppestown amygdaloid	6
Intrusives	9

B. Analytical Methods

Samples were analysed by X-ray fluorescence spectrometry for major oxides by the fusion method of Norrish and Hutton (1969), with Na_2O and trace elements Ba, Nb, Zr, Y, Sr, Rb, Zn, Cu, Ni, Co, Cr, V, La, Ce and Nd being determined separately on pressed powder briquettes. Samples were crushed after removal of extraneous material in addition to the outer surface of the core in order to avoid the effects of weathering and contamination by the core barrel and storage trays. Details of the analytical procedure are documented in Appendix I.

C. Strategy Concerning the Presentation and Assessment of Data

The analyses are presented in the numerical order in which they were sampled and prefixed to indicate stratigraphic affinities. Both major and trace element data have been recalculated to exclude volatiles, and with total Fe content as Fe_2O_3, the oxidation state in which it is determined by the analytical method employed. While the normalization of

TABLE I: (11 pages following) Major and trace element analyses. Both major and trace elements are recalculated to 100% volatile free. Original totals and volatile contents are provided. All Fe was analysed as Fe_2O_3. Major elements are expressed as weight percent oxides, trace elements in parts per million. Trace element concentrations listed as 0 ppm are below detection limits. Asterisks indicate values below the lower limits of determination (LLD), but above detection limits (DL), which are half the LLD's (See Appendix I). Prefixes to the sample numbers are derived according to the following system:

GROUP	FORMATION	SYMBOL
	AR - Allanridge	AR
P - Platberg	R - Rietgat M - Makwassie G - Goedgenoeg	PR PM PG
K - Klipriviersberg	L - Loraine-Edenville O - Orkney A - Alberton	KL KO KA
J - Jeppestown	C -Jeppestown amygdaloid	JA
D - Dominion	P - Porphyries B - Basic Lavas	DP DB
	IN - Intrusive	IN

TABLE 1:(cont.)

OXIDES AND TRACE ELEMENTS RECALCULATED VOLATILE FREE, ALL FE AS FE2O3, TOTAL = ORIGINAL TOTAL:

SAMPLE:	DB- 1	DB- 2	DB- 3	DP- 4	DP- 5	DP- 6	DB- 7	DB- 8	DB- 9	DB- 10
SIO2	57.76	58.44	58.78	68.32	70.84	69.87	52.21	52.19	55.77	57.55
TIO2	1.084	1.041	1.004	0.849	0.809	0.830	0.883	0.889	0.843	1.171
AL2O3	14.58	13.85	13.66	12.74	12.50	12.65	13.29	13.08	13.09	14.46
FE2O3	11.35	11.48	11.72	7.35	5.66	6.71	12.87	13.66	11.46	10.05
MNO	0.29	0.15	0.14	0.11	0.08	0.07	0.18	0.23	0.17	0.15
MGO	3.51	3.54	3.17	2.50	1.75	1.70	7.71	10.07	9.52	4.94
CAO	7.35	6.82	6.79	2.05	1.45	2.20	10.92	6.68	7.36	5.57
NA2O	3.33	3.03	3.17	3.65	3.42	2.70	1.67	2.85	3.43	3.11
K2O	0.50	1.37	1.34	2.16	3.22	3.03	0.08	0.11	0.15	0.57
P2O5	0.255	0.265	0.257	0.271	0.278	0.243	0.191	0.194	0.180	0.421
TOTAL:	99.21	99.86	99.73	99.69	99.49	99.11	99.32	99.30	100.12	99.55
LOI	5.72	1.65	1.48	1.52	1.68	2.33	6.89	2.62	2.13	1.71
BA	204	395	484	846	853	889	25	48	77	244
NB	8.5	7.5	7.1	12.9	13.4	15.0	4.2	2.4	5.5	7.7
ZR	173	162	171	256	277	275	91	89	93	174
Y	30.1	26.9	27.7	28.9	27.3	27.1	22.7	25.0	22.7	30.2
SR	266	460	465	214	111	71	386	132	165	147
RB	11.9	51.0	44.5	56.9	81.5	114.7	1.3	2.2	1.9	9.8
ZN	125	100	103	91	87	82	107	126	99	95
CU	28	16	42	10	9	7	58	60	43	53
NI	19	23	25	12	9	12	310	446	322	125
CO	55	54	53	26	16	21	68	87	71	58
CR	5	6	12	12	2*	4	1344	1510	1290	34
V	297	261	245	106	53	87	236	257	221	230
LA	27	25	27	44	46	35	10	13	7*	21
CE	48	59	50	77	94	76	29	27	15	45
ND	28	24	28	37	40	34	17	19	11	25

SAMPLE:	DB- 11	DB- 12	DB- 13	DB- 14	DB- 15	DB- 16	DB- 17	DB- 18	DB- 19	DB- 20
SIO2	54.10	61.12	57.18	60.41	53.72	52.45	50.82	52.78	52.70	52.51
TIO2	1.323	1.684	2.076	1.596	0.787	0.758	0.744	0.682	0.660	0.641
AL2O3	15.34	11.41	13.16	12.98	14.26	13.25	13.56	14.45	16.37	14.55
FE2O3	12.69	11.45	14.78	10.94	11.32	11.57	13.93	10.48	9.78	10.43
MNO	0.16	0.10	0.18	0.16	0.14	0.16	0.18	0.18	0.14	0.13
MGO	5.21	1.48	2.43	2.99	7.26	8.86	7.83	8.27	7.36	8.53
CAO	5.56	10.67	4.17	6.03	8.06	9.44	11.13	9.62	8.25	9.52
NA2O	4.76	0.29	3.74	3.63	3.18	2.73	1.44	2.69	3.94	2.96
K2O	0.44	1.16	1.51	0.73	1.08	0.64	0.19	0.69	0.65	0.62
P2O5	0.397	0.637	0.778	0.546	0.189	0.168	0.168	0.163	0.152	0.109
TOTAL:	99.79	100.03	98.97	99.08	99.31	99.99	99.97	99.99	99.32	99.86
LOI	1.77	1.89	2.72	2.62	1.91	2.02	3.69	2.94	2.35	2.53
BA	149	549	557	176	676	406	138	273	427	213
NB	9.3	12.5	16.5	12.9	5.6	2.9	2.8	2.6	4.5	5.4
ZR	196	260	351	259	105	90	89	80	95	82
Y	33.2	44.6	54.4	41.2	22.6	21.3	23.2	17.7	20.5	18.9
SR	121	2015	179	297	462	444	523	435	564	486
RB	7.9	37.9	90.7	28.4	17.2	11.0	5.9	13.9	14.1	15.8
ZN	123	93	142	116	104	90	96	83	85	77
CU	56	34	12	32	60	55	83	70	66	67
NI	135	19	28	67	262	290	360	318	240	258
CO	67	43	53	48	69	66	75	65	58	62
CR	41	9	17	7	772	926	1197	784	548	850
V	243	291	326	270	208	209	217	194	166	191
LA	20	34	43	31	12	13	8*	8	9	12
CE	50	79	88	86	25	27	22	25	18	20
ND	29	45	52	45	18	17	16	8	14	9

SAMPLE:	DB- 21	DB- 22	DB- 23	DB- 24	DP- 25	DB- 26	DB- 27	DB- 28	DB- 29	DB -30
SIO2	56.13	57.20	54.96	62.01	70.65	56.82	53.75	57.56	58.35	57.48
TIO2	0.624	0.644	0.715	1.430	0.795	0.625	1.251	1.413	1.541	1.134
AL2O3	15.26	15.50	16.11	12.75	12.55	15.94	14.79	15.51	13.99	14.17
FE2O3	9.47	9.19	9.95	12.30	6.28	7.95	13.58	16.43	15.19	14.19
MNO	0.11	0.12	0.14	0.16	0.07	0.12	0.17	0.15	0.13	0.16
MGO	5.59	5.18	5.73	1.94	1.06	5.57	3.67	2.80	2.85	5.29
CAO	8.00	7.66	7.41	4.89	3.60	7.29	8.90	2.44	4.21	5.60
NA2O	3.62	3.49	3.74	2.85	2.89	3.50	3.01	2.90	2.81	2.99
K2O	1.04	0.84	1.04	1.20	1.88	2.00	0.59	0.83	0.69	0.66
P2O5	0.163	0.171	0.195	0.465	0.253	0.177	0.297	0.171	0.458	0.319
TOTAL:	99.58	99.72	99.75	98.55	98.99	99.16	99.11	97.87	99.13	98.54
LOI	2.03	2.09	1.96	2.72	1.29	2.08	5.08	5.14	5.32	5.25
BA	341	327	504	373	637	567	306	341	423	214
NB	4.7	4.3	4.7	11.0	13.5	3.9	8.5	11.3	10.4	6.4
ZR	117	121	133	258	297	106	202	230	237	156
Y	19.7	20.7	22.7	35.5	30.8	18.9	33.0	25.4	38.2	27.4
SR	303	530	628	406	401	593	423	134	413	280
RB	22.2	17.0	20.2	42.1	37.3	52.3	14.8	15.6	21.9	24.7
ZN	76	76	86	73	69	77	117	146	149	146
CU	75	66	52	23	12	73	56	23	33	57
NI	90	94	98	14	12	131	35	27	21	35
CO	50	49	52	48	18	54	52	68	67	63
CR	53	51	49	9	9	52	0	0	10	10
V	161	164	169	285	48	166	223	259	435	329
LA	13	15	17	42	45	14	21	18	52	23
CE	26	29	31	76	85	35	56	39	72	42
ND	19	16	18	43	38	16	30	24	43	27

TABLE 1:(cont.)

OXIDES AND TRACE ELEMENTS RECALCULATED VOLATILE FREE, ALL FE AS FE2O3, TOTAL = ORIGINAL TOTAL:

SAMPLE:	DB- 31	DP- 32	DP- 33	DP- 34	DP- 35	DP- 36	DP- 37	DP- 38	DP- 39	DP- 40
SIO2	55.68	67.18	58.44	64.02	71.41	71.65	70.04	71.04	71.61	76.74
TIO2	1.085	0.891	1.489	0.894	0.774	0.819	0.820	0.809	0.788	0.747
AL203	14.52	13.25	21.63	14.70	11.73	12.99	12.88	12.44	12.90	12.00
FE203	15.33	6.62	6.58	12.54	4.19	5.41	6.26	5.81	7.13	1.81
MNO	0.16	0.08	0.05	0.11	0.08	0.07	0.06	0.12	0.06	0.02
MGO	3.77	1.14	1.40	2.17	1.35	0.40	0.60	0.48	0.74	0.52
CAO	7.06	4.15	1.70	1.14	0.67	1.24	1.85	2.23	0.90	0.51
NA20	3.33	4.03	1.29	1.01	1.85	4.12	4.16	3.48	4.26	3.45
K20	0.77	2.35	7.14	3.10	2.69	3.03	3.07	3.31	1.36	4.14
P205	0.300	0.292	0.517	0.319	0.255	0.279	0.267	0.279	0.246	0.259
TOTAL:	98.90	98.50	98.91	99.87	99.44	99.93	99.37	97.89	99.42	99.05
LOI	3.11	3.60	3.02	3.06	2.12	1.46	1.98	2.54	1.62	0.80
BA	388	805	1121	390	430	1042	769	861	311	1207
NB	5.6	15.1	28.5	14.7	11.7	13.3	14.1	13.5	14.4	13.5
ZR	153	313	545	315	279	299	296	279	290	271
Y	29.2	30.2	60.7	33.8	27.5	29.2	30.6	28.4	31.7	24.6
SR	691	262	66	51	94	233	201	164	87	108
RB	28.6	40.8	204.4	90.9	90.4	68.2	56.1	74.5	57.5	112.0
ZN	116	86	46	145	183	58	65	83	127	51
CU	74	8	8	8	20	11	11	10	7	7
NI	38	7	16	10	11	10	9	7	10	6
CO	67	19	15	24	28	14	16	15	20	9
CR	7	0	5	2*	4	4	4	0	8	0
V	325	59	97	65	54	54	52	53	55	41
LA	25	72	21	118	40	50	52	46	48	49
CE	50	124	59	194	72	93	100	92	91	100
ND	28	54	36	77	34	40	44	38	41	45

SAMPLE:	DB- 41	DB- 42	IN- 43	IN -44	IN- 45	IN -46	DP- 47	DP- 48	DP- 49	DB- 50
SIO2	57.78	57.72	50.26	50.53	50.86	50.91	69.37	67.68	68.38	62.50
TIO2	1.324	0.539	0.459	0.423	0.433	0.462	0.749	0.766	0.744	1.045
AL203	15.43	17.38	14.40	14.37	15.01	14.85	12.65	12.83	12.76	14.67
FE203	15.09	12.72	10.27	9.56	9.51	10.10	7.53	8.16	8.74	8.65
MNO	0.14	0.16	0.14	0.14	0.15	0.15	0.09	0.11	0.18	0.16
MGO	5.02	5.03	10.58	10.19	9.67	9.06	0.70	0.50	0.26	1.94
CAO	5.80	0.79	11.07	12.57	12.19	12.05	2.02	2.87	1.90	6.47
NA20	2.72	3.95	1.02	1.54	1.43	1.58	4.01	4.39	3.33	5.14
K20	0.55	1.66	1.77	0.63	0.70	0.79	2.67	2.48	3.41	1.16
P205	0.148	0.045	0.059	0.035	0.044	0.041	0.211	0.208	0.234	0.251
TOTAL:	99.20	99.39	99.85	100.34	101.46	99.46	99.68	99.47	98.63	98.59
LOI	5.90	3.65	2.67	2.54	2.62	2.49	2.16	2.86	2.39	4.99
BA	226	214	513	108	111	130	628	492	669	788
NB	7.7	2.4	0.7	0.4	0.5	1.2	14.8	15.7	14.5	9.5
ZR	144	42	34	32	33	37	246	248	256	187
Y	28.5	6.9	17.9	16.7	16.3	17.9	35.6	36.7	32.9	29.8
SR	287	62	209	192	173	182	237	346	165	174
RB	15.9	46.4	63.0	27.6	31.0	35.1	87.8	90.1	126.8	44.4
ZN	133	118	85	59	61	73	94	116	82	76
CU	49	155	83	75	73	87	13	115	9	64
NI	19	143	246	220	192	171	12	11	9	21
CO	64	60	59	55	55	58	19	21	22	40
CR	4	164	814	1119	755	463	5	4	0	2*
V	479	237	229	225	214	234	17	20	25	173
LA	23	0	0	5*	0	4*	43	42	46	25
CE	38	0	0	0	0	0	82	83	92	51
ND	20	0	4*	0	0	15	39	38	35	26

SAMPLE:	DP- 51	DB- 52	DB- 53	DB- 54	DB- 55	DB- 56	DB- 57	DB- 58	DP- 59	DB- 60
SIO2	69.84	51.82	55.56	57.93	53.89	55.50	53.14	58.31	70.87	60.28
TIO2	0.785	0.806	1.152	1.669	0.752	0.664	0.647	0.970	0.771	0.990
AL203	12.63	12.68	14.36	12.93	13.68	14.96	14.93	14.40	12.31	13.54
FE203	6.25	12.51	11.65	12.21	10.22	8.96	9.60	10.28	5.57	10.42
MNO	0.08	0.21	0.15	0.14	0.16	0.14	0.16	0.14	0.06	0.13
MGO	0.97	11.36	4.67	2.18	7.54	6.17	7.56	3.52	1.21	3.45
CAO	2.12	7.57	7.25	7.07	10.25	9.13	9.74	3.22	1.85	7.70
NA20	4.40	2.51	3.99	3.54	2.61	3.64	2.77	2.88	1.43	1.96
K20	2.64	0.35	0.85	1.71	0.73	0.70	1.32	0.97	5.68	1.20
P205	0.265	0.184	0.363	0.619	0.170	0.144	0.128	0.315	0.260	0.320
TOTAL:	99.49	99.66	99.79	98.50	100.42	100.55	99.81	99.83	99.33	100.86
LOI	0.80	2.63	1.24	3.61	2.59	1.41	4.31	1.73	1.26	1.76
BA	589	190	271	836	369	372	542	552	1695	1011
NB	12.9	3.1	7.5	13.0	3.1	3.7	3.2	6.2	11.3	6.6
ZR	272	76	167	270	85	79	82	163	259	167
Y	29.0	18.8	30.8	41.3	19.4	18.4	19.7	25.2	25.3	26.3
SR	156	244	419	402	374	685	420	743	254	704
RB	83.9	8.8	23.4	65.3	11.2	11.0	22.9	14.5	107.1	18.3
ZN	86	168	103	142	84	74	77	91	112	89
CU	12	52	66	59	80	68	64	57	14	43
NI	10	364	86	54	513	182	242	46	12	27
CO	21	76	56	53	68	50	64	55	19	51
CR	5	1301	41	11	928	682	670	20	4	10
V	69	233	255	291	218	188	190	214	70	222
LA	47	9	20	58	8*	6	12	19	50	27
CE	85	18	50	77	17	20	21	44	91	42
ND	36	14	32	47	14	13	16	30	42	27

TABLE 1:(cont.)

OXIDES AND TRACE ELEMENTS RECALCULATED VOLATILE FREE, ALL FE AS FE2O3, TOTAL = ORIGINAL TOTAL:

SAMPLE:	DB- 61	DB- 62	DB- 63	DP- 64	DP- 65	DB- 66	DB- 67	DB- 68	DB- 69	DB- 72
SIO2	56,49	58,47	55,05	71,19	70,82	56,32	57,38	56,39	60,67	60,33
TIO2	0,603	1,435	1,210	0,749	0,783	1,155	1,172	1,138	1,958	1,849
AL2O3	15,51	12,92	15,55	12,22	12,38	14,40	14,94	14,16	11,94	11,42
FE2O3	8,53	14,02	13,09	5,56	5,58	11,56	11,68	11,76	13,03	13,58
MNO	0,12	0,16	0,22	0,07	0,07	0,17	0,17	0,14	0,14	0,14
MGO	5,75	2,60	2,12	0,61	0,64	4,61	5,94	4,69	2,28	2,29
CAO	8,66	6,63	7,97	2,46	2,31	6,18	3,65	6,33	5,24	5,18
NA2O	2,96	2,34	3,96	3,83	4,35	4,06	3,43	3,98	2,89	2,63
K2O	1,21	1,01	0,69	3,06	2,80	1,19	1,27	1,07	1,14	2,11
P2O5	0,165	0,420	0,353	0,255	0,267	0,354	0,372	0,332	0,710	0,677
TOTAL:	100,50	100,14	98,71	100,17	99,50	98,40	97,99	99,73	99,32	99,99
LOI	1,78	3,05	4,68	1,66	1,74	1,67	2,93	1,54	2,76	2,06
BA	362	536	524	877	737	415	508	386	664	688
NB	3,8	9,2	7,6	11,9	13,5	7,8	6,4	8,0	14,8	13,9
ZR	95	214	165	267	271	173	174	168	316	285
Y	19,1	34,4	30,3	27,6	28,0	31,9	29,4	31,7	48,0	44,0
SR	750	514	715	299	300	437	234	485	375	264
RB	38,4	45,3	29,6	73,3	67,5	29,4	27,4	36,1	53,5	106,2
ZN	75	106	107	73	78	111	240	108	137	149
CU	86	34	65	13	11	79	70	78	26	18
NI	108	19	37	8	11	87	96	93	28	25
CO	54	58	72	17	16	56	62	57	49	37
CR	60	4	10	4	3	42	46	52	13	10
V	174	392	350	60	53	247	274	244	312	326
LA	16	33	22	52	50	20	24	18	40	37
CE	27	72	47	98	92	40	50	45	86	85
ND	18	39	28	44	43	29	32	27	50	52

SAMPLE:	DB- 73	DB- 75	DB- 76	DB- 77	DB- 78	DB- 79	DP- 80	DP- 81	DB- 82	DB- 83
SIO2	59,41	60,46	59,97	60,74	48,79	53,20	70,60	71,32	53,12	52,92
TIO2	1,889	1,823	1,706	1,632	1,037	0,722	0,746	0,744	0,682	0,679
AL2O3	12,00	12,49	12,47	12,98	20,33	16,00	12,25	12,31	13,28	13,57
FE2O3	13,87	12,66	13,05	10,65	14,60	9,96	5,51	5,99	11,49	10,99
MNO	0,15	0,14	0,15	0,15	0,20	0,14	0,07	0,09	0,18	0,17
MGO	2,15	2,32	3,21	2,72	7,98	8,32	0,88	0,83	8,46	8,38
CAO	4,95	5,52	5,05	6,44	5,09	6,74	1,80	4,58	10,18	10,02
NA2O	3,32	2,86	2,65	2,86	2,99	3,19	2,20	2,14	2,19	2,75
K2O	1,56	1,04	1,16	1,22	0,78	1,58	5,70	1,76	0,29	0,38
P2O5	0,702	0,684	0,592	0,596	0,204	0,147	0,246	0,241	0,136	0,136
TOTAL:	99,70	98,80	99,42	99,35	99,44	99,18	99,89	99,57	99,87	101,33
LOI	2,36	2,68	3,35	4,54	4,70	2,30	0,69	1,22	3,27	2,27
BA	617	473	549	711	184	1090	1230	645	135	230
NB	14,9	12,9	13,1	12,3	5,2	5,0	13,5	13,6	2,9	3,6
ZR	300	291	278	268	109	89	267	277	80	80
Y	46,6	45,5	43,9	37,1	26,0	20,4	27,4	29,2	17,5	19,0
SR	263	530	306	510	227	242	165	565	323	391
RB	93,8	39,8	44,7	30,3	21,2	29,7	121,0	33,6	5,1	8,0
ZN	146	128	141	119	155	92	78	74	85	75
CU	32	35	30	35	56	41	9	13	64	78
NI	25	32	31	34	601	220	12	11	318	320
CO	50	53	52	44	110	62	17	18	70	67
CR	10	9	9	8	1589	734	8	5	1012	974
V	310	315	311	264	269	204	50	49	204	198
LA	38	36	31	37	8	8	45	47	8	8
CE	81	76	75	65	30	23	94	100	19	24
ND	50	47	44	47	17	14	41	43	7*	14

SAMPLE:	DB- 85	IN- 86	IN- 87	DB- 88	DP- 89	IN- 90	DB- 91	DB- 92	DB- 93	DB- 94
SIO2	58,80	51,23	52,74	57,23	71,54	51,25	52,27	56,22	51,70	55,20
TIO2	0,794	0,409	0,614	1,167	0,832	0,468	1,880	1,598	0,763	0,676
AL2O3	14,76	14,99	14,38	14,61	12,47	14,64	13,30	13,05	13,06	13,70
FE2O3	9,24	9,15	11,21	13,90	6,58	9,11	14,44	14,50	12,36	10,36
MNO	0,14	0,15	0,17	0,17	0,06	0,16	0,26	0,18	0,18	0,14
MGO	4,86	9,12	7,69	4,43	1,17	10,13	7,75	3,41	9,15	8,47
CAO	4,95	12,18	9,99	4,15	0,78	10,71	7,08	6,91	9,54	9,46
NA2O	2,55	1,67	2,33	2,55	3,70	1,80	1,92	2,74	2,50	3,08
K2O	3,69	1,07	0,80	1,50	2,61	1,69	0,11	0,84	0,57	0,78
P2O5	0,219	0,033	0,064	0,292	0,259	0,046	0,987	0,546	0,172	0,135
TOTAL:	98,65	100,80	100,62	99,40	99,56	100,58	100,00	98,75	99,54	101,02
LOI	1,74	2,08	2,08	4,32	1,18	2,46	6,82	2,81	3,54	2,46
BA	2752	265	177	426	816	1470	105	510	223	304
NB	7,3	0,1	1,2	6,4	13,8	0,7	17,2	11,6	3,6	2,0
ZR	157	28	52	169	286	34	284	257	80	75
Y	23,3	15,2	21,4	28,9	27,4	16,7	57,4	42,1	20,3	17,5
SR	334	168	168	322	143	224	216	422	343	422
RB	59,7	41,9	39,2	41,5	73,1	101,0	6,5	31,4	14,7	18,3
ZN	90	61	78	122	84	69	167	137	93	77
CU	59	74	95	38	10	68	24	43	71	41
NI	64	181	117	28	10	186	187	40	321	292
CO	50	56	59	12	17	56	71	63	79	66
CR	28	774	120	7	12	932	659	19	1158	658
V	196	212	260	334	54	236	283	302	239	205
LA	17	0	5*	29	47	4*	52	40	9	10
CE	43	0	8*	68	88	0	122	84	24	20
ND	23	0	7	32	40	5*	64	45	16	16

TABLE 1:(cont.)

OXIDES AND TRACE ELEMENTS RECALCULATED VOLATILE FREE, ALL FE AS FE2O3, TOTAL = ORIGINAL TOTAL:

SAMPLE:	DB- 95	DP- 96	DB- 97	DP- 98	DP- 99	KA-100	KA-101	KA-102	KA-103	KA-104
SIO2	56.06	71.09	56.94	70.79	71.46	56.26	57.07	55.49	57.29	55.29
TIO2	0.855	0.811	1.112	0.764	0.678	1.040	1.080	1.094	1.040	1.076
AL2O3	15.35	12.38	13.42	12.63	11.45	14.44	14.45	15.62	14.47	14.92
FE2O3	11.52	5.95	14.23	7.16	8.82	11.02	11.90	11.60	11.19	10.72
MNO	0.14	0.05	0.13	0.05	0.08	0.14	0.12	0.11	0.11	0.15
MGO	5.23	1.01	4.43	0.73	1.30	5.61	5.69	5.69	5.35	4.85
CAO	5.84	1.16	6.51	0.98	1.04	9.77	5.16	5.59	5.65	7.27
NA2O	3.44	3.37	2.86	2.56	2.76	0.67	3.70	4.09	4.08	4.00
K2O	1.30	3.93	0.21	4.34	2.22	0.91	0.69	0.75	0.66	1.54
P2O5	0.250	0.258	0.140	0.205	0.185	0.144	0.140	0.159	0.153	0.183
TOTAL:	98.98	100.14	100.42	99.43	100.15	100.74	100.50	99.95	100.76	99.65
LOI	2.33	1.64	6.58	1.78	2.41	10.35	2.99	3.47	2.83	3.51
BA	590	1019	104	853	482	1024	340	226	231	495
NB	5.4	13.6	5.5	14.5	14.0	4.9	5.1	6.2	6.3	6.2
ZR	152	275	114	244	220	113	119	126	120	124
Y	24.6	26.9	24.4	29.5	29.3	20.7	21.5	23.0	23.5	22.3
SR	539	173	282	71	54	507	278	232	245	396
RB	24.4	84.8	6.9	139.3	63.0	38.5	18.0	29.4	23.2	51.6
ZN	101	57	158	59	91	82	85	86	87	84
CU	55	11	61	15	14	85	86	88	77	107
NI	71	12	51	18	10	115	123	172	155	164
CO	62	17	67	22	21	61	58	65	61	57
CR	22	7	79	3	12	133	143	89	84	66
V	208	59	342	41	19	191	192	201	193	169
LA	21	48	21	39	39	11	5*	13	12	11
CE	47	89	36	116	79	25	28	33	28	32
ND	26	41	17	45	34	14	17	19	14	15

SAMPLE:	KA-105	KA-106	KA-107	KO-108	KO-109	KO-110	KO-111	KO-112	KO-113	KO-114
SIO2	53.96	55.46	56.70	53.85	55.80	54.30	52.31	53.26	53.20	51.77
TIO2	1.097	1.017	1.114	1.032	1.078	1.046	1.097	0.996	1.023	1.024
AL2O3	15.18	15.00	15.59	15.07	14.90	14.77	15.54	14.96	14.58	15.43
FE2O3	11.61	10.66	11.56	12.86	13.94	13.22	14.46	12.77	12.42	14.15
MNO	0.12	0.14	0.11	0.15	0.17	0.15	0.17	0.15	0.17	0.17
MGO	4.60	4.71	4.14	5.29	5.53	5.19	5.79	4.69	5.22	4.91
CAO	8.64	8.18	5.91	6.89	5.81	6.49	5.66	9.82	9.66	8.25
NA2O	3.22	3.38	4.02	3.99	3.43	3.91	3.90	2.69	2.73	2.89
K2O	1.40	1.29	0.70	0.75	1.22	0.79	0.95	0.76	0.85	1.28
P2O5	0.169	0.171	0.162	0.122	0.127	0.120	0.126	0.121	0.149	0.131
TOTAL:	100.77	100.23	99.35	100.56	100.06	99.64	100.18	100.58	98.94	100.69
LOI	2.13	3.36	3.17	1.99	2.19	2.00	2.11	1.89	2.38	2.15
BA	573	344	155	289	505	249	278	251	262	560
NB	5.1	4.9	8.1	5.6	4.2	5.6	5.4	6.6	6.8	4.0
ZR	123	117	131	105	103	104	109	98	105	101
Y	22.2	21.7	23.2	24.3	23.6	23.4	24.8	23.4	23.9	22.4
SR	493	517	147	330	532	369	282	671	497	304
RB	46.0	46.6	24.6	27.3	43.5	28.1	34.3	27.0	29.4	46.7
ZN	84	82	96	101	105	95	107	93	99	126
CU	114	108	105	104	104	113	112	119	92	64
NI	162	159	156	151	163	160	163	152	153	156
CO	64	57	63	74	75	74	79	75	66	84
CR	97	66	77	87	72	79	72	65	54	73
V	180	168	175	253	249	239	258	234	214	246
LA	10	10	17	12	9	12	8	8	8	12
CE	34	31	32	27	21	26	27	18	30	22
ND	15	12	16	12	13	13	15	10	10	15

SAMPLE:	KO-115	KO-116	KO-117	KO-118	KO-119	KO-120	KO-121	KO-122	KO-123	KO-124
SIO2	55.53	54.53	54.85	53.26	51.03	51.46	49.50	54.79	54.30	53.57
TIO2	0.991	1.025	1.015	0.931	1.068	1.022	0.940	0.934	0.879	0.887
AL2O3	13.96	14.75	14.55	15.05	15.05	14.32	16.75	14.77	14.27	14.57
FE2O3	11.47	13.23	13.16	11.78	13.90	13.31	10.01	12.35	11.83	11.62
MNO	0.14	0.14	0.14	0.13	0.17	0.18	0.10	0.18	0.16	0.14
MGO	5.29	5.77	5.44	4.80	5.74	6.21	2.53	5.39	4.58	4.50
CAO	7.49	5.67	6.02	10.66	8.13	6.48	19.61	6.82	5.89	7.65
NA2O	2.65	3.97	3.55	2.91	3.44	6.02	0.25	3.17	7.08	5.08
K2O	2.34	0.79	1.15	0.34	1.32	0.86	0.38	1.46	0.90	2.27
P2O5	0.138	0.124	0.123	0.134	0.143	0.158	0.150	0.125	0.108	0.113
TOTAL:	99.21	100.45	100.33	99.84	101.45	103.95	100.11	99.27	103.66	102.55
LOI	2.18	1.94	1.83	2.54	2.39	2.44	6.78	2.82	2.15	1.89
BA	691	392	361	148	477	358	126	494	218	1005
NB	6.0	5.5	5.2	3.1	5.6	5.6	5.1	5.1	4.2	3.9
ZR	100	103	98	91	103	100	100	97	90	91
Y	22.2	24.0	22.3	22.1	23.4	23.1	21.0	21.8	19.6	19.9
SR	356	353	303	781	504	214	266	258	174	249
RB	86.5	31.4	41.0	10.9	50.0	32.5	15.2	56.3	33.9	90.9
ZN	66	98	93	76	96	95	61	92	61	80
CU	157	103	106	65	121	77	117	96	89	91
NI	146	157	156	143	155	154	140	142	121	126
CO	64	78	71	65	70	67	55	66	58	63
CR	54	74	97	49	77	46	64	22	35	26
V	222	243	229	228	234	222	256	221	200	214
LA	10	18	12	9	11	8	12	10	11	16
CE	27	20	25	26	29	20	143	25	25	25
ND	10	15	15	12	16	11	80	11	0	15

TABLE 1:(cont.)

OXIDES AND TRACE ELEMENTS RECALCULATED VOLATILE FREE, ALL FE AS FE2O3, TOTAL = ORIGINAL TOTAL:

SAMPLE:	KO-125	KO-126	KO-127	KO-128	KO-129	KO-130	KL-131	KL-132	KL-133	KL-134
SIO2	55.61	51.87	55.34	55.06	51.11	55.65	54.10	56.19	57.24	56.31
TIO2	0.908	0.925	0.914	0.903	1.014	0.902	0.769	0.765	0.780	0.649
AL2O3	14.89	15.27	14.42	14.61	15.59	14.59	13.79	14.10	13.33	12.53
FE2O3	11.99	12.87	12.43	11.99	15.72	11.55	11.51	11.05	11.09	10.72
MNO	0.13	0.16	0.16	0.15	0.16	0.16	0.18	0.13	0.12	0.18
MGO	4.90	5.47	4.52	4.59	4.85	4.47	6.62	6.48	6.19	6.54
CAO	6.45	8.24	6.60	7.18	9.28	7.58	7.12	7.06	6.82	9.15
NA2O	3.89	3.22	3.70	3.04	3.22	2.32	3.72	3.75	3.45	3.12
K2O	1.13	1.85	1.78	2.37	0.91	2.63	2.09	0.38	0.89	0.72
P2O5	0.114	0.123	0.125	0.108	0.134	0.136	0.098	0.095	0.092	0.082
TOTAL:	101.23	100.43	100.87	100.50	99.91	99.57	100.47	100.21	100.48	99.79
LOI	1.69	1.98	1.62	1.44	2.05	2.25	1.79	2.10	1.90	2.02
BA	299	453	477	655	178	816	328	134	209	179
NB	3.2	4.5	5.3	5.6	5.7	4.6	3.2	3.5	4.9	2.0
ZR	96	96	97	97	107	97	86	85	84	68
Y	23.0	21.6	23.1	22.8	25.5	21.2	19.1	20.0	20.1	17.8
SR	263	247	251	410	207	411	64	227	141	155
RB	44.0	65.9	68.0	95.2	33.9	108.9	74.7	12.7	29.8	19.5
ZN	87	94	86	86	104	87	90	77	84	77
CU	92	96	91	97	103	91	79	78	123	71
NI	127	133	115	111	131	111	172	180	164	190
CO	64	63	63	63	72	59	64	60	64	59
CR	29	26	26	20	28	16	233	272	238	400
V	216	209	212	222	235	215	193	187	193	195
LA	10	8	10	10	10	9	9	6	8	11
CE	22	25	30	15	28	31	22	23	17	15
ND	11	12	15	9	12	9	11	13	9	10

SAMPLE:	KL-135	KL-136	KL-137	KL-138	KL-139	KL-140	KL-141	KL-142	KL-143	KL-144
SIO2	53.10	53.47	51.80	51.82	55.96	53.32	52.54	50.97	53.12	54.56
TIO2	0.487	0.655	0.665	0.694	0.700	0.533	0.571	0.627	0.612	0.616
AL2O3	10.35	13.61	14.10	15.13	14.69	11.30	11.87	13.46	12.96	13.69
FE2O3	11.88	11.83	12.28	11.94	12.15	10.99	11.69	12.06	11.46	11.20
MNO	0.18	0.16	0.19	0.20	0.17	0.21	0.18	0.18	0.17	0.18
MGO	13.62	7.28	7.71	6.84	7.55	9.91	10.60	8.33	8.32	7.59
CAO	8.29	9.54	9.72	8.46	6.91	9.44	9.21	10.55	9.31	7.18
NA2O	1.85	2.09	2.82	3.37	3.08	2.39	1.58	3.08	2.69	3.09
K2O	0.18	1.30	0.59	1.46	0.70	1.85	1.68	0.68	1.29	1.83
P2O5	0.046	0.075	0.099	0.087	0.097	0.059	0.078	0.064	0.070	0.076
TOTAL:	101.14	100.44	99.26	100.01	99.99	101.31	99.12	99.80	100.96	98.85
LOI	3.35	2.18	3.51	2.94	3.42	1.55	2.74	2.69	2.20	2.29
BA	70	403	227	644	186	468	599	208	534	641
NB	1.3	1.9	3.5	2.2	3.9	0.7*	1.7*	1.8	2.6	2.0
ZR	43	63	70	71	74	45	52	56	56	64
Y	12.5	18.5	18.2	18.4	18.1	14.6	14.9	17.4	17.6	18.8
SR	54	561	244	173	77	107	270	208	209	176
RB	8.8	60.4	22.6	45.3	20.8	55.2	79.7	20.3	56.9	78.6
ZN	78	79	107	81	98	81	76	93	74	80
CU	52	80	67	80	52	55	64	79	73	74
NI	438	206	196	166	173	281	308	221	225	220
CO	78	70	71	67	69	66	75	71	67	67
CR	2086	381	344	215	251	783	900	475	482	446
V	171	211	217	197	155	201	219	224	214	217
LA	0	10	5*	10	9	6*	4*	6*	9	5*
CE	10*	18	14	21	16	13*	9*	21	20	13
ND	0	11	0	10	6*	6*	0	11	6*	6*

SAMPLE:	KL-145	KL-146	KL-147	KL-148	KL-149	KL-150	KL-151	KL-152	KL-153	KL-154
SIO2	54.50	51.77	53.93	54.12	55.26	52.11	56.82	54.87	52.25	55.54
TIO2	0.604	0.519	0.595	0.571	0.553	0.670	0.642	0.666	0.737	0.477
AL2O3	13.76	12.72	13.07	13.51	13.68	14.80	14.24	14.73	15.38	12.73
FE2O3	11.46	11.08	11.63	11.10	11.01	11.85	10.23	10.64	12.10	10.79
MNO	0.17	0.19	0.24	0.15	0.15	0.15	0.15	0.15	0.23	0.18
MGO	7.65	12.87	7.85	7.93	8.35	7.36	5.23	6.27	7.11	10.75
CAO	9.86	7.19	7.50	8.16	8.11	8.54	6.91	7.96	6.29	7.75
NA2O	0.15	1.98	3.48	3.11	3.03	3.01	3.38	3.42	3.31	2.16
K2O	1.75	1.60	1.39	1.26	1.78	1.43	2.27	1.20	2.49	1.52
P2O5	0.071	0.078	0.083	0.071	0.068	0.082	0.131	0.105	0.102	0.070
TOTAL:	99.50	100.01	100.87	99.83	100.35	98.81	99.56	100.13	99.61	100.55
LOI	1.98	4.00	0.27	2.45	2.20	2.79	2.02	2.48	2.57	3.12
BA	251	433	249	337	866	669	735	331	680	435
NB	6.1	2.3*	1.3	2.2	1.7	1.5	2.4	1.7*	3.0	1.6
ZR	113	60	62	60	55	73	75	77	81	56
Y	23.4	12.7	15.6	17.4	15.2	20.8	18.6	17.5	20.2	14.6
SR	54	109	44	259	213	258	314	524	140	561
RB	35.1	60.4	37.6	56.2	72.8	42.2	74.3	43.8	59.5	60.5
ZN	106	118	77	76	71	80	74	79	97	92
CU	69	48	63	65	60	62	80	72	82	56
NI	230	422	209	231	223	209	145	153	163	244
CO	63	72	65	66	65	66	56	60	67	67
CR	421	1369	449	526	543	423	156	158	171	1200
V	225	190	204	209	207	213	182	197	207	156
LA	15	6*	9	7	7	6*	9	8	9	9
CE	32	8*	16	18	16	18	23	20	18	16
ND	17	0	9	6*	7	10	12	8	9	9

TABLE 1:(cont.)

OXIDES AND TRACE ELEMENTS RECALCULATED VOLATILE FREE, ALL FE AS FE2O3, TOTAL = ORIGINAL TOTAL:

SAMPLE:	KL-155	KL-156	KL-157	KL-158	KL-159	PG-160	PG-161	PG-162	PG-163	PG-164
SIO2	54.46	54.02	54.23	50.81	53.82	62.04	60.57	60.07	56.13	51.85
TIO2	0.514	0.409	0.416	0.458	0.409	1.198	1.284	1.251	1.628	1.644
AL203	13.01	10.64	10.58	11.25	10.57	13.78	13.64	14.54	13.71	14.33
FE203	10.22	10.96	10.86	12.05	11.24	9.83	9.01	9.68	11.48	11.60
MNO	0.16	0.19	0.17	0.18	0.19	0.09	0.11	0.13	0.15	0.16
MGO	11.22	13.43	14.27	14.89	14.07	5.84	4.55	5.37	6.60	6.96
CAO	6.56	8.23	7.66	8.37	7.94	2.94	4.78	3.38	5.87	8.65
NA20	2.33	1.80	1.64	1.54	1.40	2.58	3.29	2.56	2.46	2.46
K20	1.45	0.29	0.14	0.40	0.28	1.18	2.73	2.49	0.98	1.53
P205	0.084	0.052	0.042	0.060	0.066	0.520	0.540	0.535	0.795	0.815
TOTAL:	99.55	100.63	99.11	102.44	99.23	98.80	99.60	98.33	98.90	98.36
LOI	3.84	3.88	4.40	4.32	4.42	3.58	2.56	2.77	5.67	4.39
BA	430	111	49	146	120	777	1085	1010	886	806
NB	2.7	0.7*	1.1	1.6	0.0	17.4	17.5	16.6	14.2	13.5
ZR	63	38	41	45	41	302	310	313	253	254
Y	14.1	11.6	12.4	14.4	12.2	47.9	48.1	48.0	51.1	51.7
SR	445	215	137	126	180	494	351	228	401	1093
RB	52.8	11.0	4.1	9.4	5.9	27.9	60.5	60.9	23.9	35.0
ZN	78	84	114	101	112	120	112	149	141	131
CU	53	51	45	51	40	23	19	29	48	31
NI	304	385	402	344	405	96	88	93	159	162
CO	70	75	76	72	78	41	37	40	50	52
CR	1287	1935	2289	1577	1771	250	255	258	337	378
V	153	162	171	190	171	155	167	172	225	236
LA	6*	5*	6	5*	4*	51	60	55	48	50
CE	14	10*	13*	10*	9*	123	130	129	116	117
ND	5*	4*	6*	4*	0	60	59	66	66	66

SAMPLE:	PG-165	PG-166	PG-167	PG-168	PG-169	PG-170	PG-171 A	PG-171 B	PG-172	PG-173
SIO2	53.31	53.50	57.48	54.17	56.97	57.07	55.08	57.13	56.13	61.89
TIO2	1.637	1.579	1.686	1.614	1.569	1.667	1.666	1.611	1.599	1.460
AL203	13.49	14.84	14.49	14.70	13.97	15.55	15.71	14.15	15.32	13.70
FE203	12.81	11.67	10.83	12.51	10.55	10.35	9.71	10.04	9.25	7.77
MNO	0.16	0.14	0.14	0.18	0.14	0.11	0.11	0.13	0.12	0.09
MGO	7.09	6.20	5.28	7.13	5.71	5.61	3.71	3.61	3.83	2.88
CAO	6.74	6.95	5.70	5.24	6.74	4.86	7.29	8.15	7.42	6.16
NA20	2.62	3.73	3.41	2.80	3.12	3.10	3.61	3.01	3.44	3.17
K20	1.18	0.65	0.18	1.05	0.51	0.88	2.54	1.41	2.11	2.16
P205	0.760	0.742	0.793	0.799	0.735	0.805	0.792	0.765	0.794	0.715
TOTAL:	100.19	98.40	98.26	99.15	100.13	98.17	99.45	99.71	98.63	99.52
LOI	3.12	2.77	4.21	3.53	3.85	4.73	5.28	3.76	4.77	2.86
BA	522	443	172	659	584	977	1029	689	999	1131
NB	13.8	16.6	16.9	17.2	16.5	18.7	18.4	17.2	17.4	18.2
ZR	244	272	304	292	287	333	325	307	314	309
Y	50.7	51.9	55.8	51.6	50.1	56.9	58.7	51.6	50.5	45.4
SR	566	470	564	502	1022	469	555	830	587	596
RB	26.1	12.4	3.0	19.0	8.3	21.3	44.0	24.3	41.8	44.5
ZN	144	131	132	140	109	125	124	125	117	88
CU	43	33	29	36	38	41	38	36	33	42
NI	161	159	145	167	118	105	109	103	124	107
CO	53	49	48	51	46	43	44	42	45	36
CR	369	371	376	380	242	167	191	186	253	207
V	236	247	219	214	200	204	204	188	197	168
LA	53	51	58	47	54	46	65	56	60	55
CE	113	112	129	116	120	112	141	124	123	123
ND	58	60	71	59	64	60	75	65	65	63

SAMPLE:	PG-174	PG-175	PG-176	PG-177	PM-178	PM-179	PM-180	PR-181	PR-182	PR-183
SIO2	50.47	60.16	59.27	78.24	64.95	66.79	60.51	56.53	57.53	56.32
TIO2	1.733	1.431	1.399	0.254	1.122	1.172	1.300	1.434	1.280	1.440
AL203	17.27	14.83	14.57	5.91	13.97	14.21	15.38	15.39	13.66	15.74
FE203	13.65	9.20	8.62	9.05	7.79	5.75	8.83	10.69	9.84	8.86
MNO	0.16	0.11	0.12	0.13	0.08	0.08	0.09	0.16	0.10	0.11
MGO	6.26	4.22	2.86	3.85	3.38	2.08	3.69	6.52	5.79	4.14
CAO	6.09	4.03	8.12	2.03	2.21	4.52	5.45	5.33	6.61	6.78
NA20	2.69	3.14	3.02	0.09	1.31	4.04	2.99	3.03	3.41	3.35
K20	0.86	2.23	1.38	0.41	4.72	0.80	1.19	0.43	1.17	2.34
P205	0.796	0.658	0.658	0.036	0.461	0.542	0.560	0.683	0.609	0.735
TOTAL:	98.70	98.48	98.93	99.10	99.72	98.90	98.41	98.83	98.62	99.54
LOI	4.28	3.76	4.42	5.84	3.00	1.96	2.71	5.97	5.28	5.82
BA	1034	984	590	204	1670	171	1054	293	809	1291
NB	21.6	19.8	18.6	26.7	30.2	32.1	32.6	14.3	13.5	14.3
ZR	376	326	316	360	491	549	560	276	245	245
Y	61.0	48.6	46.8	57.4	62.1	73.4	66.0	42.1	39.6	44.5
SR	670	303	805	67	115	926	1270	315	585	432
RB	18.0	45.6	29.6	12.1	158.2	34.0	27.6	10.8	22.4	53.9
ZN	101	105	107	57	99	93	100	117	100	99
CU	40	30	31	10	12	13	23	27	36	33
NI	169	90	89	26	30	17	31	146	170	105
CO	54	42	39	21	23	20	29	50	50	42
CR	258	196	168	0	26	15	24	386	520	150
V	221	182	174	25	98	89	140	179	169	189
LA	64	56	56	52	73	100	94	48	47	45
CE	149	125	126	89	174	205	205	102	101	109
ND	79	61	62	35	81	94	94	53	51	55

TABLE 1:(cont.)

OXIDES AND TRACE ELEMENTS RECALCULATED VOLATILE FREE, ALL FE AS FE2O3, TOTAL = ORIGINAL TOTAL:

SAMPLE:	PR-184	PR-185	PR-186	PR-187	PR-188	PR-189	PR-190	PR-191	PR-192	PR-193
SIO2	47.50	54.51	52.79	56.45	56.96	55.72	57.43	52.23	54.41	56.38
TIO2	2.202	1.831	1.924	1.713	1.711	1.642	1.602	1.601	1.444	1.386
AL2O3	16.47	13.66	14.66	14.31	14.62	14.59	13.91	16.79	15.85	14.89
FE2O3	14.26	12.92	12.52	11.11	11.21	10.90	10.09	13.11	6.29	11.90
MNO	0.16	0.18	0.15	0.13	0.13	0.14	0.13	0.14	0.07	0.16
MGO	5.41	6.48	5.68	4.43	4.50	5.45	4.24	5.50	2.59	5.41
CAO	9.39	6.22	7.97	5.72	6.51	6.55	6.22	5.60	8.14	5.91
NA2O	3.23	2.65	2.69	3.17	2.94	4.02	3.30	3.29	5.97	2.60
K2O	0.21	0.58	0.63	2.13	0.53	0.15	2.28	0.92	1.58	0.69
P2O5	1.168	0.966	0.975	0.831	0.877	0.842	0.788	0.820	0.657	0.674
TOTAL:	99.10	98.92	99.21	99.20	98.14	98.33	99.90	98.10	98.64	99.18
LOI	6.76	3.89	6.79	5.55	4.65	2.92	3.16	5.32	6.45	6.77
BA	312	696	482	1182	398	164	1599	799	852	435
NB	19.8	17.7	21.2	19.9	19.1	21.2	20.6	18.8	20.4	17.7
ZR	321	305	334	348	355	385	363	369	387	351
Y	67.6	55.8	59.2	56.7	55.4	56.8	54.0	58.2	48.4	50.4
SR	775	740	448	291	829	813	702	963	679	562
RB	8.4	12.8	12.8	40.1	7.9	3.2	39.7	15.0	63.6	24.3
ZN	162	152	143	129	119	146	121	151	75	116
CU	58	44	41	40	47	31	36	41	39	31
NI	153	166	133	120	101	115	106	135	82	115
CO	62	60	51	48	46	46	43	56	35	48
CR	562	479	306	260	211	246	300	318	184	294
V	314	234	229	234	227	218	202	240	184	195
LA	65	56	57	66	64	60	65	64	63	53
CE	144	132	131	151	139	139	147	136	135	123
ND	78	67	71	76	68	70	74	71	63	60

SAMPLE:	PR-194	AR-195	AR-196	AR-197	AR-198	AR-199	KA-200	KO-201	KO-202	KL-203
SIO2	53.93	58.33	56.70	55.38	61.26	57.15	57.47	56.84	54.06	54.55
TIO2	1.465	1.242	1.229	1.167	1.182	1.146	1.074	0.982	1.014	0.674
AL2O3	15.48	14.35	14.70	14.88	15.66	13.80	14.42	13.92	14.82	15.97
FE2O3	10.72	12.04	11.86	15.12	10.05	11.46	11.62	12.38	13.31	11.58
MNO	0.12	0.16	0.15	0.15	0.09	0.12	0.12	0.14	0.15	0.16
MGO	7.36	3.27	2.21	4.05	3.20	4.18	4.62	4.68	5.36	6.94
CAO	7.73	5.99	8.17	5.36	3.25	6.45	6.57	6.74	6.99	7.63
NA2O	1.05	4.12	4.15	3.16	3.80	4.05	2.70	2.21	3.21	3.05
K2O	1.47	0.30	0.62	0.53	1.30	1.42	1.45	2.18	0.97	1.38
P2O5	0.671	0.207	0.218	0.198	0.210	0.228	0.161	0.127	0.127	0.075
TOTAL:	100.43	99.30	100.36	99.56	100.13	99.98	98.77	99.32	100.28	98.26
LOI	9.30	5.92	7.77	6.12	5.19	3.32	6.48	2.02	2.14	2.12
BA	385	524	259	271	362	565	1189	617	254	518
NB	20.2	10.4	10.5	10.3	10.5	7.7	5.5	4.3	4.5	3.0
ZR	367	178	180	177	180	157	124	101	105	68
Y	51.6	27.5	26.9	28.2	28.0	27.4	24.4	22.9	23.7	18.6
SR	217	723	690	802	678	1472	353	358	461	526
RB	51.2	10.7	24.2	11.8	29.3	40.0	39.8	86.9	36.4	58.6
ZN	129	115	111	138	93	94	82	89	97	77
CU	11	118	123	104	115	123	95	114	122	80
NI	115	110	106	116	113	143	163	148	151	190
CO	46	62	62	64	56	60	64	63	69	71
CR	286	10	13	14	16	20	98	57	62	390
V	213	164	180	166	164	177	199	213	221	217
LA	64	26	30	25	24	26	16	15	11	4*
CE	138	55	60	51	55	54	38	25	25	12*
ND	69	25	30	25	27	25	17	11	13	5*

SAMPLE:	KL-204	KL-205	PG-206	PG-207	PG-208	PM-209	PM-210	PM-212	PM-213	PM-217
SIO2	55.60	54.90	58.23	53.67	54.50	59.75	68.29	66.24	68.03	65.41
TIO2	0.499	0.427	1.285	1.599	1.897	1.375	1.064	1.226	1.217	1.151
AL2O3	12.42	10.53	13.96	15.60	16.10	15.48	13.09	15.19	13.91	15.74
FE2O3	10.17	10.43	10.15	11.84	12.41	8.59	6.05	6.38	5.86	7.45
MNO	0.17	0.18	0.12	0.16	0.16	0.05	0.05	0.09	0.02	0.10
MGO	9.22	12.24	5.15	6.42	5.74	3.76	0.77	1.66	1.72	1.71
CAO	7.99	8.82	5.43	6.15	5.86	2.44	2.65	2.04	2.51	4.09
NA2O	2.39	1.90	2.86	3.04	3.88	0.51	2.96	6.56	1.54	3.36
K2O	1.47	0.52	2.24	0.75	0.42	7.47	4.64	0.07	4.68	2.31
P2O5	0.073	0.060	0.564	0.782	1.029	0.584	0.436	0.545	0.517	0.478
TOTAL:	98.91	101.56	100.78	99.72	99.92	99.43	99.07	98.63	99.14	99.56
LOI	2.54	3.16	2.78	3.74	3.15	2.92	2.04	1.70	2.74	2.62
BA	419	187	745	541	395	2784	2017	25	1721	1942
NB	2.2	0.7*	16.4	14.8	18.9	36.9	28.3	34.6	33.9	28.2
ZR	66	45	315	271	317	594	476	561	527	511
Y	16.5	13.9	48.0	51.7	68.4	76.8	66.4	76.7	78.1	75.2
SR	67	256	493	672	583	191	330	203	207	888
RB	51.4	23.6	53.2	17.5	7.6	207.2	112.3	2.0	234.4	55.8
ZN	84	60	121	123	136	125	96	99	74	112
CU	52	50	49	40	42	15	11	10	13	17
NI	258	338	98	138	168	38	25	17	27	26
CO	62	69	44	50	59	25	19	20	18	21
CR	1032	1697	272	342	398	27	20	21	27	21
V	180	167	172	209	223	120	91	98	109	100
LA	10	4*	60	49	77	104	88	107	128	96
CE	15	12*	135	114	159	208	192	205	243	193
ND	11	5*	64	59	82	96	85	94	102	93

TABLE 1:(cont.)

OXIDES AND TRACE ELEMENTS RECALCULATED VOLATILE FREE, ALL FE AS FE2O3, TOTAL = ORIGINAL TOTAL:

SAMPLE:	PM-219	PM-222	PM-228	PM-231	PM-233	PR-234	AR-236	AR-238	AR-241	AR-244
SIO2	65,71	68,23	66,00	61,88	59,78	58,46	56,15	58,43	55,90	51,43
TIO2	1,249	1,082	1,068	1,341	1,187	1,346	1,322	1,193	1,251	1,228
AL2O3	14,55	13,54	12,96	16,87	14,78	14,26	15,53	14,54	14,79	14,31
FE2O3	9,86	6,04	6,42	7,70	13,11	9,91	5,09	10,15	12,46	14,47
MNO	0,12	0,10	0,09	0,08	0,15	0,13	0,25	0,11	0,18	0,22
MGO	3,28	1,70	1,06	2,51	5,22	4,71	2,02	2,28	3,55	5,38
CAO	1,84	3,85	7,93	2,64	2,01	6,61	14,66	8,29	6,83	9,14
NA2O	2,86	3,94	3,42	3,33	2,24	3,21	0,16	4,26	3,67	2,99
K2O	1,96	1,05	0,60	2,77	1,00	0,74	4,59	0,54	1,14	0,58
P2O5	0,538	0,460	0,453	0,669	0,531	0,636	0,228	0,208	0,228	0,252
TOTAL:	98,99	99,65	99,41	98,25	98,63	99,61	99,60	99,62	99,21	98,54
LOI	2,93	1,99	3,15	2,98	4,29	4,57	12,61	6,95	6,50	8,62
BA	660	337	229	1104	568	686	998	386	379	233
NB	32,8	28,8	23,6	40,1	31,0	15,9	10,1	11,0	9,9	7,2
ZR	540	489	464	678	515	341	187	179	179	174
Y	69,2	69,9	65,4	84,6	63,1	49,1	30,1	27,6	28,9	26,2
SR	178	962	2945	488	428	1395	402	874	305	342
RB	82,7	45,5	22,2	103,2	34,7	9,6	172,4	16,3	25,8	15,2
ZN	151	113	78	140	204	112	117	119	96	121
CU	14	16	28	17	10	42	130	129	125	103
NI	27	22	22	28	20	107	76	104	146	193
CO	26	16	19	19	33	42	51	54	64	64
CR	24	23	30	25	17	283	21	11	32	78
V	108	95	90	134	94	184	184	166	176	211
LA	45	94	85	140	58	63	28	30	27	31
CE	112	193	176	282	132	134	60	57	61	48
ND	65	88	83	106	61	68	31	26	29	27

SAMPLE:	DB-247	DB-251	DB-254	DB-257	DB-259	DP-261	DP-263	DP-265	DP-269	DB-273
SIO2	59,56	54,52	51,84	53,85	49,95	69,32	55,93	78,93	68,93	60,28
TIO2	1,660	0,664	0,691	0,624	1,319	0,845	1,080	0,660	0,788	1,147
AL2O3	12,45	15,89	14,76	14,37	17,25	13,17	15,11	10,93	12,63	13,70
FE2O3	12,81	9,46	12,34	9,42	17,15	6,74	11,78	2,43	7,46	15,20
MNO	0,18	0,15	0,17	0,16	0,21	0,09	0,12	0,03	0,11	0,17
MGO	3,18	6,76	7,85	8,20	5,53	1,57	5,34	0,85	0,50	2,39
CAO	6,66	7,39	8,37	9,87	4,76	1,70	5,32	0,42	2,79	4,65
NA2O	1,72	3,93	3,40	2,33	2,72	4,36	4,39	0,20	3,21	2,29
K2O	1,20	1,08	0,45	1,03	0,75	1,92	0,76	5,34	5,37	2,01
P2O5	0,567	0,166	0,140	0,138	0,362	0,286	0,156	0,208	0,219	0,168
TOTAL:	99,83	99,28	100,54	100,18	100,25	99,16	99,13	99,48	99,53	98,09
LOI	3,72	2,02	2,24	2,04	4,22	2,21	2,57	1,55	2,84	5,35
BA	951	662	232	321	278	516	475	1015	692	576
NB	11,7	3,4	2,5	2,9	8,2	12,8	16,1	11,4	14,5	5,9
ZR	258	97	85	80	172	271	353	233	245	139
Y	40,0	18,9	18,7	17,3	30,7	25,7	36,0	23,4	33,8	24,2
SR	505	441	325	465	337	159	205	43	213	244
RB	31,8	16,8	6,5	29,2	13,3	40,1	56,3	150,1	97,6	91,4
ZN	121	81	94	76	166	68	93	40	90	116
CU	31	57	77	76	6	6	9	3	9	44
NI	31	216	389	275	44	9	10	13	10	26
CO	50	57	69	61	78	19	17	10	18	61
CR	10	299	883	746	5	3	2*	9	3	0
V	281	180	201	182	402	76	59	50	26	387
LA	51	13	8	11	29	38	50	27	47	25
CE	80	27	21	25	60	77	97	51	88	51
ND	45	12	8	7	27	35	42	22	55	18

SAMPLE:	DP-276	DB-278	DB-281	DB-285	DB-286	DP-288	KA-291	KO-295	AR-300	AR-304
SIO2	73,65	55,35	52,78	55,49	56,56	69,39	56,60	55,55	61,89	60,38
TIO2	0,322	1,252	0,671	0,818	1,413	0,814	1,047	1,074	1,222	1,271
AL2O3	12,70	15,79	14,39	15,69	14,31	12,57	15,39	14,66	14,36	14,80
FE2O3	5,04	11,28	10,65	9,85	14,26	6,39	11,74	13,47	9,75	7,64
MNO	0,07	0,18	0,16	0,14	0,18	0,09	0,12	0,15	0,12	0,13
MGO	0,68	5,93	8,53	5,20	3,20	0,94	5,07	5,23	3,64	2,88
CAO	0,98	5,01	9,81	7,88	6,02	3,46	5,23	5,52	2,80	5,60
NA2O	3,14	3,99	2,51	3,22	2,90	3,36	3,92	3,34	2,81	3,62
K2O	5,09	0,83	0,55	1,48	0,81	2,72	0,74	0,90	3,18	3,46
P2O5	0,125	0,383	0,151	0,258	0,344	0,259	0,140	0,124	0,220	0,227
TOTAL:	99,41	98,10	100,47	96,24	98,76	98,98	100,53	99,35	99,69	98,69
LOI	1,86	1,86	2,11	1,64	3,06	3,38	3,48	2,89	3,52	4,96
BA	370	416	230	837	501	625	304	233	707	741
NB	14,8	8,1	3,3	3,4	8,3	13,4	3,5	3,4	11,9	12,2
ZR	269	185	76	150	223	272	122	110	187	193
Y	24,4	33,8	17,7	24,8	34,5	28,7	21,4	21,3	23,1	24,3
SR	89	203	428	607	409	275	360	197	71	95
RB	102,5	11,6	12,9	26,5	14,0	73,4	25,8	31,9	69,3	75,1
ZN	51	132	84	91	140	80	92	105	84	64
CU	13	48	71	67	39	5	74	68	10	5
NI	8	115	292	71	25	9	167	161	113	96
CO	11	61	63	53	62	20	59	76	57	47
CR	5	47	601	29	0	0	81	60	18	4
V	21	276	199	210	372	73	180	208	179	147
LA	52	22	6	19	31	43	14	9	14	16
CE	95	55	22	50	69	83	23	23	37	38
ND	38	31	7*	22	34	35	10	7	18	19

TABLE 1:(cont.)

OXIDES AND TRACE ELEMENTS RECALCULATED VOLATILE FREE, ALL FE AS FE2O3, TOTAL = ORIGINAL TOTAL:

SAMPLE:	AR-305	AR-307	PG-312	PG-314	PG-316	PG-319	PG-322	PG-325	PG-328	PM-329
SIO2	56,00	57,97	59,07	50,68	65,42	57,89	59,32	56,96	60,06	54,93
TIO2	1,295	1,201	1,292	1,732	1,289	1,281	1,364	1,530	1,267	1,729
AL2O3	14,79	14,27	14,15	19,44	13,48	13,95	15,14	13,57	15,34	18,55
FE2O3	14,04	10,00	11,59	14,50	8,10	9,99	9,87	11,01	8,68	10,18
MNO	0,13	0,16	0,14	0,12	0,14	0,18	0,16	0,14	0,11	0,12
MGO	4,78	4,95	5,54	4,60	2,35	3,97	5,61	6,66	4,46	4,07
CAO	2,43	6,23	4,28	2,76	4,99	7,03	3,08	5,62	4,38	3,16
NA2O	2,78	3,45	2,72	3,00	2,81	2,54	4,11	3,19	4,38	2,93
K2O	1,58	1,50	0,87	2,63	2,87	2,62	0,81	0,57	0,73	3,64
P2O5	0,176	0,266	0,551	0,748	0,541	0,550	0,542	0,754	0,591	0,687
TOTAL:	99,85	98,33	99,92	98,60	98,73	98,75	98,42	97,62	99,23	97,08
LOI	3,87	4,84	5,83	4,25	2,10	3,22	2,87	2,56	2,86	2,90
BA	501	349	865	1042	1198	1475	522	549	413	2147
NB	9,5	7,6	18,4	32,6	24,4	18,1	22,8	18,0	21,5	45,8
ZR	180	185	355	705	493	323	425	297	410	748
Y	22,2	28,9	50,1	93,5	64,2	48,5	54,4	52,2	54,6	92,9
SR	53	451	421	380	775	851	414	491	525	523
RB	33,8	24,6	24,4	103,0	67,3	56,6	21,8	15,6	13,8	132,7
ZN	116	103	136	174	100	114	110	130	102	139
CU	7	41	12	15	11	28	18	11	12	17
NI	162	198	70	59	33	94	60	161	55	57
CO	72	63	40	39	26	43	38	47	33	51
CR	21	128	171	100	68	253	213	442	120	39
V	197	208	189	253	151	181	158	219	182	157
LA	14	24	65	90	93	62	51	49	81	123
CE	41	57	136	196	199	126	121	113	163	265
ND	20	29	64	96	93	60	58	60	75	119

SAMPLE:	PM-332	PM-335	PM-338	AR-339	AR-341	AR-343	AR-345	KA-346	KA-347	KA-348
SIO2	66,91	68,75	67,40	59,05	55,76	52,42	57,15	52,56	58,13	53,26
TIO2	1,090	1,116	1,082	1,190	1,332	1,174	1,071	1,129	1,005	1,078
AL2O3	13,24	12,75	13,61	14,42	14,67	14,27	14,91	14,87	14,13	15,13
FE2O3	6,76	6,60	6,13	9,93	11,70	12,76	11,82	12,51	10,10	12,27
MNO	0,14	0,07	0,08	0,18	0,14	0,16	0,15	0,14	0,14	0,13
MGO	1,56	0,76	2,42	3,35	4,03	4,91	4,81	7,29	4,89	5,16
CAO	2,94	2,53	3,93	8,06	7,35	9,36	5,37	8,24	6,43	8,13
NA2O	3,30	3,16	2,79	1,18	3,78	4,06	3,93	2,04	4,46	3,80
K2O	3,56	3,78	2,10	2,41	0,97	0,65	0,58	1,07	0,58	0,87
P2O5	0,462	0,468	0,459	0,225	0,271	0,241	0,224	0,152	0,137	0,165
TOTAL:	99,92	100,18	100,51	99,16	100,07	101,05	98,79	101,77	100,21	100,72
LOI	2,06	1,85	3,62	8,74	6,43	5,06	3,58	10,11	2,25	2,23
BA	1350	1310	509	509	208	349	347	445	204	391
NB	28,8	31,9	30,4	11,4	9,0	7,3	6,5	2,0	5,2	6,4
ZR	478	468	452	178	178	168	167	60	108	118
Y	67,9	67,9	63,9	28,3	25,3	28,3	24,4	17,7	20,7	23,7
SR	493	202	224	209	283	606	499	280	257	588
RB	88,0	91,2	85,5	98,5	23,9	17,4	17,4	87,7	11,7	26,7
ZN	104	87	91	96	127	93	135	81	67	103
CU	10	10	8	114	92	50	57	70	77	122
NI	22	23	20	102	176	184	165	211	101	167
CO	20	19	18	56	78	71	71	69	54	63
CR	11	17	20	18	48	57	55	413	124	64
V	96	106	106	167	215	201	195	211	179	171
LA	93	84	70	25	23	23	24	11	13	11
CE	191	177	140	51	51	42	51	17	25	34
ND	88	79	68	22	26	26	27	8	13	16

SAMPLE:	KA-349	KA-350	KO-352	KO-355	KO-356	AR-359	AR-360	AR-361	AR-362	AR-363
SIO2	55,12	54,83	54,75	53,50	50,88	57,76	53,96	55,38	55,09	54,18
TIO2	0,973	1,092	0,984	0,919	0,925	1,240	1,241	1,321	1,181	1,102
AL2O3	15,54	14,98	14,62	15,10	15,77	14,38	15,06	14,14	14,15	13,39
FE2O3	10,83	11,12	12,45	13,37	11,07	9,93	13,16	12,89	11,75	12,04
MNO	0,13	0,15	0,15	0,18	0,11	0,13	0,18	0,13	0,14	0,16
MGO	4,41	4,82	4,65	5,79	3,57	3,12	5,00	4,71	4,98	5,32
CAO	7,43	6,41	7,42	6,21	5,17	7,71	5,93	6,55	8,13	8,75
NA2O	4,57	3,67	3,52	3,21	3,64	3,44	4,11	2,80	3,26	3,54
K2O	0,84	2,77	1,32	1,61	0,75	2,08	1,14	1,80	1,06	1,47
P2O5	0,144	0,169	0,132	0,106	0,114	0,207	0,220	0,282	0,259	0,241
TOTAL:	101,66	102,31	100,51	101,55	101,62	100,63	100,97	100,22	99,55	99,73
LOI	1,94	2,18	1,96	2,42	2,57	5,56	4,22	6,20	5,09	4,79
BA	255	730	408	1208	164	649	550	555	255	396
NB	5,8	6,0	2,9	4,0	4,1	10,6	9,6	8,7	8,7	5,5
ZR	116	120	97	96	96	183	180	194	176	170
Y	23,3	24,4	22,2	19,6	19,1	25,1	26,5	31,6	26,0	27,7
SR	244	332	466	317	128	426	311	122	519	579
RB	24,5	86,8	52,5	57,4	22,1	57,1	34,0	24,6	14,2	20,2
ZN	94	84	94	104	67	99	125	106	98	106
CU	92	97	99	77	16	104	118	97	83	90
NI	100	152	139	148	126	112	128	164	209	220
CO	61	62	63	69	47	54	73	67	69	67
CR	64	66	59	25	29	15	17	53	147	176
V	171	186	225	235	188	164	187	207	201	195
LA	14	19	11	11	10	23	23	23	25	20
CE	33	34	23	27	25	55	47	50	51	53
ND	16	17	13	13	12	26	25	27	26	28

TABLE 1:(cont.)

OXIDES AND TRACE ELEMENTS RECALCULATED VOLATILE FREE, ALL FE AS FE203, TOTAL = ORIGINAL TOTAL:

SAMPLE:	AR-364	AR-365	JA-366	JA-367	JA-368	JA-369	JA-370	JA-371	KA-373	KA-376
SIO2	57.10	57.86	64.68	64.52	66.82	65.09	65.58	50.22	55.74	52.77
TIO2	1.135	1.002	0.998	1.046	1.042	1.026	1.017	1.670	1.015	1.174
AL203	14.05	14.37	12.92	12.50	11.94	12.94	12.88	19.57	14.36	16.66
FE203	9.66	10.49	11.46	11.69	12.65	11.92	11.28	16.75	10.59	12.23
MNO	0.11	0.13	0.13	0.17	0.17	0.17	0.16	0.26	0.17	0.16
MGO	4.32	3.37	0.84	0.86	1.09	0.86	0.89	1.61	4.66	4.66
CAO	7.05	6.70	3.27	3.25	2.90	3.37	1.96	3.26	9.05	6.81
NA2O	4.03	3.77	3.65	4.20	2.72	3.61	3.84	4.20	3.43	3.39
K2O	2.27	1.99	1.33	1.45	0.15	0.51	1.90	1.59	0.86	1.97
P2O5	0.248	0.231	0.503	0.504	0.512	0.517	0.496	0.869	0.140	0.172
TOTAL:	101.00	101.34	99.51	99.82	98.31	98.58	100.17	98.88	99.79	98.45
LOI	3.52	5.82	2.40	2.29	2.52	2.91	2.07	3.20	2.42	5.54
BA	556	360	554	644	122	363	840	1210	403	555
NB	7.9	8.8	14.2	16.1	15.7	14.4	15.2	23.4	6.1	6.0
ZR	179	177	235	241	255	247	233	383	114	137
Y	26.4	25.8	51.7	52.1	54.3	51.4	46.8	72.3	22.1	22.4
SR	636	386	594	219	194	554	211	487	929	249
RB	28.6	24.0	48.2	66.8	4.3	12.1	55.5	34.5	26.7	63.7
ZN	90	84	161	155	164	164	160	232	79	95
CU	103	56	23	30	13	21	22	26	78	59
NI	121	133	13	14	15	11	12	18	113	173
CO	52	55	26	29	29	29	24	37	51	59
CR	50	57	9	6	3	6	9	8	115	86
V	189	202	15	18	18	17	17	27	172	188
LA	24	24	42	43	40	47	41	59	6	13
CE	50	60	87	88	90	98	81	124	23	32
ND	26	27	47	46	46	48	41	57	10	12

SAMPLE:	KL-382	KL-392	PR-395	PR-398	AR-400	AR-403	PG-406	PG-417	IN-419	IN-421
SIO2	54.47	53.56	48.52	56.06	55.60	54.32	59.06	56.70	49.28	58.73
TIO2	0.500	0.505	1.654	1.531	1.167	1.167	1.425	1.501	1.834	1.402
AL203	12.79	14.50	15.99	14.17	14.77	14.38	13.85	13.39	14.95	13.42
FE203	10.86	11.08	9.14	11.13	11.58	14.70	10.07	11.05	16.29	10.00
MNO	0.17	0.17	0.24	0.18	0.19	0.16	0.13	0.17	0.18	0.16
MGO	9.00	8.83	7.19	5.09	4.59	5.57	5.74	6.00	6.51	4.26
CAO	8.04	6.88	12.68	6.97	9.93	6.77	4.33	6.19	6.86	5.56
NA2O	2.15	3.05	3.38	2.48	2.02	1.50	2.25	2.83	3.33	3.48
K2O	1.95	1.36	0.50	1.66	1.88	1.22	2.58	1.50	0.46	2.35
P2O5	0.071	0.070	0.687	0.713	0.277	0.224	0.579	0.677	0.293	0.606
TOTAL:	101.17	98.95	98.24	98.82	98.54	98.55	98.99	98.03	100.18	99.55
LOI	2.34	3.17	10.65	6.76	9.59	9.78	5.82	3.31	2.60	1.74
BA	297	384	213	899	261	104	1005	821	231	845
NB	1.4*	0.0	19.6	16.4	6.6	9.2	18.7	14.9	6.7	18.7
ZR	59	66	336	288	181	180	286	276	159	348
Y	15.9	15.5	59.3	52.3	28.1	27.6	46.5	49.9	47.3	51.1
SR	217	144	266	986	524	207	374	759	484	616
RB	89.6	36.0	15.9	30.3	54.1	39.7	88.8	35.2	8.8	46.5
ZN	74	117	100	127	108	109	143	115	118	82
CU	53	49	3	34	57	97	28	27	85	62
NI	216	202	192	134	214	124	150	136	92	88
CO	66	65	51	48	67	70	46	49	60	43
CR	584	503	542	347	49	189	457	374	233	277
V	178	179	199	221	226	211	181	207	331	159
LA	7	8	49	53	21	21	49	46	9	56
CE	14	13	105	118	57	54	113	103	28	124
ND	6*	4*	58	61	29	20	56	57	18	62

SAMPLE:	PG-426	PG-433	AR-442	AR-446	AR-451	KA-452	KA-455	KO-457	KO-460	KO-462
SIO2	55.85	54.54	53.96	58.88	58.44	53.91	54.76	56.09	54.26	54.11
TIO2	1.614	1.580	1.498	1.076	0.891	1.046	1.081	1.008	0.951	0.946
AL203	14.06	16.78	16.66	14.67	14.37	13.76	15.21	13.69	14.89	14.95
FE203	10.67	10.46	12.58	10.64	8.11	12.30	11.84	13.35	12.14	12.94
MNO	0.17	0.09	0.17	0.15	0.14	0.15	0.14	0.16	0.13	0.15
MGO	5.50	5.62	5.17	4.02	4.49	6.57	4.50	5.54	5.17	4.91
CAO	6.02	5.16	5.60	4.62	6.95	9.52	7.07	5.92	6.62	5.99
NA2O	2.63	4.46	3.76	4.03	4.05	2.23	3.24	3.18	4.13	2.98
K2O	2.71	0.70	0.50	1.68	2.41	0.38	1.99	0.92	1.57	2.40
P2O5	0.762	0.635	0.278	0.237	0.164	0.139	0.163	0.125	0.123	0.121
TOTAL:	96.06	98.04	98.81	98.37	99.32	101.56	99.30	100.66	98.96	99.37
LOI	3.33	4.83	6.02	3.14	3.46	4.15	1.76	2.00	1.70	1.95
BA	1201	391	213	741	924	241	638	348	293	835
NB	17.2	28.6	8.1	8.7	6.6	4.0	5.6	6.5	4.6	4.7
ZR	309	515	191	177	141	106	122	100	101	100
Y	49.1	66.1	30.8	26.1	22.5	22.0	25.3	23.1	22.5	23.2
SR	527	430	532	393	451	566	512	258	213	190
RB	71.1	15.0	13.0	38.2	52.8	10.1	68.5	36.6	61.3	111.9
ZN	119	102	136	99	52	73	84	90	85	96
CU	27	18	5	08	95	109	105	79	45	105
NI	154	98	226	145	104	226	162	152	146	138
CO	49	41	82	66	49	64	65	69	64	66
CR	446	277	66	61	145	415	85	63	68	27
V	227	186	252	192	187	194	179	236	221	238
LA	53	70	20	43	21	14	15	10	11	10
CE	126	156	44	53	41	27	34	20	31	27
ND	66	75	23	22	17	14	15	9	16	17

TABLE I:(cont.)

OXIDES AND TRACE ELEMENTS RECALCULATED VOLATILE FREE, ALL FE AS FE2O3, TOTAL = ORIGINAL TOTAL:

SAMPLE:	KL-465	KL-467	KL-468	KL-469	KL-471	PR-472	PR-474	PR-476	PR-477	PR-479
SIO2	55.52	56.34	52.81	54.78	56.61	56.14	56.59	61.59	58.92	58.24
TIO2	0.878	0.736	0.400	0.637	0.599	1.667	1.264	1.350	1.427	1.355
AL2O3	14.31	14.47	8.59	14.92	17.75	17.01	13.54	14.46	14.49	13.74
FE2O3	11.98	10.90	12.17	11.08	10.55	10.96	10.15	7.38	10.15	10.32
MNO	0.14	0.14	0.17	0.18	0.12	0.13	0.14	0.07	0.10	0.15
MGO	4.10	5.53	17.46	6.65	4.37	2.96	5.54	3.04	4.83	5.19
CAO	7.77	7.90	8.06	6.54	2.66	4.01	6.97	5.19	5.56	6.22
NA2O	3.40	3.09	0.19	3.61	4.30	4.23	2.74	3.74	3.20	2.49
K2O	1.70	0.82	0.11	1.53	2.92	2.24	2.52	2.59	0.68	1.72
P2O5	0.118	0.081	0.039	0.077	0.125	0.657	0.540	0.595	0.670	0.590
TOTAL:	100.06	100.83	99.59	99.56	100.81	100.86	101.68	100.88	99.19	100.31
LOI	1.25	2.08	4.95	3.71	3.88	3.03	4.08	4.07	4.53	4.35
BA	457	262	16	235	376	1054	987	1481	482	703
NB	3.6	3.4	1.2	5.3	3.5	33.3	15.1	24.0	16.1	17.7
ZR	97	78	34	63	84	750	288	421	283	311
Y	22.3	20.6	10.4	16.1	19.9	85.7	50.3	52.1	48.2	49.1
SR	400	498	20	90	173	328	741	367	664	545
RB	66.6	25.2	7.6	43.4	80.2	64.6	67.9	66.1	15.5	41.7
ZN	84	73	76	80	70	101	107	88	115	110
CU	19	88	43	65	113	10	37	12	18	23
NI	108	123	516	180	163	25	165	103	144	124
CO	58	57	88	64	58	29	46	36	46	40
CR	21	186	4618	336	437	17	421	302	457	432
V	221	206	178	224	215	158	196	159	201	187
LA	12	5*	0	5*	15	113	58	75	49	57
CE	24	19	8*	20	29	169	127	166	109	124
ND	12	10	0	10	13	84	61	81	58	61

SAMPLE:	PR-480	PR-481	PR-483	PR-484	PR-485	PR-486	PR-487	PR-489	PR-491	PR-492
SIO2	56.72	56.53	58.06	55.32	55.20	55.80	59.85	59.56	59.29	59.82
TIO2	1.486	1.426	1.241	1.469	1.513	1.377	1.435	1.381	1.376	1.744
AL2O3	15.33	14.73	13.96	13.62	13.78	12.02	13.65	13.96	14.02	13.68
FE2O3	9.98	11.59	10.12	11.03	11.78	11.99	8.54	9.55	9.92	10.17
MNO	0.11	0.12	0.13	0.15	0.16	0.18	0.13	0.13	0.13	0.14
MGO	4.39	7.90	4.04	6.05	5.49	8.20	3.75	3.90	3.90	2.87
CAO	6.04	3.92	6.76	7.67	6.91	6.66	7.56	6.20	5.45	6.12
NA2O	3.31	2.92	2.05	1.90	2.88	1.93	3.30	2.62	2.95	2.75
K2O	1.98	0.17	3.10	2.14	1.57	1.24	1.03	2.09	2.34	1.91
P2O5	0.665	0.693	0.544	0.655	0.718	0.625	0.752	0.602	0.624	0.801
TOTAL:	100.48	98.72	100.20	101.03	99.68	99.21	100.41	98.78	100.31	100.66
LOI	5.45	3.64	5.00	3.10	5.87	2.93	2.92	3.51	3.73	5.82
BA	1025	83	1202	929	992	477	788	991	987	913
NB	19.6	14.6	16.8	14.8	14.5	14.7	16.8	17.2	19.6	25.6
ZR	349	299	310	276	273	244	318	350	354	426
Y	51.4	45.1	48.6	48.5	51.1	45.4	53.4	51.4	51.0	62.4
SR	488	291	537	529	460	400	955	837	1045	607
RB	49.1	3.2	78.3	50.1	33.1	24.3	23.0	45.4	38.8	34.3
ZN	124	116	111	114	126	123	78	104	109	104
CU	21	9	34	57	44	34	39	30	35	39
NI	92	165	92	157	139	220	66	78	89	50
CO	47	57	45	50	53	58	35	41	39	35
CR	257	546	241	462	415	936	126	252	276	55
V	195	218	169	199	223	195	183	170	168	233
LA	58	48	57	52	52	44	65	59	61	77
CE	142	122	124	106	113	98	136	128	133	163
ND	66	62	60	55	62	51	70	62	63	81

SAMPLE:	PR-494	AR-495	AR-496	AR-497	AR-498	AR-500
SIO2	51.80	52.68	53.74	51.76	56.77	56.74
TIO2	1.775	1.276	1.201	1.210	1.146	1.018
AL2O3	14.13	16.37	15.35	15.75	15.16	14.29
FE2O3	13.37	12.73	12.23	13.67	11.41	11.16
MNO	0.17	0.11	0.13	0.16	0.14	0.18
MGO	5.31	5.06	4.07	5.78	5.61	4.96
CAO	7.63	7.49	9.17	7.76	5.64	5.86
NA2O	2.47	2.34	2.46	3.34	3.52	5.29
K2O	2.47	1.78	1.38	0.34	0.37	2.29
P2O5	0.879	0.266	0.264	0.229	0.233	0.220
TOTAL:	100.87	99.13	99.54	100.12	98.70	100.38
LOI	10.47	8.60	12.88	7.72	5.06	3.36
BA	580	416	175	97	202	705
NB	16.9	8.4	7.8	7.4	8.1	8.1
ZR	300	192	182	181	189	159
Y	54.8	32.1	28.7	24.2	32.0	28.0
SR	555	403	196	242	553	539
RB	66.5	58.8	48.2	10.9	5.7	31.8
ZN	152	117	97	106	105	93
CU	41	182	129	137	95	88
NI	166	210	157	215	166	97
CO	50	71	63	64	69	56
CR	426	61	51	213	56	83
V	253	265	258	242	208	188
LA	51	21	27	16	25	23
CE	118	53	57	46	50	52
ND	62	30	29	22	27	27

trace element data is not usually employed in the literature, it is considered to be more compatible with the major element data in this form in view of the hydrated nature of the secondary mineral assemblage as well as the strongly carbonated nature of a few extremely altered samples, for which volatile loss may be up to 10 wt%. The volatile-free data is thus considered to be more representative of the original liquid composition. Although space limitations have prevented the presentation of the original analyses inclusive of volatiles, the original totals as well as the wt% loss of volatiles on ignition at 1000°C (L.O.I.) are provided in Table I to enable recalculation back to the original form.

In the following sections, variation diagrams are presented for all oxides and trace elements using Zr as the abscissa in place of the more common indices of differentiation such as MgO, Differentiation Index, Mg-number etc. The reasons for this are:

(a) Zr is widely recognised as behaving in a typically incompatible fashion over a broad compositional range as a result of its high field strength (charge to mass ratio).

(b) For the same reason, Zr is generally not transported in aqueous fluids (Pearce and Norry, 1979) and is thus widely regarded and, indeed, has been shown to behave as an immobile element during most processes of secondary alteration and low grade metamorphism (e.g. Winchester and Floyd, 1977; Floyd and Winchester, 1975; Pearce and Norry, 1979; Finlow-Bates and Stumpfl, 1981).

(c) It commonly occurs in concentrations ideally suited to X-ray fluorescence analysis, and precise determinations are thus readily obtainable.

Before any petrogenetic interpretations are made, it is essential that the effects of secondary alteration, metamorphism or possible pervasive regional metasomatism, as proposed by Cornell (1978), be assessed in order to establish whether the data, in terms of magma compositions, have been invalidated by mobilization of some elements. Assuming then that Zr is immobile during post-solidification processes, its use as the abscissa in the succeeding diagrams serves a dual purpose, firstly as an index of

differentiation and secondly as a means of evaluating qualitatively the degrees of mobility of the other elements by observing the coherency of the variation and the degree of scatter within coherent trends. This is only valid if it is assumed that the variations are caused by simple magmatic processes resulting in continuous, rational trends. In addition the risk of masking real magmatic trends by the use of a differentiation index which may be susceptible to secondary processes is avoided. A brief digression may be in order at this stage to justify the above strategy in terms of the relevant literature.

In order to overcome the problem of mobilization of elements due to hydrothermal alteration and metamorphism of volcanic sequences, various approaches have been adopted by different workers. Perhaps the most widely used approach has been to avoid the use of highly altered samples altogether by rejecting samples which fail to meet certain criteria established to suit the requirements of a particular study, as suggested by Irvine and Baragar (1971). Reid (1979) for example, in a study of Precambrian metavolcanics of the Haib Supergroup in Namibia, avoided samples which could be observed to be excessively altered in hand specimen, or which displayed a penetrative schistosity, were substantially veined or contained a high proportion of combined water.

Another approach, devised by Beswick and Soucie (1978), makes use of molecular ratio plots from which mobile oxides may be isolated by comparison with standard trends produced by a representative number of unaltered Mesozoic lavas of wide compositional range. Theoretically this procedure enables one to correct back to the original composition, the assumption being that the original composition does lie on the standard trends. Davies et al. (1979) adopted a modified version of this approach for Archaean volcanics of the Timmins mining area, Ontario, using Cartesian molecular ratio plots with a known mobile oxide as the common denominator. By using various combinations of oxides they were able to establish which were mobile by isolating those producing deviations from the straight line which would be expected had both numerators been immobile. A basic assumption of this method is that the variation of the mobile denominator is almost entirely a result of secondary remobilization and that primary compositional variations are small.

Another method is to compare analyses of fresh and altered portions of a

sample, or by comparing similar but progressively more altered samples from the same sequence and preferably from the same flow, as suggested by Floyd (1976). Such an approach is useful when the type of remobilization is in the form of relatively small-scale metasomatic migration of certain elements giving rise to easily recognisable "alteration regimes", such as those described by Smith (1968), and Smith and Smith (1976), in Ordovician volcanics of New South Wales, Australia, and Morrison (1978) in Paleocene basalts from northwest Scotland. Alternatively petrogenetic interpretation may be restricted to those elements which are known to remain relatively immobile during secondary processes, such as Zr, Ti, Y, Nb and certain rare earths, which have been used for purposes of classification (Winchester and Floyd, 1977), identification of tectonic setting (Pearce and Cann, 1973; Floyd and Winchester, 1975) and petrogenetic modelling (Pearce and Norry, 1979).

The strategy adopted in this study has been of a more empirical nature, although many aspects of the abovementioned works have been taken into consideration. Thus the basis of sampling was such that the more altered, fractured and veined material was avoided, and while this did not eliminate highly altered samples of homogeneous outward appearance, these are relatively few in number and provide a good indication of the extremes of secondary compositional modification which may be expected. L.O.I. contents of analyzed samples fluctuate considerably but different levels characterize different formations, a possible result of original chemistry and texture, and a cut-off level would thus be difficult to apply. Strongly carbonated samples are reflected in excessive L.O.I. levels (up to 10%) due to loss of CO_2. While the recognition of alteration regimes is difficult as samples were taken from borehole core and not from laterally extensive outcrops, different types of alteration have nevertheless been observed petrographically, with some samples being epidotized and others carbonated, and these features may imply the presence of such regimes. This being the case, a large proportion of the chemical modification can be regarded as a closed-system metasomatic redistribution of elements. Real magmatic trends should thus be defined by the average trends of a statistically large enough sample population taken over a large enough area, depending on the scale of the alteration regimes. However, if the degree of scatter exceeds the degree of magmatic variation, the original trend will be obliterated. The use of the molar-ratio techniques of Beswick and Soucie (1978) and Davies et

al. (1979) have been avoided, since dangers inherent in applying their basic assumptions to the Witwatersrand triad lavas are considered to outweigh their usefulness.

In the following sections, the relative mobilities of elements along with their variation trends are described and it will be demonstrated that petrogenetic interpretation need not be restricted to the immobile trace elements, which nevertheless will be used as the basis for the interpretation. Furthermore, in the light of the chemical data presented here, it will be argued in a later section that the large scale, open system metasomatic process envisaged by Cornell (1978) for the Ventersdorp Supergroup is unlikely to have occurred, at least in the area under consideration.

D. Description of Chemical Trends Relative to Zirconium

1. Dominion Basic Lavas

(a) Major Oxide Variations : The major oxide variations of the Dominion basic lava sequence plotted against Zr are presented in Figure 11. This suite displays the largest variation of all the magma groups under consideration, forming an apparently continuous differentiation sequence which exhibits a range in Zr content from around 75 to 350ppm, and representing a spectrum of lavas from basic through to intermediate types. Well-defined trends are displayed by SiO_2, TiO_2, Al_2O_3, MgO and P_2O_5. Visually approximated average trends with increasing Zr content are as follows :

SiO_2 shows a steady increase from around 52% to 60%, accompanied by a progressive depletion of both MgO and CaO from 10% to 2.5%, and 10% to 5% respectively. Al_2O_3 displays a slight initial increase from around 14% to 15%, subsequently decreasing to 12% in the most evolved samples. Fe_2O_3 is enriched from around 11% to 13.5%, although a large degree of scatter between 8% and 15% is exhibited. MnO remains essentially constant at .15%. The alkalies display a large

Figure 11: Oxide versus Zr variation diagrams - Dominion basic lavas.

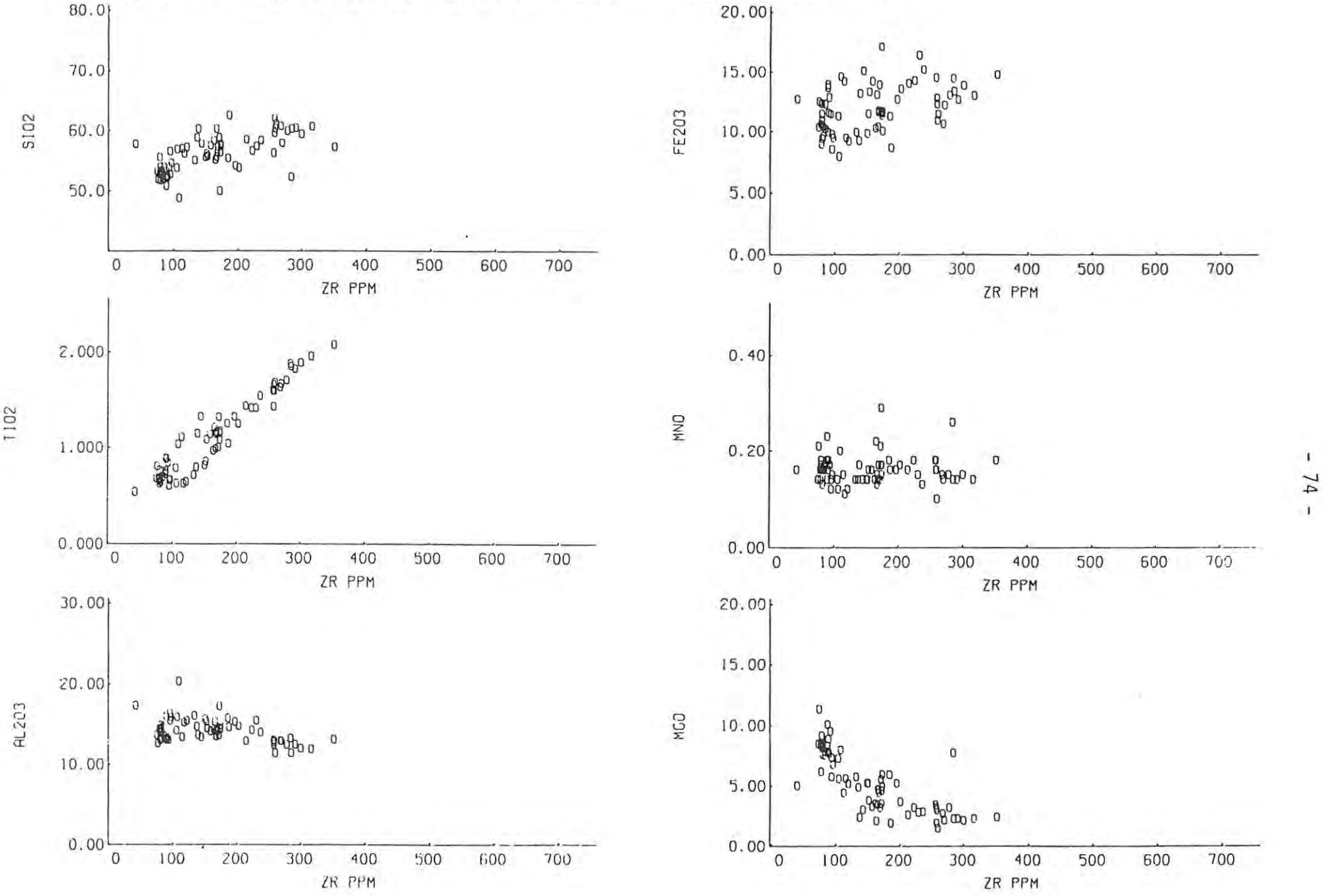

Figure 11: (cont.)

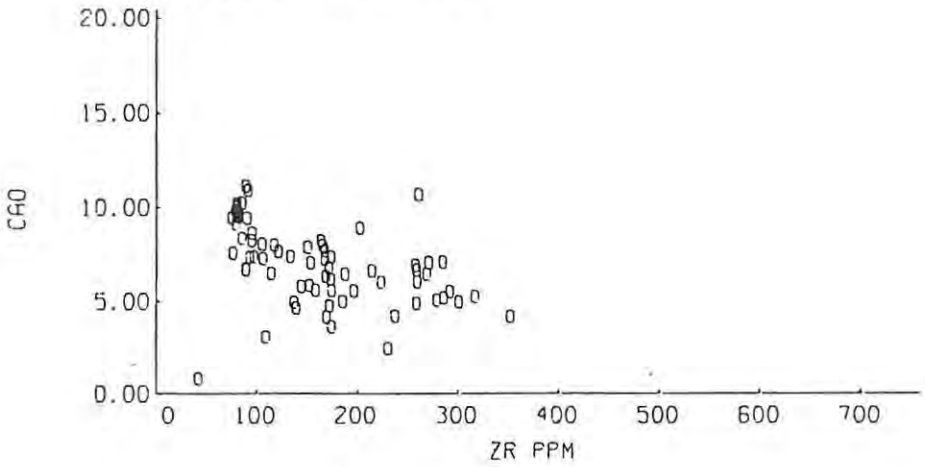

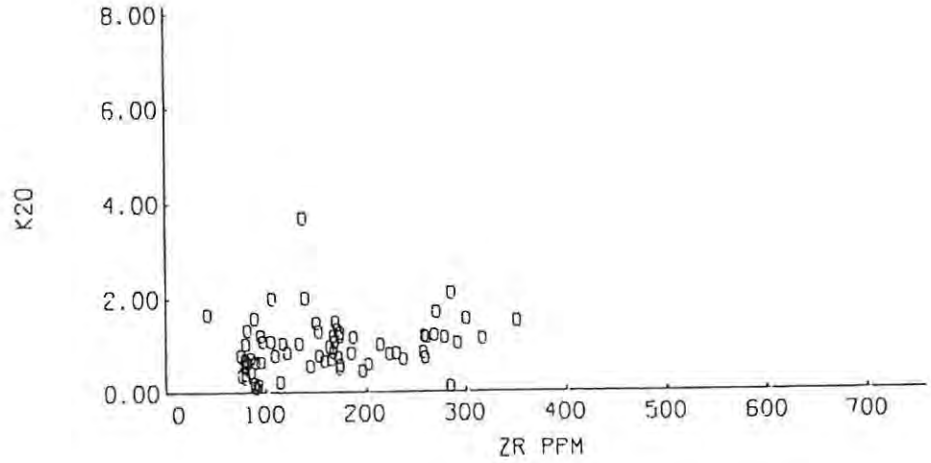

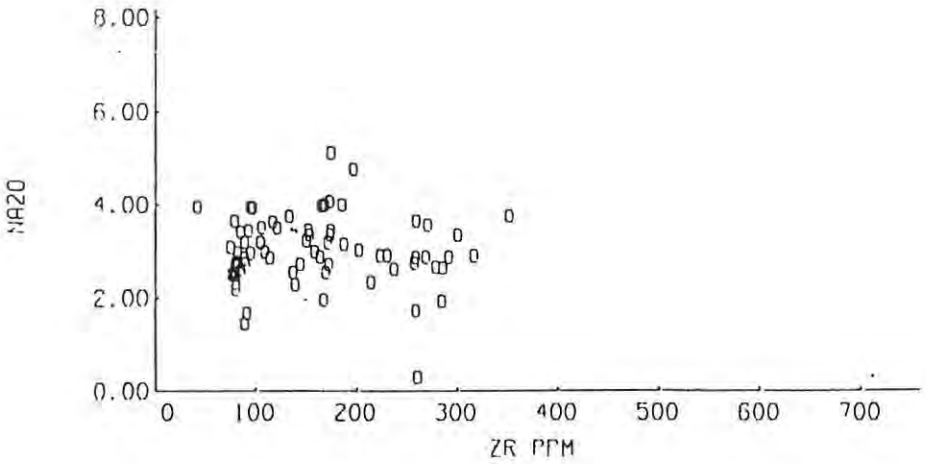

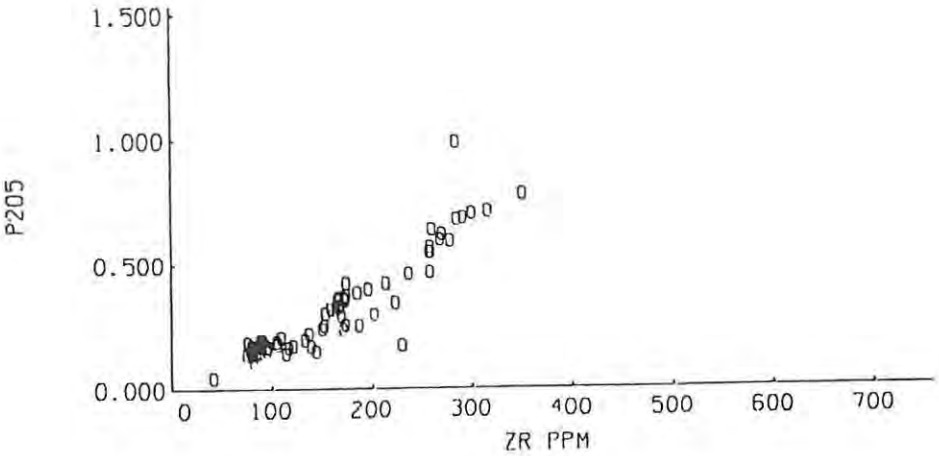

degree of scatter, with both showing no coherent trend, Na_2O varying between 2% and 4%, and K_2O between 0% and 2%. TiO_2 and P_2O_5 both show linear enrichments from .7% to 2% and from .2% to .75% respectively.

It is evident from Figure 11 that useful constraints may be placed on petrogenetic interpretation of these lavas by virtue of the coherent trends displayed by the oxides, with the possible exception of Na_2O, K_2O and Fe_2O_3. Most of the trends are clearly only distinguished by virtue of the large Zr variation.

(b) Trace Element Variations : Trace element concentrations of the Dominion basic lavas plotted against Zr are presented in Figure 12. Nb, Y, La, Ce and Nd predictably display the most well-defined trends by virtue of their expected immobility, all behaving incompatibly and defining linear positive correlations with Zr. Approximate ranges are as follows :

Nb	3-15ppm
Y	18-55ppm
La	10-40ppm
Ce	20-80ppm
Nd	10-50ppm

Both Cr and Ni similarly display well-defined trends. Cr is very rapidly depleted from 1500ppm to around 20ppm within the most basic lavas, thereafter remaining essentially constant. Ni exhibits a similar behaviour, although the initial rapid rate of depletion from 450ppm is more subdued between 100 and 200ppm Zr, levelling out at around 30ppm in the more evolved lavas. Although Zn and V exhibit considerable scatter, both show definite enrichments with increasing Zr. Both Co and Cu exhibit depletion trends, the latter from 70 to around 25ppm, while the former is more subdued, decreasing from 65 to 50ppm. Ba and Rb both show a sense of enrichment with differentiation although a large degree of scatter is present. The average trend of Ba increases from around 300 to 600ppm, and that of Rb from 15 to 50ppm. Sr remains essentially constant at around 400ppm,

Figure 12: Trace element versus Zr variation diagrams - Dominion basic lavas.

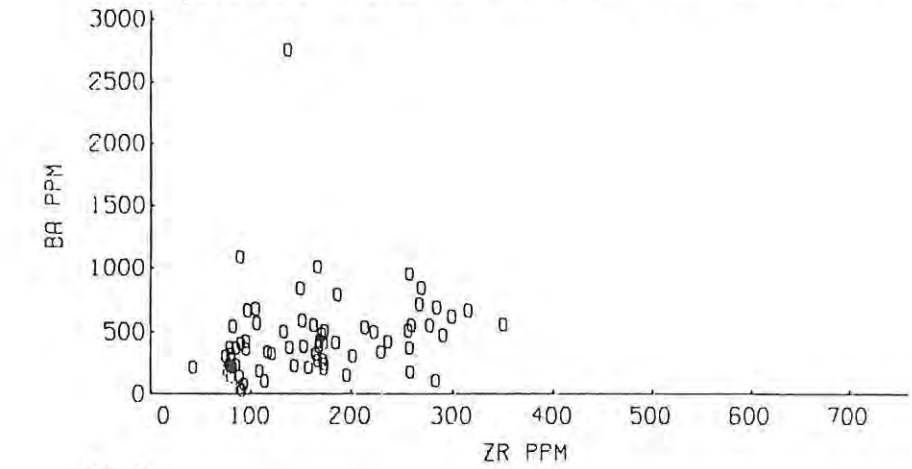

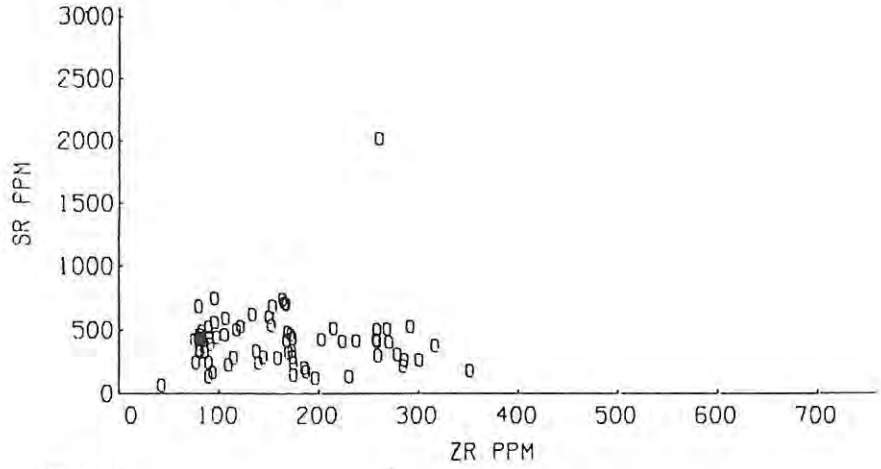

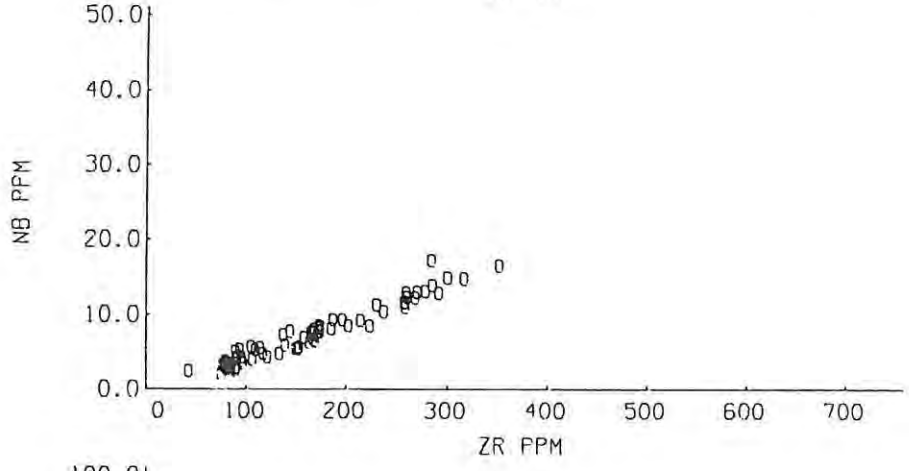

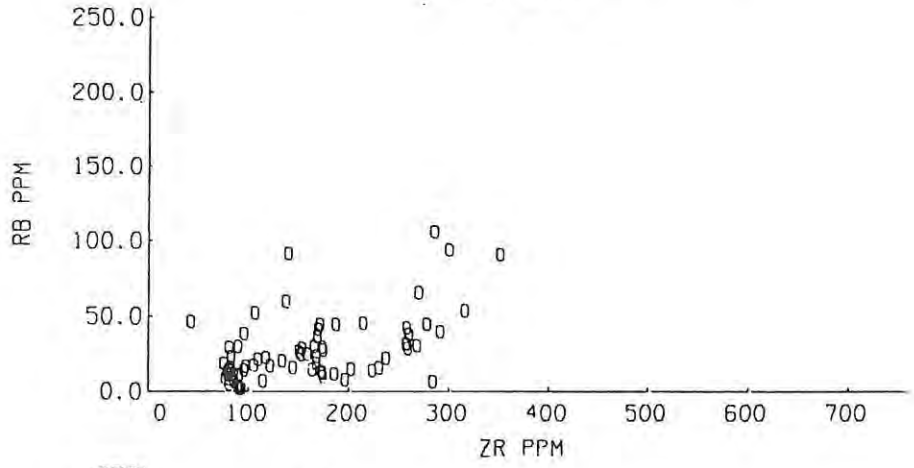

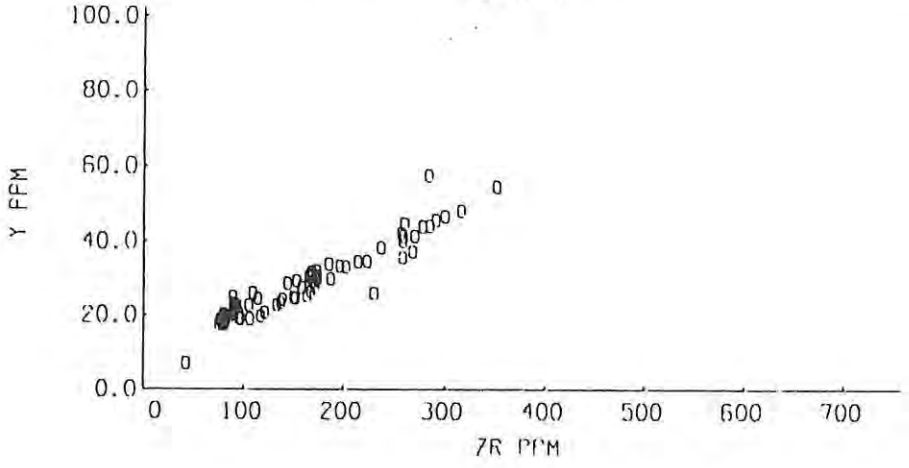

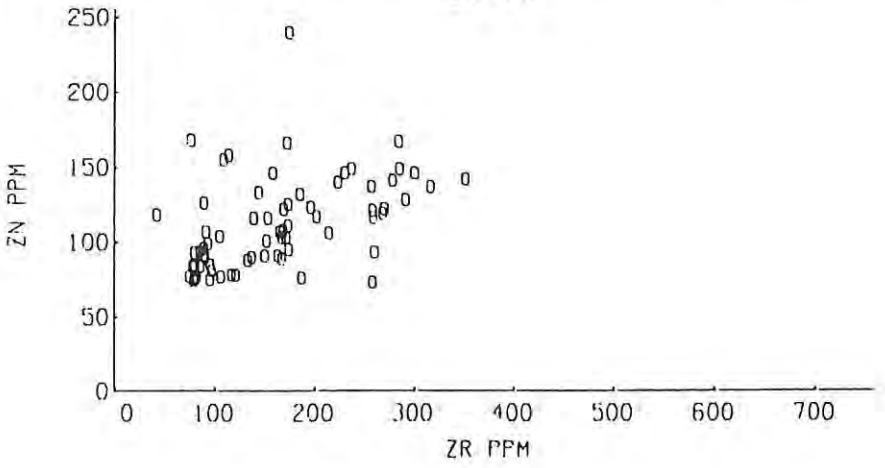

Figure 12: (cont.)

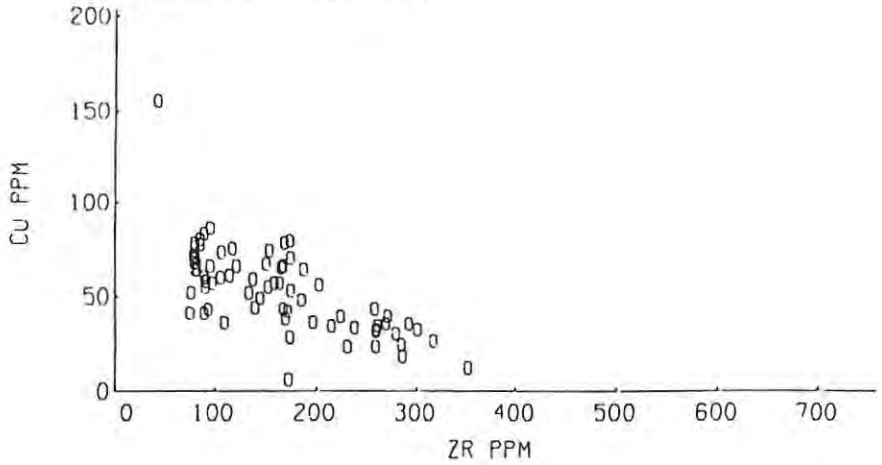

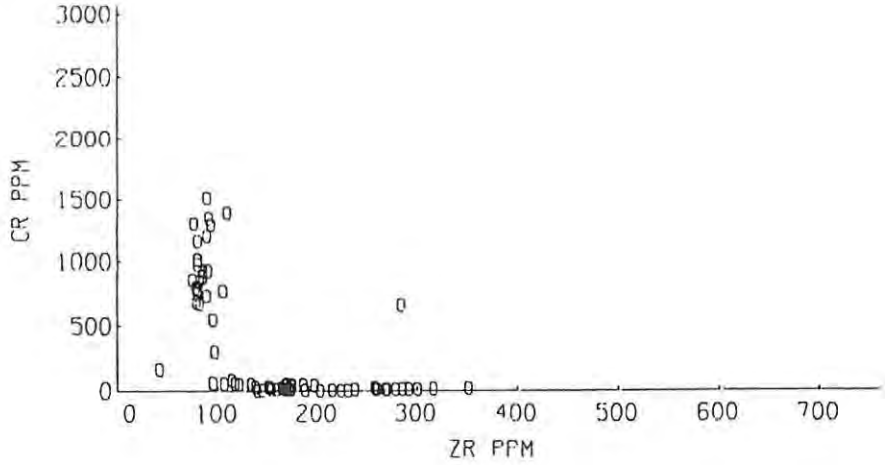

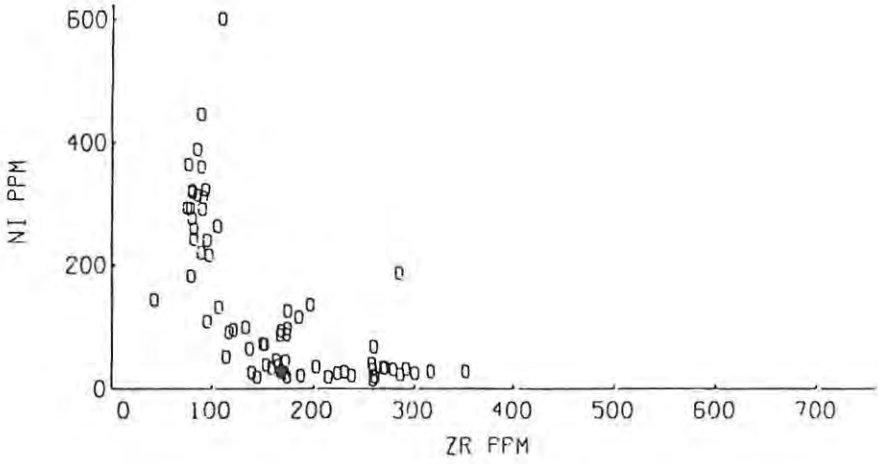

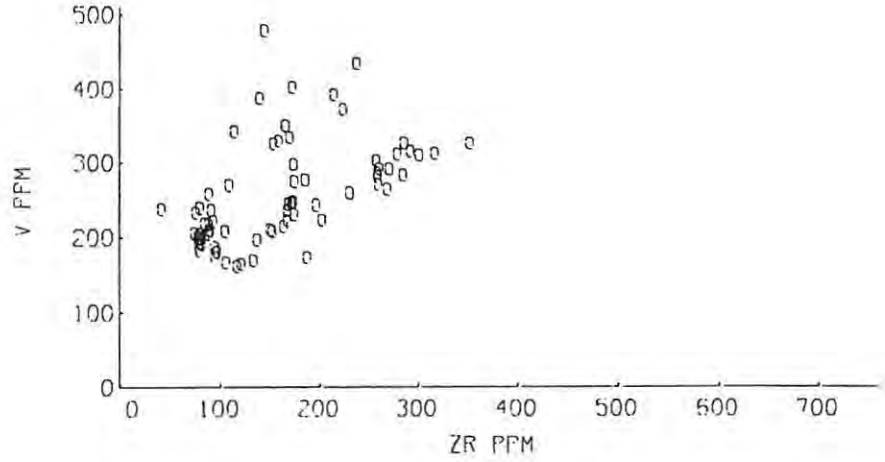

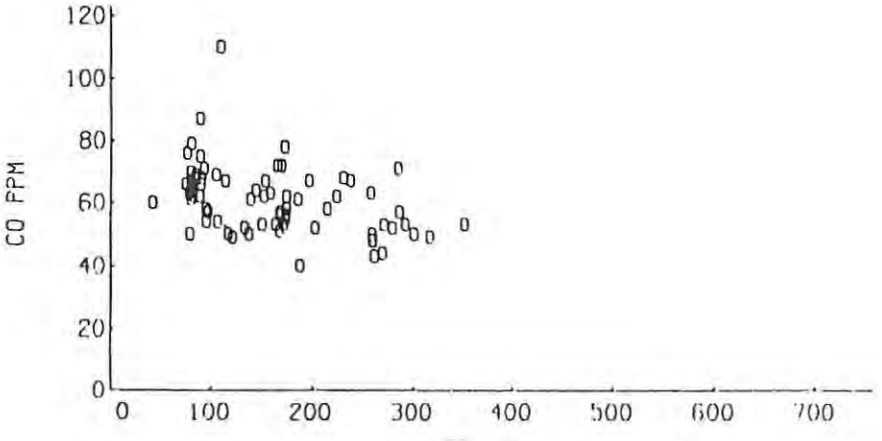

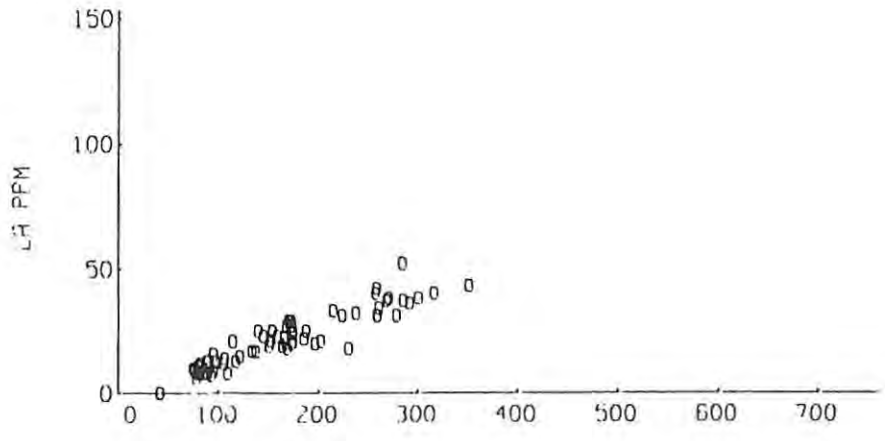

Figure 12: (cont.)

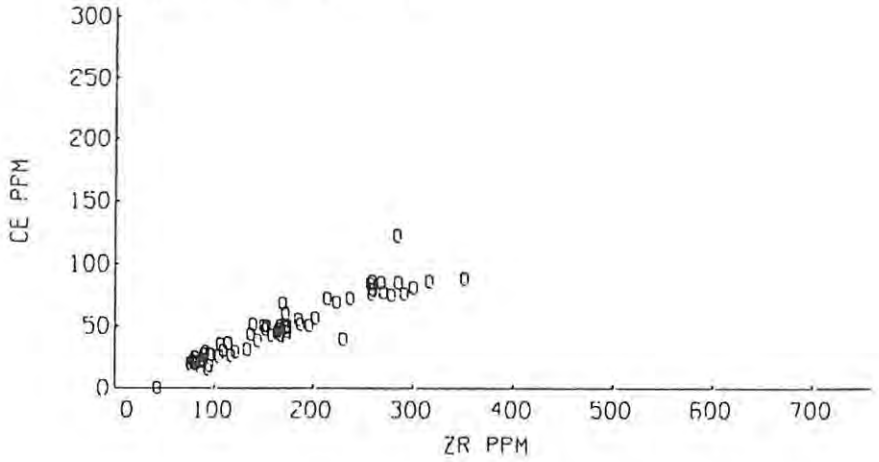

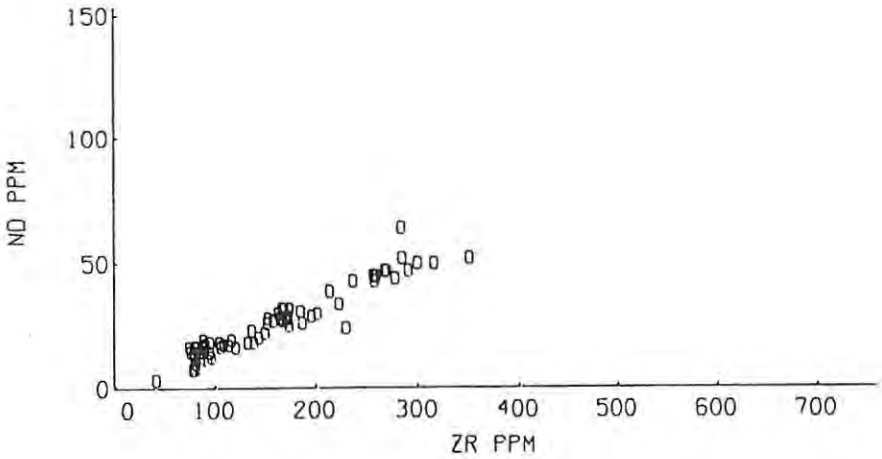

possibly decreasing slightly with increasing Zr content, and also shows a large degree of scatter.

The incompatible elements Nb, Zr, Y, La, Ce and Nd, along with Cr and Ni, thus appear to be the most favourable candidates for use in quantitative or semi-quantitative geochemical calculations. The remaining elements, especially Cu, provide important constraints on petrogenetic interpretation, although their use in a quantitative sense should be approached with caution because of the scatter probably produced by secondary processes.

2. Dominion Porphyries

(a) Major Oxide Variations : Variation diagrams for the Dominion porphyries are presented in Figure 13. The outlines of the basic lava trends, taken from Figure 11, have been included to facilitate comparison. In contrast to the basic lavas, and despite overlap in certain diagrams, the porphyries are chemically quite distinctive and display little coherent chemical variation with Zr. While the use of Zr as an index of differentiation might be questionable in such acid lavas, zircon was not observed in thin section and the lack of coherent variation using any other element as the abscissa, suggests that the observed variation in most instances is random scatter which has obscured any rational magmatic trends which may have existed. The TiO_2, Al_2O_3 and P_2O_5 variations are exceptions and are discussed below.

The bulk of the samples fall within a Zr range of 240 to 320ppm. Sample DP-33 (545ppm Zr) plots some distance away from the bulk of the samples and will be discussed later. In contrast to the Dominion basic lavas of equivalent Zr contents, the porphyries are richer in SiO_2 (70.14%) and K_2O (3.03%)(the figures in parentheses represent the mean oxide concentrations exclusive of sample DP-33), and depleted in TiO_2 (.79%), Fe_2O_3 (6.71%), MnO (.08%), MgO (1.12%), CaO (2.02%) and P_2O_5 (.24%). Al_2O_3 (12.64%) and Na_2O (3.22%) contents are equivalent to the basic lavas, although

Figure 13: (2 pages following) Oxide versus Zr variation diagrams - Dominion porphyries. Dashed line indicates the Dominion basic lava trend.

Figure 13: (cont.)

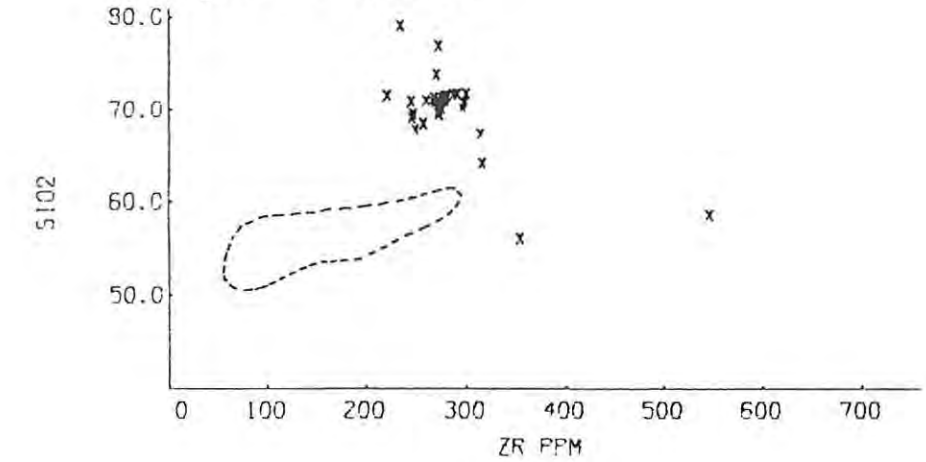

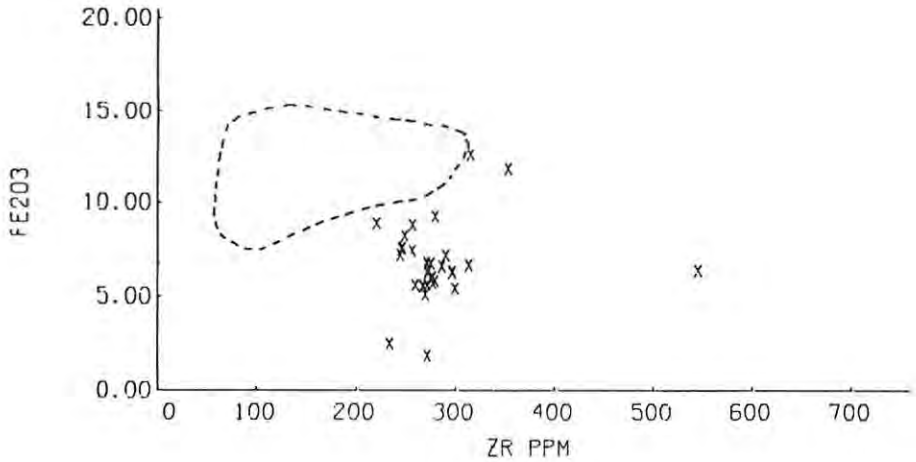

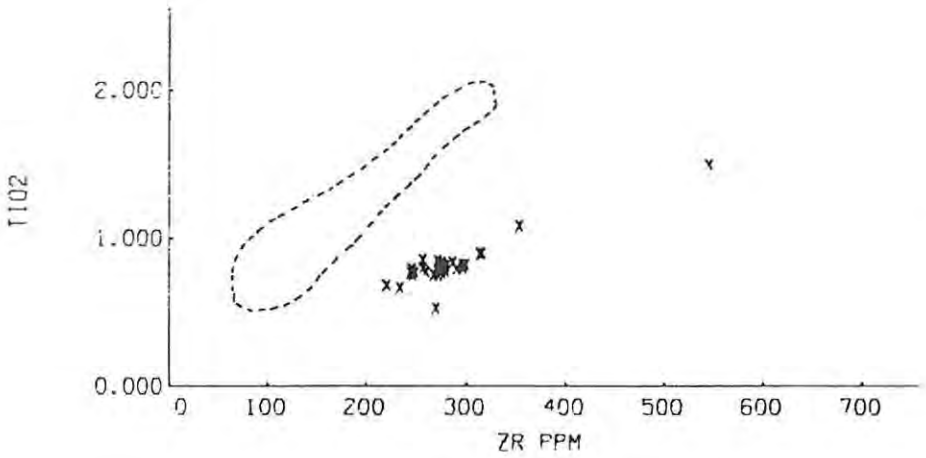

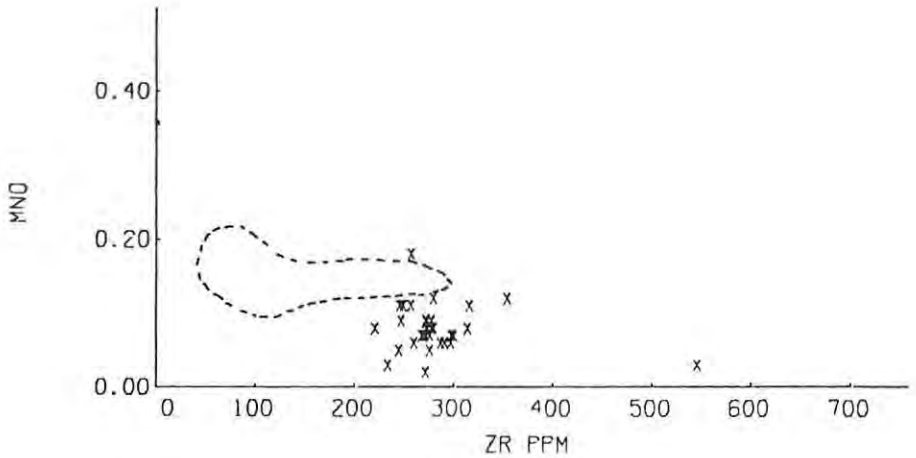

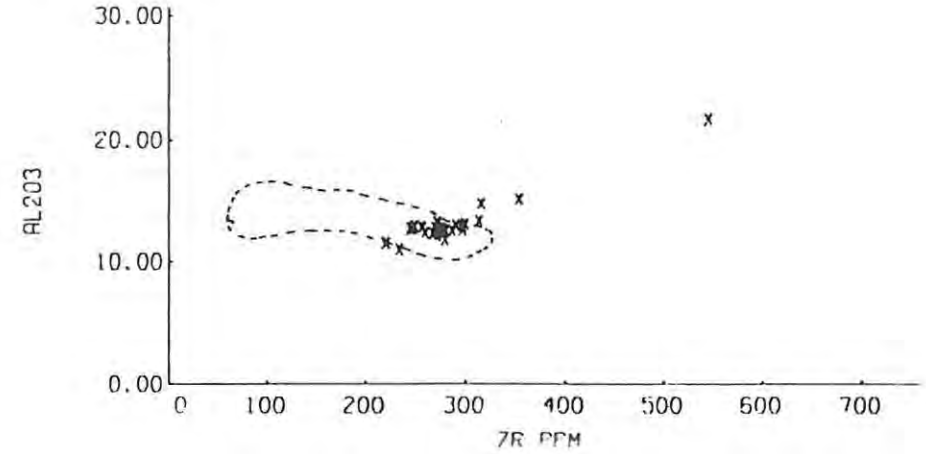

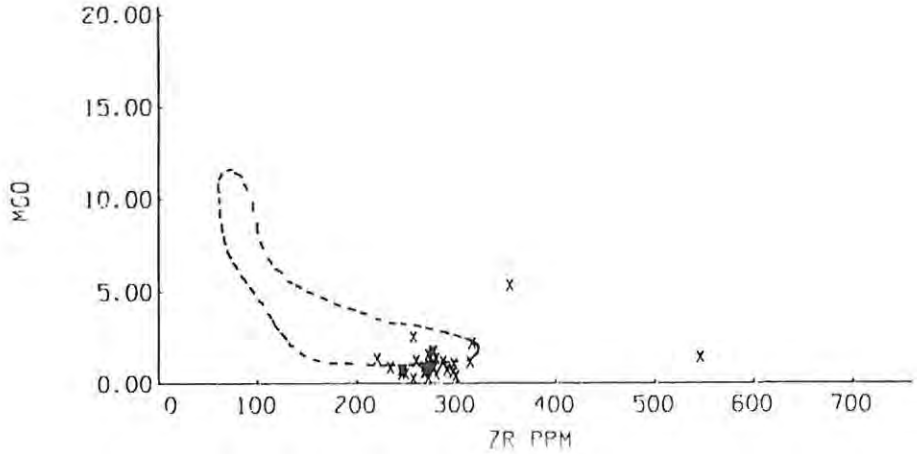

Figure 13: (cont.)

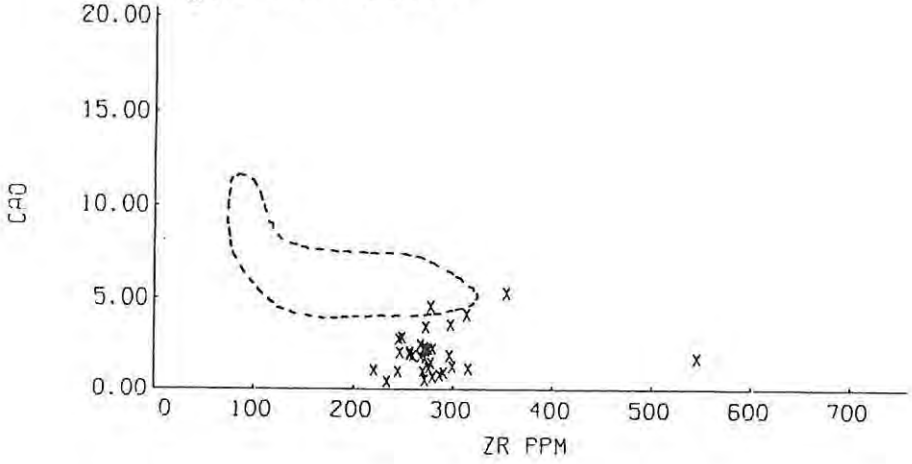

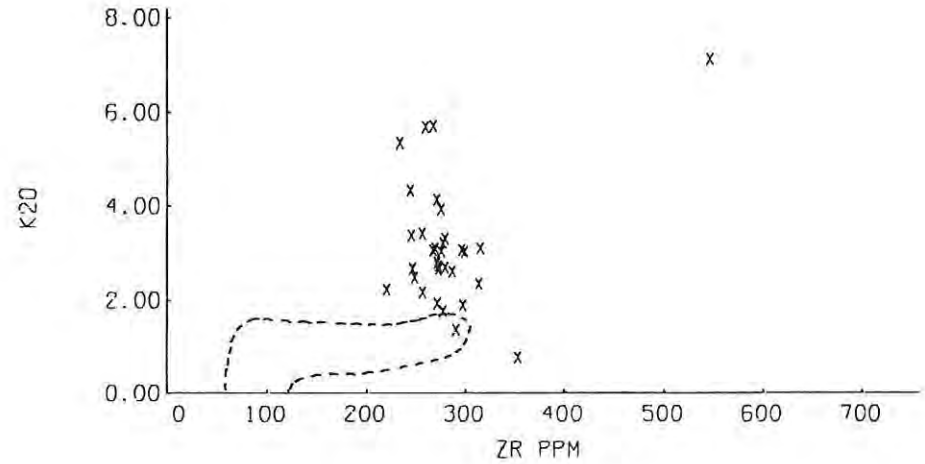

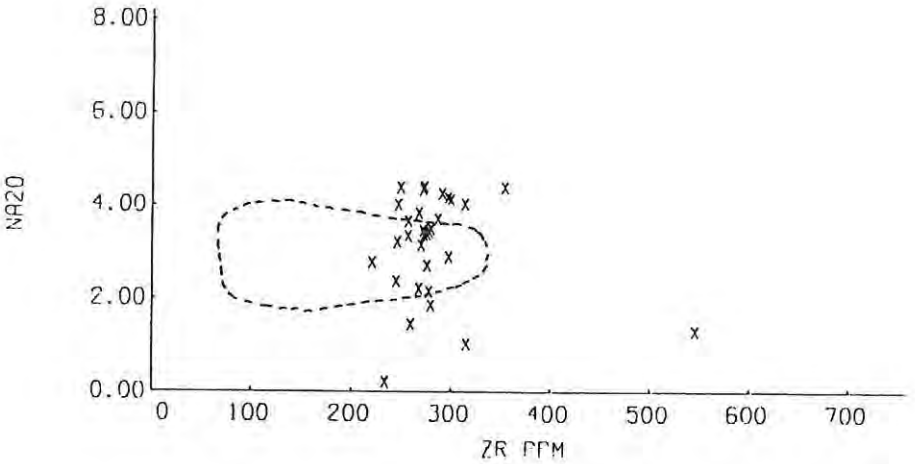

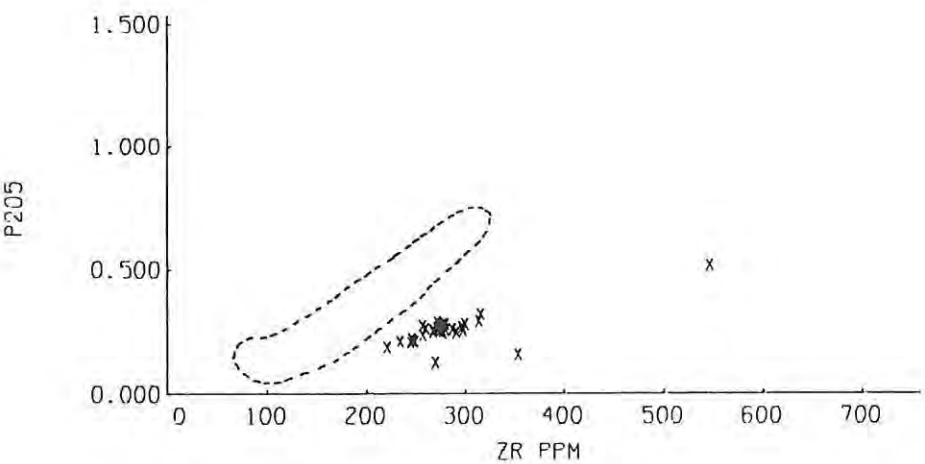

Na_2O might be slightly enriched in the porphyries. K_2O, Na_2O and to a lesser extent Fe_2O_3 again appear to be the most mobile oxides, with K_2O scattered between 1.5 and 6%, while TiO_2, P_2O_5 and Al_2O_3 display the smallest amount of scatter, and may thus be regarded as immobile.

Relative to the average porphyry composition, sample DP-33 is depleted in SiO_2 and Na_2O, and strongly enriched in TiO_2, Al_2O_3, K_2O and P_2O_5. In the case of TiO_2, K_2O and P_2O_5, this sample lies on a projection of a line passing through the origin and the mean porphyry composition, while with Al_2O_3 this line cuts the Y-axis at around 3% Al_2O_3. The relationship of sample DP-33 to the mean composition in respect of the remaining oxides is obscure because of scatter, although Fe_2O_3 and MnO may be slightly depleted and MgO slightly enriched.

(b) Trace Element Variations : As in the case of the major oxides, the mean trace element concentrations of these lavas (excluding DP-33) may be considered representative of the porphyries as a whole, as the variation in most cases appears to be random scatter (Figure 14). The incompatible elements Nb and Y, as well as TiO_2, Al_2O_3 and P_2O_5 mentioned above, exhibit straight-line positive trends which in most cases project through the origin. These trends reflect the coherency in behaviour of these elements with Zr, probably as a result of their expected immobility during secondary processes, although a magmatic origin for the trends cannot be ruled out.

In relation to the basic lavas of similar Zr contents, the porphyries are enriched in Rb (82ppm) (although considerable overlap exists due to large degrees of scatter) and La (49ppm). They are depleted in Y (29ppm), Zr (191ppm), Zn (84ppm), Cu (14ppm), Ni (10ppm), Cr (5ppm) and strongly depleted in Co (18ppm) and V (52ppm). Concentrations of Ba (757ppm), Nb (14ppm), Ce (93ppm) and Nd (40ppm) are similar to those of the basic lavas. The mean Zr content is 273ppm.

Once again Ba, Sr and Rb appear to be the most mobile elements,

Figure 14: (3 pages following) Trace element versus Zr variation diagrams - Dominion porphyries. Dashed line indicates the Dominion lava trend.

Figure 14: (cont.)

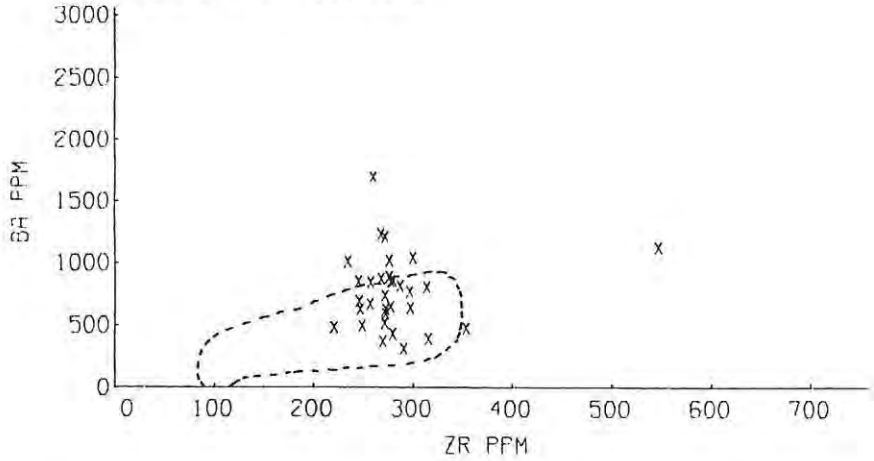

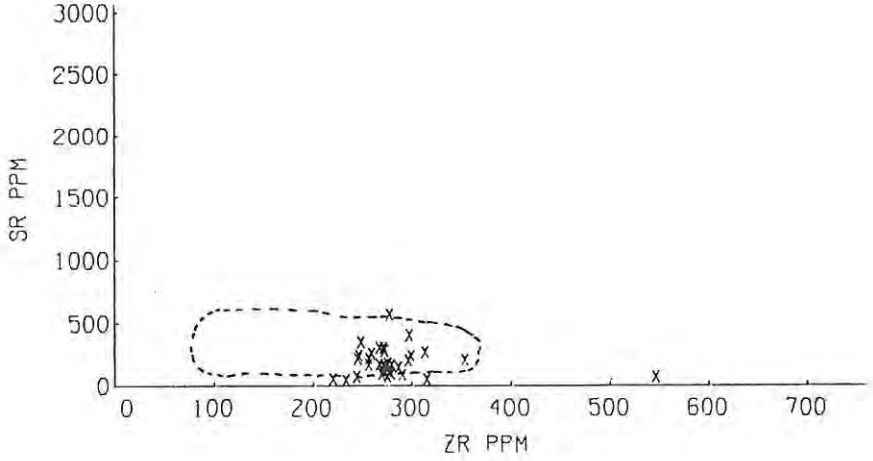

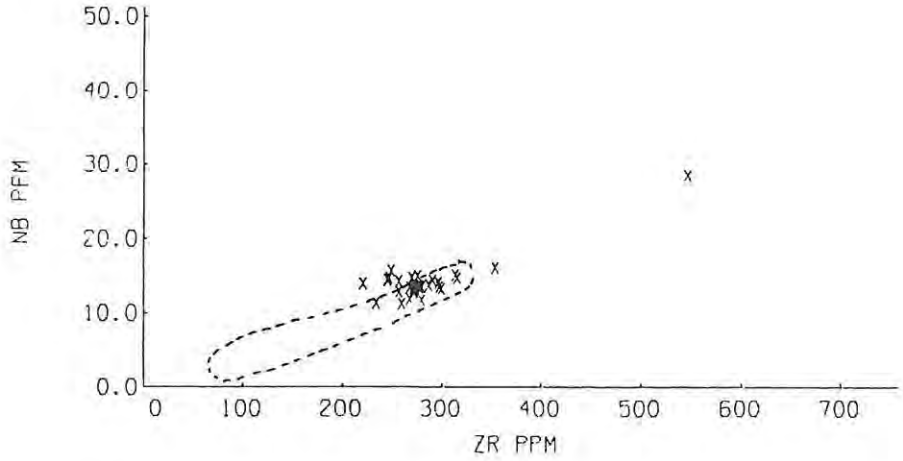

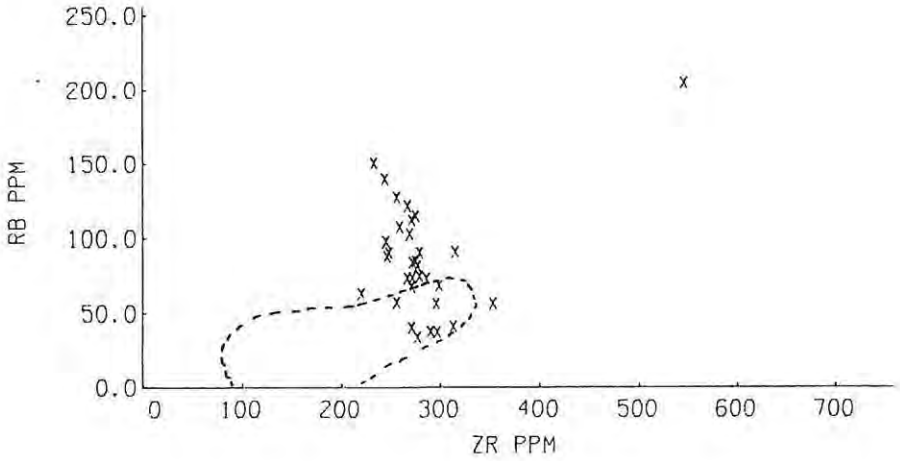

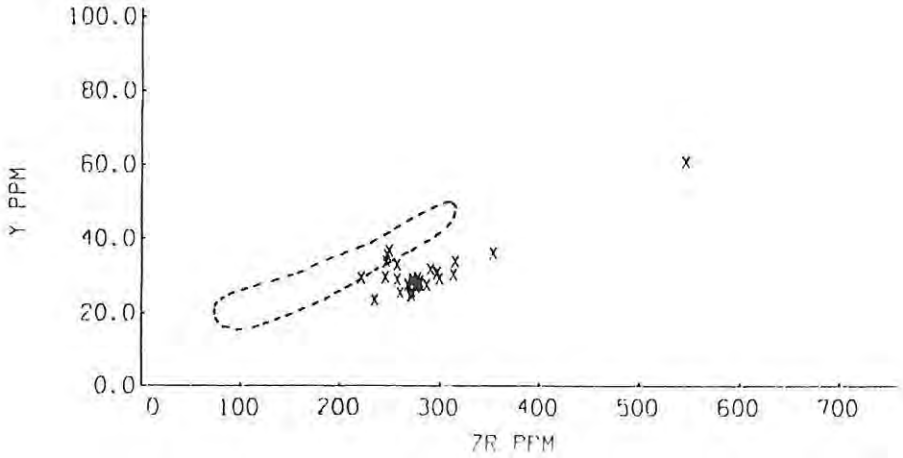

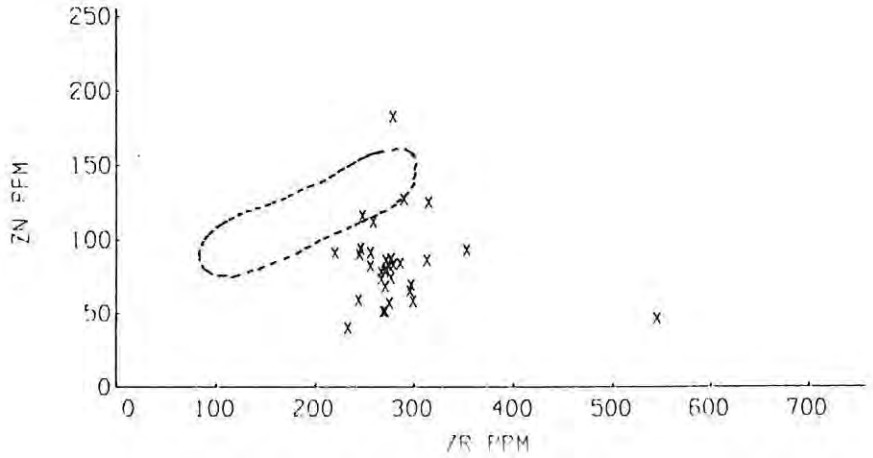

Figure 14: (cont.)

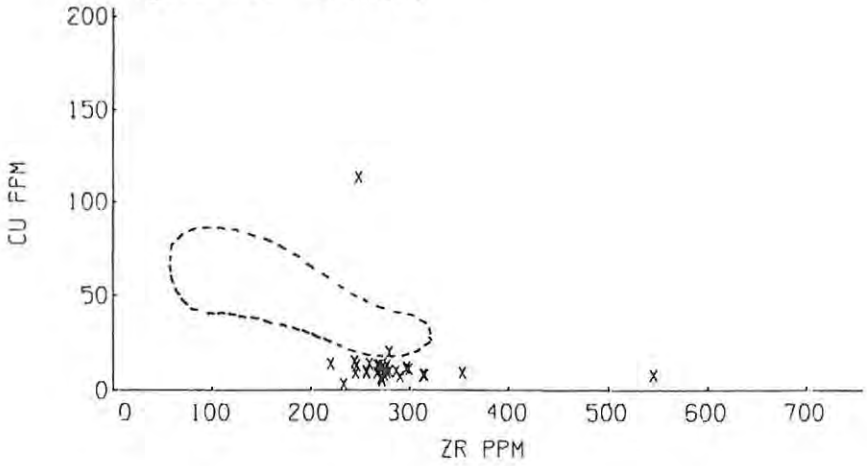

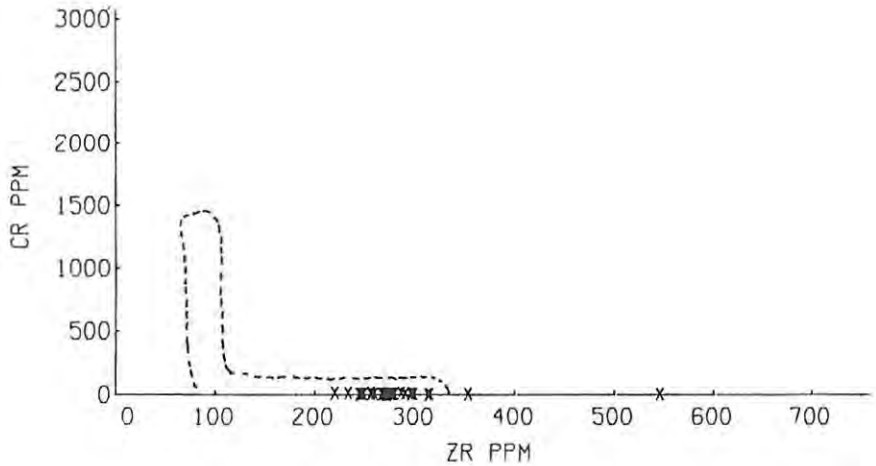

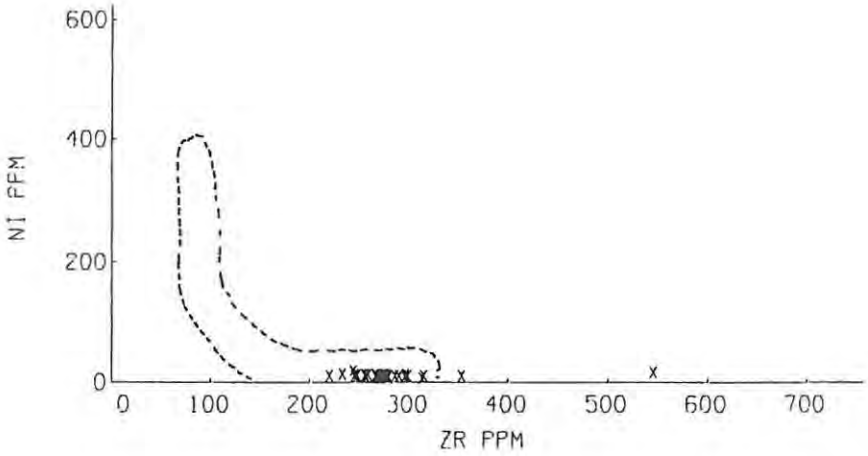

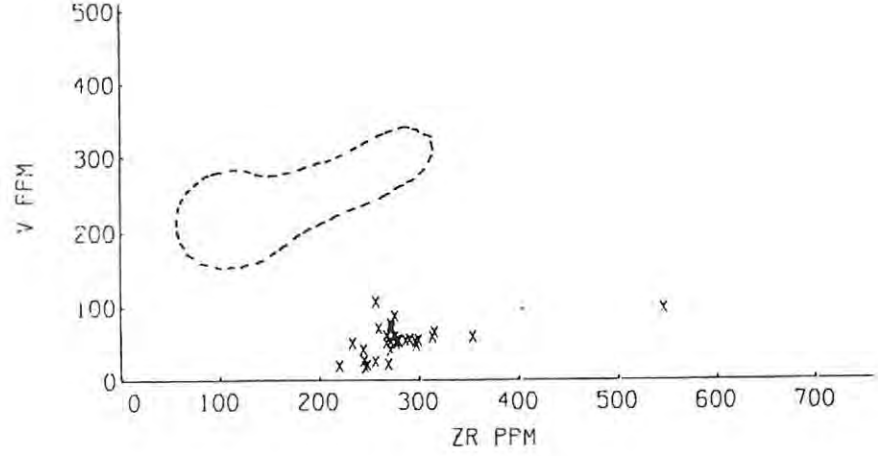

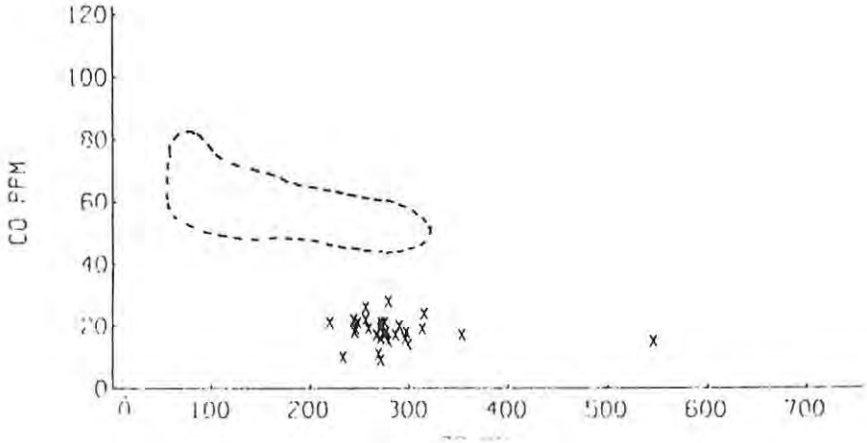

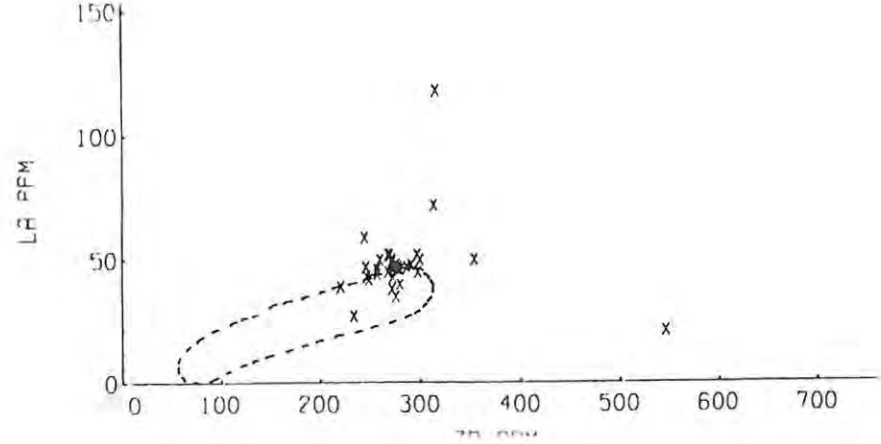

Figure 14: (cont.)

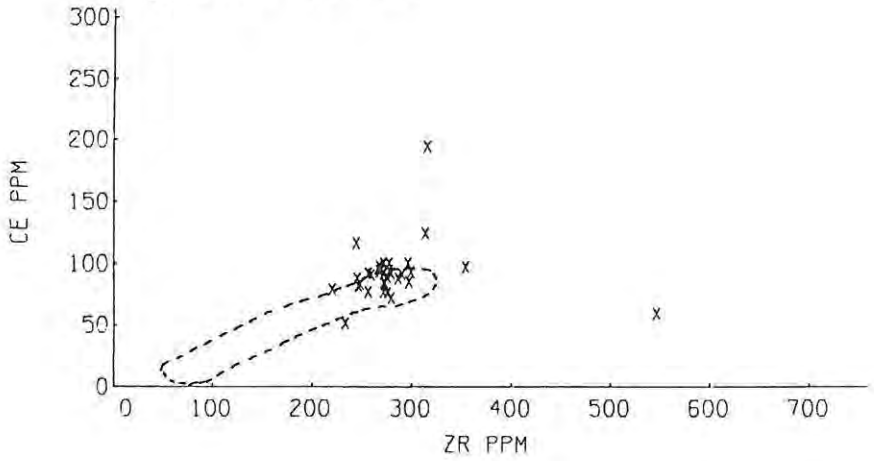

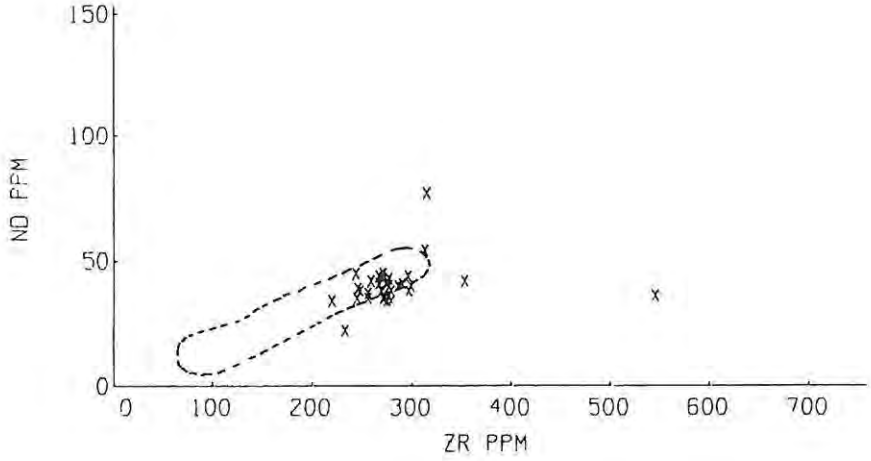

followed by Zn, as indicated by their large degrees of scatter.

Relative to the bulk of the porphyries, sample DP-33 is enriched in Ba, Nb, Y, Rb and possibly V, falling on a projection of a line passing through or close to the origin and the bulk of the samples. The remaining elements are more difficult to evaluate, although Sr, Zn, La, Ce and Nd appear to be depleted. The implications of these relationships are important as they appear to be duplicated in several formations, and will be considered further in a later chapter.

3. Ventersdorp Supergroup (including Jeppestown Amygdaloid)

(a) General : Variation diagrams for the lavas of the Ventersdorp Supergroup and including the Jeppestown amygdaloid samples are presented in Figures 15 (major oxides) and 17 (trace elements). The axes are identical to those used for the Dominion Group diagrams, and where possible the Dominion basic lava trend is indicated to facilitate comparison.

The discrete ranges in Zr content of the major compositional groups within the Ventersdorp Supergroup allow these groups to be easily accommodated with very little overlap on the variation diagrams. As a whole, Zr in these lavas ranges from approximately 40ppm to over 700ppm. Lavas of the Klipriviersberg Group are chemically the most primitive, with Zr content ranging between 40 and 150ppm, followed by the Allanridge lavas which show limited variation about a mean of 178ppm Zr. With the exception of sample JA-371, the Jeppestown amygdaloid samples are clustered about a mean of 242ppm Zr. The Goedgenoeg and Rietgat formations cannot be separated geochemically and are thus treated together. They fall within the range of 240 to 750ppm Zr, although all but 4 samples lie between 240 and 430ppm. The 4 high-Zr samples resemble rocks of the Makwassie formation both petrographically and chemically. They were taken from the highly porphyritic units occurring within the Goedgenoeg formation in boreholes JBF-1 and VHD-1, which were referred to at the end of Chapter III. These samples are excluded from the general description of the chemistry of

Figure 15: (2 pages following) Oxide versus Zr variation diagrams - Ventersdorp Supergroup and Jeppestown amygdaloid lavas. Dashed line indicates the Dominion basic lava trend.

Key to symbols:-
X - Klipriviersberg lavas
O - Allanridge lavas
+ - Goedgenoeg/Rietgat lavas
M - Makwassie porphyries
* - Jeppestown amygdaloid lavas

Figure 15: (cont.)

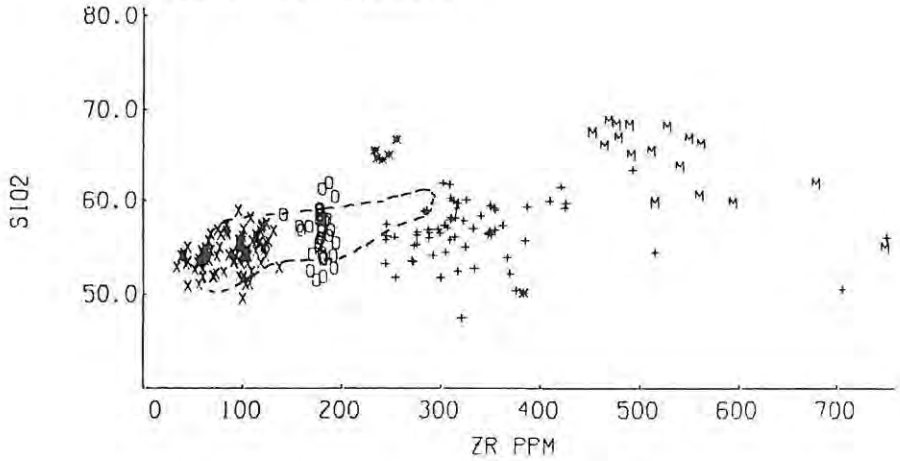

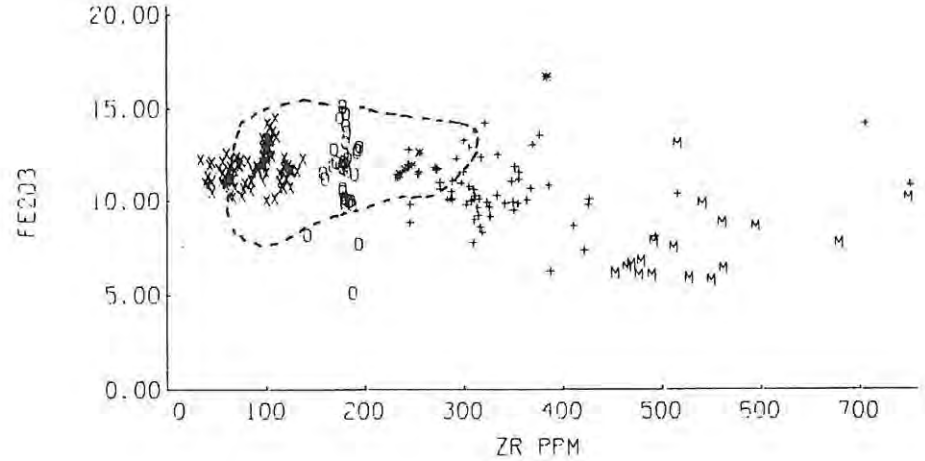

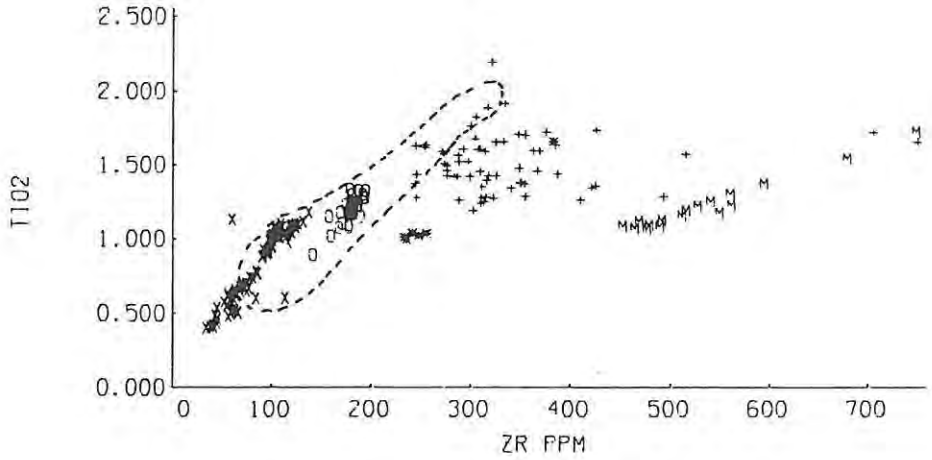

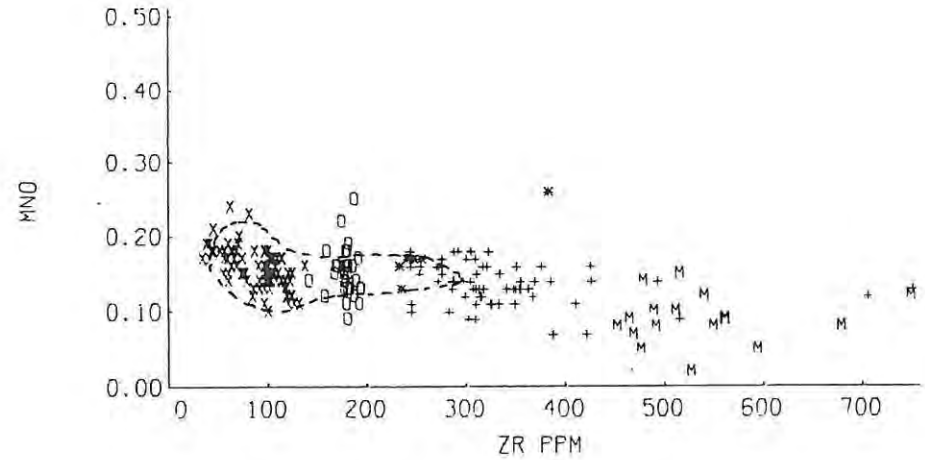

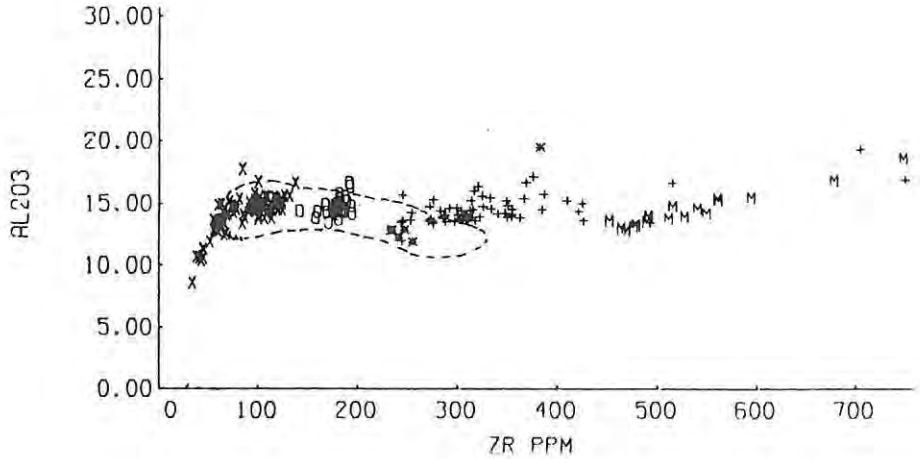

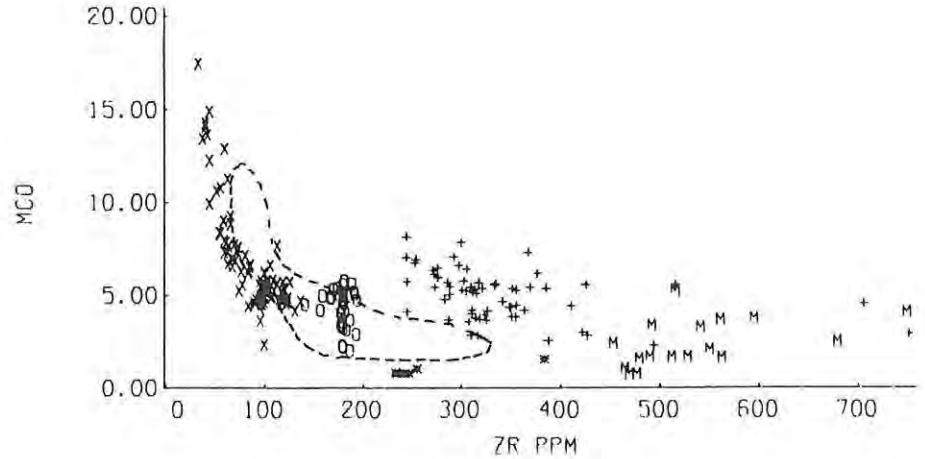

Figure 15: (cont.)

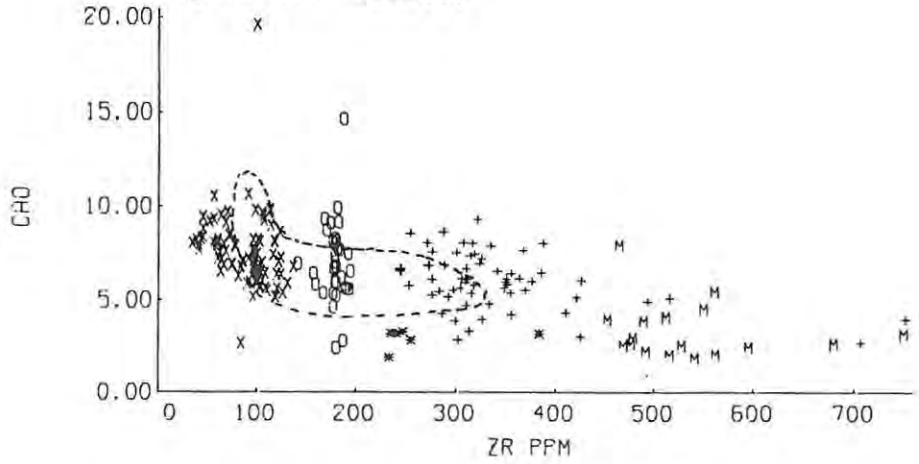

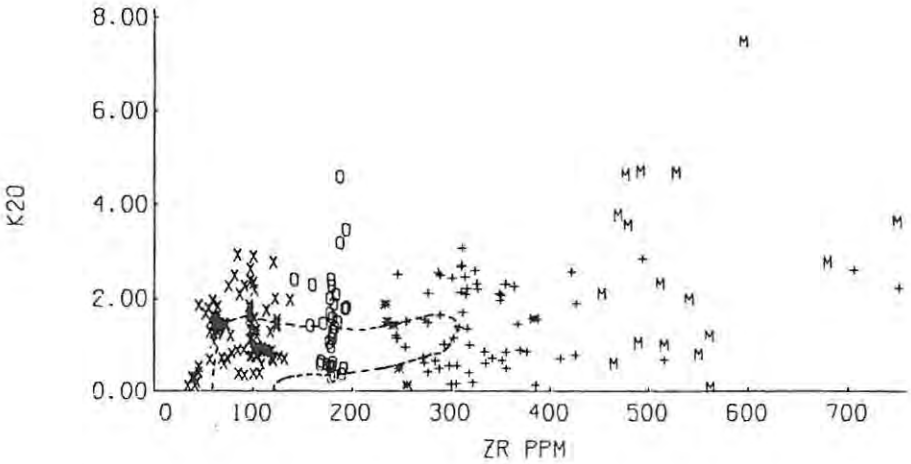

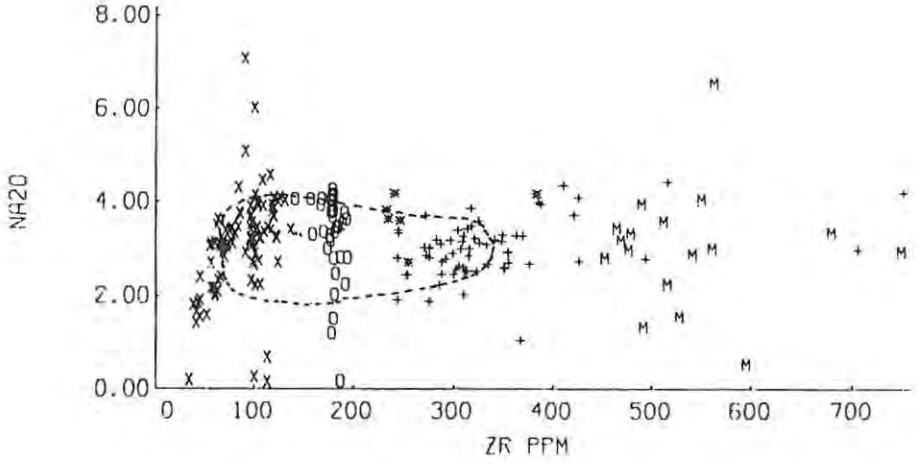

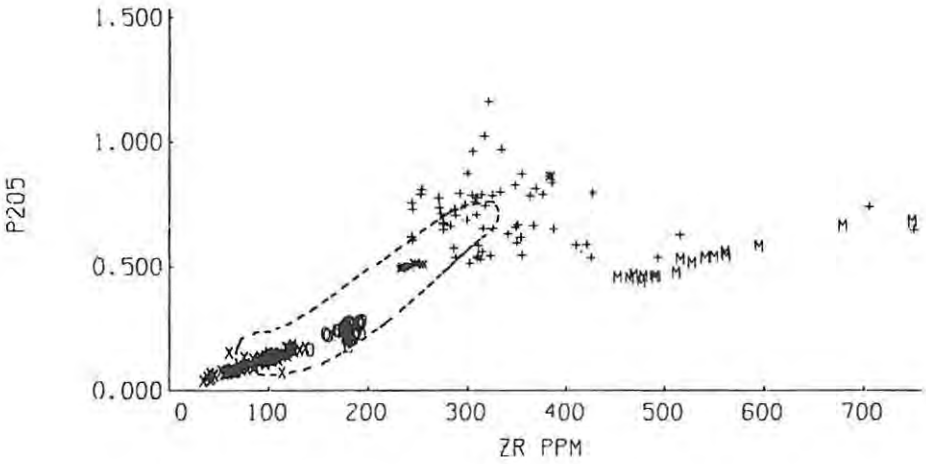

the Goedgenoeg/Rietgat lavas below, but will be considered later in Chapter VIII.

The Zr concentrations in the Makwassie porphyry samples vary between 450 and 750ppm. Because of the relatively high levels of Zr and the presence of zircon in these specimens, Zr may not behave as an incompatible element, and magmatic trends may not be obvious in the plots.

(b) Major Element Variations : Only lavas of the Klipriviersberg, Goedgenoeg/Rietgat and Makwassie sequences display ranges in Zr of sufficient magnitude to indicate coherent intra-formational trends which are not obscured by the scatter of the data. Of these only the Klipriviersberg and Makwassie samples do in fact display coherent trends. The Allanridge samples display a relatively wide range in the concentrations of many elements despite the limited Zr range, a feature which probably reflects the variability in type and degree of alteration described in Chapter V. Thus all the oxides with the exception of TiO_2, Al_2O_3 and P_2O_5 display varying degrees of mobility, with MgO slightly mobile and Na_2O and K_2O extremely mobile.

It has been stated in Chapter III that the Alberton, Orkney and Loraine/Edenville formations of the Klipriviersberg Group are distinguishable on geochemical grounds. This is best exemplified in the TiO_2 versus Zr and Fe_2O_3 versus Zr plots which are reproduced on an expanded scale in Figures 16(a) and (b). Figure 16(a) shows a small gap between .8 and .85% TiO_2 and 86 to 90ppm Zr. This gap represents a boundary between the Loraine/Edenville and Orkney formations. All Orkney formation samples lie within the range of 90 to 110 ppm Zr, while only 3 Alberton samples plot below 110ppm Zr. The Orkney/Alberton formation boundary is well illustrated in Figure 16(b), where Orkney samples generally have higher Fe_2O_3 concentrations than those of the Alberton lavas. The significance of these compositional breaks will be evaluated in Chapter VIII. The Orkney and Alberton formations display no discernible magmatic trends within their limited Zr ranges. In contrast, the Loraine/Edenville lavas exhibit a number of

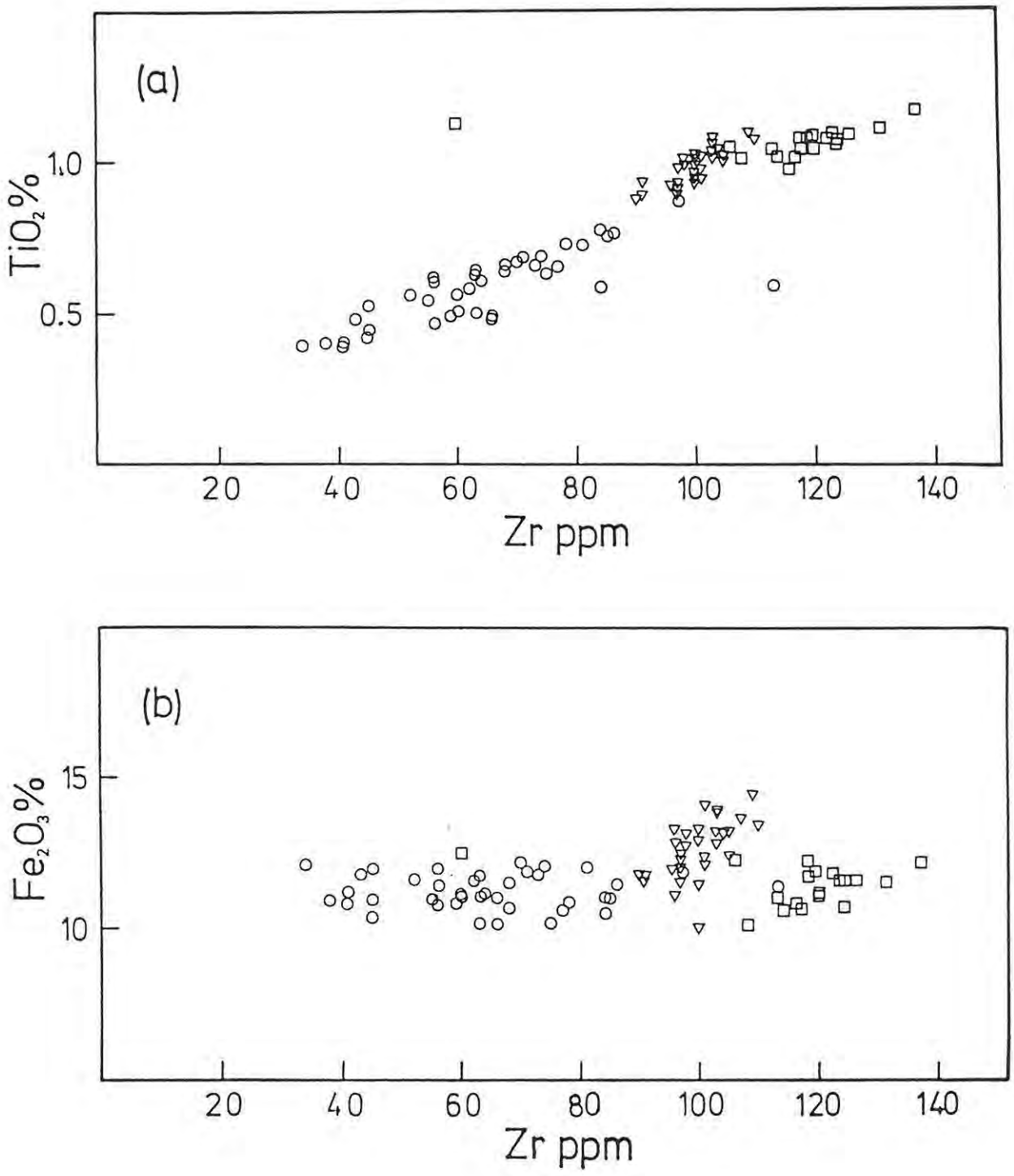

Figure 16: Variation of TiO_2(a) and Fe_2O_3(b) versus Zr - Klipriviersberg lavas, illustrating the discrete compositional fields of the constituent formations. Circles - Loraine/Edenville formations; triangles - Orkney formation; squares - Alberton formation.

well-defined trends, the most significant being that of MgO, which decreases with increasing Zr from 17.5% to around 5%. SiO_2 varies between 50 and 57%, showing a very ill-defined increase with increasing Zr. No variation of Fe_2O_3 is discernible through the scatter and it presumably remains relatively constant at between 10 and 12.5%, while MnO is scattered about a .17% mean. CaO, although scattered, shows a general depletion from 9% to 6%, while any trend for K_2O has been obliterated by secondary alteration, and concentrations now vary between 0% and 2%. Al_2O_3, TiO_2, P_2O_5, and Na_2O display linear enrichments with increasing Zr, reflecting both an incompatible and, with the exception of Na_2O, an immobile behaviour. TiO_2 increases from .4% to .8%, Al_2O_3 from 8% to 15%, P_2O_5 from around .06% to .1% and Na_2O from around 1.3% to 3.8%, with the most basic sample containing .2%, but this may well be a secondary depletion due to alteration.

Orkney and Alberton lavas show very little coherent intra-formational variation but exhibit some significant differences between them, most clearly illustrated, as has already been demonstrated, by Fe_2O_3, which ranges from 11% to just below 15% in the Orkney formation, with a mean of 12.67%, while in the Alberton samples it varies between 10% and 12.5% with a mean of 11.4%, and is thus similar to the levels in the Loraine/Edenville formation. MnO, although scattered, is generally more depleted in the Alberton formation. SiO_2 contents are scattered in both formations between 50% and 57%, while MgO varies between 4% and 6%. CaO, Na_2O and K_2O display wide ranges due to their high mobility, with average concentrations in both formations being very similar, viz. 7.45%, 3.45% and 1.32% for CaO, Na_2O and K_2O respectively in the Orkney formation, and 7.19%, 3.40% and 1.13% for these elements in the Alberton formation. Al_2O_3 is scattered between 14% and 16% (means = 14.85% in the Orkney, and 14.95% in the Alberton formation), showing a distinct flattening of the enrichment trend exhibited by the Loraine/Edenville formation. A more subtle break occurs with TiO_2 concentrations, which in the Orkney and Alberton formations cluster about means of .98% and 1.07% TiO_2 respectively. The Alberton formation samples

lie on a projection of the Loraine/Edenville trend, but the Orkney samples lie above this projected trend (Figure 16(a)). P_2O_5 forms a linear trend continuous with that of the Loraine/Edenville formation, with concentrations increasing to just below .2% in the Alberton lavas.

Lavas of the Allanridge formation have major oxide concentrations spread over the range covered by the Alberton and Orkney formations, and often exceed the upper and lower limits of the latter, while mean concentrations are similar. TiO_2 contents are slightly higher, with a mean of 1.2% which, because of the higher Zr contents, lies below the projected Klipriviersberg trend. P_2O_5, with a mean of .23%, falls on a projection of the Klipriviersberg trend. MgO contents are generally lower, averaging 4.22%.

Lavas of the Goedgenoeg/Rietgat formations, while displaying a relatively wide range in Zr, exhibit a large degree of scatter which in most cases appears to be random. Mean concentrations of SiO_2, Al_2O_3 and K_2O are almost identical to those of the Allanridge formation. Fe_2O_3, MnO and Na_2O are slightly lower, while MgO is higher (5.1%). TiO_2 and P_2O_5 concentrations are higher with respective means of 1.5% and .7%. It is significant that these lavas do not display the usual linear coherence of TiO_2 and P_2O_5 with Zr. Finally the similarity in distribution patterns in the TiO_2 and P_2O_5 versus Zr plots suggests a close coherence in the behaviour of these two elements. The implications of these features will be discussed in Chapter VII.

Samples of the Jeppestown amygdaloid (excluding sample JA-371) are characterized by considerably higher mean contents of SiO_2 (65.3%) and lower TiO_2 (1.03%), Al_2O_3 (12.6%), MgO (.9%) and CaO (3.0%) compared to the Allanridge and Goedgenoeg/Rietgat lavas, whose Zr contents are respectively less than and greater than those of the Jeppestown amygdaloid. Fe_2O_3 (11.8%) and MnO (.16%) contents are similar to those of the Allanridge formation. Na_2O and K_2O (3.6% and 1.1% respectively) are the only oxides which show an appreciable amount of scatter, the

former being slightly higher, and the latter slightly lower than the mean concentrations in the Allanridge and Goedgenoeg/Rietgat formations. P_2O_5 content averages .57% and is thus intermediate between the Allanridge and Goedgenoeg/Rietgat means for this element.

Relative to the bulk of the Jeppestown samples, sample JA-371 (383ppm Zr) is strongly depleted in SiO_2 and enriched in TiO_2, Al_2O_3, Fe_2O_3, MnO, MgO and P_2O_5, while the CaO, K_2O and Na_2O concentrations fall in the same range as the other samples. This relationship is thus similar to that of sample DP-33 to the rest of the Dominion porphyries.

The Makwassie quartz porphyries exhibit a large Zr variation, between 450 and 750ppm, and while some oxides exhibit a large degree of scatter, others are linearly correlated with Zr. SiO_2 exhibits a general decrease with increasing Zr, from around 68% down to 55% with a mean of 64.6%. Fe_2O_3 (7.6%) and MnO (.09%) are widely scattered although a crude enrichment trend may be present. CaO and MgO exhibit similar configurations to those of Fe_2O_3, with means of 3.34% and 2.43% respectively. Na_2O (3.02%) and K_2O (2.72%) show a pronounced scatter with no suggestion of coherence with Zr. TiO_2, Al_2O_3 and P_2O_5 display very well-defined linear enrichment trends. TiO_2 increases from about 1% to 1.7%. Al_2O_3 increases from 12.5% to 18%, and P_2O_5 from .44% to .7%. It may be noteworthy that the TiO_2 and P_2O_5 trends project back through the origin, while that of Al_2O_3 intersects the Y-axis at 4% Al_2O_3. An important feature of the chemistry of the Makwassie porphyries is that the trends displayed by SiO_2 and the immobile oxides, TiO_2, Al_2O_3 and P_2O_5, are similar to those produced by samples DP-33 and JA-371 in relation to the bulk of the Dominion porphyries and the Jeppestown amygdaloid samples respectively. The significance of this observation will be assessed in Chapter VII.

(c) Trace Element Variations : A feature of the trace element variation diagrams (Figure 17) is the relative consistency of slope defined by the most incompatible, immobile elements, Nb,

Figure 17: (3 pages following) Trace element versus Zr variation diagrams - Ventersdorp Supergroup and Jeppestown amygdaloid lavas. Dashed line indicates the Dominion basic lava trend. Symbols as in Figure 15.

Figure 17: (cont.)

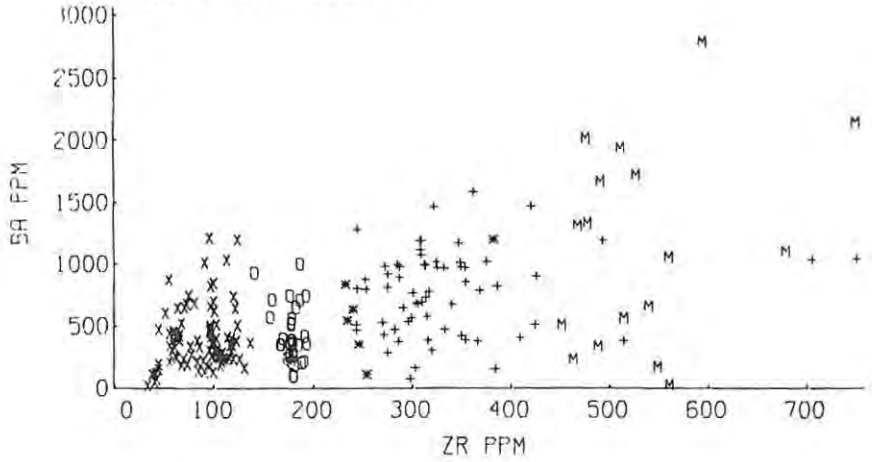

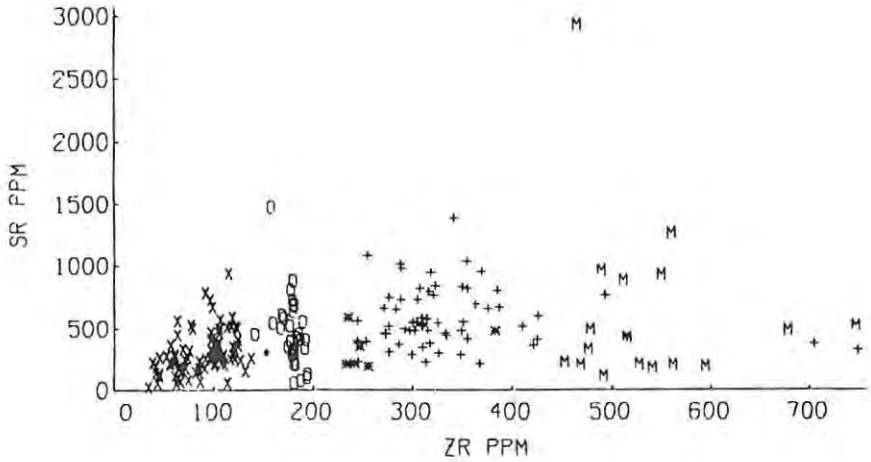

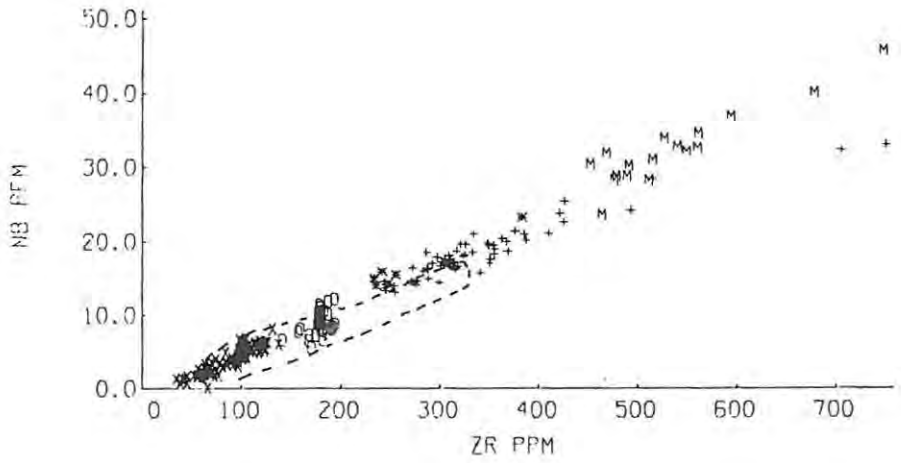

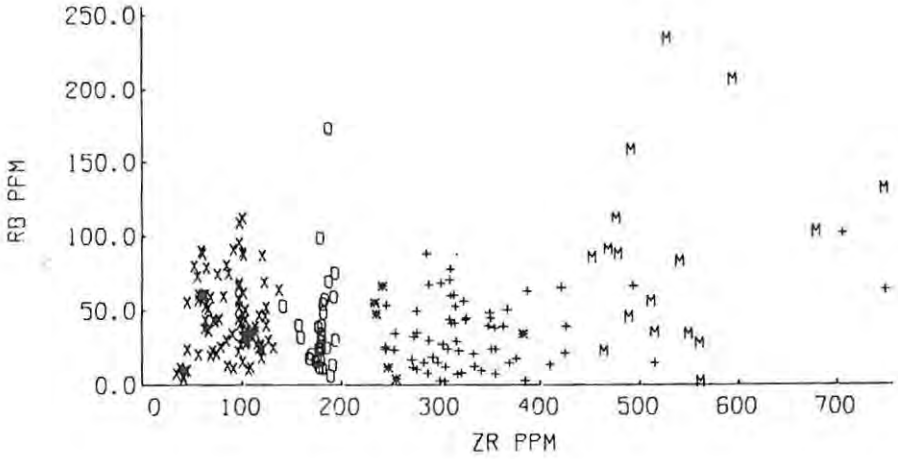

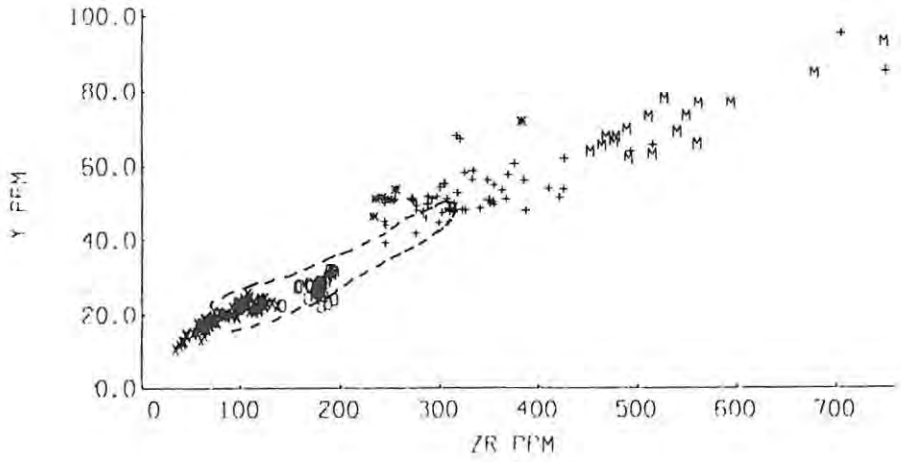

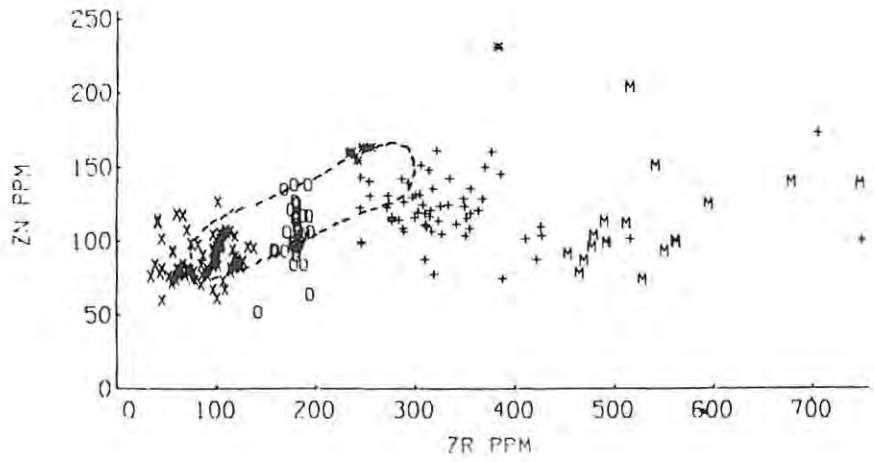

Figure 17: (cont.)

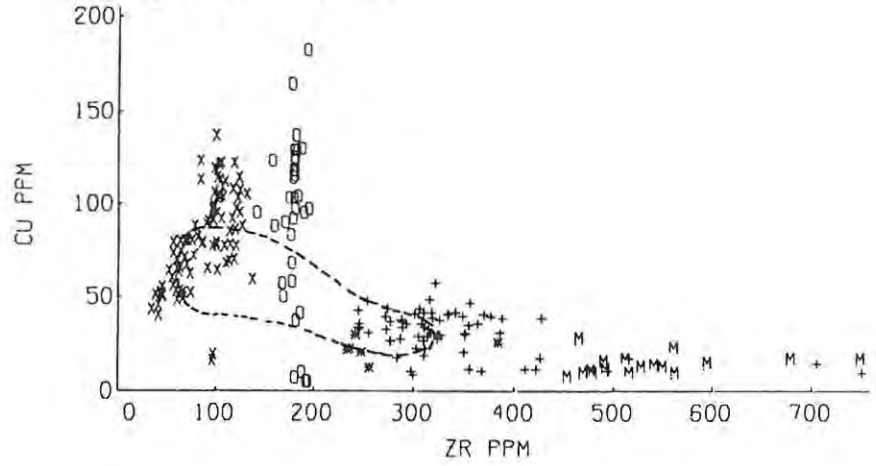

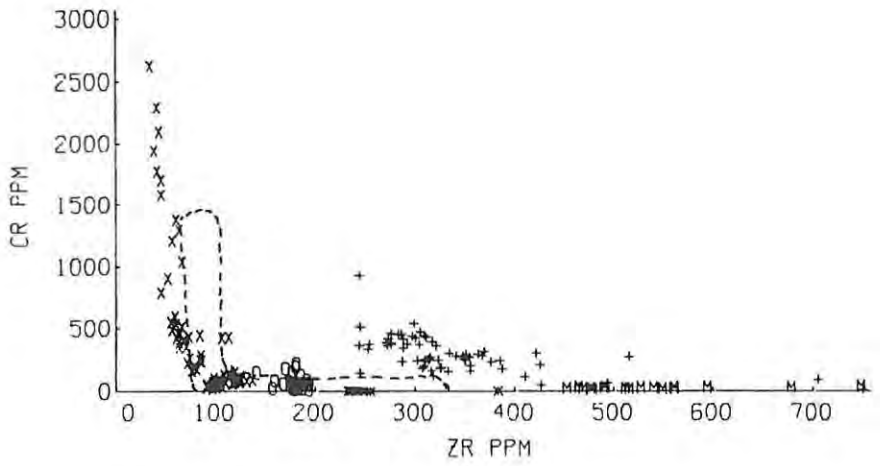

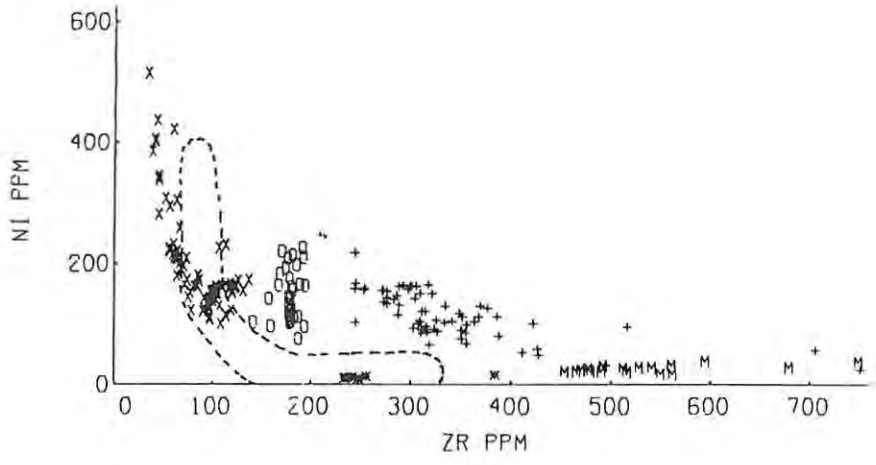

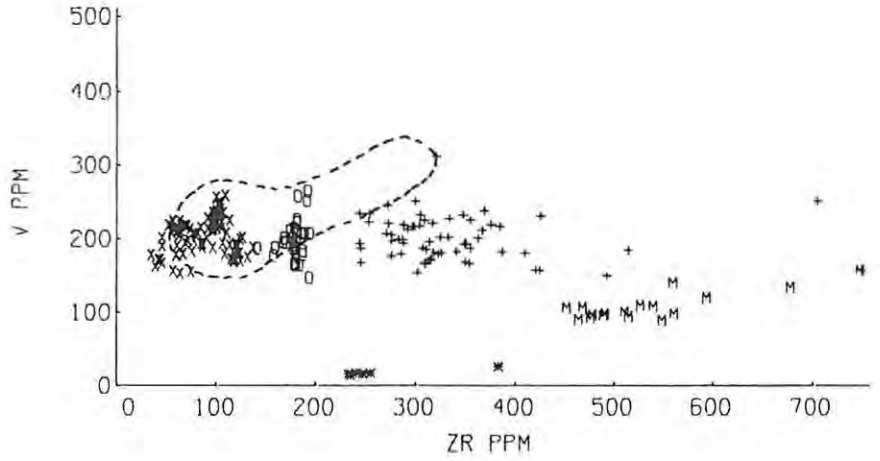

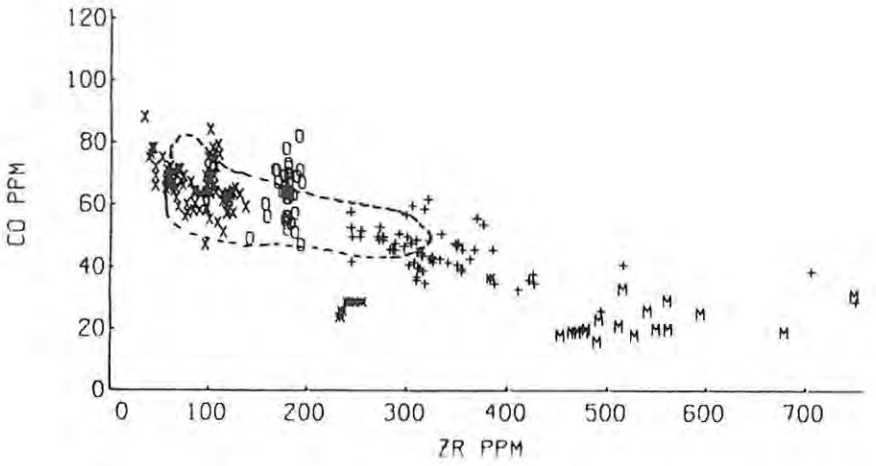

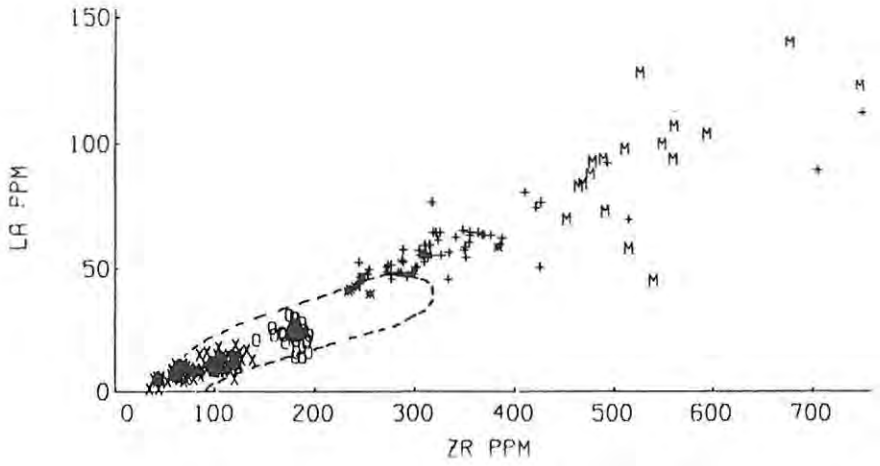

Figure 17: (cont.)

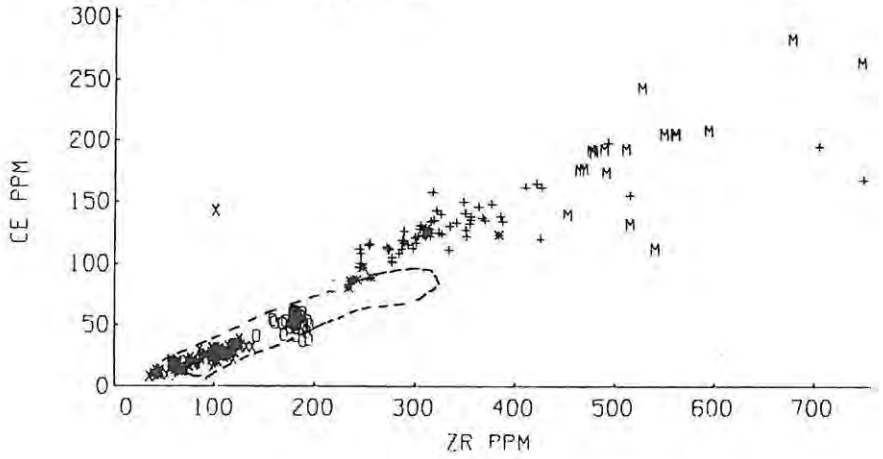

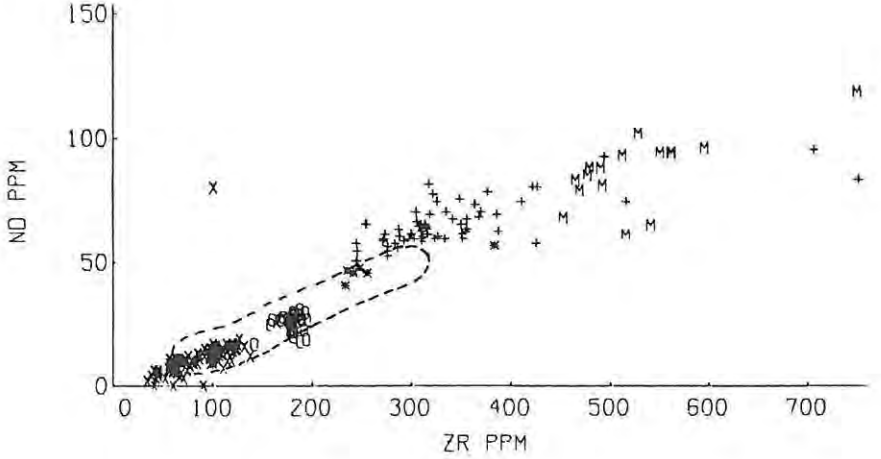

La, Ce, Nd and to a lesser extent Y plotted against Zr, for all the lava groups of the Witwatersrand triad, thus forming apparently continuous variation trends both within and between the various lava groups. It is also noteworthy that TiO_2 and P_2O_5, which in most instances appear to behave as incompatible elements, do not display this consistent relationship, as has been demonstrated in the previous sections.

Nb shows the most consistent trend. It ranges between 0 and 8ppm in the Klipriviersberg Group, clusters about means of 8.9 and 15.1ppm in the Allanridge and Jeppestown lavas respectively, and is enriched from 15 to 25ppm in the Goedgenoeg/Rietgat formations, and from 25 to 45ppm in the Makwassie porphyries.

The trend produced by Y is not as consistent as the Nb trend, and the Y versus Zr variation in the Klipriviersberg Group as a whole is non-linear, displaying a gradually decreasing rate of enrichment of Y relative to Zr. Y concentrations in the Allanridge formation cluster about a mean of 27.2ppm, falling on a projection of the Klipriviersberg trend. The remaining formations are enriched in Y relative to the latter trend, with the Jeppestown samples clustering about a 51.3ppm mean, and the Goedgenoeg/Rietgat and Makwassie samples increasing from around 40 to 60ppm and 60 to 90ppm respectively.

The rare-earth elements La, Ce and Nd show similar trends to Nb, although the Jeppestown amydaloid and Goedgenoeg/Rietgat samples again show a slight relative enrichment, and the Makwassie porphyries show appreciable scatter. Overall ranges exhibited by the lavas are approximately from below detection limits to 130, 270 and 120ppm for La, Ce and Nd respectively.

In contrast to these coherent trends, Ba, Sr and Rb are highly scattered. This reflects their mobility during low-grade regional metamorphism, and they are thus of little petrogenetic value.

In the Klipriviersberg samples, the transition elements Co, V, Zn and Cu exhibit similar breaks in the variation trends to

those displayed by Fe_2O_3, thus illustrating the subtle compositional differences between the Loraine/Edenville, Orkney and Alberton formation lavas. This is best illustrated by Co, which is depleted from 80ppm to below 60ppm in the Loraine/Edenville formations. The Orkney formation shows a scatter of between 60 and 80ppm Co, with a mean of 67ppm, which distinguishes it from the Alberton formation which clusters about a 60ppm mean. A similar relationship is displayed by V, which shows a similar configuration to that of Fe_2O_3 on the variation diagrams. Concentrations in the Loraine/Edenville formation are scattered about a mean of 194ppm, while the Orkney formation is appreciably enriched, averaging 226ppm. The Alberton formation, with V values showing a similar degree of scatter to those in the latter samples, is more depleted, with an average of 184ppm V. Zn shows a similar distribution to that of V, although more scattered. The mean Zn content of the Loraine/Edenville formations is 85ppm, although this may be an overestimate as the scatter appears to be biased towards higher Zn levels. The Orkney samples have a higher mean Zn content of 92ppm, while the Alberton formation averages 85ppm. Cu is highly scattered, yet is noteworthy in that the Loraine/Edenville lavas show a crude enrichment between 40 and 80ppm, as opposed to the depletion observed in the Dominion basic lavas. The Orkney and Alberton lavas have mean Cu levels of 95ppm and 92ppm respectively, although it appears that the former are, in general, more enriched in Cu than the latter, with the lower mean resulting from several samples being extremely depleted in Cu, a feature which is probably of secondary origin.

Cr and Ni display a strong coherence with MgO. Cr is rapidly depleted from 2600ppm to around 200ppm in the Loraine/Edenville formations and clusters about means of 51ppm and 124ppm in the Orkney and Alberton formations respectively. It is interesting to note the higher levels of Cr in the Alberton lavas, despite their higher incompatible element concentrations. (A similar situation is also evident in the MgO vs Zr plot, although masked by scatter.) Ni exhibits a similar pattern, decreasing from over 500ppm to around 180ppm in the Loraine/Edenville formations, while the Orkney and Alberton formations average

142ppm and 158ppm respectively.

The Allanridge formation displays a large variation in transition element abundances relative to Zr. However, as in all cases this appears to be random scatter, the means (in brackets below) may be considered representative. The average Zn level (105ppm) is higher than that of the Klipriviersberg lavas, while the remaining elements fall within the range of the Orkney and Alberton formations. Cu (91ppm) shows an extremely large degree of secondary variation, far surpassing that of the other formations. The degree of scatter in Ni (148ppm), Co (63ppm) and V (196ppm) is slightly higher than that observed for the Orkney and Alberton formations combined, while Cr (61ppm) forms a relatively tight cluster, and is lower than in the Orkney formation.

The Goedgenoeg/Rietgat lavas are characterized by poorly-defined to non-existent trends in their transition element variations relative to Zr. Zn is randomly scattered between 100 and 150ppm, with a mean of 121ppm being slightly higher than that of the Allanridge lavas. Cu (31ppm) is much lower than in the formations already discussed and is also randomly scattered, as is V (202ppm) whose levels are equivalent to those of the Allanridge and Klipriviersberg lavas. Ni (123ppm), Co (46ppm) and Cr (315ppm) all display crude depletion trends, approximately from 150 to 80ppm, 50 to 35ppm and 400 to 200ppm respectively. While Ni and Co is lower than in the Alberton, Orkney and Allanridge lavas, Cr is higher.

Relative to the Goedgenoeg/Rietgat lavas, the Jeppestown amygdaloid (excluding sample JA-371) has higher Zn (161ppm) slightly lower Cu (22ppm) and much lower Ni (13ppm), Co (27ppm), Cr (7ppm) and V (17ppm). In all cases, sample JA-371 is enriched relative to the mean, such that it falls on the projection of a line passing through the mean and through or close to the origin, although in the case of Cr this relationship is obscured because of extremely low concentrations.

The Makwassie porphyries display pronounced linear trends for

the transition element variations with Zr, projecting through or close to the origin, although the Zn trend is poorly defined due to pronounced scatter. The concentrations of all these elements are lower than in the Goedgenoeg/Rietgat formations. Zn shows an approximate enrichment from 80 to 130ppm, Cu from 10 to 20ppm, Ni from 20 to 40ppm, Co from 20 to 30ppm, Cr from 20 to 40ppm and V from 90 to 160ppm. These trends are thus similar to those produced by sample JA-371 relative to the mean Jeppestown compositions, and similar in some respects to the relationship of sample DP-33 relative to the bulk of the Dominion porphyry samples. These relationships are consistent with those noted for the major element concentrations in these samples.

E. Discussion : Geochemistry and Classification of the Witwatersrand Triad Lavas

1. Introduction

A systematic attempt to classify the lavas, and to demonstrate how they compare compositionally with other lava sequences, is currently being undertaken by T.B. Bowen (1984) and these aspects will thus not be considered in detail in this thesis. A brief summary of the general geochemical characteristics of these lavas is presented here in order to demonstrate the broad compositional differences between lava suites, to emphasize the unifying features of these lavas and to present a basis for the interpretations presented in the succeeding chapters. As a means to this end, Table II has been compiled. It contains both representative and average analyses of the Witwatersrand triad lavas. The means of the Dominion porphyries, exclusive of sample DP-33, the Jeppestown amygdaloid, exclusive of sample JA-371, and the Alberton, Orkney and Allanridge formations are considered representative of these lava types in view of the limited compositional variation occurring within them. Means of the Dominion basic lavas, the Loraine/Edenville, Geodgenoeg/Rietgat and Makwassie formations, as well as the intrusive samples, should be treated with caution because of the significant degrees of compositional variation within these suites which are probably due to magmatic processes and

TABLE II: Representative analyses and means of the various magma types, with C.I.P.W. norms (See text for source of data).

	1	2	3	4	5	6	7	8	9	10
SiO_2	51.70	53.61	56.86	58.84	52.81	53.97	54.00	55.41	50.54	52.75
TiO_2	0.763	0.728	1.093	1.681	0.400	0.588	0.980	1.067	0.423	0.614
Al_2O_3	13.06	14.64	14.72	12.89	8.59	13.15	14.85	14.95	14.37	14.38
Fe_2O_3	12.36	11.05	11.95	13.33	12.17	11.26	12.67	11.44	9.56	11.21
MnO	0.18	0.16	0.16	0.16	0.17	0.17	0.15	0.13	0.14	0.17
MgO	9.15	7.64	4.17	2.88	17.46	9.03	5.00	5.12	10.19	7.69
CaO	9.54	8.31	6.31	5.84	8.06	7.90	7.45	7.19	12.57	9.99
Na_2O	2.50	2.95	3.33	2.69	0.19	2.62	3.45	3.40	1.54	2.33
K_2O	0.57	0.75	1.11	1.11	0.11	1.24	1.32	1.13	0.63	0.80
P_2O_5	0.172	0.156	0.296	0.583	0.039	0.078	0.126	0.156	0.035	0.064
Ba	223	320	522	531	16	346	421	438	108	177
Nb	3.6	3.6	7.3	12.6	1.2	2.2	4.9	5.5	0.4	1.2
Zr	80	89	165	269	34	64	100	116	32	52
Y	20.3	19.8	28.6	41.9	10.4	16.7	22.5	22.2	16.7	21.4
Sr	343	402	412	453	20	206	344	393	192	168
Rb	14.7	16.6	28.8	44.4	7.6	42.7	50.0	39.4	27.6	39.2
Zn	93	95	116	130	76	85	92	85	59	78
Cu	71	67	52	30	43	66	95	92	75	95
Ni	321	268	58	38	516	248	142	158	220	117
Co	79	66	59	55	88	68	67	61	55	59
Cr	1158	763	21	45	2618	778	51	124	1119	120
V	239	209	271	312	178	194	266	184	225	260
La	9	10	23	36	1	7	11	12	5	5
Ce	24	23	48	80	8	16	29	30	1	8
Nd	16	14	27	45	2	7	14	14	4	7
Ap	0.40	0.38	0.71	1.40	0.09	0.19	0.28	0.38	0.09	0.14
Il	1.45	1.37	2.07	3.19	0.75	1.11	1.80	2.03	0.81	1.16
Or	3.43	4.49	6.62	6.62	0.65	7.39	8.27	6.74	3.78	4.79
Ab	21.41	25.21	28.43	23.01	1.61	22.42	29.87	29.02	13.11	19.88
An	22.95	24.71	22.19	20.07	22.51	20.65	20.57	22.44	30.69	26.68
C	0.00	0.00	0.00	0.00	0.00	0.00	0.00	0.00	0.00	0.00
Mt	2.77	2.46	2.67	2.99	2.73	2.51	2.83	2.55	2.13	2.51
Dien	5.73	3.75	1.35	0.76	5.02	4.54	2.78	2.54	8.51	5.38
Difs	3.74	2.60	1.79	1.56	1.75	2.77	3.14	2.61	3.94	3.83
Diwo	9.92	6.63	3.13	2.25	7.35	7.69	5.98	5.23	13.32	9.60
Wo	0.00	0.00	0.00	0.00	0.00	0.00	0.00	0.00	0.00	0.00
Hyen	16.51	15.45	9.14	6.48	38.91	18.17	10.52	10.34	13.69	13.94
Hyfs	10.76	10.74	12.13	13.18	13.59	11.09	11.87	10.62	6.34	9.91
Q	0.00	2.21	9.79	18.52	5.03	1.49	2.11	5.51	0.00	2.17
Fo	0.56	0.00	0.00	0.00	0.00	0.00	0.00	0.00	2.36	0.00
Fa	0.40	0.00	0.00	0.00	0.00	0.00	0.00	0.00	1.21	0.00
Ne	0.00	0.00	0.00	0.00	0.00	0.00	0.00	0.00	0.00	0.00
D.I.	25	32	45	48	7	31	40	41	17	27
$\frac{100An}{Ab + An}$	52	49	44	47	93	48	41	44	70	57
M-value	63	62	45	34	77	65	49	51	71	62

TABLE II (cont.)

	11	12	13	14	15	16	17	18	19	20
SiO_2	51.12	56.34	53.31	61.88	56.73	65.34	59.75	68.29	64.56	70.14
TiO_2	0.464	1.190	1.637	1.460	1.515	1.026	1.373	1.064	1.222	0.790
Al_2O_3	14.66	14.66	13.49	13.70	14.45	12.60	15.48	13.09	14.46	12.64
Fe_2O_3	9.84	11.44	12.81	7.77	10.62	11.80	8.59	6.05	7.62	6.71
MnO	0.15	0.15	0.16	0.09	0.14	0.16	0.05	0.05	0.09	0.08
MgO	9.49	4.22	7.09	2.88	5.16	0.91	3.76	0.77	2.43	1.13
CaO	11.51	7.00	6.74	6.18	6.24	2.95	2.44	2.65	3.34	2.02
Na_2O	1.62	3.26	2.82	3.17	2.98	3.60	0.51	2.96	3.03	3.22
K_2O	1.06	1.50	1.18	2.16	1.45	1.11	7.47	4.64	2.73	3.03
P_2O_5	0.043	0.233	0.760	0.713	0.717	0.506	0.584	0.436	0.521	0.245
Ba	371	419	522	1131	776	504	2784	2017	1151	757
Nb	0.7	8.9	13.8	18.2	17.7	15.1	30.9	28.3	32.4	13.7
Zr	35	178	244	309	318	242	594	476	535	273
Y	17.4	27.2	50.7	45.4	51.8	51.3	76.8	66.4	71.6	29.3
Sr	188	448	566	596	596	314	191	330	622	191
Rb	48.4	37.3	26.1	44.5	33.4	37.4	207.2	112.3	89.2	81.7
Zn	69	105	144	88	121	161	125	96	112	84
Cu	79	91	43	42	33	22	15	11	14	14
Ni	188	148	161	107	123	13	38	25	25	10
Co	57	63	53	36	46	27	25	19	22	18
Cr	708	61	369	207	315	7	27	20	23	5
V	230	196	236	168	202	17	120	91	107	52
La	3	23	53	55	57	43	104	88	93	49
Ce	4	51	113	123	127	89	208	192	194	93
Nd	6	25	58	63	64	46	96	85	93	40
Ap	0.09	0.57	1.82	1.71	1.71	1.21	1.40	1.04	1.23	0.59
Il	0.88	2.25	3.12	2.76	2.87	1.95	2.59	2.01	2.31	1.48
Or	6.32	8.92	7.03	12.82	8.63	6.62	44.44	27.54	16.25	18.02
Ab	13.79	27.84	24.11	26.99	25.47	30.80	4.32	25.21	25.81	27.41
An	29.88	21.16	20.91	16.90	21.96	11.45	8.35	8.77	13.27	8.44
C	0.00	0.00	0.00	0.00	0.00	1.33	3.55	0.00	1.69	0.99
Mt	2.19	2.55	2.87	1.73	2.36	2.64	1.91	1.35	1.70	1.49
Dien	7.17	2.30	1.77	1.84	0.99	0.00	0.00	0.16	0.00	0.00
Di'fs	3.66	2.83	1.40	1.97	0.87	0.00	0.00	0.52	0.00	0.00
Diwo	11.53	5.16	3.27	3.86	1.92	0.00	0.00	0.65	0.00	0.00
Wo	0.00	0.00	0.00	0.00	0.00	0.00	0.00	0.00	0.00	0.00
Hyen	14.97	8.31	16.09	5.39	11.98	2.29	9.44	1.75	6.10	2.84
Hyfs	7.65	10.24	12.73	5.79	10.58	13.81	8.90	5.60	7.96	7.48
Q	0.00	7.88	4.92	18.28	10.69	27.94	15.13	25.41	23.71	31.27
Fo	1.18	0.00	0.00	0.00	0.00	0.00	0.00	0.00	0.00	0.00
Fa	0.67	0.00	0.00	0.00	0.00	0.00	0.00	0.00	0.00	0.00
Ne	0.00	0.00	0.00	0.00	0.00	0.00	0.00	0.00	0.00	0.00
D.I.	20	45	36	58	45	65	64	78	66	77
$\frac{100An}{Ab + An}$	68	43	46	38	46	27	66	26	34	24
M-value	69	46	56	46	53	6	51	23	43	28

not alteration. For this reason some individual analyses have been included in Table II, although these too may not be strictly representative because of varying degrees of scatter of individual elements as demonstrated in the previous section. They do, however, in conjunction with the means, serve to illustrate the pertinent features of these lavas.

2. Source of Data in Table II

Analyses 1 to 4 in Table II are from the Dominion basic lava suite. Analysis 1 is that of sample DB-93, and is typical of the most basic samples of the suite, which in the following chapter will be shown to be parental to the more evolved lavas. Analyses 2 to 4 represent means of progressively more evolved lavas of this sequence, and were determined by arbitrarily subdividing the sample population on the basis of Zr content, at the 125ppm and 210ppm Zr levels. On this basis, analyses 2, 3 and 4 represent means of 29, 25 and 18 samples respectively.

The Klipriviersberg lavas are represented by analyses 5 to 8. Analysis 5 is that of sample KL-468, the most basic sample of the Loraine/Edenville formation, while analysis 6 represents the mean of 39 Loraine/Edenville samples, within which a significant component of magmatic variation is present. Analyses 7 and 8 are the means of 32 Orkney and 19 Alberton formation samples respectively.

Although very little mention has been made of the intrusive samples, the majority of those analysed appear to have Klipriviersberg affinities. Analyses 9 and 10 are those of samples IN-44 and IN-87, representing a basic and more evolved composition respectively. Analysis 11 is the mean of the seven intrusive samples from boreholes DSF-7 and DRS-6. Other intrusives listed in Table I, namely IN-395, IN-419 and IN-421 appear to have Goedgenoeg/Rietgat affinities, although IN-419 has an anomalously low P_2O_5 content, while IN-395 and IN-419 are anomalously low in SiO_2. This may be due to secondary alteration. It should be noted that the intrusive nature of these three samples has not been established with certainty, and time limitations have prevented further investigation of this problem.

Analysis 12 is the mean Allanridge formation composition (34 samples). Although many elements exhibit large degrees of scatter in the Zr variation diagrams (Figures 15 and 17), this is probably of a secondary origin, since the immobile elements are not significantly affected. Analysis 12 is thus considered to be representative of the Allanridge formation magma, since secondary alteration is thought to be effectively of a closed-system type (see subsection 5 below).

The Goedgenoeg/Rietgat formations are represented by analyses 13 to 15. As mentioned in previous sections, a substantial proportion of incoherent compositional variation occurs within this suite and analyses 13 and 14, respectively representing samples PG-165 and PG-173, serve to illustrate the degree of chemical diversity, although they do not necessarily represent end-members of a differentiated sequence. Analysis 15 is the mean of 62 samples with the omission of the four samples previously mentioned as being more akin to the Makwassie porphyries.

The remaining analyses in Table II are of the more acid members of the Witwatersrand triad, with analysis 16 being the mean composition of the Jeppestown amygdaloid exclusive of sample JA-371, and analysis 20 the mean composition of the Dominion porphyries exclusive of sample DP-33. Analyses 17 and 18 represent samples PM-209 and PM-210, of the Makwassie porphyries respectively. These serve to demonstrate the compositional variation of these porphyries as illustrated in the Zr-variation diagrams (Figures 15 and 17), with analysis 18 being of a low-Zr sample, and 17 an example of the high-Zr types. Analysis 19 represents the mean of the 17 analysed Makwassie samples.

3. General Observations

From the variation diagrams presented in Section D and the analyses and means tabulated in Tables I and II, it is clear that only the Dominion basic lavas and those of the Loraine/Edenville formations contain truly basaltic types. Despite high MgO contents (i.e. up to 17.5%; analysis 5, Table II), only some of the most basic samples, including some of the intrusives, are olivine normative. This is a result of the high SiO_2 contents of these lavas in comparison to

younger tholeiitic rocks of equivalent MgO levels. Another feature of the high MgO lavas is their high concentrations of Cr and Ni. The majority of samples from all the formations excluding the Jeppestown amygdaloid, Makwassie and Dominion porphyries, are basic-intermediate to intermediate in composition, and have hence often been referred to in the literature as "andesites", a term which has been incorporated into the formal stratigraphic nomenclature of these rocks (see Chapter II).

Within the basic-intermediate to intermediate samples, considerable overlap is present between the major oxide compositions of samples of various suites, while certain minor oxides and trace elements display major between-suite differences and serve to discriminate between the various lava types (see T.B. Bowen, 1984). This feature is best illustrated by the incompatible elements, Zr, Ti and P. Although overlap occurs between the Dominion basic lava sequence and various Ventersdorp suites, combinations of the latter elements have proved to be efficient discriminators (see T.B. Bowen, 1984). In practice, the most useful discriminating variables are the Ti/P and Ti/Zr ratios, which when plotted against one another, yield a useful discrimination diagram which is presented in Figure 18. Thus, while superficially many of the lavas are compositionally similar, minor elements show them to be quite diverse.

Each of the more acid suites, namely the Jeppestown amygdaloid, Dominion and Makwassie porphyry formations, also displays distinctive chemical features. Although in Figure 18 the Jeppestown samples overlap with the Goedgenoeg/Rietgat formation samples, absolute abundances of various elements, especially SiO_2, Ni, Cr and V, serve to distinguish them unequivocally.

4. Tentative Classification and Nomenclature

A systematic classification of the Witwatersrand triad lavas is a difficult exercise in view of the unusual chemistry displayed by these rocks. This discussion is intended merely to point out the problematical features and to suggest a tentative nomenclature for these lavas, which may be superceded by conclusions reached by T.B. Bowen (1984).

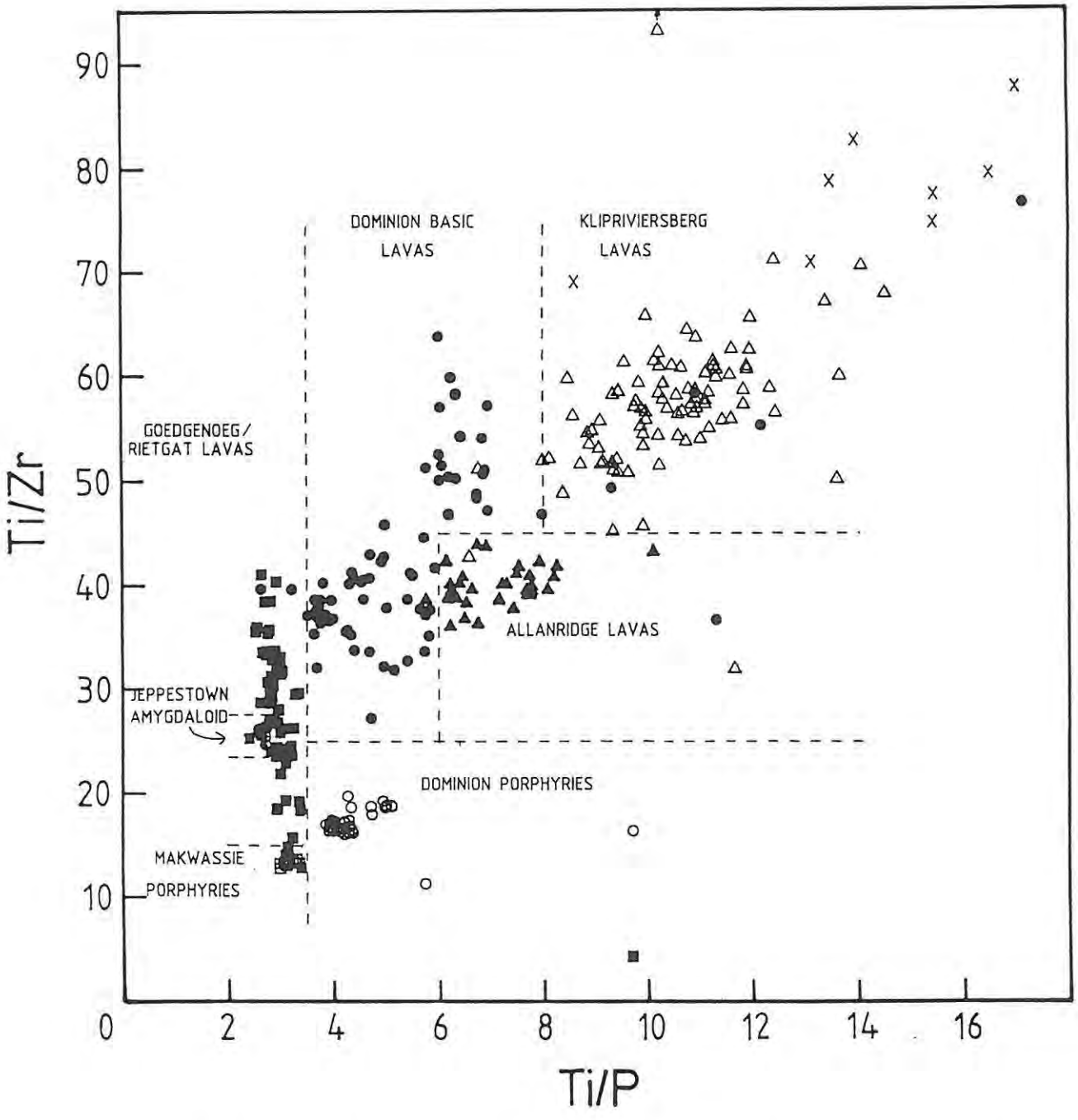

Figure 18: Ti/Zr versus Ti/P discrimination diagram. Open triangles - Klipriviersberg lavas; solid squares - Goedgenoeg/Rietgat lavas; open squares - Makwassie porphyries; solid triangles - Allanridge lavas; solid circles - Dominion basic lavas; open circles - Dominion porphyries; crossed circles - Jeppestown amygdaloid lavas; crosses - intrusives.

Since the term "andesite" has generally been applied to these lavas, it might be appropriate at this stage to assess its suitability. Wyatt (1976) discussed the systematic classification of Klipriviersberg lavas from an area near Johannesburg. These lavas are identical compositionally to the bulk of the Klipriviersberg samples analysed in the current study, although Wyatt's study did not reveal the presence of high-Mg lavas in the upper Klipriviersberg formations. He showed that while the lavas displayed some features characteristic of calc-alkaline provinces, the bulk of the evidence suggested they were more akin to tholeiitic flood basalts, despite their relatively high SiO_2 and alkali contents. An important factor leading to this conclusion was the low Al_2O_3 contents. Irvine and Baragar (1971) noted that the main difference between calc-alkaline and tholeiitic basalts was in the Al_2O_3 content, being between 16% and 20% in the former, and between 12% and 16% in the latter. All the basic to intermediate lava groups of the Witwatersrand triad have mean Al_2O_3 contents of less than 15%, suggesting tholeiitic affinities for the bulk of these lavas. Furthermore Taylor (1968) showed that low Ni abundances (less than 50ppm) are characteristic of andesites and high-alumina basalts, while the mean Ni concentrations of all the basic to intermediate lava groups in this study, except in the more evolved part of the Dominion basic sequence, are greater than 100ppm. Although differences are not always as pronounced as with Ni, trace element levels on the whole, including those of TiO_2 and P_2O_5, are generally typical of tholeiitic basalts.

In view of the presence of intermediate SiO_2 levels as well as intermediate to low MgO contents in the more evolved lavas, it would seem appropriate to employ the nomenclature outlined by Wilkinson and Binns (1977). According to their scheme, the majority of the Witwatersrand triad lavas lie within their definition of "tholeiitic andesites", in that they have normative plagioclase between An_{30} and An_{50}, contain less than 10 wt% normative quartz (may be olivine normative), D.I. greater than 35, and M-values less than 50. In contrast, olivine tholeiite and tholeiitic basalt has a more calcic normative plagioclase composition, D.I.'s generally less than 30, and M-values often greater than 60. At the opposite extreme, tholeiitic dacites (or icelandites) have a normative quartz content greater than

10 wt%, normative plagioclase compositions between An_{20} and An_{30}, and D.I.'s greater than 60.

Applying this scheme to the Witwatersrand triad lavas (see Table II), the Dominion basic lavas extend from the tholeiite field into the tholeiitic andesite field, which contains the majority of samples. For the more evolved lavas of this sequence most criteria indicate tholeiitic andesite, but normative quartz contents are too high. The intrusives can all be classified as tholeiites, while the lavas of the Loraine/Edenville formation range from tholeiites to tholeiitic andesites. The mean Loraine/Edenville lava composition is approximately intermediate between these two fields. Tholeiitic andesites predominate in the Alberton and Orkney formations, although some samples are tholeiites. Samples from the Allanridge and Goedgenoeg/Rietgat formations are predominantly tholeiitic andesites, although lavas from the latter formation are unusual in that mean normative quartz levels are just over 10% and mean M-value is just over 50. These contradictory features of the Goedgenoeg/Rietgat lavas have important petrogenetic implications which will be discussed in Chapter VII. The Jeppestown, Dominion and Makwassie samples plot as tholeiitic dacites, although the Makwassie porphyries have a mean normative plagioclase composition which is too calcic. The validity of the Wilkinson and Binns classification scheme for the more acid rocks is open to question since the assumed Fe_2O_3/FeO ratio of .2 is possibly not applicable to these lavas. The Dominion porphyries are the most silicic of the lavas analysed, and mean SiO_2 contents of 70.14% is sufficiently diagnostic to classify them as rhyolites. More systematic work is required, however, to classify the acid lavas with more confidence.

In general, while the Wilkinson and Binns classification scheme is not entirely satisfactory for the Witwatersrand triad lavas, it is attractive because it describes both the tholeiitic nature and the intermediate compositions of the bulk of the lavas, and avoids the implications that the lavas are a calc-alkaline succession, a superficial conclusion which may result were the terms "andesites" or "basaltic andesites" employed. Some of the lavas are similar in some respects to the SiO_2- and MgO-rich bonninites and high-Mg andesites which have recently received much attention in the literature (e.g.

Dallwitz, 1968; Jenner, 1981; Tatsumi, 1981), but are generally too SiO_2-poor for equivalent MgO contents. A few of the high-Mg samples may resemble basaltic komatiites, the criteria for classification of which has recently undergone various modifications (e.g. Arndt et al., 1977). A group of high-Mg lavas at the base of the Ventersdorp succession in Wyatt's (1976) study area, making up part of the Westonaria formation (see Chapter II), has been interpreted by McIver et al. (1982) as having komatiitic affinities. While some of the high-Mg samples of the Loraine/Edenville formation are compositionally similar to these basal volcanics, trace element concentrations are irreconcilable and they are unlikely to be related genetically. Furthermore, the lack of spinifex texture and the relative rarity of high-Mg samples of true basaltic komatiite composition in the lavas of the present study is considered to render any attempt to equate these lavas with a komatiite sequence of dubious value.

It is suggested that the term "magnesian tholeiite" might be more appropriate for the Mg, Cr and Ni-rich lavas of the Dominion and Loraine/Edenville sequences. There appears to be no established classification scheme present which adequately caters for the Witwatersrand triad lavas.

5. Comments on the Possible Occurrence and Effects of Metasomatism in the Witwatersrand Triad Lavas.

Cornell (1978) has proposed that a burial metamorphic and metasomatic event may have affected the rocks occupying the vast area once covered by the Transvaal Supergroup. The purpose of this section is to examine this proposal, and to assess whether such a process may have significantly affected the igneous compositions of the lavas.

Cornell's (1978) hypothesis was based on seven samples (four of which were tuffaceous) taken from correlates of the Platberg Group which outcrop in the Prieska district, where they form the extreme south-western extension of the Ventersdorp Supergroup. His main lines of evidence were, firstly, that four samples defined a Rb-Sr isochron which yielded an age of 1920 $\pm$ 100 Ma. He considered this age to be too young, and the initial Sr-isotope ratio too high, to

represent a realistic magmatic isochron. Secondly, five of the seven samples were corundum-normative.

Cornell (1978) thus postulated that the Sr-isotope system of the lavas homogenized with that of associated basement-derived sediments by the migration of fluids under burial metamorphic conditions. He ascribed these conditions to an enhanced geothermal gradient associated with the emplacement of the Bushveld Complex, dated at between 1670 and 2095 Ma (see SACS, 1980). Elements such as Na_2O, K_2O and CaO were mobilized under these conditions, and a resultant loss of CaO caused an effective alumina oversaturation to which he attributed the corundum in the norms and a bulk compositional shift towards the compositions of the associated sediments.

Cornell (1978) furthermore attributes the compositional uniformity of the "upper Klipriviersberg lavas" studied by Wyatt (1976) to this metasomatic event. It is thus essential that the applicability of Cornell's (1978) hypothesis to the data from the Klerksdorp area be evaluated before any petrogenetic interpretation is attempted.

In the current study, petrographic evidence presented in Chapter V shows undoubtedly that the lavas have been metamorphosed to greenschist facies assemblages. Furthermore the geochemical data shows that a substantial number of samples from the Dominion porphyries, Makwassie porphyries, Jeppestown amygdaloid and Goedgenoeg/Rietgat formations do contain corundum in their norms (see T.B. Bowen, 1984), as do occasional samples from some of the other formations. Inspection of individual analyses, however, shows that the reasons for this alumina oversaturation are not consistent and result from depletions of one or all of Na_2O, K_2O and CaO, in various combinations, and occasionally from enrichment of Al_2O_3.

This is best illustrated in a sequence which does not appear to display any magmatic trends, such as the Dominion porphyries and Jeppestown amygdaloid. As suggested in Chapter V, the Jeppestown amygdaloid is probably the most prone to metasomatic modification, as it is of limited thickness and surrounded by thick sedimentary sequences. Thus samples JA-366 to 371 have normative corundum

contents which range from 0% in JA-366 to 3.8% in JA-371. Excluding sample JA-371, samples JA-368 and JA-370 display the highest normative corundum contents, viz. 3.3% and 2.1% respectively. The former occurs 12m from the top of the sequence in borehole JY-8, and the latter in the middle of the sequence in borehole R-1. Relative to the mean composition (analysis 16, Table II), sample JA-368 is strongly depleted in K_2O and to a lesser extent Na_2O, while the CaO level remains constant and Al_2O_3 is slightly depleted. In contrast, sample JA-370 is enriched in K_2O and Na_2O, and depleted in CaO, whereas Al_2O_3 is constant. As a result, their respective norms (see T.B. Bowen, 1984) display vastly different feldspar components, with JA-368 containing .89% orthoclase as opposed to 11.35% in JA-370, while a nett depletion in total Na_2O, K_2O and CaO could explain the presence of corundum.

The chemistry of sample JA-371 as a whole is anomolous, and its high Al_2O_3 content (19.57%) almost certainly accounts for its corundum-normative character. Similar samples are occasionally present in other formations, an example being DP-33 of the Dominion porphyries, with 21.63% Al_2O_3 and 10.00% corundum in the norm. This appears to be a localized process, however, since immobile element levels are also affected, and, as discussed in the previous section, such a process may account for the observed Makwassie trends.

The highly carbonated sample, KA-100 (see Chapter V), which occurs 2m above the Witwatersrand Supergroup sediments, is enriched in CaO and depleted in Na_2O relative to the mean Alberton formation composition (analysis 8, Table II), resulting in 5.44% orthoclase, 5.75% albite and 34.02% anorthite appearing in the norm, as compared with mean proportions of 6.74%, 29.02% and 22.44% respectively for these normative minerals.

Similar examples may be quoted from all formations studied, and while avoiding any petrogenetic interpretation at this stage, these observations lead to the conclusion that no systematic chemical variation due to metasomatic interaction with associated sediments is present, and the proximity of samples to these sediments is not reflected in any consistent manner in their chemical compositions. In most cases the corundum-normative character can be explained by

nett depletions of alkalies and CaO, which results in an effective alumina oversaturation, while other samples may have suffered a counterbalancing enrichment of these elements. Table II demonstrates that the mean of the Goedgenoeg/Rietgat formations is not corundum normative, while those of the Jeppestown amygdaloid, Dominion and Makwassie porphyries are, with a maximum of 1.6% corundum occurring in the Makwassie formation. Thus all mean compositions are within the 2% corundum limit considered by Cornell (1978) to be acceptable for acid igneous rocks. It is probably not fortuitous that the Makwassie porphyries have the highest mean corundum content, since as mentioned previously, the trends displayed by these rocks are similar to those displayed by samples DP-33 and JA-371 relative to their respective means, and may reflect some process other than a magmatic one. There is furthermore doubt as to the liquid character of the Makwassie samples (see Chapter V, Section D).

In general, the mean compositions listed in Table II and the Zr variation diagrams (Figures 11 to 17) support the assumption made earlier, that while elements such as K_2O, Na_2O and CaO are mobile to varying degrees in different formations, the mobilities are largely random due to small-scale metasomatic redistribution in small-scale alteration regimes. Thus on a larger scale the alteration would effectively be of a closed-system type, hence average trends should be representative of original magmatic trends, and concentrations of the less mobile elements should be realistic. While limited open-system metasomatic effects may be expected near sediment-lava boundaries, and boundaries between compositionally diverse lavas, it is evident that no widespread systematic alteration has occurred. Furthermore, the subtle but consistent bulk chemical differences between the constituent formations of the Klipriviersberg Group negates any suggestion that metasomatic homogenization of these lavas has occurred. The approach adopted in this study, outlined in Section C of this chapter, thus appears to be justified by the analytical data. i.e. If trends are reasonably coherent despite scatter of data, the use of average trends for petrogenetic modelling is valid.

VII EVALUATION OF THE COMPOSITIONAL VARIATION WITHIN SPECIFIC LAVA SUITES

A. Introduction

The objective of this chapter is to determine the possible evolutionary processes which have resulted in the compositional variations displayed within certain lava sequences as described and illustrated in Chapter VI. Consideration will be restricted to the formations which display compositional variations of sufficient magnitude as to allow rational geochemical trends to be resolved despite the scatter of data due to secondary processes. The compositional variation of the Dominion basic lava, Loraine/Edenville, Goedgenoeg/Rietgat and Makwassie formations will thus be evaluated.

Compositional variations within the Dominion porphyry, Jeppestown amygdaloid, Alberton, Orkney and Allanridge formations are generally too limited and/or too irrational to warrant attention in this chapter. Utilization of the mean compositions of these formations is therefore considered valid for the assessment of inter-formation relationships in Chapter VIII. However, it was noted in Chapter VI (Section D), that projections through compositionally anomalous samples of the Dominion porphyry and Jeppestown amygdaloid formations, and the respective means of these formations, produce trends similar to those defined by the Makwassie porphyry samples. For this reason the relationship of these anomalous samples to their respective formations will briefly be discussed in Section E, where the Makwassie porphyry trends are evaluated.

B. Dominion Basic Lavas

The high MgO, Cr and Ni contents of the more primitive lavas of the Dominion basic lava sequence warrant an assessment as to whether partial melting trends or reflections of source heterogeneities might be preserved in the data.

The chief criterion for the identification of primary mantle melts is an M-value of between 68 and 72, the range in which a liquid may be in equilibrium with mantle olivine (Green and Ringwood, 1967; Green et al., 1974). The more primitive Dominion basic lavas have a mean M-value of 62 (Table II), with a maximum of 68 displayed by sample DB-52. It is thus unlikely that any primary liquids are represented, and a limited amount of fractional crystallization has probably affected even the most primitive samples.

Moreover both Cr and Ni display rapid initial depletions with increasing Zr content (Figure 12), a feature which is to be expected for fractional crystallization and which is not compatible with partial melting. It may nevertheless be significant that in Figures 11 and 12, certain elements, particularly the siderophile elements, display relatively large degrees of scatter towards the low Zr side of the compositional spectrum. This is well illustrated by the plot of TiO_2 vs Zr (Figure 11). Since Ti and Zr are regarded as two of the most immobile elements, the observed scatter may be a reflection of source heterogeneity or variable degrees of partial melting rather than of secondary remobilization. Although such processes may have resulted in numerous sub-parallel liquid lines of descent which are only partially reflected by the data, the general trends, as evidenced by Cr and Ni vs Zr, appear to reflect a fractional crystallization control.

It is thus concluded that partial melting or source heterogeneity effects have not played a significant role in the generation of the observed variation trends, although they may have produced slight variations in the parent melt compositions resulting in excessive scatter of data in the subsequent differentiation curves. The rapid decrease in Cr and Ni concentrations with increasing Zr and the wide range of Zr concentrations are strong indicators of differentiation by fractional crystallization, which is considered below.

Petrographic examination (see Chapter V, Section B) has shown that the majority of samples are aphyric, and only the more evolved samples contain scattered, embayed plagioclase microphenocrysts. The generally aphyric nature of the samples is strong evidence that they represent a liquid line of descent, the proportion of plagioclase phenocrysts in the more evolved samples being insufficient to significantly affect the

liquid compositions. The presence of plagioclase suggests that it was a liquidus phase during the later stages of differentiation. Petrography does not provide any further clues to the identities of other participating phases, however, and all the common major liquidus phases in basaltic to intermediate magmas need to be considered. These are olivine, orthopyroxene (or pigeonite), augite, plagioclase and hornblende.

Figure 19 shows the variation of Al_2O_3, MgO and CaO relative to SiO_2. Both MgO and CaO show continuous depletion trends with increasing SiO_2, while Al_2O_3 is enriched initially and subsequently depleted. Insets in Figure 19 show to scale the visually estimated best fit curves for the respective plots. These curves are reproduced in Figure 20, on which suitable phenocryst compositions are plotted. The phenocryst compositions selected are presented in Table III.

The olivine composition was obtained from Deer et al., (1966). All others are those used by Reid (1979) for lavas of comparable composition. Vectors in Figure 20 illustrate the relative effects of removal of individual phenocryst phases on the liquid composition at both the most basic end of the trend and at the point where the Al_2O_3 curve is inflected.

Superficially, it appears from Figure 20 that the initial part of the differentiation trends may be produced by the removal of an assemblage comprising the common low-pressure phases, olivine, augite and plagioclase. However, the application of graphical methods, as described by Cox et al. (1979) (page 158), shows that no consistent proportions of these three phases can provide a solution to all three trends in Figure 20. The inclusion of orthopyroxene in the assemblage results in an even poorer fit, as does the exclusion of one or more of the anhydrous phases. Fractionation of hornblende alone, however, can account for the trends. Although hornblende may exhibit a relatively wide compositional range, Cawthorn (1976) has demonstrated that the CaO content of igneous amphibole remains fairly constant regardless of magma composition. It is thus probably not fortuitous that the selected hornblende composition lies almost directly on a projection of the Dominion trends.

Major oxide variation trends thus appear to favour a model whereby the initial stages of differentiation were dominated by hornblende

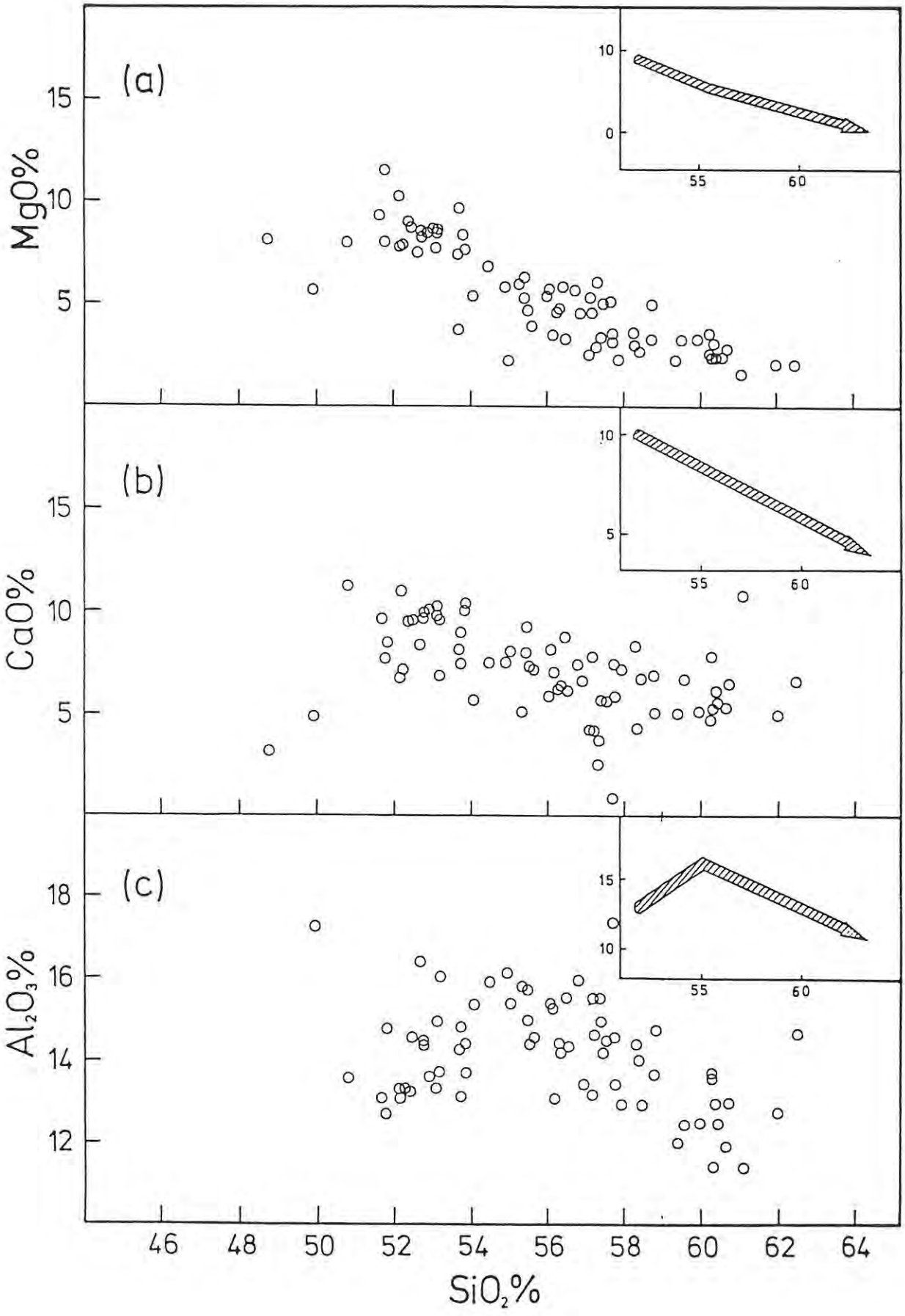

Figure 19: Variation of MgO, CaO and Al_2O_3 versus SiO_2 - Dominion basic lavas. Insets show visually-estimated best fit curves.

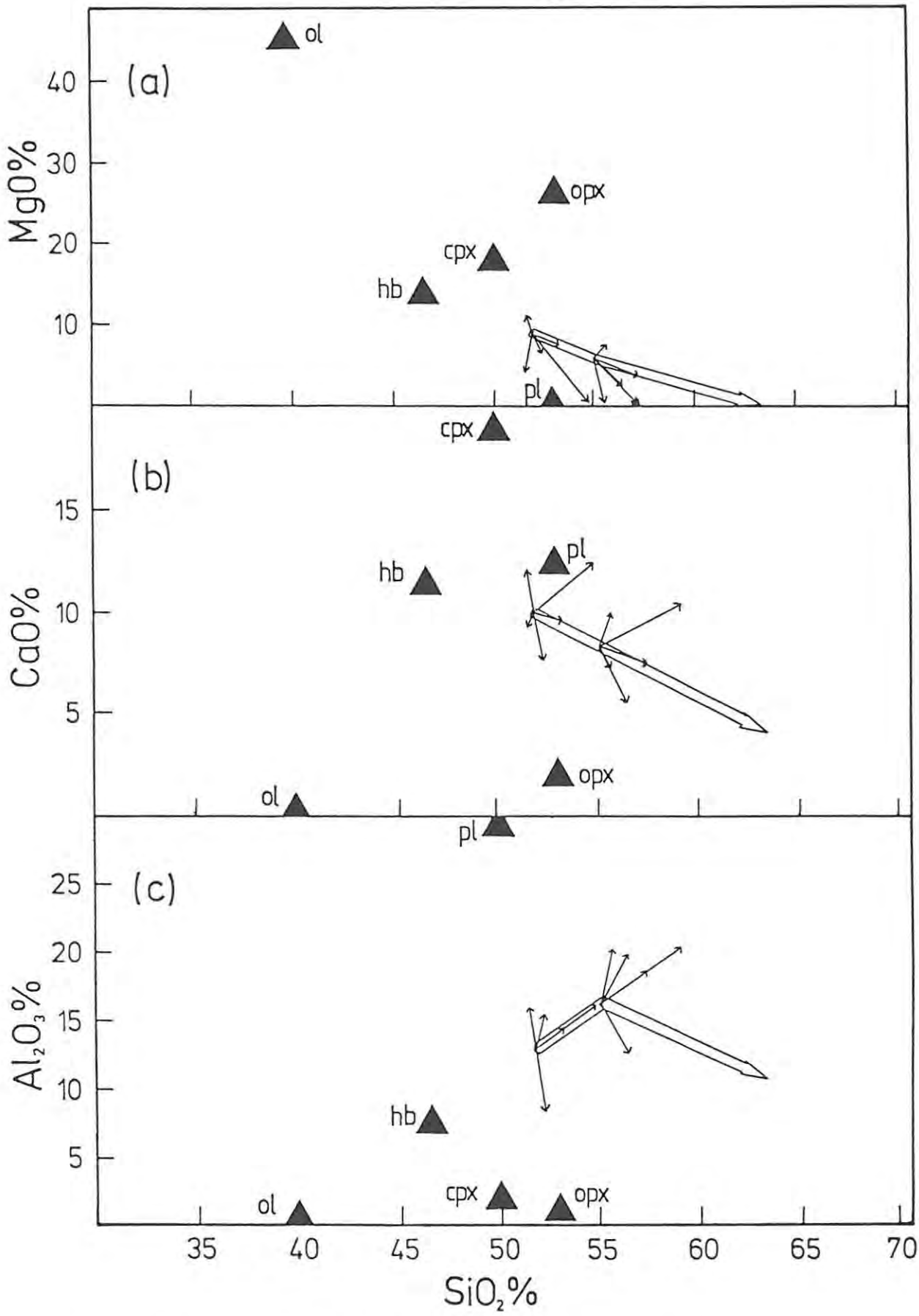

Figure 20: MgO, CaO and Al_2O_3 versus SiO_2 variation curves reproduced from Figure 19, with hypothetical phenocryst compositions and vectors illustrating the relative effects that the extraction of individual phenocrysts would have on the liquid composition.

TABLE III: Selected phenocryst compositions used for modelling the oxide trends of the Dominion basic lavas. (For source of data, see text).

	ol	opx	cpx	hb	pl
SiO_2	39.87	53.0	50.0	46.5	53.0
TiO_2	.03	.2	.5	2.0	-
Al_2O_3	-	1.0	2.0	7.7	30.0
Fe_2O_3	.86	-	-	-	-
FeO	13.20	17.0*	10.5*	16.1*	-
MnO	.22	-	-	-	-
MgO	45.38	26.8	17.8	13.7	-
CaO	.25	2.0	19.0	11.5	12.5
Na_2O	.04	-	.2	1.4	4.5
K_2O	.01	-	-	1.1	-

* All Fe as FeO

fractionation, although the possible participation of additional anhydrous phases cannot be ruled out at this stage. Assuming that hornblende represents the total extract, it can be shown by crude mass-balance type calculations that approximately 45% crystallization would be required to drive the liquid composition to the point where the Al_2O_3 content attains a maximum.

The second stage of differentiation is characterised by a depletion of Al_2O_3. This suggests that plagioclase must have become a dominating influence on the liquid line of descent. The fact that a change in the fractionating assemblage is required to satisfy the Al_2O_3 versus SiO_2 plot suggests that the liquid has transgressed the hornblende stability limits, possibly as a result of decreasing H_2O pressure or a change in temperature and total pressure conditions. Alternatively hornblende may persist as a liquidus phase and the commencement of plagioclase precipitation may simply be a result of the changing magma composition. The latter is considered unlikely in the light of trace element constraints which are discussed later. It is also unlikely that olivine could be a liquidus phase at this stage of the evolution of the magma. Whether hornblende persists or not, inspection of Figure 20 shows that a low-Ca pyroxene is required to counteract the effect of plagioclase fractionation on the rate of CaO depletion.

Plagioclase and a low-Ca pyroxene are thus the only essential components for the second stage of differentiation. Assuming these to be the only phases involved, calculations show that plagioclase must make up approximately 65% of the extract. Furthermore, 70% crystallization of the plagioclase/orthopyroxene assemblage is required to account for the compositional range observed in the second stage of differentiation.

The generation of the most evolved magmas of the Dominion basic lava sequence thus requires a total of 80% to 85% fractional crystallization of the most primitive magmas by the two-stage mechanism postulated above.

The model may be tested using trace element data. Pearce and Norry (1979) have demonstrated the usefulness of the immobile, incompatible elements as petrogenetic indicators, with the Zr/Y versus Zr relationship being particularly diagnostic.

Figure 21 illustrates the Zr/Y versus Zr relationship in the Dominion basic lavas. An arrow indicates the point along the trend which corresponds to the point of inflection of the Al_2O_3 versus SiO_2 trend in Figure 20. This point was determined graphically from the oxide-oxide plots in Figure 20 and the oxide-Zr plots in Figure 11. Vectors in Figure 21 indicate the direction in which fractional crystallization of individual mineral phases will shift the liquid composition, calculated according to the Rayleigh fractionation law (see Arth, 1976) using D's compiled by Pearce and Norry (1979) which are listed in Table IV. Plotted on a logarithmic scale, the geometry of the vectors is independent of source composition.

Application of the Rayleigh law, using F-parameter's estimated from the oxide-SiO_2 relationships, yields the trends shown in Figure 21. The initial trend represents 45% fractional crystallization of hornblende (hence F = .55) from a parent composition taken as 80ppm Zr, 18.5ppm Y, Zr/Y = 4.3, which corresponds to the densest cluster of the most primitive samples in Figure 21. The resultant differentiate contains 108ppm Zr, 18.5ppm Y, Zr/Y = 5.8. These values were used as the parent composition for the second stage of fractional crystallization, where F = .30 and the extract comprised 65% plagioclase and 35% orthopyroxene. The final differentiate contains 353ppm Zr and 55.4ppm Y, with Zr/Y = 6.4. Figure 21 shows that the modelled trend closely approximates that of the analytical data. The close correspondence of the calculated point of inflection and the inflection point transferred from the Al_2O_3 versus SiO_2 plot (arrow in Figure 21), lends more weight to the model. Moreover, the vectors in Figure 21 demonstrate that an anhydrous or partially anhydrous assemblage would be unable to fractionate the Zr/Y ratio to the required extent during the initial stage of differentiation, and that significant proportions of hornblende and/or clinopyroxene could not be accommodated in the fractionating assemblage during the second stage.

Support of the fractionation hypothesis by the behaviour of other trace elements is more obscure, but not contradictory. Figures 22 and 23 show the relationships of Zr/Nb versus Zr and Zr/Ti versus Zr respectively. These relationships, used in the same way as that of Zr/Y versus Zr, show the following :

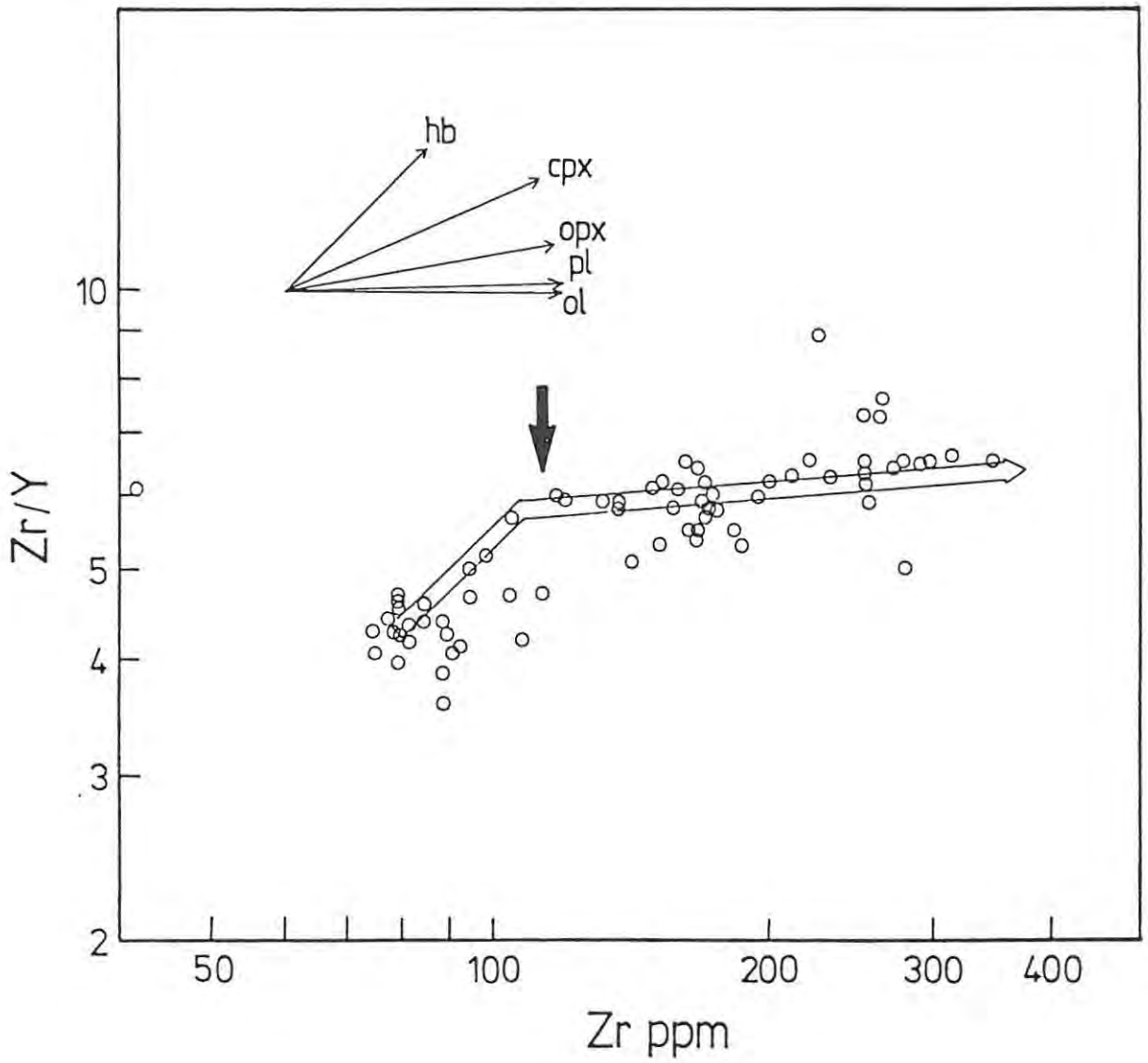

Figure 21: Zr/Y versus Zr variation - Dominion basic lavas, showing the modelled trend (see text). The arrow along the trend corresponds with the inflection point in the Al_2O_3 - SiO_2 curve (Figure 20). Vectors indicate the direction in which the fractionation of individual phases would shift the liquid composition, from any point along the trend.

TABLE IV: Distribution coefficients used in Rayleigh fractionation calculations involving the immobile, incompatible elements (from Pearce and Norry, 1979).

	ol	pl	cpx	opx	hb
Ti	0.02	0.04	0.3	0.1	1.5
Zr	0.01	0.01	0.1	0.03	0.5
Y	0.01	0.03	0.5	0.2	1.0
Nb	0.01	0.01	0.1	0.15	0.8

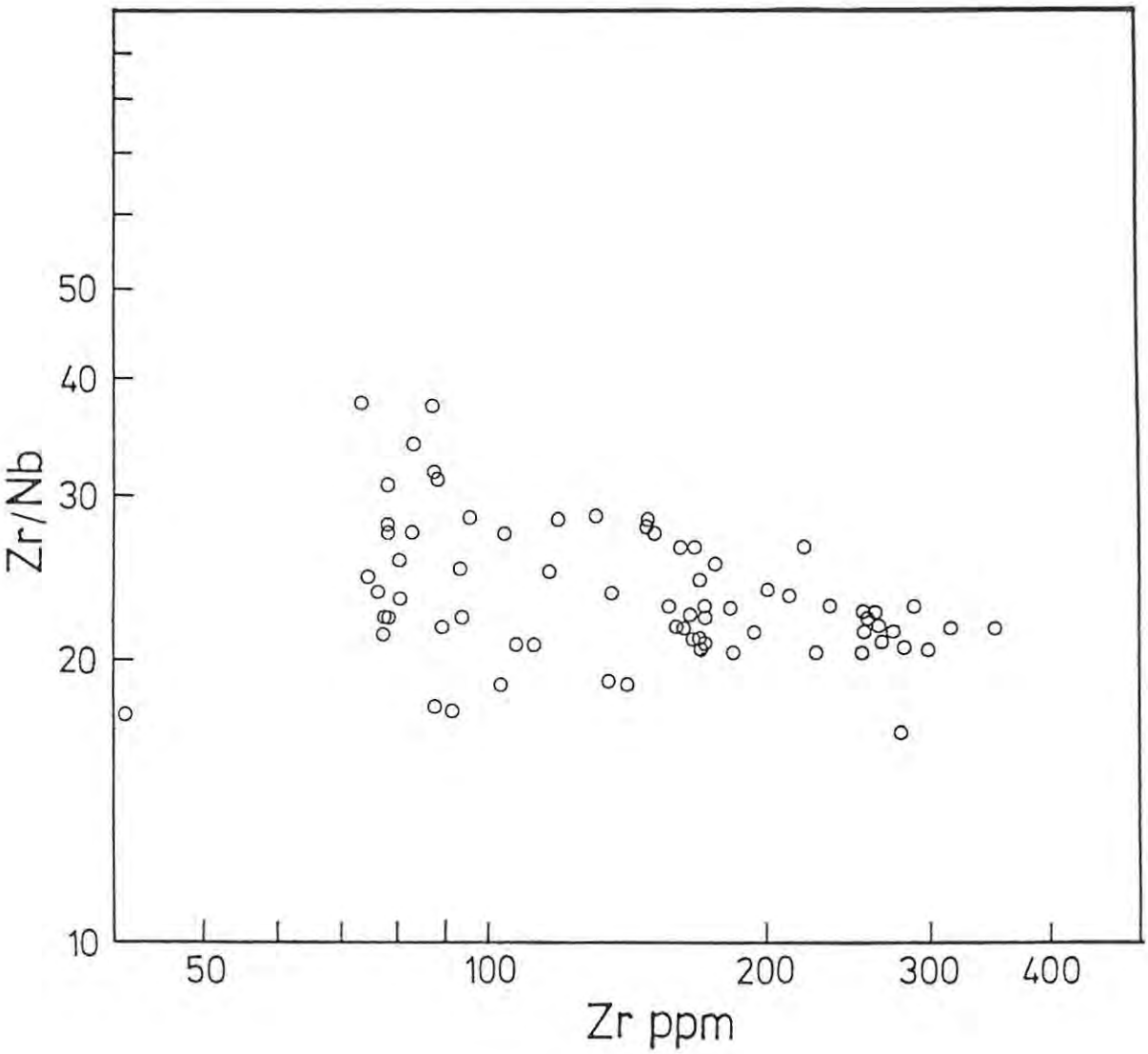

Figure 22: Zr/Nb versus Zr variation - Dominion basic lavas, illustrating the consistency of Zr/Nb. Scatter in the low-Zr part of the trend is due to poor analytical precision where Nb concentrations approach detection limits.

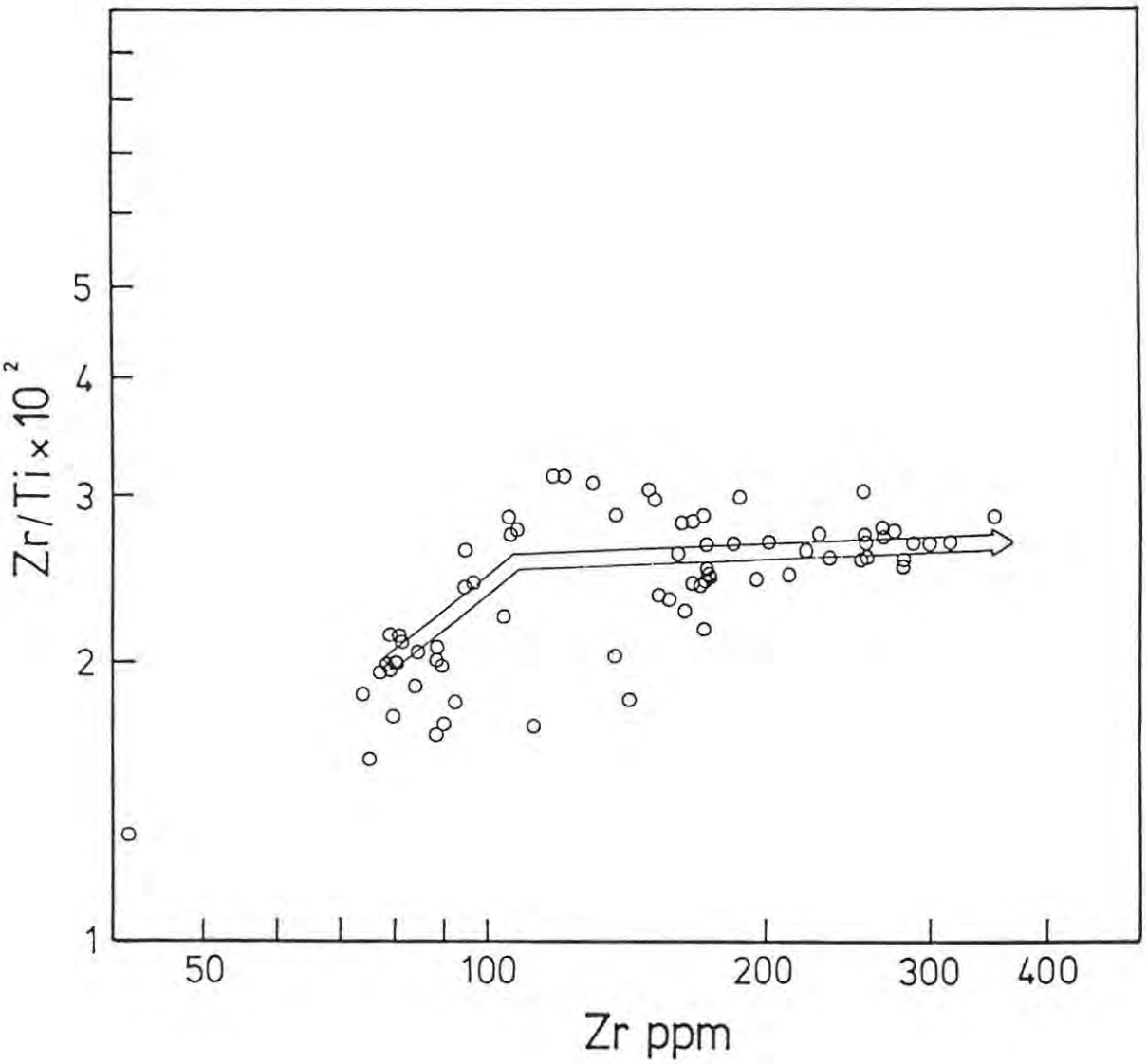

Figure 23: Zr/Ti versus Zr variation - Dominion basic lavas, showing the trend modelled using a D of .9 for Ti in hornblende.

The differences in D's between Zr and Nb (Pearce and Norry, 1979) are insufficient to significantly fractionate the Zr/Nb ratio, which consequently remains relatively constant between 20 and 25 (Figure 22). A fairly substantial degree of scatter is present in the low-Zr part of the trend, which may be attributed to poorer analytical precision as Nb levels approach detection limits. The relative consistency of the Zr/Nb ratio with increasing Zr content, although not diagnostic, is nevertheless supportive of the fractionation model.

The Zr/Ti - Zr relationship (Figure 23) is more problematical, since Pearce and Norry (1979) report a D for Ti in amphibole of 1.5. The postulated initial stage of hornblende fractionation results in a significantly higher Zr/Ti ratio than is reflected by the data. Furthermore, the trend in the low-Zr range is obscured by excessive scatter which may be attributable to source heterogeneity or variable degrees of partial melting, as suggested earlier. If a D for Ti in hornblende of .9 is assumed, the postulated model yields the trend shown in Figure 23. A D of .9 lies within the error limits reported by Pearce and Norry (1979), and is reasonable considering the variable TiO_2 contents of hornblende, which Cawthorn (1976) suggests may be pressure dependent. Allowing for the possible melting origins of the scatter in the low-Zr data, the modelled trend is an adequate approximation of the observed trend, and the Zr/Ti versus Zr relationship does not detract from the proposed model.

The variation diagrams for Cr, Ni and Cu relative to Zr are reproduced in Figure 24. By manipulation of the Rayleigh equation, it can be shown that in order to approximate the observed Cr and Ni trends (Figure 24) by the postulated model, D's of 8 and 3.5 respectively for Cr and Ni in hornblende, and 6 and 6 in orthopyroxene are required. Reported D's for Cr and Ni in hornblende are scarce. Leeman (1976) has reported values of 12.0 and 3.0 for Cr and Ni respectively. Considering the wide range of reported D's for these elements in pyroxene, a similar range may be expected in amphibole, and the D's inferred from the Cr and Ni variations are thus acceptable. Similarly, the inferred D's of these elements in orthopyroxene are acceptable. Jahn et al. (1980) quote ranges of between 5 and 10 for Cr, and 1 and 10 for Ni, while Leeman (1976) reported values of 2 and 3.8, and Sun et al. (1978), values of 3 and 2.5 for Cr and Ni respectively.

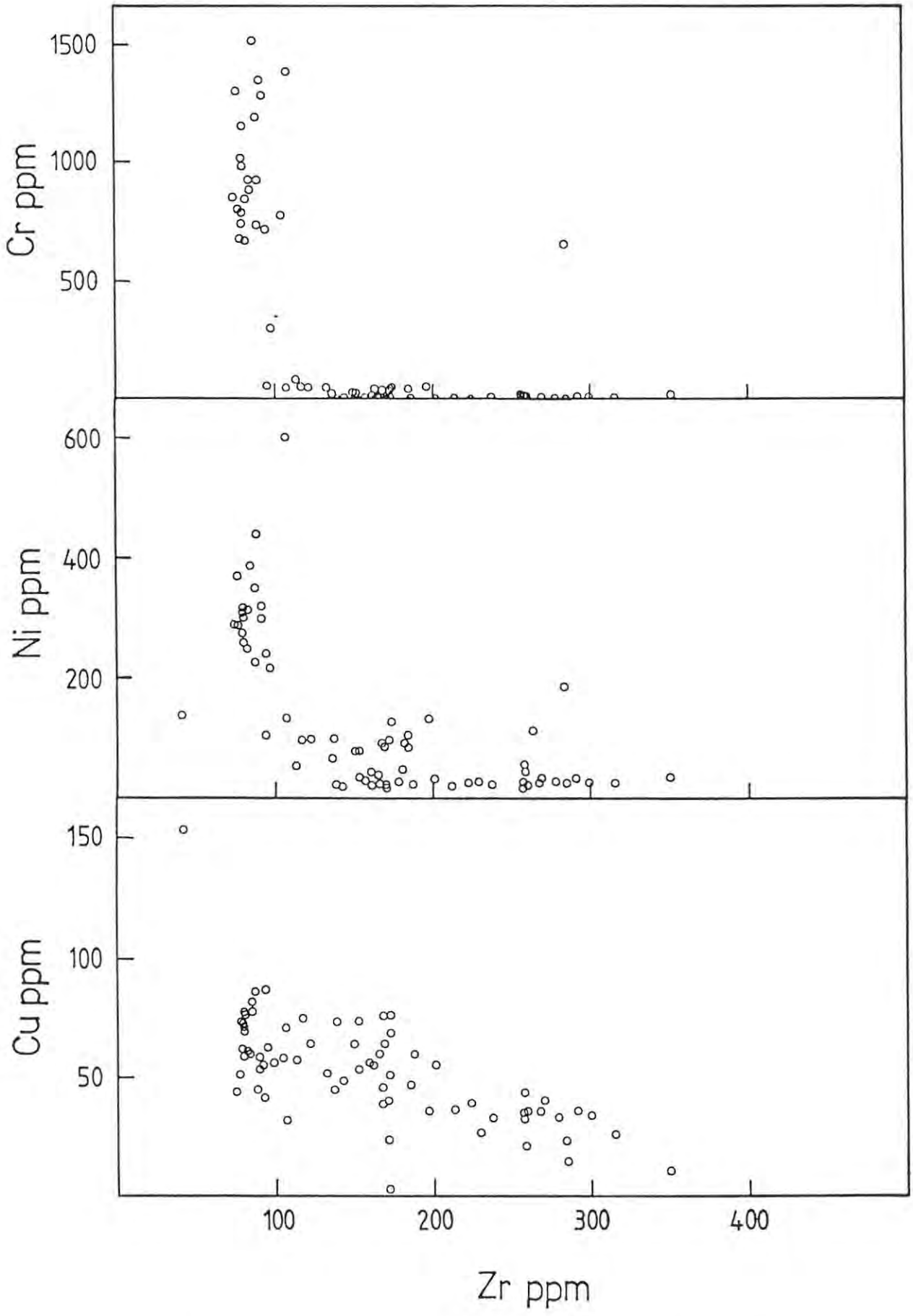

Figure 24: Variation of Cr, Ni and Cu relative to Zr - Dominion basic lavas (see text).

Evaluation of the other trace elements which display reasonably defined trends similarly produces consistent results, with the exception of Cu. Reported D's for Cu in most silicate phases are generally less than unity. An exception is a value of 1.5 to 2.4 quoted by Irving (1978), which was determined by Seward (1971) for calcic pyroxene crystallized from a synthetic silicate melt, and the applicability of these values to natural systems is thus questionable. If the bulk D's for Cu in the postulated fractionating assemblages are in fact less than unity, it appears that the participation of a minor amount of sulphide need be invoked to account for the depletion of Cu with differentiation (Figure 24).

In order to model the above trend, a bulk D for Cu of approximately 2 is required. Taking a D for Cu in sulphide of 50 (Maclean and Shimazaki, 1976) the inferred bulk D is readily obtainable by the inclusion of ~4% sulphide in the fractionating assemblage. This amount would have an insignificant effect on the relevant oxide variations, but would be expected to have a pronounced influence on the behaviour of Ni, since Sun et al. (1979) report a D for Ni in sulphide of 150. Scatter of data in the 80 to 110ppm Zr range (representing the initial stage of differentiation) prevents the resolution of a Cu variation trend. It is nevertheless unlikely that sulphide fractionation commenced during the early stage, since this would require that Ni behaves incompatibly towards hornblende in order to maintain the observed bulk D for Ni of 3.5. Up to 3% sulphide fractionation could readily be accommodated during the second stage of differentiation. The nett effect of this would be to reduce the inferred D for Ni in orthopyroxene from 6 to around 1.5, which is near the lower limits of reported values.

To summarise, trace element modelling supports the fractional crystallization model, deduced largely from the oxide variations, whereby the most evolved lavas of the Dominion basic lava sequence may be derived from the most basic lavas by 45% fractional crystallization of hornblende, followed by 70% crystallization, from the residual liquid, of an assemblage comprising 65% plagioclase and 35% orthopyroxene. The model also accommodates the inclusion of up to 3% sulphides in the second-stage assemblage, which is necessitated by the observed depletion of Cu with differentiation. The subdued participation of other phases has not been ruled out.

The postulated model is rather crude, since it relies on hypothetical liquidus phase compositions, and variations in phase compositions with changing liquid composition have not been taken into account. However, scatter of data, attributed to both primary and secondary processes, imposes limitations on the applicability of more complex models. Nevertheless, the model is significant in that hornblende dominates the initial stages of fractionation and the Zr/Y-Zr relationship infers that no significant participation of the anhydrous phases could have occurred. Although unusual, hornblende-dominated assemblages have been reported in the literature. Experimental work on natural systems has shown that under certain conditions, hornblende may be the only liquidus phase for a range of magma compositions. Experiments on "wet" (5% H_2O) andesites (see Jakes and White, 1972) have shown that hornblende may be the first liquidus phase at low to moderate pressures (2.5 to 12 kbars) and is joined at higher pressures or lower temperatures by clinopyroxene. Cawthorn et al. (1973) have studied an unusual sequence of lavas from Grenada, which range in composition from nepheline-normative basanites through to quartz-normative basaltic andesites. They have shown this sequence to be derived by fractional crystallization of hornblende at intermediate pressures in the presence of H_2O. Moreover, they confirmed by melting experiments that the precipitation of olivine and clinopyroxene is inhibited once amphibole appears as a liquidus phase.

The occurrence of hornblende as the sole fractionating phase in the initial stages of differentiation of the Dominion magmas thus appears to be an acceptable situation. Since the model further requires that hornblende becomes unstable during the second stage of differentiation (see Figure 21), it follows that refinement of the model may enable some important constraints to be placed on the physico-chemico conditions operative during the pre-eruptive history of the Dominion lavas, and more so if the involvement of a sulphide phase were verified.

C. Loraine/Edenville Formations

In order to evaluate whether mantle heterogeneity and/or partial melting effects are reflected in the Loraine/Edenville data, the same rationale has been applied as in the previous section. The mean M-value of the Loraine/ Edenville lavas is 65, and that of the most primitive sample is 77 (Analyses 5 and 6, Table II). Thus the more basic lavas of this group may represent primary liquids, a conclusion supported by the high Cr and Ni contents of these lavas. However, the strong depletion of Cr and Ni with increasing Zr (Figure 26a, b) suggests that the bulk trends were produced by fractional crystallization. These trends are nevertheless not smooth, and it is likely that this reflects variable degrees of partial melting and/or heterogeneous source compositions, resulting in numerous subparallel liquid lines of descent. The average trend will thus be evaluated below in terms of a fractional crystallization model.

Relative to that of the Dominion basic lavas, the degree of chemical variation of the Loraine/Edenville lavas as indicated by the Zr-variation diagrams (Figures 15 to 17) is more limited. Furthermore, the most basic samples of the Loraine/Edenville formations do not define a tight cluster as do their Dominion Group counterparts, and a parental magma composition is thus difficult to define. Consequently a slightly different approach is required in interpreting the observed chemical variation of the Loraine/Edenville lavas, since the above factors reduce the diagnostic value of oxide-oxide diagrams. Textures are, however, better preserved than those of the Dominion lavas, and petrographic evidence will thus form the basis from which an hypothesis will be formulated and subsequently tested and further constrained by geochemical methods similar to those utilized in the preceding section.

A phenocryst phase, pseudomorphed by chlorite, was noted in some of the MgO-rich lavas (see Chapter V, Section D). This phase was identified on rather tenuous grounds as representing an MgO-rich orthopyroxene. Augite occurs as microphenocrysts, as overgrowths on the postulated orthopyroxene pseudomorphs and as groundmass laths, and appears to represent the second phase in the order of crystallization, followed by plagioclase, which occurs only as a groundmass phase. It is thus postulated that a fractionation sequence would initially be controlled by

the extraction of orthopyroxene from the magma, followed at a later stage by augite and possibly plagioclase in the final stages. Other phases need also to be considered, however, especially in view of the high MgO content of the more primitive lavas, from which olivine might be expected to precipitate.

As a preliminary test of the viability of the postulated sequence of crystal fractionation, Figure 25 illustrates the variation of Zr/Y with respect to Zr. Although poorly defined because of scatter, a slight initial increase of Zr/Y with increasing Zr content is apparent, followed by a more rapid enrichment of Zr/Y. Vectors drawn on Figure 25 illustrate the effects of 50% Rayleigh fractionation of various phases, calculated using the distribution coefficients of Pearce and Norry (1979) (see Table IV). The geometry of the vectors is applicable to any point along the observed trend, since logarithmic scales have been used. Despite the subjectivity of the observed trend imposed by scatter of data, the diagram provides several important constraints. It shows that neither clinopyroxene nor amphibole could have dominated the initial stages of fractionation, and the later stages of fractionation were either dominated by clinopyroxene or involved the extraction of an amphibole-bearing assemblage in order to produce the observed enrichment of the Zr/Y ratio. While these deductions reinforce the petrographic evidence, the behaviour of other elements needs to be assessed in order to further constrain the possibilities.

Figures 26a, b and c illustrate the variation of Cr, Ni and Cr/Ni relative to Zr. In the low Zr range between 34 and 55ppm Zr, samples show a rapid depletion in both Cr and Ni from 2600ppm to 600ppm Cr and 520 to 230ppm Ni, with increasing Zr content. All the porphyritic samples occur in this region of the trend, although not all the samples in this range, including the most primitive sample (KL-468), contain phenocrysts. It is thus unlikely that the trend has resulted from phenocryst accumulation. The bulk of the samples fall within the range between 55 and 85ppm Zr, where Cr decreases from 600ppm to 150ppm, and Ni from 230ppm to 150ppm.

The 55ppm Zr level corresponds with a break in the data on the Cr and Ni versus Zr plots (Figure 26), with the point where the rate of Zr/Y enrichment relative to Zr increases (Figure 25), and represents the upper

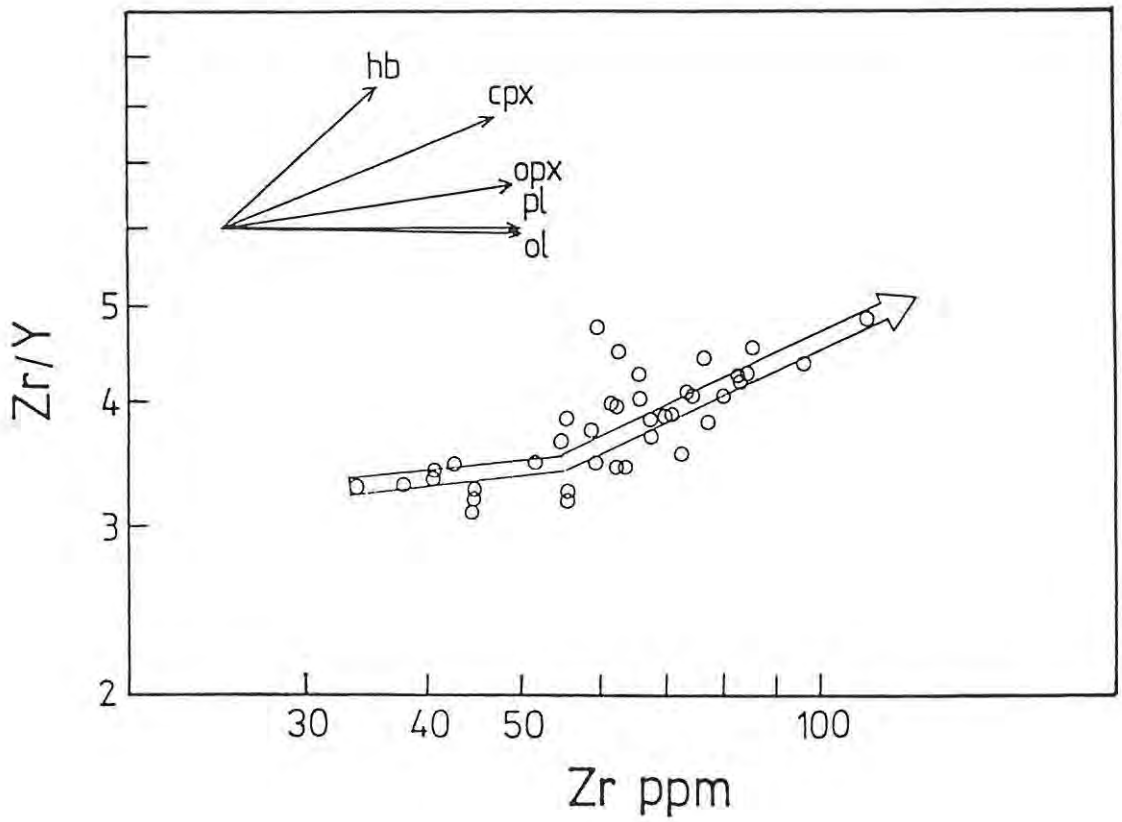

Figure 25: Zr/Y versus Zr variation - Loraine/Edenville lavas, showing the modelled trend (see text). Vectors indicate the direction in which the fractionation of individual phases would shift the liquid composition, from any point along the trend.

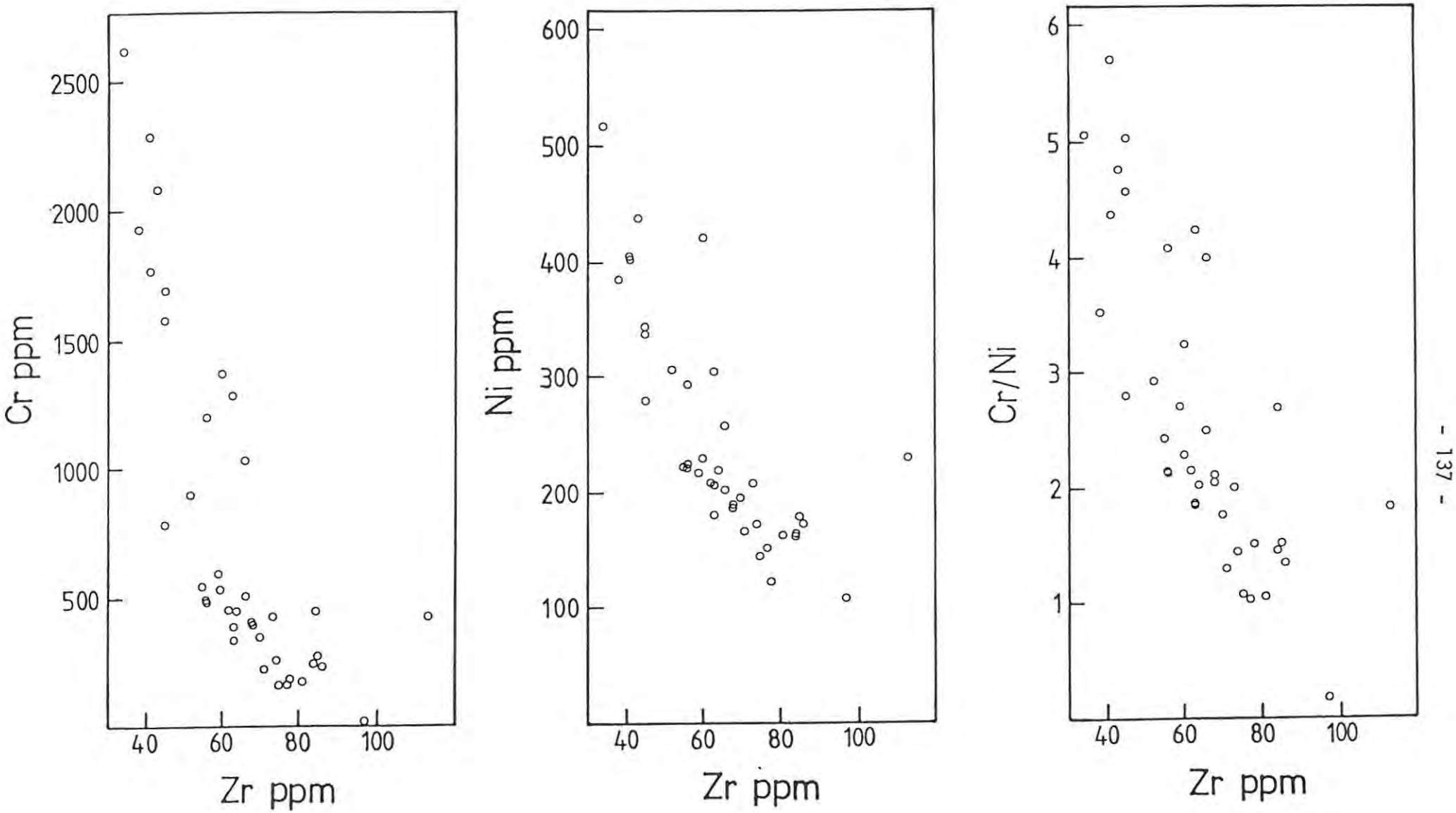

Figure 26: Variation of Cr, Ni and Cr/Ni relative to Zr - Loraine/ Edenville lavas (see text).

Zr limit of the orthopyroxene-phyric lavas. This point will thus be taken to represent the change in the fractionating assemblage postulated earlier.

Using Zr enrichment factors to estimate F, the observed trends may be approximated by 38% fractional crystallization (F = .62) of the most primitive composition (sample KL-468), followed by 35% (F = .65) fractional crystallization of the residual liquid. Calculated bulk distribution coefficients for Cr and Ni for the two respective stages are: Cr - 4.1 and 4.2; Ni - 2.9 and 2.0.

The bulk D for Ni is too low to be attributable to olivine-controlled fractionation, since D for Ni in olivine is greater than 5 in an MgO-rich liquid and increases with decreasing MgO content (Hart and Davis, 1978). Furthermore the strong depletion trend in Cr/Ni ratios (Figure 26c) is contrary to what would be expected for an olivine-dominated extract, since D for Cr in olivine is less than 1 (Leeman, 1976; Jahn et al., 1980). Thus, unless olivine is accompanied by a substantial proportion of plagioclase in order to explain the low bulk D for Ni, and sufficient chromite to deplete Cr relative to Ni, the involvement of olivine can be ruled out. It is considered unlikely that plagioclase would be involved during the early stages of fractionation because of the low Al_2O_3 content of the liquid (see Green and Ringwood, 1967), while there is probably a good chance of chromite crystallizing in view of the high Cr content of the magma.

Fractionation of orthopyroxene, clinopyroxene and hornblende could suitably explain the observed Cr and Ni trends throughout the postulated crystallization sequence, but only orthopyroxene is permissible as a candidate for the initial stages of fractionation because of constraints imposed by the Zr/Y versus Zr variation. The Cr and Ni versus Zr relationships do not allow any further constraints to be placed on the postulated second-stage assemblage, since both clinopyroxene and hornblende can be accommodated.

The other trace elements are less diagnostic, either due to ambiguous solutions or, more commonly, due to excessive scatter of data. The enrichment of Cu and depletion of Co with increasing Zr content

(Figure 17) are, however, not in conflict with the constraints already formulated.

Evaluation of major oxide trends plotted against MgO confirms the initial orthopyroxene control on the compositional variation of the magma, and although the second stage is more obscure, it could be explained by the extraction of clinopyroxene, hornblende and possibly plagioclase. These conclusions are illustrated in Figure 27, which shows the variation of SiO_2, Al_2O_3, Fe_2O_3 and CaO with MgO. Mixing lines have been fitted to project through the estimated phenocryst compositions, and through the data.

The phenocryst compositions used to evaluate these variation diagrams are presented in Table V. The clinopyroxene composition is that of a microphenocrystal augite obtained by electron microprobe analysis from sample NL-789, (see Chapter V), the bulk chemistry of which (presented in Appendix II) suggests that it belongs to the MgO-rich group of the Loraine/Edenville lavas. The augites in this sample are relatively diopside-rich, and similar in composition to basic augite of the Skaergaard intrusion, which occur in equilibrium with orthopyroxenes of bronzite composition (Brown and Vincent, 1957). From this relationship, it may be inferred that orthopyroxenes crystallizing from the high-MgO Loraine/Edenville lavas would similarly be of bronzite composition. The orthopyroxene composition presented in Table V thus represents a bronzite analysis selected from Brown and Vincent (1957). The hornblende and plagioclase compositions used are the same as those employed in the previous section for the Dominion lavas.

The postulated mechanisms thus provide a good approximation of the observed trends in the initial stage of fractionation. There is no strong evidence for the involvement of hornblende in the second stage, although it cannot be ruled out. The limited involvement of plagioclase in the final stages similarly cannot be ruled out. However, since the augite composition may be expected to become progressively more Fe-rich with differentiation, an augite-dominated assemblage is favoured, and is supported by petrographic evidence.

Phase chemistry has very limited applicability in the interpretation of these lavas because of scatter of data which results in widely ranging normative compositions, as discussed in the previous chapter. Two

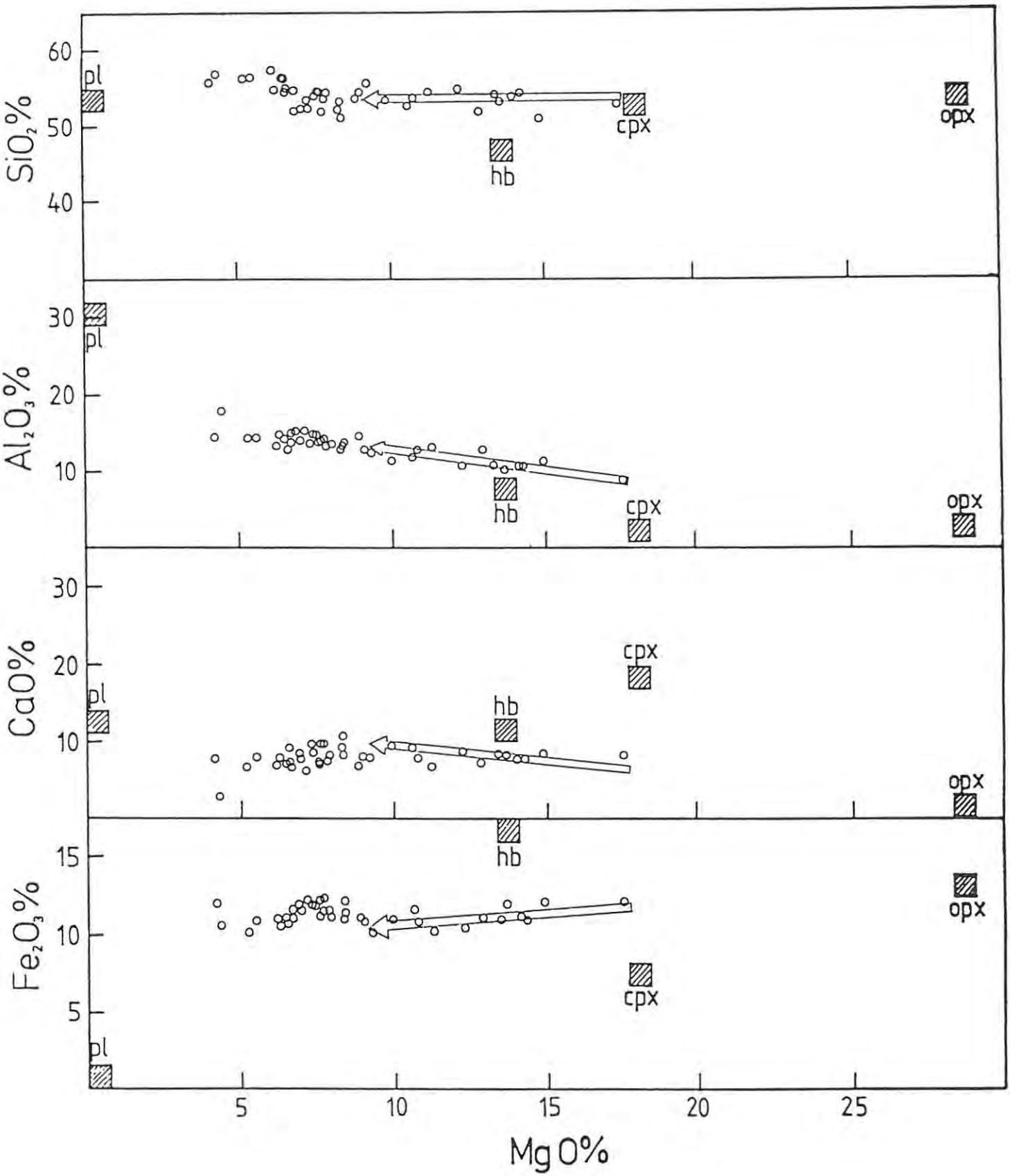

Figure 27: Variation of SiO_2, Al_2O_3, CaO and Fe_2O_3 relative to MgO - Loraine/Edenville lavas, with hypothetical phenocryst compositions. The postulated fractionation of orthopyroxene during the initial stage of differentiation fits the data well, as indicated by the arrows. The second stage is more obscure, but appears to require clinopyroxene, hornblende and possibly plagioclase as components of the extract, although not necessarily simultaneously.

TABLE V: Phenocryst compositions selected for modelling the oxide trends of the Loraine/Edenville lavas. (See text for source of data).

	opx	cpx	hb	pl
SiO_2	53.6	53.15	46.5	53.0
TiO_2	.5	.15	2.0	-
Al_2O_3	2.3	2.04	7.7	30.0
Fe_2O_3	1.3	-	-	-
FeO	10.8	6.58*	16.1*	-
MnO	.3	.18	-	-
MgO	28.7	18.26	13.7	-
CaO	2.0	18.46	11.5	12.5
Na_2O	.2	.23	1.4	4.5
K_2O	-	-	1.1	-
Cr_2O_3	-	.97	-	-
NiO	-	.05	-	-

* All Fe as FeO

projections in the system SiO_2-olivine-clinopyroxene-plagioclase are nevertheless presented in Figure 28, calculated by the method of Walker et al. (1979). Since the phase relations were determined for mid-oceanic ridge basalts, the phase boundaries are probably not applicable to the Klipriviersberg lavas, especially if hornblende is involved. It is useful, however, purely from a geometric point of view. The projection from SiO_2 indicates that the MgO-rich lavas have a strong olivine control. This is in fact misleading, since the high-MgO trend extends well above the ol-di-plag plane, showing a strong orthopyroxene control which is well-illustrated in the projection from diopside, thus reinforcing the conclusion that orthopyroxene dominated the initial stages of fractionation.

To summarise, petrographic, incompatible element, compatible element and major oxide evidence supports a fractional crystallization model for the generation of the observed compositional variation of the Loraine/Edenville lavas. The initial stages of fractionation were dominated by the extraction of Mg-rich orthopyroxene, possibly accompanied by a minor proportion of chromite. This stage represents approximately 38% crystallization of the inferred parental liquid. The latter stages of differentiation represent a further 35% crystallization, and, although the phase relationships are more obscure, petrographic and trace element evidence favours a clinopyroxene-dominated assemblage. The possible participation of hornblende and plagioclase can nevertheless not be ruled out on the basis of available geochemical evidence.

D. Goedgenoeg/Rietgat Formations

The analysed Goedgenoeg/Rietgat lavas display a mean M-value of 53 (see Table II), with a maximum of 62 in samples PR-194 and PR-486. It is thus unlikely that any primary mantle melts are represented, since this requires M-values to be between 68 and 72 (Green and Ringwood, 1967; Green et al.,1974).

Mean Ni concentrations are similar to those of the Alberton, Orkney and Allanridge formations and Cr concentrations (Mean = 315ppm) are significantly higher (see Table II and Figure 17). Paradoxically,

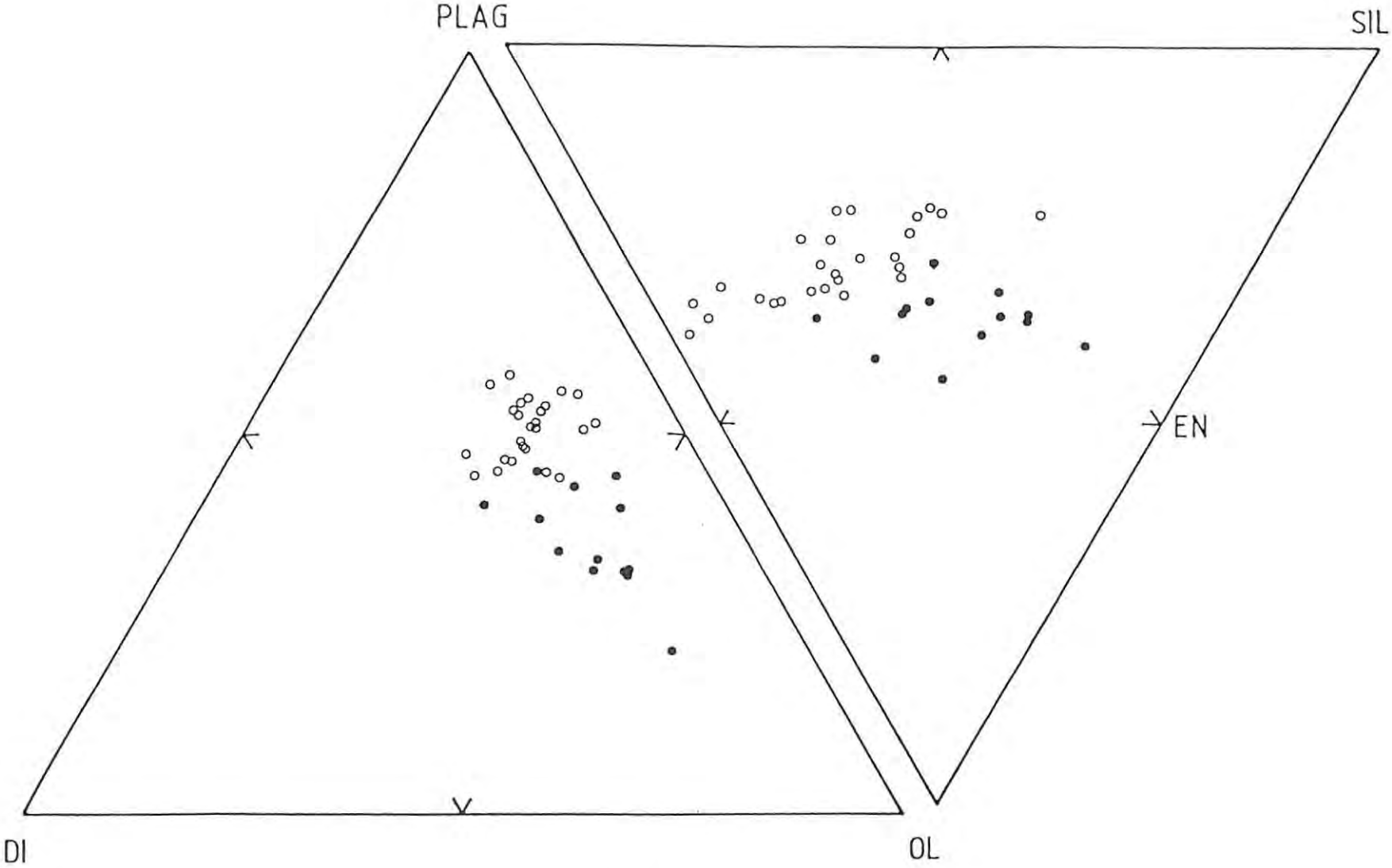

Figure 28: Projections from SiO_2 and diopside of the Loraine/Edenville lavas in the system SiO_2-ol-di-plag, calculated by the method of Walker et al. (1979). The most primitive lavas (MgO>8%, Cr>700ppm; solid circles) clearly display an enstatite control.

incompatible element levels are much higher than those of the Klipriviersberg and Allanridge lavas (see Chapter VI). Zr contents higher than 240ppm, in comparison with the low Zr levels of the more primitive lavas of the Loraine/Edenville and Dominion basic lava sequences, suggest that the Goedgenoeg/Rietgat lavas are highly evolved despite the high Cr levels, if a mantle origin is assumed.

It is thus unlikely that any partial melting trends are preserved, but a general lack of trends (see Figures 15 and 17) prevents any particular evolutionary process being inferred from the character of the compatible element-incompatible element trends (as used in the previous sections to infer fractional crystallization). The lack of well-defined trends using Zr as an index of differentiation furthermore does not permit a fractional crystallization model to be adequately tested. Employment of various other conventional indices of differentiation failed to improve the resolution of the trends. Petrographic evidence summarized in Chapter V suggests that if fractional crystallization was operative, plagioclase and a ferromagnesian mineral, tentatively identified as Ti-rich augite, were likely components of the extract.

The large Zr range of these lavas cannot be attributed to alteration and metamorphism, since petrographic evidence shows that they have not undergone more intense alteration than the other lavas of the Witwatersrand triad. As Zr, Ti and P appear to have remained immobile in the other Witwatersrand triad lavas, it is a reasonable assumption that their respective behaviour reflects primary magmatic processes. The interrelationships of Zr, Ti and P thus allow important constraints to be placed on possible evolutionary models.

Neither Ti nor P displays any correlation with increasing Zr (see Figure 15). In contrast, P shows a good linear correlation with Ti, illustrated in Figure 29. A least squares fit of the data intersects the TiO_2-axis at approximately 0.4% TiO_2.

In order to explain the observed Zr, Ti and P behaviour by a fractional crystallization model, either Zr or Ti and P or all three must have behaved compatibly at some stage during the fractionation process. It is unlikely that Zr would be compatible, despite its relatively high concentrations, since the major oxide composition of these lavas is

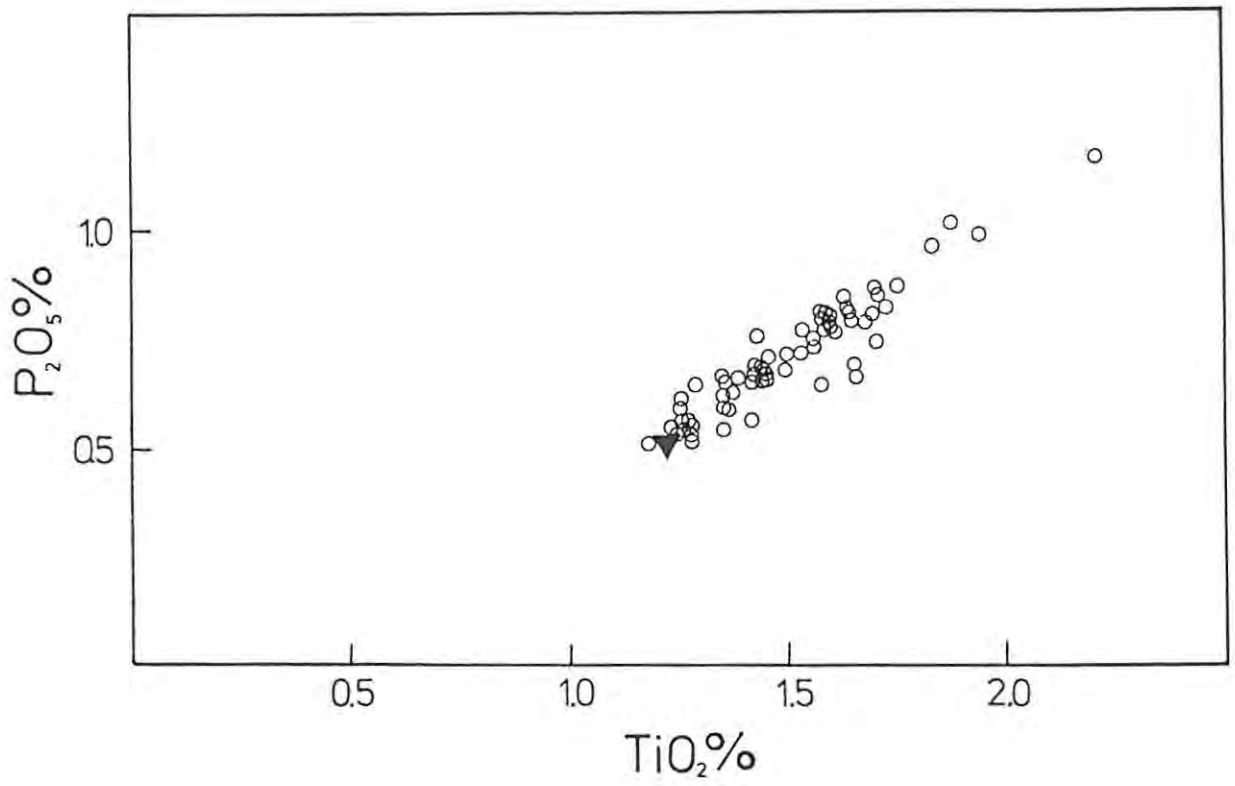

Figure 29: P_2O_5 versus TiO_2 - Goedgenoeg/Rietgat lavas, illustrating the strong covariance of these elements. The triangle represents the mean of the Makwassie porphyries (see text).

relatively basic, being similar to that of the Alberton, Orkney and Allanridge formations. Moreover, the expected correlation of Nb, Y, La, Ce and Nd with Zr is preserved. The compatible behaviour of Ti would be consistent with petrographic evidence suggesting a Ti-rich augite on the liquidus. However, the close correlation of Ti and P requires that P also behaved compatibly. It is feasible that Ti and P become compatible simultaneously when critical concentrations are achieved by fractional crystallization, a case in point being the Birds River Complex in the Dordrecht district (Eales and Booth, 1974) where a fairly late-stage precipitation of ilmenite and apatite resulted in the above elements being depleted simultaneously after displaying strong enrichment trends (Robey, 1976). Thus if the precipitation of a Ti-rich augite resulted in the compatible behaviour of Ti, the co-precipitation of a small proportion of apatite would have to be invoked to explain the covariance of these two elements.

Such a model is still inadequate, however, since it fails to account for the incoherent Zr-Ti and Zr-P relationships in addition to the lack of well-defined trends displayed by most of the other elements. Such problems may be overcome by invoking the type of case referred to by Cox et al. (1979) as "proliferation of the liquid lines of descent". Where in nature the generation of a single liquid line of descent is a rare and ideal case, the majority of volcanic sequences consist of a large number of overlapping similar lines of descent which approximate the ideal case, and may thus be modelled as such. The various liquid lines of descent may, however, be subparallel, resulting in incoherent trends. Cox et al. (1979) quote data from Appleton (1972) on the Roman province of Quaternary volcanoes, where certain oxide pairs display totally incoherent trends while others show relatively well-defined trends, resulting from varying degrees of proliferation of the liquid lines of descent.

Such may conceivably be the case for the Goedgenoeg/Rietgat lavas, where in addition the degree of scatter has been enhanced by the effects of secondary processes. Proving or disproving this model with the available data would be difficult, however, and virtually impossible to refine to any extent.

An alternative model would be one in which the Goedgenoeg/Rietgat lavas

represent crustal melts. However, because the relatively high Cr and Ni contents would be difficult to reconcile with such a model, a hybridization model is considered to be more plausible. In addition, a hybridization model can explain certain unusual features of these lavas which will be discussed later.

In the present study, a hybridization model involves too many unknown variables to be pursued to any detail. Various mechanisms may be involved, including magma mixing, contamination and assimilation, preceded, followed and/or accompanied by fractional crystallization. The latter possibility would further complicate the model. De Paolo (1981) has suggested that combined assimilation and fractional crystallization is an important process in nature, and has devised mathematical equations to model this process. He showed that results thus obtained may be very different from those obtained if fractional crystallization (see Arth, 1976) and binary mixing models (see Langmuir et al., 1978) are applied separately.

A likely end-member component in a hybridization model would be material of Makwassie-type composition, since the Makwassie porphyries are intimately associated with the Goedgenoeg/Rietgat lavas spatially, and complete textural gradations between the two have been observed by the writer. Moreover, Ti/P ratios of the Makwassie and the Goedgenoeg/Rietgat lavas coincide (see Figure 18) and the mean Makwassie composition falls precisely on a projection of the P_2O_5-TiO_2 trend of the Goedgenoeg/Rietgat lavas, close to the lower TiO_2 and P_2O_5 limits of the latter (Figure 29). If the Makwassie porphyries do represent an end-member component, then none of the remaining Witwatersrand triad magma types could represent a basic component, because their Ti/P ratios are very different (see Figure 18), a feature which would not permit the observed Ti-P relationship to be preserved in the Goedgenoeg/Rietgat lavas. A postulated basic end-member would thus be required to have a Ti/P ratio similar to that of the Makwassie and Goedgenoeg/Rietgat lavas.

Titanaugite has been inferred from petrographic evidence (see Chapter V) to have been a liquidus phase. It is thus tempting to postulate a basic end-member component of alkaline affinity, since titanaugite commonly occurs in undersaturated alkaline magmas. A composition similar to the mean basanite composition presented by Le Maitre (1976), characterised by

high TiO_2 and P_2O_5 contents, along with high MgO and low SiO_2, would be a suitable candidate. Due to its basic character, such a magma would conceivably contain high Cr and Ni levels.

It can be shown that, if two hypothetical end-members, each containing certain distinctive features, are mixed, then those features will be preserved in the resultant hybrid, provided they were sufficiently prominent in the end-members. High incompatible element levels and high normative quartz contents may be considered to be prominent features of the Makwassie lavas, while analogous features in the hypothetical basic component would be high MgO, Cr and Ni concentrations. A mixing model can thus explain the following somewhat contradictory features which broadly serve to distinguish the Goedgenoeg/Rietgat lavas from those of the Alberton, Orkney and Allanridge formations (see Table II and Figures 15 and 17): Despite the similar major element chemistry of the lavas of all the above formations, the Goedgenoeg/Rietgat samples contain substantially higher incompatible element levels, yet Ni concentrations are similar, while Cr concentrations are substantially higher. Similarly, while mean MgO content is higher, so is the normative quartz component. In relation to the classification scheme discussed in Chapter VI, the latter features result in the mean Goedgenoeg-Rietgat lava composition having a M-value of 53, which is too basic for the normal tholeiitic andesite range, while the mean normative quartz content (10.69%) suggests that the mean composition is too acid to be classified as tholeiitic andesite.

The above inconsistencies may thus readily be explained by a hybridization model, superimposed on or by the effects of fractional crystallization, and this model is therefore preferential to one involving fractional crystallization alone. The nebulous nature of both models, however, prevents the application of quantitative modelling to these lavas, and more definite conclusions must await more detailed study and the accumulation of further evidence in the form of rare earth element (REE) and isotopic data.

E. Makwassie Formation

Evaluation of the chemical variation of the Makwassie porphyries is

hampered by several factors, viz. uncertainty as to a pyroclastic or liquid mode of effusion; a certain loss of chemical control resulting from the secondary redistribution of the mobile elements, and finally the general lack of knowledge concerning petrogenetic processes operative in acid-intermediate magmas compared to what is known of the more basic types.

The behaviour of K_2O, Na_2O, Ba, Rb and Sr becomes critical for the petrogenetic interpretation of more felsic magmas, since the feldspars usually play a dominant role which may be monitored by the behaviour of the above elements. Unfortunately these elements, as demonstrated in the previous chapter, are extremely mobile and are thus of little value as petrogenetic indicators.

Nevertheless, the behaviour of the more immobile elements provides certain constraints. The fact that all discernible trends relative to Zr appear to be linear (see Figures 15 and 17) and that a unique geochemical signature manifested by immobile element ratios is preserved, permits several basic assumptions to be made with a reasonable degree of confidence.

(i) The original magma composition has not been significantly modified by any processes other than those which may be approximated by theoretical closed-system magmatic differentiation models, and post-depositional secondary alteration and metamorphism. Contamination of the porphyries at any stage after attainment of their geochemical signature is thus ruled out, unless it involved a purely mineralogical component having no effect on the immobile incompatible element ratios, or a component having very similar incompatible element ratios.

(ii) The trends displayed by the less mobile elements relative to Zr (see Chapter VI) all approximate positive straight lines with the notable exception of SiO_2, which is depleted relative to Zr. Thus it would appear that simple mixing relationships could explain the chemical variation, and that if fractional crystallization was involved, the role of mafic phases was negligible.

Thus whatever differentiation processes are invoked, a SiO_2-rich mineral clearly must play a dominant role, and Al_2O_3 would be involved to a limited extent, since the well-defined trend relative to Zr intersects the Y-axis at about 4.5% Al_2O_3. (This implies that Al_2O_3 was not enriched to the same extent as Zr.) The remaining elements, with the exception of the highly mobile elements mentioned previously whose roles cannot be assessed, have thus behaved passively, suffering only concentration and/or dilution effects, since their trends, relative to Zr, appear to project through the origin.

(iii) It follows from (i) and (ii) above, that the observed chemical variation of these porphyries can shed no light on their mode of effusion. Whether the mixing trends originated during the effusive phase, or whether they represent compositional gradients in a pre-effusive magma chamber, the final results, in this case, would be the same.

Conversely, the mode of effusion, whether liquid or pyroclastic, need not have any bearing on the interpretation of the chemical variation, since this may be interpreted from an empirical point of view. If a solution is thus obtained, geological and petrographical evidence may then be utilized to determine the plausibility of such a solution and to provide further constraints.

Accepting the above assumptions, feldspar and quartz would be the most favourable candidates for a fractionation model, since they make up by far the bulk of the phenocryst assemblage (see Chapter V). Removal or accumulation of a feldspar-quartz assemblage would furthermore account for the depletion trend displayed by SiO_2 relative to Zr, the slightly subdued enrichment trend of Al_2O_3 and the passive behaviour of the other elements not involved in this assemblage.

A plot of Al_2O_3 versus SiO_2 is presented in Figure 30. The trend line has been calculated by least squares linear regression, which yields a slope of -0.33, a y-intercept of 35.92% Al_2O_3, and a correlation coefficient of -0.86. Feldspar and quartz compositions are plotted.

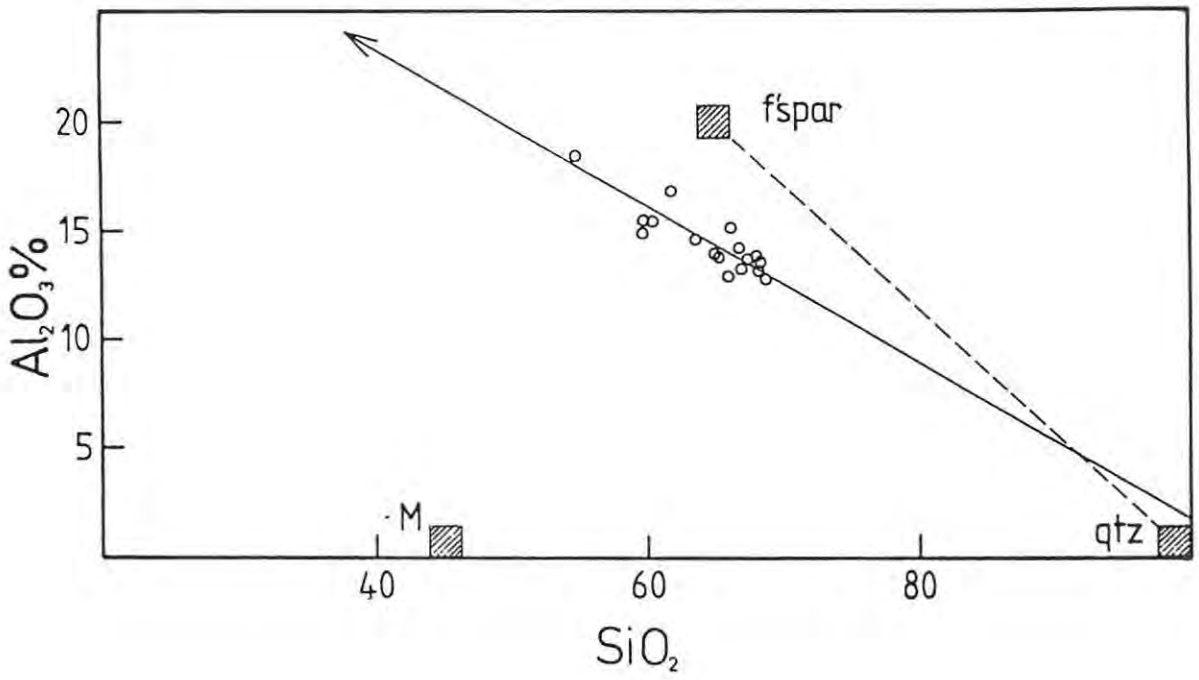

Figure 30: Al_2O_3 versus SiO_2 - Makwassie porphyries. The intersection of a regression line and a quartz-feldspar tie-line (as shown) suggests a quartz-dominated extract, unless a hypothetical mafic phase (M) is included in a postulated fractionating assemblage (see text).

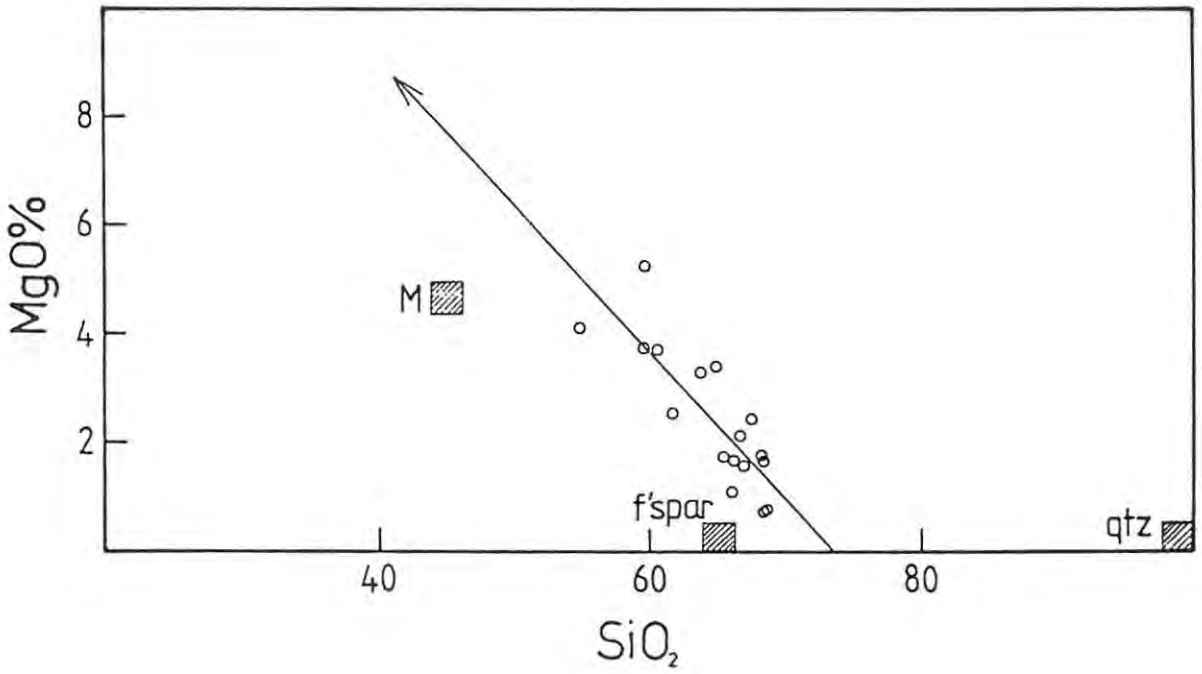

Figure 31: MgO versus SiO_2 - Makwassie porphyries. A regression line through the data requires a feldspar-dominated extract in a quartz-feldspar fractionating assemblage. The inclusion of a hypothetical mafic phase (M) is required to reconcile the MgO-SiO_2 variation with the Al_2O_3-SiO_2 trend (Figure 30) if a fractional crystallization model is invoked.

The feldspar composition is an approximation and is representative of both plagioclase in the albite to oligoclase range and alkali-feldspar. Both have similar SiO_2 and Al_2O_3 contents (Deer et al., 1966) and both may be expected to occur in lava of Makwassie-type composition. It is thus unnecessary to differentiate between plagioclase and alkali-feldspar for present purposes.

It can be shown by simple mass-balance calculations that the observed SiO_2 versus Al_2O_3 trend may be produced by the addition or removal of an assemblage comprising 68% quartz and 32% feldspar. This is in contradiction to the petrographic observation that feldspar is the dominant phenocryst phase (see Chapter V). The quartz phenocrysts are, however, more strongly resorbed and their original size is impossible to assess. More contradictory evidence results from a plot of MgO versus SiO_2, presented in Figure 31. The trend line was determined by least squares linear regression. The data shows a reasonable fit, with a correlation coefficient of -0.83. However, this trend requires an extract of 23% quartz and 77% feldspar. The two plots are thus irreconcilable if the variation is attributed solely to feldspar and quartz fractionation. The discrepancy may readily be resolved, however, by the introduction of a third phase. It can be shown that a mafic phase containing roughly 40% to 50% SiO_2, less than 10% MgO and making up 10% to 20% of the fractionating assemblage (e.g. certain amphiboles and Fe-rich augite), provides a solution to the trends involving SiO_2, Al_2O_3 and MgO. In this case feldspar must make up between 60% and 65% of the assemblage, and quartz approximately 20%. These proportions are more consistent with those of the quartz and feldspar observed petrographically. Excessive scatter in the other pertinent major-element trends prevents further refinement of this model.

The trace elements lend no positive support for the participation of a mafic phase, as all the useful trace and minor elements display similar enrichment factors. However, because the required proportion of the hypothetical mafic phase is small, the effect on the bulk distribution coefficients may be negligible and the model can thus not be rejected on these grounds.

Other evidence, however, does not appear to favour the above model. While variations in texture, relative phenocryst proportions and total

phenocryst content were observed, as described in Chapter V, none of these variations could be related to the immobile element chemistry.

The incompatible trace element concentrations across the entire compositional range of the Makwassie samples show an enrichment factor of approximately 1.6, which by the above fractionation model implies a 38% variation in total phenocryst content between the "end member" samples. No such variation could be detected. The fractionation model furthermore requires that the relative phenocryst proportions remain constant, again in contradiction to petrographic observation.

If more indirect evidence is considered it becomes even more difficult to sustain a crystal fractionation model. In Chapter VI the reader's attention has repeatedly been drawn to the similarity of the Makwassie trends to those produced by the compositionally anomalous samples of the Dominion porphyries and the Jeppestown amydaloid relative to their respective mean compositions. It was therefore suggested earlier that a solution to the Makwassie porphyry variations may also be applicable to the Dominion porphyry and Jeppestown amydaloid trends.

The Dominion porphyry immobile element trends are also reflected to a limited extent by the bulk of the samples, which do not, however, vary by more than 70 ppm Zr to either side of mean of 273 ppm Zr, while sample DP-33, with 545 ppm Zr, is clearly anomalous. Five Jeppestown amygdaloid samples cluster tightly about a mean of 242 ppm Zr, with the anomalous sample, JA - 371, having 383 ppm Zr. Both anomalous samples show strong SiO_2 depletion and Al_2O_3 enrichment relative to the respective means (despite the fact that both contain resorbed quartz phenocrysts/ xenocrysts).

It is evident from petrographic examination that the anomalous chemistry of these samples can be ascribed to secondary mineralization. Sample JA-371, described in Chapter V, comprises a fine, uniform groundmass of green chlorite with scattered segregations of altered secondary Fe-Ti oxides, which can explain the low SiO_2 (50.22%), high Al_2O_3 (19.57%) and high Fe_2O_3 (16.75%) contents of this sample. The groundmass of sample DP-33 comprises a fine sericite felt which is reflected by the high Al_2O_3 (21.63%) and K_2O (7.12%) and low SiO_2 (58.44%) contents of the sample relative to the mean (see Table II for

representative mean compositions). Because these samples are compositionally anomalous, statistics would favour a secondary rather than a primary origin for these anomalies.

It thus appears that special circumstances prevailing during the breakdown of the primary mineral assemblages and the formation of the secondary metamorphic assemblages have inhibited the formation of quartz from SiO_2 released by the breakdown reactions, and resulted in the nett removal, primarily of SiO_2, either metasomatically or in aqueous solution, resulting in the passive enrichment of the immobile elements. Such a migration of SiO_2 may possibly have been stress-induced, where the mobilized SiO_2 may have contributed to localized fracture filling, thereby maintaining constant overall mass and volume.

Extending the above model to the Makwassie porphyries, the lack of correlation between chemistry and petrography may be attributed to the original variability of textures and phenocryst distribution, and the more uniform spread of data across the compositional spectrum.

Evidence thus appears to favour a post-depositional, secondary origin for the generation of the chemical variation of the Makwassie porphyries. However, because this model is based largely on evidence obtained indirectly via the Dominion porphyry and Jeppestown amygdaloid samples, it should be regarded as tentative until it can be verified by more detailed and quantitative study.

A crystal fractionation model can explain the chemical variation but is difficult to reconcile with petrographic evidence.

F. Summary of Conclusions

In order to consolidate the foregoing chapter, the conclusions reached for each of the individual lava sequences which were evaluated are briefly summarized below:

(a) The compositional variation occurring within the Dominion basic lava sequence may be ascribed to fractional crystallization processes.

The initial stages of differentiation were controlled by 45% crystallisation of hornblende, while the later stages represent 70% crystallization from the residual liquid of an assemblage dominated by plagioclase and orthopyroxene in the proportions .65:.35, and including up to 3% sulphides. Thus the entire sequence represents a total of 84% crystallization of the original basic parent magma, of which the most basic Dominion samples are assumed to be representative.

Comparison with data of several workers obtained from natural lava sequences and from experimental work, suggests that at least the initial stages of fractionation occurred at moderate pressures in an hydrous magma.

(b) Differentiation of the Loraine/Edenville lavas was achieved by 38% fractional crystallization of an Mg-rich orthopyroxene which was probably accompanied by a minor proportion of chromite. This was followed by a further 35% crystallization from the residual melt of an assemblage in which augite appears to have been dominant.

The entire compositional spectrum has thus resulted from a total of 60% fractional crystallization from a parent magma whose composition is assumed to be approximated by that of the most basic sample, KL-468.

(c) The large degree of compositional variation displayed by samples from the Goedgenoeg/Rietgat formations has been attributed to the interaction of hybridization and fractional crystallization processes.

The postulated end-members of the hybridization process are material of Makwassie porphyry-type composition and a basic magma unrepresented in the Ventersdorp lava pile with an inferred basanitic composition. More detailed work is required in order to verify and refine this model.

Plagioclase and Ti-rich augite appear to have been liquidus phases at the time the lavas were extruded.

(d) The coherent trends of the Makwassie porphyries may be explained by

crystal fractionation, but a model is favoured whereby the observed trends have resulted from the nett removal, mainly of SiO_2, either metasomatically or in aqueous solution, as a result of post-depositional secondary processes.

Only a few samples have been markedly affected by the above process and the composition of these porphyries prior to alteration was probably fairly close to the mean reported in Chapter VI, Table II.

VIII INTER MAGMA-TYPE RELATIONSHIPS

A. Introduction

The aim of this chapter is to determine if there are any genetic relationships between the various magma types (as defined in Figure 18).

Several factors hamper investigation of between-type relationships. Firstly, it is likely that most of the magma types under consideration have undergone low-pressure fractional crystallization which would have obscured any record of high-pressure relationships. Secondly, the identity and composition of participating phenocryst phases, especially at moderate and high pressures, are generally unknown or highly speculative. Thirdly, the dependance of most trace element distribution coefficients on pressure and magma composition is unknown. Finally, the applicability of experimentally-determined phase relationships to the Witwatersrand triad magma compositions is dubious because these magmas do not appear to be compositionally equivalent to any of the common major magma types.

Also important in any evaluation is the geological evidence such as stratigraphical, chronological and petrographical considerations. More stringent evaluation and testing of the models which will be proposed would be facilitated by the accumulation of REE and isotopic data.

B. General Considerations

According to theoretical magmatic differentiation models the incompatible elements remain covariant during both melting and crystallization processes. Ratios of such elements should thus remain constant throughout these processes.

Pearce and Norry (1979) have demonstrated that differences in certain incompatible, immobile element ratios between oceanic lavas from different tectonic regimes can best be explained by nett enrichments and

depletions of the pertinent elements in the mantle source.

Similarly Marsh and Eales (in press) have demonstrated the presence of both chemically and stratigraphically distinct magma types within the Karoo tholeiitic lava succession in Lesotho and the NE Cape. Despite extensive overlap in major element chemistry, these magma types each display distinctive incompatible element ratios. Using major element, trace element and REE modelling techniques, supplemented by isotopic data, they convincingly showed that the different basalt types were unlikely to be related by any of the following processes (including various combinations): Closed and open-system, high- and low-pressure fractional crystallization, contamination, and various types of partial melting. They thus concluded that heterogeneous source compositions had resulted in the unique geochemical signatures which were retained throughout the various evolutionary stages to be manifested in the final extrusive products.

The ability to discriminate between the various stratigraphically and chemically distinct units of the Witwatersrand triad lavas by virtue of their immobile incompatible element ratios (see Figure 18), is thus a strong argument for ruling out consanguinity between the different magma types. However, such a statement should be treated with caution. Some of the lavas under consideration are of intermediate and acid compositions. Distribution coefficients of immobile, incompatible elements compiled by Pearce and Norry (1979) generally increase in magnitude as more acid compositions are approached. Bulk distribution coefficients of these elements can thus be expected to increase with differentiation and differences in D's between different elements may become significant, resulting in fractionation of the inter-element ratios.

In addition, samples from all groups appear in certain variation diagrams to plot along continuous trends (e.g. Figure 17, Nb versus Zr) and in a general sense approximate a compositional continuum from basic through to acid types. Genetic links between the various magma types can thus not be ruled out.

Because of the problems concerning genetic interpretation mentioned in Section A of this chapter, much reliance needs to be placed on geological

evidence to support the geochemical constraints in making a realistic assessment of the inter magma-type relationships. Initially, the broad between-group relationships are considered below, followed by the relationships between formations within specific groups.

C. Between-Group Relationships

1. Dominion Group - Ventersdorp Supergroup

Despite trivial manifestations of volcanicity within the intervening Witwatersrand Supergroup, the fact that approximately 7500m of sediment accumulated after extrusion of the Dominion lavas and prior to extrusion of the Ventersdorp lavas demonstrates the existence of a long-lived hiatus in volcanicity during Witwatersrand times. Radiometric age dating (see Chapter II) confirms an age difference between the Dominion and Ventersdorp lavas of somewhere in the region of several hundred million years.

Hildreth (1981) considers the normal duration of the activity of a magmatic system resulting in the formation of a volcanic field to be in the order of 10^7 years, thus less by an order of magnitude than the age discrepancy between Dominion and Ventersdorp times.

It is thus concluded that the Dominion and Ventersdorp successions represent two separate magmatic events. Compositional similarities between the more basic lavas of the Dominion and Ventersdorp sequences have been demonstrated in Chapter VI. These suggest that similar conditions existed in the mantle during both magmatic episodes, although the lavas evolved along different paths (see Chapter VII). Differences in source composition are reflected in the ability to discriminate between the pertinent magma types by virtue of incompatible element ratios. This topic will be discussed further in Chapter IX.

2. Klipriviersberg Group - Platberg Group :

Superficially, it appears that a major time break existed between the

extrusion of the Klipriviersberg and Platberg Group magmas, with the intervening Kameeldoorns sediments resting upon a major unconformity which represents the boundary between the two Groups.

However, it was noted in Chapter III that a more complex situation appears to exist. Boreholes WS-4 and WS-5 contain a short sequence of Platberg type lava sandwiched between the top of the Klipriviersberg lavas and the base of the Kameeldoorns sediments. Furthermore, borehole JHA-1 contains a thick succession of Kameeldoorns type sediments intercalated with Platberg lava (see Figure 10). The writer has subsequently observed similar situations in areas removed from the present study area.

It is thus suggested that no significant time lapse occurred between Klipriviersberg and Platberg times. The immature nature of the Kameeldoorns sediments supports this contention. It thus appears that the onset of Platberg volcanism was contemporaneous with the deposition of the Kameeldoorns sediments. Such a model does not detract from conclusions reached by Winter (1965, 1976) that the sediments were deposited as clastic wedges adjacent to fault scarps.

Brink (1982) concluded from a structural study of the Witwatersrand strata in the Buffelsdoorn gold mine situated to the east of Klerksdorp, that no major faulting occurred during Klipriviersberg times. A period of enhanced tectonic activity, manifested by the development of major fault systems, commenced after the Klipriviersberg lavas were extruded (Brink, 1982).

It is thus suggested that the onset of Platberg type volcanism coupled with the deposition of the Kameeldoorns sediments reflect a change in tectonic regime within the crust. Such a change may also be reflected in the significant compositional differences between the Klipriviersberg and Platberg magma types, and will be further discussed in Chapter X. There is thus no chronological basis for rejecting a genetic link between the lavas of the two Groups.

Despite a large degree of overlap in major element chemistry between lavas of the two Groups, they display widely divergent minor and

trace element concentrations, and are widely separated on the Ti/Zr versus Ti/P discrimination diagram (Figure 18). It was demonstrated in the previous chapter that Ti and P appear to have behaved compatibly at some stage during the evolution of the Goedgenoeg/Rietgat lavas. Nevertheless, the observed coherency of Ti and P (see Figure 29) suggests that it is unlikely that the Ti/P ratios could have been modified sufficiently by differentiation processes to produce the observed discrepancy in Ti/P ratio between tne Klipriviersberg and Platberg lavas (see Figure 18). A simple differentiation relationship can thus be ruled out. Moreover, Ti/P ratios were invoked in Chapter VII to show that the Klipriviersberg lavas could not have represented a basic end-member in an hybridization model for the generation of the Goedgenoeg/Rietgat lavas.

Derivation of the Goedgenoeg/Rietgat lavas by differentiation of the evolved Klipriviersberg lavas is unlikely because the former have higher Cr, M-values, normative anorthite and similar Ni, despite being more evolved on the basis of SiO_2, normative quartz and incompatible element content (Table II). The Goedgenoeg/Rietgat lavas are furthermore strongly depleted in Cu relative to the Alberton and Orkney lavas. This feature could only be explained by sulphide fractionation. This would, however, be accompanied by a strong depletion in Ni, which is not the case.

It is unlikely that the two Groups could be genetically related by different degrees of partial melting of the same source material, since this would still not account for the contradictory geochemical characteristics of the Goedgenoeg/Rietgat lavas. Derivation of the Goedgenoeg/Rietgat lavas by complex processes involving crustal melting along with extensive remelting of Klipriviersberg material previously trapped within the crust (e.g. Cox, 1980), has not been considered in the present study. This may, however, be a fruitful line to pursue in a more detailed investigation.

It is thus concluded that no simple genetic relationship exists between the lavas of the Klipriviersberg and Platberg Groups.

3. Allanridge Formation - Platberg Group :

Relative to the Allanridge lavas, the Goedgenoeg/Rietgat lavas have higher Cr, M-values, normative anorthite and similar Ni, but normative quartz and incompatible element levels are also higher (Table II). All the Platberg Group lavas have much lower Ti/P ratios than the Allanridge lavas. Therefore arguments similar to those applied above for the Klipriviersberg lavas may be used to show that there is no evidence to suggest a genetic relationship between the Allanridge and the Platberg magmas.

Additionally, the intervening Bothaville formation sediments are mature, flat-lying, and were laid down after a period of extensive peneplanation (Winter, 1976; Tankard et al., 1982). This definite hiatus in volcanic activity suggests that the Allanridge lavas might represent a separate magmatic episode.

4. Allanridge Formation - Klipriviersberg Group :

A large time interval separates the Allanridge from the Klipriviersberg lavas, during which the Platberg Group and Bothaville Formation rocks were deposited and which includes the Bothaville period of peneplanation.

Compositionally, the Allanridge lavas are more evolved than the Klipriviersberg lavas, containing higher SiO_2, normative quartz and incompatible elements, and lower MgO, M-values and normative anorthite (see Table II). Moreover, inspection of the variation diagrams in Figures 15 and 17 shows that the Allanridge samples generally plot on a projection of the Klipriviersberg trends to more evolved compositions. The only readily detectable exception is TiO_2, where the Allanridge samples have lower TiO_2 than the projected trend of the Klipriviersberg samples. This feature alone provides the means for distinguishing the Allanridge lavas from the Klipriviersberg lavas on the basis of Ti/Zr and Ti/P ratios (Figure 18).

The above observations suggest that the Allanridge lavas could be derived by fractional crystallization of Klipriviersberg type magma.

Precipitation of a Ti-bearing mineral such as magnetite or ilmenite could be invoked to explain the reduction in the rate of TiO_2 enrichment. However, this would be expected to be reflected in other elements such as Ni, Co and V, which does not appear to be the case.

Alternatively the lower Ti/Zr and Ti/P ratios of the Allanridge relative to the Klipriviersberg lavas may be attributed to source heterogeneity, in which case the Allanridge lavas would have evolved independently (although along a similar path) of the Klipriviersberg lavas. This is considered to be more feasible, especially if the large time interval between the two is taken into account.

5. Jeppestown Amygdaloid :

The stratigraphic position of the Jeppestown amygdaloid within the Witwatersrand Supergroup, and the trivial volume of lava relative to the sediments, suggests that it can be regarded as representing an isolated magmatic event. Secondly, the mean composition of the Jeppestown amydaloid samples is clearly distinct from that of the other magma types under investigation (cf. Table II).

It is thus concluded that the possibility of genetic relationships existing between the Jeppestown amygdaloid lavas and the lavas of the remaining members of the Witwatersrand triad is highly remote.

D. Within-Group Relationships

1. Dominion Group:

The occurrence through time and space of bimodal volcanic suites has for years presented a perplexing problem to igneous petrologists.

The intimate association of basic and acid volcanics, with a distinct compositional break between them, has generally been explained by two broad models. The first postulates a fractional crystallization relationship between the two components (e.g. Ewart et al., 1976), and the second postulates the derivation of the acid volcanics by

crustal melting as a result of the heat flux provided by the mantle-derived basic magmas (e.g. Blake et al., 1965; Robertson, 1981; Condie, 1982; Condie and Nuter, 1981).

Neither of the above models is universally applicable, and various combinations and modifications, combined with the introduction of more complex processes (see Hildreth, 1981) have been invoked to satisfy various constraints in specific situations.

In the Dominion Group lavas, significant features are :

(a) The basic lava sequence displays a broad compositional spectrum, where the most evolved lavas have been shown in Chapter VII to be representative of the final 16% residual liquid derived by continuous, closed-system fractional crystallization of the most primitive magmas sampled.

(b) The acid lavas may be regarded as an isochemical unit, the limited compositional variation present being attributable to secondary alteration and metamorphic processes (see Chapter VI and VII). The mean (Table II) is considered to be representative of the original magma composition.

(c) A distinct compositional gap is present between the basic and acid lava suites. This is well-illustrated by a 6% discrepancy in SiO_2 between the most evolved lavas of the basic suite and the mean acid lava composition (Figure 32). Nevertheless, the latter contains lower Zr concentrations than the former (see Chapter VI).

(d) The intimate spatial and chronological association between the two suites is indicated by field relationships, where each suite contains minor intercalations of the other (see Chapter III).

(e) Available information shows the basic lava sequence to be volumetrically subordinate to the acid lavas, the full succession of which is not represented in the boreholes sampled in the present study (SACS, 1980; Watchorn, 1980).

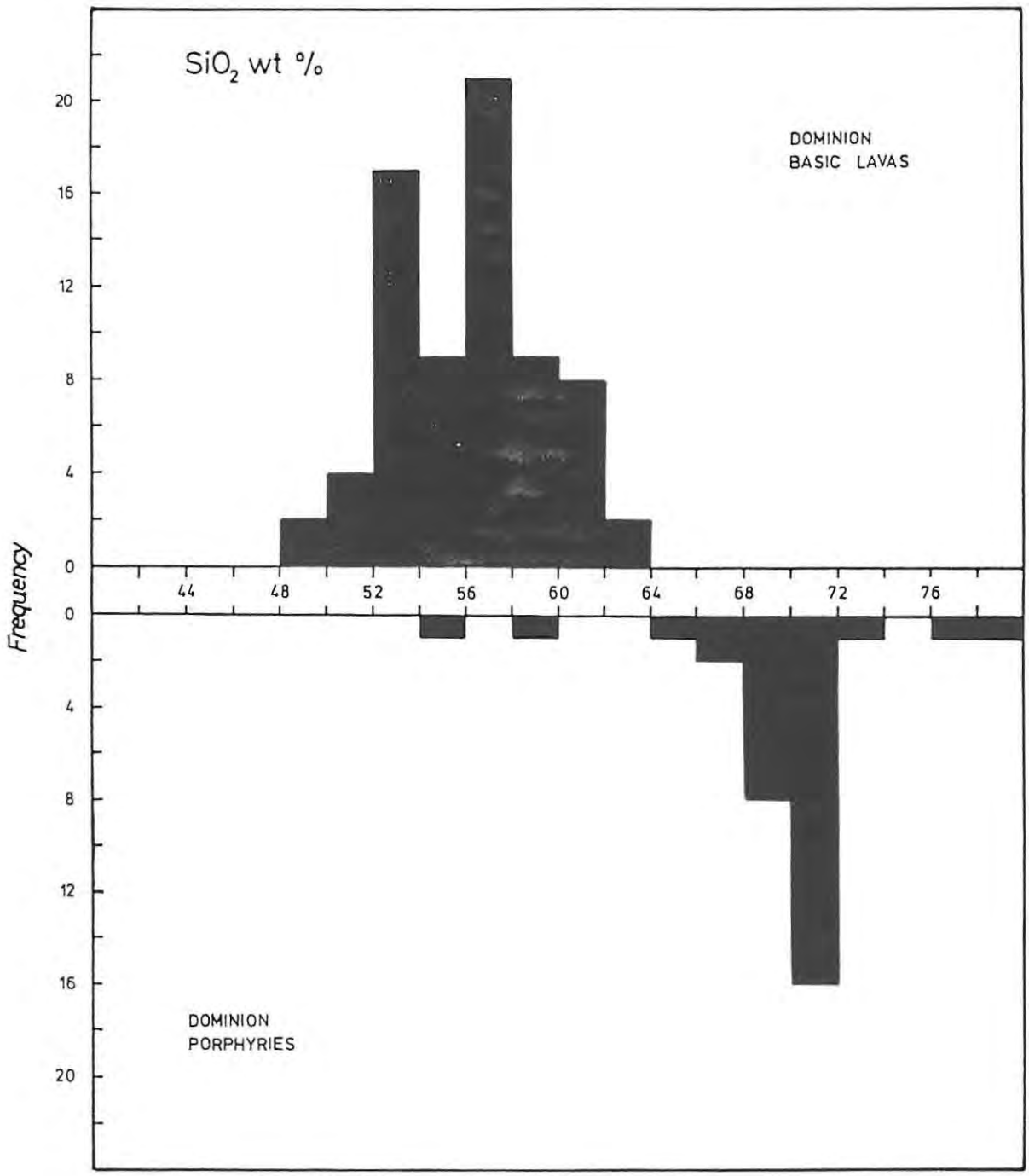

Figure 32: Comparison of the distributions of SiO_2 in the Dominion basic lavas and the Dominion porphyries.

Hildreth (1981) has documented five postulated mechanisms for the generation of bimodal volcanic suites. In addition to fractional crystallization and partial melting, differentiation processes involving convective separation of liquid from partially molten diapirs and remelting of igneous forerunners are also considered. Each model takes into account both physical and chemical constraints. The possibility of two or more of the postulated mechanisms occurring concurrently or successively is stressed.

Stringent application of the various models to the Dominion Group lavas is outside the scope of this study, especially since the limited compositional variation of the porphyries obscures their pre-eruptive history. Nevertheless, the characteristic features of the Dominion volcanics listed above fit well with a model whereby the acid volcanics are a product of partial melting of older crustal rocks. Describing such a model, Hildreth (1981) states that :

"An extensional tectonic stress regime that favoured the brittle failure of crustal rocks that were partially melted by intruding basalt could permit extraction of rhyolitic liquids in tabular bodies. At the same time it would suppress hybridization, entrainment of residues, and melting extensive enough to generate liquids much less silicic than rhyodacite. ... shallow aggregation could produce predominantly rhyolitic magma chambers of any size ... ... most of these extensional magmatic systems are apparently bimodal, erupting little or no magma of intermediate composition. This is thought to be a leading mechanism for the generation of continental rhyolites on all scales."

The main criteria for rejecting a model whereby the acid porphyries represent differentiation products of the basic lavas are as follows :

The most evolved samples of the Dominion basic lava sequence have been shown to represent the residual liquid after 84% crystallization of the assumed parental magma. Substantially more crystallization would be required to produce the compositions of the acid porphyries. (Such a process would be difficult to monitor, since the lower Zr, Ti and P contents of the porphyries would require that these

elements became compatible at some stage.) The large volume of extruded acid volcanics relative to that of the basic lavas would be difficult to reconcile with a differentiation model, where the acid component would be expected to be very subordinate. However, the density filtering capability of the crust may have caused preferential extrusion of the less-dense acid volcanics, with the bulk of the basic magmas remaining ponded within the crust. A crustal melting model is thus favoured, although more detailed work is required to prove this model and to eliminate other possibilities.

2. Klipriviersberg Group :

It has been demonstrated in Chapter VI that the Klipriviersberg Group can be chemically subdivided into three distinct units corresponding to different formations within the Group. The chemical variation of the Loraine/Edenville formations is attributable to fractional crystallization (see Chapter VII), while the Orkney and Alberton formations each display more limited compositional variation and the mean compositions (see Table II) are considered representative of the bulk of the lavas in these suites.

It was further demonstrated in Chapter VI (see Figures 15, 16 and 17) that, where trends are discernible, the Alberton samples generally lie on projections of the Loraine/Edenville trends to more evolved compositions. The compositions of samples of the Orkney formation are generally intermediate between those of the more evolved Loraine/Edenville and Alberton formation samples, but show a tendency to be more enriched in Ti, Fe, Co and V relative to the latter. While this enrichment in Ti is insufficient to permit chemical discrimination between the component units on the Ti/Zr versus Ti/P diagram (Figure 18), it is nevertheless significant in that it demonstrates that the three units are discrete entities which are not on a continuous liquid line of descent. Nevertheless, the fact that they cannot be discriminated between using immobile incompatible element ratios is strong evidence in favour of them effectively being evolved by slightly different fractionation paths from a common parent. The resolution of the data is insufficient to determine whether parent compositions were slightly different.

Field evidence suggests that there were no significant time breaks and that the volcanism was continuous. This may be taken as evidence of consanguinity but is not decisive.

It was noted in Chapter V that the Alberton and Orkney lavas contain plagioclase phenocrysts and microphenocrysts. These are not present in the Loraine/Edenville lavas. Thus, if the Orkney and Alberton lavas are more differentiated products of the Loraine/Edenville sequence, plagioclase may have become part of the fractionating assemblage. A plot of Al_2O_3 versus Zr (Figure 33) supports this contention, where the strong enrichment of Al_2O_3 with increasing Zr in the Loraine/ Edenville lavas is not continued through to Orkney and Alberton lava compositions. The enrichment of the siderophile elements in the Orkney formation requires that the fractionation paths of the Orkney and Alberton magmas diverged after the more evolved Loraine/Edenville compositions had been attained. This could be attributed to variable roles of oxides or minerals such as plagioclase (which exclude the siderophile elements) in the later stages of differentiation.

Alternative explanations are equally plausible, however, and the Loraine/Edenville, Orkney and Alberton magmas may have evolved independently from a common parent, with only the most differentiated magmas of the latter two formations reaching the surface. A third possibility is that the lavas of the three formations may have been derived by separate batch melting episodes of a mantle source which was progressively more depleted in incompatible element levels, or by variable degrees of melting of the same source, resulting in parent magmas with slightly varying incompatible element levels which subsequently evolved along parallel liquid lines of descent. These alternatives are illustrated in Figure 34 using a plot of Cr versus Zr.

There is insufficient resolution of data to adequately test the above proposals, and other alternatives cannot be ruled out. The only conclusions which may be drawn from the present level of study are that the three chemically distinct units of the Klipriviersberg Group may effectively be regarded as consanguinous, but that they do not represent a continuous differentiation sequence.

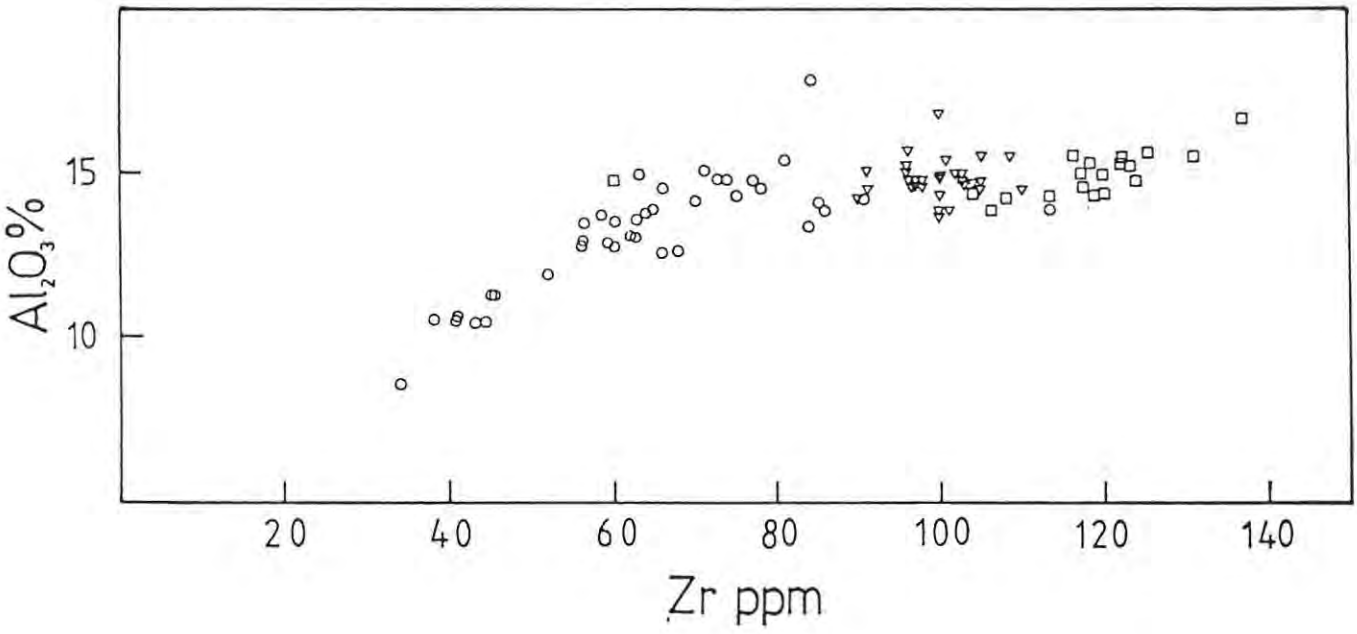

Figure 33: Variation of Al_2O_3 with Zr in the Klipriviersberg lavas. Suppression of the strong initial Al_2O_3 enrichment trend is probably attributable to the introduction of plagioclase as a liquidus phase. Symbols: Circles - Loraine/Edenville formations; triangles - Orkney formation; squares - Alberton formation.

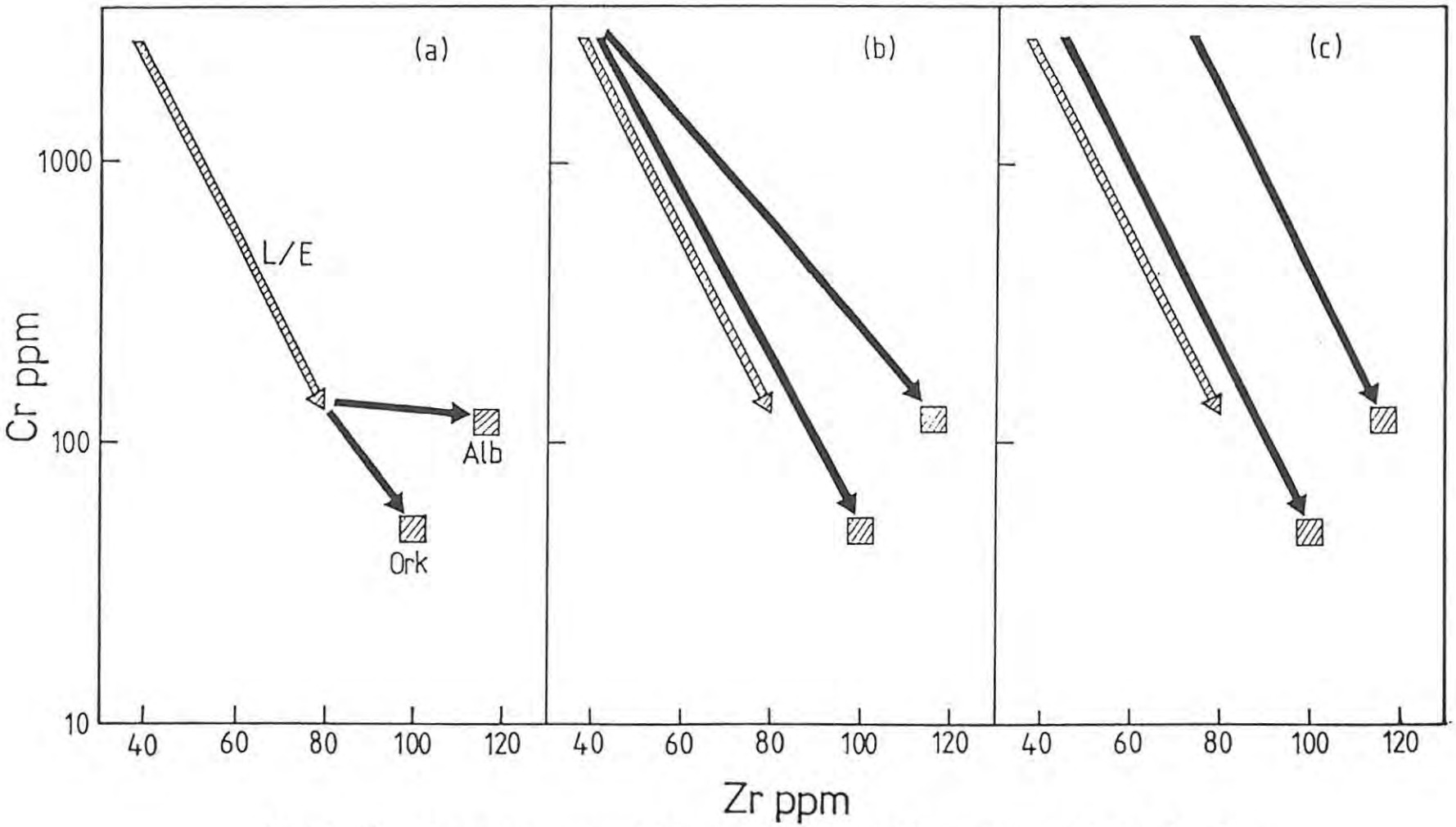

Figure 34: Schematic representation of 3 possible modes of origin for the Orkney and Alberton lavas, using their Cr-Zr relationships. Shaded arrow and squares represent the Loraine/Edenville trend and mean Orkney and Alberton compositions respectively. Solid arrows represent hypothetical trends: a) Independent differentiation from evolved Loraine/Edenville composition. b) Differentiation along sub-parallel paths from a common parent. c) Differentiation along parallel paths from different parent compositions resulting from successive batch melting or variable degrees of partial melting.

3. Platberg Group:

Relationships between the three volcanic formations of the Platberg Group are obscured by the fact that the Goedgenoeg and Rietgat formations are chemically indistinguishable, and the origin of the Makwassie porphyries is uncertain.

Several factors nevertheless suggest that the three formations are cogenetic: Field relationships discussed previously suggest that no significant time breaks occurred during Platberg times. The Goedgenoeg and Rietgat formations cannot be distinguished on a chemical basis, yet are separated stratigraphically by the Makwassie porphyries and are petrographically distinguishable by virtue of the characteristic feldspar phenocryst morphologies (see Chapter V). Furthermore, petrographical gradations have been observed where the feldspar phenocryst density in the Goedgenoeg lavas may increase to the extent where the lava resembles the Makwassie porphyries (see Chapter V), although the flows still retain their amygdaloidal tops and bases which are more characteristic of the Goedgenoeg lavas. In extreme cases these samples become compositionally similar to the Makwassie porphyries (see Chapter VI, Section D,3).

In Chapter VII, a hybridization model was proposed to account for the compositional features of the Goedgenoeg/Rietgat lavas. The Makwassie porphyries were thought to represent an acid end-member, the basic end-member being unrepresented in the Ventersdorp volcanic pile. While the above model most certainly represents a drastic oversimplification, the fact that such a model is required by the available evidence suggests that the Goedgenoeg/Rietgat lavas are not simple differentiates of mantle-derived magma, and a crustal component is implied.

It is thus tentatively suggested that the Makwassie porphyries represent crustal melts which, in addition, have interacted by contamination, assimilation or magma-mixing, with unrepresented basic magma to form the Goedgenoeg/Rietgat lavas. Considering the controversy which surrounds the concept of hybridization on a large scale (see Hughes, 1982, p. 208), a lot more work is required before this hypothesis can be accepted or rejected.

E. Conclusions

A brief summary of the conclusions reached in the foregoing chapter is presented below :

(a) The Dominion Group rocks have no genetic links with any of the other Witwatersrand triad lavas. The bimodal nature of the Dominion volcanics is probably a result of melting of separate source rocks (i.e. mantle and crustal) during the same magmatic event.

(b) The lavas of the Jeppestown amygdaloid represent an isolated magmatic event and are compositionally unrelated to the other lava types of the Witwatersrand triad.

(c) The Klipriviersberg lavas are not consanguinous with any of the other magma types. The lavas of the three chemically-definable formations within the Klipriviersberg group are probably consanguinous, but do not lie on a common liquid line of descent.

(d) Lavas of the Platberg Group are not related genetically to any of the other magma types. Extrusion of the Platberg lavas commenced directly after Klipriviersberg times, and was accompanied by a period of enhanced tectonic activity. The Goedgenoeg and Rietgat lavas are thought to represent hybrid magmas containing both mantle and crustal components, where the Makwassie porphyries represent the crustal-derived acid end-member. The basic end-member is not represented in the Ventersdorp lava pile.

(e) The Allanridge lavas represent an isolated magmatic event. Despite compositional similarities, they are unlikely to represent more evolved products of Klipriviersberg-type magma.

IX MANTLE SOURCE CHARACTER

A. Source Heterogeneity

It has frequently been suggested in preceeding chapters that fundamental chemical differences between different magma types, and variations within magma types, might be attributable to heterogeneous source compositions. Erlank et al. (1980) have demonstrated that the upper mantle beneath Southern Africa has been chemically heterogeneous since Archaean times. It is thus important to assess whether such heterogeneities are reflected in the data from the Witwatersrand triad.

The rationale behind using immobile incompatible element ratios as indicators of source heterogeneity was discussed in Section B of the previous chapter, and is briefly reviewed here: Since differences between distribution coefficients of the highly incompatible elements are negligible, they remain covariant during partial melting and fractional crystallization processes, and ratios involving these elements should thus remain constant (Gast, 1968; Arth, 1976). However, because D's increase in magnitude with progressively more differentiated liquid compositions (Pearce and Norry, 1979), differences in D's may become significant, resulting in the fractionation of interelement ratios which may mask discrete differences in source composition.

This problem arises in the Witwatersrand triad lavas, since most magma types are differentiated to varying degrees, showing diverse ranges in incompatible element levels. Furthermore, certain magma types are thought to be wholly or partially derived from crustal material. Possible effects of partial melting variables on the interelement ratios is another unknown entity, since melting processes have not been modelled.

In order to minimize these problems, only the most basic lavas of the Dominion Group are considered below, namely those with less than 125 ppm Zr, for which the mean composition appears in Table II (analysis 2). Selected interelement ratios of these samples are compared by means of histograms with those for the Loraine/Edenville samples, which represent the most basic lavas of the Klipriviersberg Group. Both these groups contain the most primitive lavas in the Witwatersrand triad, and there is little doubt that they represent mantle-derived liquids. Differences in interelement ratios should thus reflect differences in their respective

sources.

Histograms comparing the Zr/Nb, Zr/Y, Ti/Zr, Ti/P and Ce/Nd ratios of the two magma types are presented in Figure 35. Arithmetic means are indicated by means of arrows.

The distributions of Zr/Nb ratios of the two magmas are indistinguishable, while those of Zr/Y, Ti/Zr and Ce/Nd ratios show definite differences, but a large degree of overlap is evident. The Ti/P ratio distributions display the least variance, and there is very little overlap. The Ti/P ratio has thus proved to be an efficient discriminating variable (see Figure 18).

Several factors may have contributed to the spread of the data: Possible fractionation effects have already been discussed. Secondary alteration and metamorphism have probably caused a certain amount of scatter. A major factor is undoubtedly error due to the low concentration levels of Nb, Nd and possibly Y in many of the samples, since analytical precision deteriorates as concentrations approach detection limits (see Appendix I). In such cases, underestimates of concentrations of the denominator have a more pronounced influence on the ratio than overestimates, resulting in the skewed distributions which are evident in the Zr/Nb, Ce/Nd and, to a lesser degree, in the Zr/Y histograms.

Although interelement ratio differences between the two magma types are readily apparent, the above factors have caused a smearing of the data and these differences are possibly not as conspicuous as they may have been in the pristine liquids. Ideally, the relative distributions of the interelement ratios can nevertheless be taken as evidence for mantle heterogeneity but it should be pointed out that complicating factors may be present. These are :

(a) The presence of minor residual phases in the mantle.

(b) Possible crustal contamination.

The presence of minor phases in the mantle, such as apatite and sphene, could result in very different interelement ratios being produced in liquids generated by different degrees of partial melting of the same

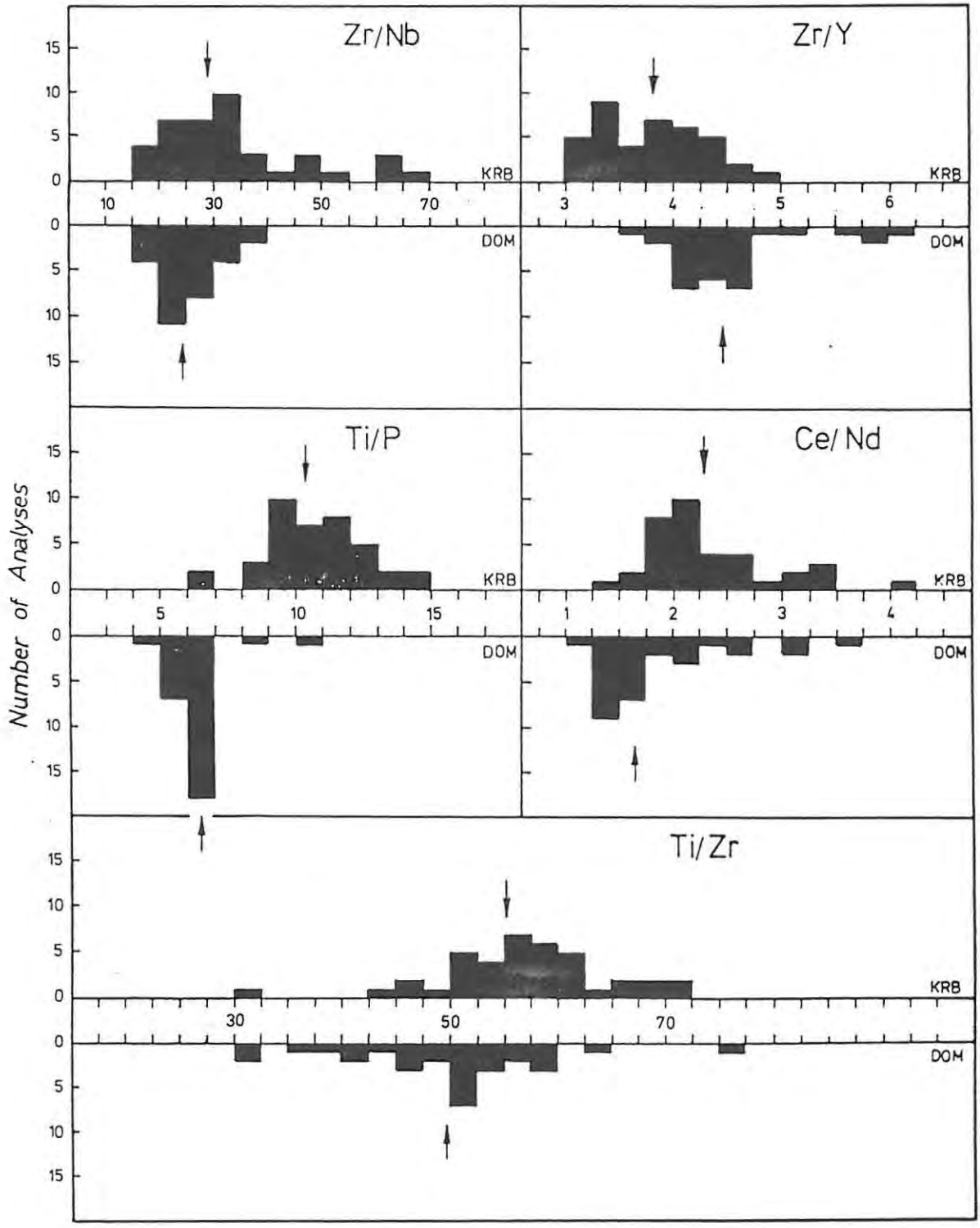

Figure 35: Comparison of immobile, incompatible element ratio distributions between the most primitive lavas of the Klipriviersberg Group (those of the Loraine/Edenville formations) and those of the Dominion basic lavas (with Zr<125ppm). Arrows indicate arithmetic means.

source. However, if minor phases are completely melted during the initial stages of partial melting, further melting will result in constant ratios which are a true reflection of source composition.

For example, Beswick and Carmichael (1978) suggested that phosphate minerals such as whitlockite and apatite may be present in the mantle, remaining stable over the entire P-T range of magma generation. However, Frey et al. (1980) have disputed the validity of the assumptions on which Beswick and Carmichael's (op. cit.) conclusions were based. Furthermore, Watson (1980) has shown that P_2O_5 is highly soluble in basaltic liquids at mantle temperatures and pressures, and that the possibility of apatite being residual after the generation of basaltic liquids is remote.

The general consensus appears to be that minor phases, as in the above example, are not residual in the mantle after the large degrees of partial melting which are required to produce basaltic liquids (Ringwood, 1975). It is thus unlikely that minor residual phases have affected the interelement ratios of the magmas under consideration.

It is possible that the interelement ratios have been modified by varying degrees of crustal contamination of the respective magmas en route to the surface. Isotopic data is required in order to evaluate this possibility adequately. The importance of crustal contamination in the modification of magma compositions is a controversial topic (Cox et al., 1979; Hughes, 1982), but it is generally regarded as having a negligible effect when copious amounts of magma, as in flood-basalt volcanism, are involved.

It is therefore concluded that heterogeneous chemistry was a feature of the mantle source during the early Proterozoic, and has contributed to the evolution of distinct magma types within the lava pile.

B. Source Composition

The aim of this section is to review briefly certain aspects of the conclusions reached by Wyatt (1976) on the petrogenesis of the Klipriviersberg lavas in the area south of Johannesburg, and to assess

these conclusions in the light of data accumulated in the present study.

Approximately half of Wyatt's (op. cit.) analyses represent the basal Mg-rich lavas of the Westonaria formation, which Wyatt (op. cit.) showed to be unrelated to the upper Klipriviersberg lavas. Since the Westonaria formation is not present in the Klerksdorp area (see Chapter II, E), these lavas are not considered further. Wyatt's (op. cit.) study did not reveal the presence of Mg-rich lavas in the Loraine/Edenville formation. The probable reason for this is the fact that the Klipriviersberg succession in the area south of Johannesburg is truncated by an unconformity on which the Transvaal Supergroup sediments were deposited. Most of the Mg-rich lavas have thus been eroded away, since they are concentrated towards the top of the succession (see Figure 36). Wyatt (op. cit.) nevertheless noted an increase in basicity of the lavas with height. In his petrogenetic modelling, he treated all his samples together, and did not differentiate chemically between the Alberton, Orkney and Loraine/Edenville formations. The mean composition of Wyatt's (op. cit.) upper Klipriviersberg samples is compared in Table VI with those of the Orkney and Alberton formations of the present study. Wyatt's (op. cit.) mean composition is clearly representative mainly of the Alberton and Orkney formation lavas, as well as the evolved Loraine/Edenville lavas, all of which have very similar major element compositions.

Wyatt (op. cit.) was unable to produce a satisfactory fractional crystallization model to account for the limited compositional variation of his samples. This is understandable, since the present study has shown that the Alberton, Orkney and Loraine/Edenville lavas do not lie on a common liquid line of descent (see Chapter VIII; D). Wyatt (op. cit.) concluded that the Klipriviersberg lavas represent close to primary melts of a wet peridotite mantle. This conclusion was based on the results of workers such as Kushiro et al. (1968), Kushiro (1969; 1970; 1972; 1974), Mysen (1973), Nicholls and Ringwood (1972; 1973), Nicholls (1974), Green (1973) and Boettcher et al. (1975), who showed that quartz-normative liquids such as quartz-tholeiites and andesites may be produced by direct partial melting of the mantle under water-rich conditions.

The present study (see Chapter VII) has shown that the most evolved lavas

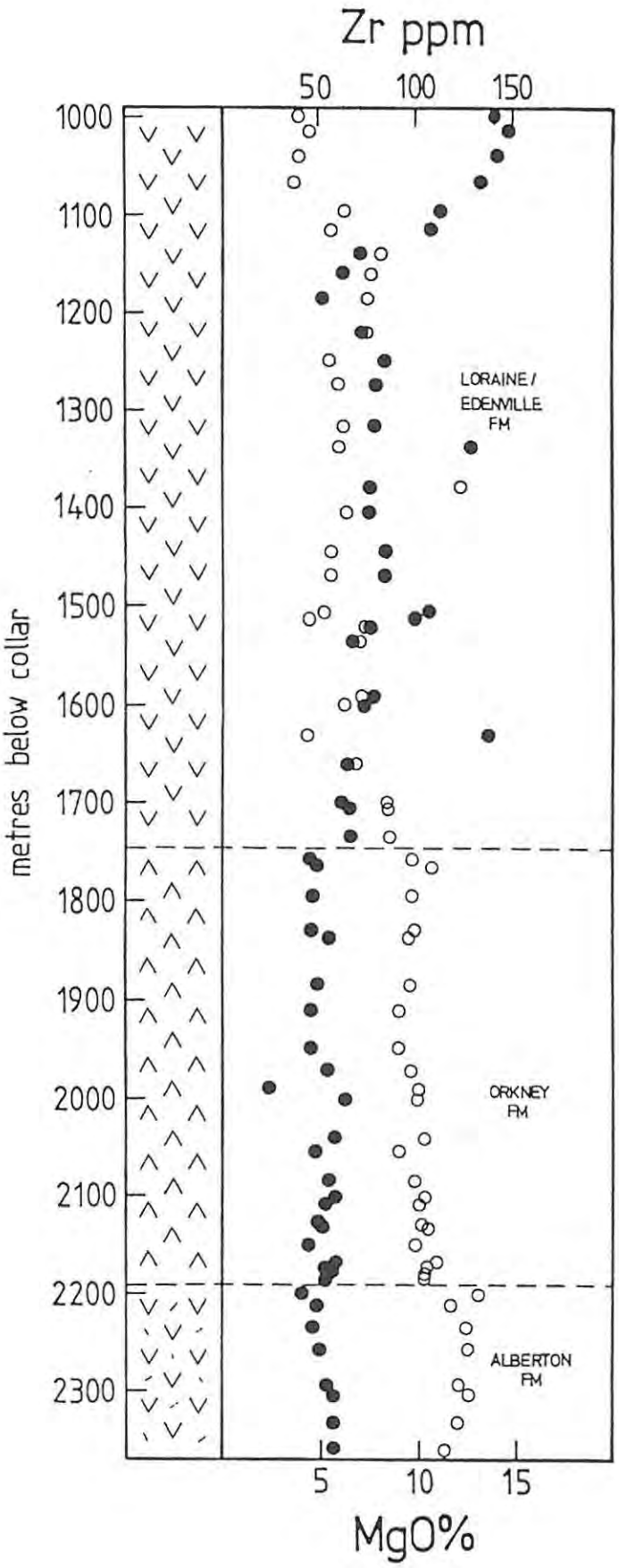

Figure 36: Variation of MgO (solid circles) and Zr (open circles) with height in the Klipriviersberg lavas from borehole WS-5. Note the general increase in basicity from the base upwards, and the compositional breaks at formation boundaries.

TABLE VI: Comparison of mean composition of Wyatt's (1976) "Upper Kliprivіersberg" lavas with means of the Alberton and Orkney formations from this study.

	1	2	3
SiO_2	55.19	55.41	54.00
TiO_2	.94	1.07	.98
Al_2O_3	14.87	14.95	14.85
Fe_2O_3	11.41	11.44	12.67
MnO	.14	.13	.15
MgO	5.00	5.12	5.00
CaO	7.64	7.19	7.45
Na_2O	2.96	3.40	3.45
K_2O	1.66	1.13	1.32
P_2O_5	.18	.16	.13
Ba	748	438	421
Nb	5.4	5.5	4.9
Zr	112	116	100
Y	20	22.2	22.5
Sr	373	393	344
Rb	60	39.4	50.0
Zn	87	85	92
Cu	94	92	95
Ni	166	158	142
Co	-	61	67
Cr	120	124	51
V	172	184	266
La	-	12	11
Ce	-	30	29
Nd	-	14	14

1. Mean "Upper Klipriviervberg lavas" from Wyatt (1976). FeO recalculated to Fe_2O_3, all elements normalized to 100% volatile free.
2. Mean Alberton lavas - this study.
3. Mean Orkney lavas - this study.

of the Loraine/Edenville formation have been derived from the most primitive lavas by 60% fractional crystallization. Hence the Alberton and Orkney lavas, being more evolved, have probably undergone at least 60% fractional crystallization. This feature, together with the relatively uniform composition of the Alberton, Orkney and evolved Loraine/Edenville lavas, supports the conclusion reached by McIver (1975), who showed that the lavas analysed by Wyatt (op. cit.) represent evolved liquids which have undergone a period of low-pressure equilibration.

The most primitive Loraine/Edenville lavas (e.g. sample KL-468) are characterized by relatively high SiO_2 levels, and are generally quartz-normative, despite MgO levels of up to 17.5% (see Table II). It was demonstrated in Chapter VII that olivine did not form part of the fractionating assemblage during crystallization. This feature is attributable to the inherently high SiO_2 content of the magma. These comments are equally true for the Dominion basic lavas.

Similarities between the Mg-rich lavas of the Witwatersrand triad, and modern high-magnesian andesites and bonninites, were pointed out in Chapter VI (E). The latter rock-types are characterized by high SiO_2 coupled with high MgO contents. There is general consensus amongst many workers that these features result from partial melting of mantle peridotite in water-saturated and/or water undersaturated environments (Crawford et al., 1981; Jenner, 1981; Tatsumi, 1981; 1982; Tatsumi and Ishizaka, 1982).

It is thus concluded that Wyatt (op. cit.) was correct in suggesting that the Klipriviersberg lavas were derived by partial melting of a hydrous mantle, but the bulk of the lavas have undergone a substantial degree of fractional crystallization, and thus represent evolved derivatives of the primary melts. Since most of the mafic lavas of the Witwatersrand triad are characterized by relatively high SiO_2 levels, and may thus be classified as tholeiitic andesites, it is suggested that all were derived from a hydrous source. Thus, while the mantle was probably chemically heterogeneous (see Section A of this chapter), the presence of H_2O appears to have been an ubiquitous feature throughout early Proterozoic times.

X SUMMARY

The lavas of the Witwatersrand triad can be subdivided into seven distinct magma types which broadly correspond with existing stratigraphic subdivisions. Chemical distinctions between the different magma types are made on the basis of their immobile, incompatible element chemistry, where Ti/P and Ti/Zr ratios together represent the most efficient discriminating variables. In addition, absolute Zr concentrations identify individual magma types within the Ventersdorp Supergroup, and are essential for further stratigraphic subdivision of the Klipriviersberg Group.

The rocks of the Witwatersrand triad have been subjected to low-grade, greenschist facies, regional metamorphism. Primary mineral assemblages have thus been partially or completely destroyed, but original textures are still preserved. No large scale metasomatic processes were operative, and in most cases alteration appears to have been effectively of a closed system type.

Compositionally, the lavas cover a broad spectrum from close to primary mantle melts to rhyolites. Despite variable trace element signatures, the bulk of the lavas display overlapping major element compositions and are characterized by broad compositional similarities. Relative to modern tholeiitic basalts, the mafic lavas are enriched in SiO_2 and depleted in MgO, but have similar Al_2O_3, transition element and, in most cases, incompatible element levels. Modern calc-alkaline andesites have between 16% and 20% Al_2O_3 (Irvine and Barager, 1971), whereas in the Witwatersrand triad lavas, Al_2O_3 content seldom exceeds 16%. It is thus suggested that the term "tholeiitic andesites", as defined by Wilkinson and Binns (1977), is appropriate for the bulk of the mafic lavas, since it describes both their tholeiitic affinities and intermediate compositions. According to this scheme, the more primitive lavas may be classified as magnesian tholeiites and tholeiites, and the felsic lavas range from tholeiitic dacites to rhyolites.

The Dominion Group lavas represent a typical example of bimodal volcanism, comprising two unrelated magma types, the Dominion basic lavas and the Dominion acid porphyries. The basic lava suite is highly

differentiated, with compositions ranging from magnesian tholeiites to tholeiitic andesites. The compositional variation has been attributed to a two-stage fractional crystallization process.

The initial stage is represented by 45% crystallization of hornblende, followed by 70% crystallization, from the residual liquid, of an assemblage comprizing plagioclase and orthopyroxene in the proportions .65:.35, possibly accompanied by up to 3% sulphide.

The Dominion porphyries are rhyolites of uniform composition, the limited variation of which has been attributed to secondary alteration effects. They are thought to represent crustal melts generated by the heat flux provided by the mantle-derived basic lavas.

The Jeppestown amygdaloid comprises tholeiitic dacites of extremely uniform composition, despite large textural variations. Their origin has not been established, but they represent an isolated magmatic event.

The Klipriviersberg Group lavas can be subdivided into three stratigraphically consistent units on the basis of Zr concentrations. The Alberton lavas, at the base of the succession, are the most evolved, and are overlain by the Orkney lavas which are characterized by lower incompatible element levels and a relative enrichment of the siderophile elements. These magmas each display very limited compositional variation and fall within the tholeiitic andesite range. The uppermost Loraine/Edenville lavas are the most primitive, ranging from magnesian tholeiites to tholeiitic andesites. The magnesian tholeiites are concentrated towards the top of the succession, and represent close to primary mantle melts. Modelling suggests that the Loraine/Edenville lavas evolved by 38% fractional crystallization of Mg-rich orthopyroxene, possibly accompanied by a minor proportion of chromite, followed by 35% crystallization, from the residual liquid, of an extract in which augite predominated.

The Alberton, Orkney and Loraine/Edenville lavas are probably consanguinous, but do not lie on a common liquid line of descent.

Platberg Group volcanism appears to have commenced directly after Klipriviersberg times, and was accompanied by a period of enhanced

tectonic activity which resulted in the contemporaneous deposition of the Kameeldoorns sediments adjacent to fault scarps. Platberg volcanism is thus related to the same tectono-thermal event which produced the Klipriviersberg magmas.

Two magma types have been recognised within the Platberg Group, the Goedgenoeg/Rietgat lavas and the Makwassie porphyries. The Goedgenoeg/Rietgat lavas represent two petrographically-distinct lava formations which are separated stratigraphically by the Makwassie porphyries, but which are chemically indistinguishable. Although essentially tholeiitic andesites, they display several anomalous compositional features and a broad compositional spectrum characterized by a lack of variation trends. This has led to the tentative conclusion that they are the products of a complex interaction of fractional crystallization and hydridization processes, containing both crustal and mantle components. The Makwassie porphyries may represent the acid, crustal-derived component, but a suitable basic component is not present within the Ventersdorp lava succession.

The Makwassie porphyries are dacitic in composition, and display rational variation trends. These have been attributed to the passive concentration of the less mobile elements due to the nett removal of a siliceous component during post-depositional secondary recrystallization.

The Allanridge lavas are tholeiitic andesites of similar composition to the Alberton and Orkney lavas, but with more evolved incompatible element levels. They similarly display very limited compositional variation. The Allanridge lavas probably evolved along similar paths to the Klipriviersberg lavas, but it is unlikely that they are consanguinous and they appear to represent a separate magmatic event.

The broad compositional similarities of the mafic types are probably a reflection of similar mantle source conditions. Results of experimental work on modern magmas with similar compositional features suggest that they were generated by partial melting of a wet peridotite mantle. However, despite similar source conditions, the distinct trace element signatures of the individual magma types show that no genetic interrelationships exist between them, and that the mantle was chemically heterogeneous during the early Proterozoic.

XI ACKNOWLEDGEMENTS

The assistance of the following people and organizations is gratefully acknowledged:

Professor H V Eales for initiating and administering this project.

Dr Goonie Marsh for his unrelenting assistance in the form of discussions, suggestions and criticisms.

Teral Bowen for her cooperation on this project.

Mr P M Strydom and the staff of Anglo American Prospecting Services, Klerksdorp, for their hospitality and logistical support during sampling operations.

David Bowen, Mark Hannam and Julian Misiewicz for assistance with sample preparation.

Mike Botha, Moose Kruger and Dennis Gouws for assistance with the XRF spectrometer, microprobe and computing, as well as helpful discussions and therapeutic diversions.

The academic staff of the Rhodes Geology Department for their willing assistance in their various fields of expertise.

Bev Bowen for drafting most of the diagrams, plotting numerous graphs and for her continued support over the duration of this project.

The Anglo American Corporation for providing sample material, borehole information and a grant to finance this study.

The C.S.I.R. for financial support.

Shirleen Reynolds and Angela Stuurman for typing this manuscript.

XII REFERENCES

APPLETON, J.D. (1972). Petrogenesis of Potassium-rich Lavas from the Roccamonfina Volcano, Roman Region, Italy. J. Petrology, 13, 425-456.

ARNDT, N.T., NALDRETT, A.J., and PYKE, D.R. (1977). Komatiitic and Iron-rich Tholeiitic Lavas of Munro Township, Northeast Ontario. J. Petrology, 18, 319-369.

ARTH, J.G. (1976). Behaviour of Trace Elements during Magmatic Processes - A Summary of Theoretical Models and their Applications. Journ. Research U.S. Geol. Survey, 4, 41-47.

BESWICK, A.E.,and CARMICHAEL, I.S.E. (1978). Constraints on Mantle Source Compositions imposed by Phosphorus and Rare-Earth Elements. Cōntr. Miner. Petrol., 67, 317-330.

BESWICK, A.E., and SOUCIE, G. (1978). A Correction Procedure for Metasomatism in an Archaean Greenstone Belt. Precambrian Research, 6, 235-248.

BLAKE, D.H., ELWELL, R.W., GIBSON, I.L., SKELHORN, R.R. and WALKER, G.P.L. (1965). Some Relationships resulting from the Intimate Association of Acid and Basic Magmas. Q. Jl. geol. Soc. Lond., 121, 31-50.

BOETTCHER, A.L., MYSEN, B.O. and MODRESKI, P.J. (1975). Melting in the Mantle: Phase Relationships in Natural and Synthetic Peridotite - H_2O-CO_2-C-H-O-S with application to Kimberlite. In: Ahrens, L.H., Dawson, J.B., Duncan, A.R. and Erlank, A.J. (Eds.), Physics and Chemistry of the Earth, 9, 855-867, Pergamon Press, Oxford, 940p.

BOWEN, T.B. (1984). The Geochemical Stratigraphy of the Volcanic Rocks of the Witwatersrand Triad in the Klerksdorp Area, Transvaal. M.Sc. thesis (unpubl.), Rhodes University.

BRINK, M.C. (1982). The Structural Geology of Buffelsfontein Gold Mine. M.Sc thesis (unpubl.), Univ. of Natal (Pietermaritzburg), 140pp.

BROWN, G.M., and VINCENT, E.A. (1957). Pyroxenes from the Early and Middle Stages of Fractionation of the Skaergaard Intrusion, East Greenland. Miner. Mag., 31, 511-543

BURGER, A.J., and COERTZE, F.J. (1973). Radiometric Age Measurements on Rocks from Southern Africa to the end of 1971. Bull. geol. Surv. S. Afr., 58, 44pp.

BURGER, A.J., and COERTZE, F.J. (1973-74). Age Determinations - April 1972 to March 1974. Ann. geol. Surv. S. Afr., 10, 135-141.

BURGER, A.J., and WALRAVEN, F. (1980). Summary of Age Determinations carried out during the period April 1978 to March 1979. Ann. geol. Surv. S. Afr., 14/2, 109-118.

CAWTHORN, R.G. (1976). Some Chemical Controls on Igneous Amphibole Compositions. Geochim. cosmochim. Acta., 40, 1319-1328.

CAWTHORN, R.G., CURRAN, E.B., and ARCULUS, R.J. (1973). A Petrogenetic Model for the Origin of the Calc-alkaline suite of Grenada, Lesser Antilles. J. Petrology, 14, 327-337.

CAWTHORN, R.G., and McCARTHY, T.S. (1977). Partitioning of Nickel between Immiscible Picritic Liquids. Earth Planet. Sc. Lett., 37, 339-346.

CAWTHORN, R.G., McIVER, J.R., McCARTHY, T.S., WYATT, B.A., FERGUSON, J., and BARNES, S.J. (1979). Possible Liquid Immiscibility Textures in High-Magnesia basalts from the Ventersdorp Supergroup, South Africa. J. Geol., 87, 105-113.

CONDIE, K.C. (1982). A Plate-Tectonics Model for Proterozoic Continental Accretion in the Southwestern United States. Geology, 10, 37-42.

CONDIE, K.C., and NUTER, J.A. (1981). Geochemistry of the Dubois Greenstone Succession: An Early Proterozoic Bimodal Volcanic Association in West-Central Colorado. Precambr. Res., 15, 131-155.

CORNELL, D.H. (1978). Petrologic Studies at T'Kuip: Evidence for Metamorphism and Metasomatic Alteration of Volcanic Formations beneath the Transvaal Volcanosedimentary Pile. Trans. geol. Soc. S. Afr., 81, 261-270.

COX, K.G. (1980). A Model for Flood Basalt Vulcanism. J. Petrology, 21, 629-650.

COX, K.G., BELL, J.D., and PANKHURST, R.J. (1979). The Interpretation of Igneous Rocks. George Allen & Unwin, London, 450pp.

CRAWFORD, A.J., BECCALUVA, L., and SERRI, G. (1981). Tectono-Magmatic Evolution of the West Phillipine-Mariana Region and the Origin of Bonninites. Earth Planet. Sc. Lett., 54, 346-356.

DALLWITZ, W.B. (1968). Chemical Composition and Genesis of Clino-enstatite-Bearing Volcanic Rocks from Cape Vogel, Papua: A Discussion. 23rd Int. Geol. Congr., 2, 229-242.

DAVIES, J.F., GRANT, R.W.E., and WHITEHEAD, R.E.S. (1979). Immobile Trace Elements and Archean Volcanic Stratigraphy in the Timmins Mining Area, Ontario. Can. J. Earth Sci., 16, 305-311.

DEER, W.A., HOWIE, R.A., and ZUSSMAN, J. (1966). An Introduction to the Rock-Forming Minerals. Longman, London, 528pp.

DE PAOLO, D.J. (1981). Trace Element and Isotopic Effects of Combined Wallrock Assimilation and Fractional Crystallization. Earth Planet. Sc. Lett., 53, 189-202.

EALES, H.V., and BOOTH, P.W.K. (1974). The Birds River Gabbro Complex, Dordrecht District. Trans. geol. Soc. S. Afr., 77, 1-15.

ERLANK, A.J., ALLSOPP, H.L., DUNCAN, A.R. and BRISTOW, J.W. (1980). Mantle Heterogeneity beneath Southern Africa: Evidence from the Volcanic Record. Phil. Trans. R. Soc. Lond., A297, 295-307.

EWART, A., MATEEN, A. and ROSS, J.A. (1976). A Review of the Mineralogy and Chemistry of Tertiary Central Volcanic Complexes, S.E. Queensland-N.E. New South Wales. In: Johnson, R.W. (Ed.), Volcanism in Australasia, Elsevier, 21-39.

FINLOW-BATES, T., and STUMPFL, E.F. (1981). The Behaviour of So-Called Immobile Elements in Hydrothermally Altered Rocks associated with Volcanogenic Submarine-Exhalative Ore Deposits. Mineral. Deposita, 16, 319-328.

FLOYD, P.A. (1976). Geochemical Variation in the Greenstones of S.W. England. J. Petrology, 17, 522-545.

FLOYD, P.A., and WINCHESTER, J.A. (1975). Magma Type and Tectonic Setting Discrimination using Immobile Elements. Earth Planet. Sc. Lett., 27, 211-218.

FREY, F.A., RODEN, M.F. and ZINDLER, A. (1980). Constraints on Mantle Source Compositions imposed by Phosphorus and Rare-Earth Elements: Critical Comments on the Paper by A.E. Beswick and I.S.E. Carmichael. Contr. Miner. Petrol., 75, 165-174.

GARCIA, M.O. (1978). Criteria for the Identification of Ancient Volcanic Arcs. Earth-Sc. Rev., 14, 147-165.

GAST, P.W. (1968). Trace Element Fractionation and the Origin of Tholeiitic and Alkaline Magma Types. Geochim. Cosmochim. Acta., 32, 1057-1086.

GREEN, D.H. (1973). Experimental Melting Studies on a Model Upper Mantle Composition at High Pressure under Water-Saturated and Water-Undersaturated Conditions. Earth Planet. Sc. Lett., 19 , 37-53.

GREEN, D.H., EDGAR, A.D., BEASLEY, P., KISS, E., and WARE, N.G. (1974). Upper Mantle Source for Some Hawaiites, Mugearites and Benmoreites. Contr. Miner. Petrol., 48, 33-43.

GREEN, D.H., and RINGWOOD, A.E. (1967). The Genesis of Basaltic Magmas. Contr. Miner. Petrol., 15, 103-190.

HART, S.R., and DAVIS, K.E. (1978). Nickel Partitioning between Olivine and Silicate Melts. Earth Planet. Sc. Lett., 40, 203-219.

HART, S.R., GUNN, B.M., and WATKINS, N.D. (1971). Intralava Variation of Alkali Elements in Icelandic Basalt. Am. J. Sc., 270, 315-318.

HILDRETH, W. (1981). Gradients in Silicic Magma Chambers: Implications for Lithospheric Magmatism. J. Geophys. Res., 86, 10153-10192.

HUGHES, C.J. (1982). Igneous Petrology. Elsevier Scientific Publishing Co., Amsterdam, 551pp.

IRVINE, T.N., and BARAGAR, W.R.A. (1971). A Guide to the Chemical Classification of the Common Volcanic Rocks. Can. J. Earth Sci., 8, 523-548.

IRVING, A.J. (1978). A Review of Experimental Studies of Crystal/Liquid Trace Element Partitioning. Geochem. Cosmochim. Acta., 42, 743-770.

JACOBSEN, W. (1943). Ausbilding und Petrographie der Südafrikanischen Ventersdorp Formation in Süd-Westlichen Transvaal und Nordlichen Oranje-Freistaat. Neues Jb. Miner. Geol. Paläont. Abt. A., Abh. Bd., 78, 217-282.

JAHN, B-M., AUVRAY, B., BLAIS, S., CAPDEVILA, R., CORNICHET, J., VIDAL, F., and HAMEURT, J. (1980). Trace Element Geochemistry and Petrogenesis of Finnish Greenstone Belts. J. Petrology, 21, 201-244.

JAKES , P., and WHITE, A.J.R. (1972). Hornblendes from Calc-Alkaline Volcanic Rocks of Island Arcs and Continental Margins. Am. Miner., 57, 887-902.

JENNER, G.A. (1981). Geochemistry of High-Mg Andesites from Cape Vogel, Papua New Guinea. Chem. Geol., 33, 307-332.

KUSHIRO, I. (1969). The System Forsterite-Diopside-Silica With and Without Water at High Pressures. Am. J. Sc., 267A, 269-294.

KUSHIRO, I. (1970). Systems Bearing on Melting of the Upper Mantle under Hydrous Conditions. Carnegie Inst. Yb., 68, 240-245.

KUSHIRO, I. (1972). Effect of Water on the Composition of Magmas formed at High Pressures. J. Petrology, 13, 311-334.

KUSHIRO, I. (1974). The System Forsterite-Anorthite-Albite-Silica-H_2O at 15 kbar and the Genesis of Andesitic Magmas in the Upper Mantle. Carnegie Inst. Yb., 73, 244-248.

KUSHIRO, I., SYONO, Y., and AKIMOTO, S. (1968). Melting of a Peridotite Nodule at High Pressures and High Water Pressures. J. Geophys. Res., 73, 6023-6029.

LABUSCHAGNE, A.N. (1974). The Petrology of the Lower Ventersdorp Lavas in the East Driefontein Gold Mine. M.Sc. thesis (unpubl.), Potchefstroom Univ., 117pp.

LANGMUIR, C.H., VOCKE, R.D., HANSON, G.N., and HART, S.R. (1978). A General Mixing Equation with Applications to Icelandic Basalts. Earth Planet. Sc. Lett., 37, 380-392.

LE MAITRE, R.W. (1976). The Chemical Variability of some Common Igneous Rocks. J. Petrology, 17, 589-631.

LEEMAN, W.P. (1976). Petrogenesis of McKinney (Snake River) Olivine Tholeiite in light of Rare - Earth Element and Cr/Ni Distributions. Geol. Soc. Am. Bull., 87, 1582-1586.

LOFGREN, G.E. (1972). Plagioclase Crystal Morphology as Determined by Growth Temperature. Abstr. 5.3 in program for Advanced Study Institute on Feldspars, July 1972, Manchester.

MACLEAN, W.H., and SHIMAZAKI, H. (1976). The Partition of Co, Ni, Cu, and Zn between Sulphide and Silicate Liquids. Econ. Geol., 71, 1049-1057.

MALAN, S.P. (1959). The Petrology and Mineralogy of the Rocks of the Dominion Reef System near Klerksdorp. M.Sc. thesis (unpubl.), Univ. Witwatersrand, Johannesburg, 82pp.

MARSH, J.S., and EALES, H.V. (in press). The Chemistry and Petrogenesis of Igneous Rocks of the Karoo Central Area, Southern Africa. Trans. geol. Soc. S. Afr. Spec. Publ., 13.

MCIVER, J.R. (1975). Aspects of some High Magnesia Eruptives in Southern Africa. Contr. Miner. Petrol., 48, 153-169.

MCIVER, J.R., CAWTHORNE, R.G., and WYATT, B.A. (1982). The Ventersdorp Supergroup - the Youngest Komatiitic Sequence in South Africa? In: Arndt, N.T., and Nisbet, E.G., (Eds.), Komatiites. George Allen and Unwin, London, 526pp.

MOLENGRAAFF, G.A.F. (1905). Note on the Geology of a Portion of the Klerksdorp District, with Special Reference to the Development of the Lower Witwatersrand Beds and the Vaal River System. Trans. geol. Soc. S. Afr., 8, 16-25.

MORRISON, M.A. (1978). The Use of "Immobile" Trace Elements to Distinguish the Palaeotectonic Affinities of Metabasalts: Applications to the Paleocene Basalts of Mull and Skye, Northwest Scotland. Earth Planet. Sc. Lett., 39, 407-416.

MYSEN, B.O. (1973). Melting in a Hydrous Mantle: Phase Relations of Mantle Peridotites with Controlled Water and Oxygen Fugacity. Carnegie Inst. Yb., 73, 237-240.

NEL, L.T., JACOBS, H., ALLAN, J.T., and BOZZOLI, G.R. (1937). Wonderstone. Bull. Geol. Surv. S. Afr., 8, 44pp.

NICHOLLS, I.A. (1974). Liquids in Equilibrium with Peridotitic Mineral Assemblages at High Water Pressures. Contr. Miner. Petrol., 45, 289-316.

NICHOLLS, I.A., and RINGWOOD, A.E. (1972). Production of Silica-Saturated Tholeiitic Magmas in Island Arcs. Earth Planet. Sc. Lett., 17, 243-247.

NICHOLLS, I.A., and RINGWOOD, A.E. (1973). Effect of Water on Olivine Stability in Tholeiites and the Production of Silica Saturated Magmas in the Island Arc Environment. J. Geol., 81, 285-300.

NICOLAYSEN, L.O., BURGER, A.J., and LIEBENBERG, W.R. (1962). Evidence for the Extreme Age of Certain Minerals from the Dominion Reef Conglomerates and the Underlying Granite in the Western Transvaal. Geochim. Cosmochim. Acta, 26, 15-23.

NORRISH, K., and HUTTON, J.T. (1969). An Accurate X-ray Spectrographic Method for the Analysis of a Range of Geological Samples. Geochim. Cosmochim. Acta., 33, 431-455.

PEARCE, J.A., and CANN, J.R. (1973). Tectonic Setting of Basic Volcanic Rocks Determined using Trace Element Analysis. Earth Planet. Sc. Lett., 19, 290-300.

PEARCE, J.A., and NORRY, M.J. (1979). Petrogenetic Implications of Ti, Zr, Y and Nb Variations in Volcanic Rocks. Contr. Miner. Petrol., 69, 33-47.

PEMBERTON, J. (1978). The Geochemistry and Petrology of Karoo Basalts of the Barkly East Area, North-Eastern Cape. M.Sc. thesis (unpubl.), Rhodes University, 139pp.

PIENAAR, P.J. (1956). Stratigraphy and Petrography of the Ventersdorp System in the Orange Free State Goldfield, South Africa. M.Sc. thesis (unpubl.), Queen's University, Kingston, Ontario, 190pp.

REID, D.L. (1979). Petrogenesis of Calc-Alkaline Metalavas in the Mid-Proterozoic Haib Volcanic Subgroup, Lower Orange River Region. Trans. geol. Soc. S. Afr., 82, 109-131.

RINGWOOD, A.E. (1975). Composition and Petrology of the Earth's Mantle. McGraw-Hill Inc., New York, 618pp.

ROBERTSON, J.M. (1981). Bimodal Volcanism in the Early Proterozoic Pecos Greenstone Belt, Southern Sangre de Cristo Mountains, New Mexico. Geol. Soc. Am. Abstr. Progs., 13, 103.

ROBEY, J.v.A. (1976). Aspects of the Geochemistry of the Dolerites and Basalts of the North-Eastern Cape Province, South Africa. M.Sc. thesis (unpubl.), Rhodes University, 118pp.

SEWARD, T.M. (1971). The Distribution of Transition Elements in the System $CaMgSi_2O_6$ - $Na_2Si_2O_5$ - H_2O at 1000 Bars Pressure. Chem. Geol., 7, 73-95.

SIMPSON, A.B. (1964). A Bibliography of the Geology of the Ventersdorp System and other Pre-Bushveld Extrusives and Associated Sediments. Inform. Circ. econ. Geol. Res. Unit, Univ. Witwatersrand, Johannesburg, 18, 66pp.

SMITH, R.E. (1968). Redistribution of Major Elements in the Alteration of Some Basic Lavas during Burial Metamorphism. J. Petrology, 9, 191-219.

SMITH, R.E., and SMITH, S.E. (1976). Comments on the use of Ti, Zr, Y, Sr, K, P and Nb in Classification of Basaltic Magmas. Earth Planet. Sc. Lett., 32, 114-120.

SOUTH AFRICAN COMMITTEE FOR STRATIGRAPHY (SACS). (1980). Stratigraphy of South Africa. Part 1 (Comp. L.E. Kent). Lithostratigraphy of the Republic of South Africa, South West Africa/Namibia, and the Republics of Bophuthatswana, Transkei and Venda. Handb. geol. Surv. S. Afr., 8, 690pp.

STOW, G.W. (1874). Geological Notes on Griqualand West. Q. Jl. geol. Soc. Lond., 30, 581-680.

SUN, S.S., NESBITT, R.W., and SHARASKIN, A.Y. (1979). Geochemical Characteristics of Mid-Ocean Ridge Basalts. Earth Planet. Sc. Lett., 44, 119-138.

TANKARD, A.J., JACKSON, M.P.A., ERIKSSON, K.A., HOBDAY, D.K., HUNTER, D.R., and MINTER, W.E.L. (1982). Crustal Evolution of Southern Africa. Springer-Verlag, 523pp.

TATSUMI, Y. (1981). Melting Experiments on a High-Magnesian Andesite. Earth Planet. Sc. Lett., 54, 357-365.

TATSUMI, Y. (1982). Origin of High-Magnesian Andesites in the Setouchi Volcanic Belt, Southwest Japan, II. Melting Phase Relations at High Pressures. Earth Planet. Sc. Lett., 60, 305-317.

TATSUMI, Y., and ISHIZAKA, K. (1982). Origin of High-Magnesian Andesites in the Setouchi Volcanic Belt, Southwest Japan, I. Petrographical and Chemical Characteristics. Earth Planet. Sc. Lett., 60, 293-304.

TAYLOR, S.R. (1968). Trace Element Chemistry of Andesites and Associated Calc-Alkaline Rocks. In: McBirney, A.R., Ed., Proceedings of the Andesite Conference. Bull. Dept. geol. Miner. Ind., 65, State of Oregon, 193pp.

TRUSWELL, J.F. (1970). An Introduction to the Historical Geology of South Africa. Purnell, Cape Town, 167pp.

TYLER, N. (1979). Correlation, Stratigraphic Relations and Geochemistry of the Ventersdorp Supergroup in the Derdepoort Area, West-Central Transvaal. Inform. Circ. econ. Geol. Res. Unit, Univ. Witwatersrand, Johannesburg, 131, 23pp.

VAN NIEKERK, C.B., and BURGER, A.J. (1964). The Age of the Ventersdorp System. Ann. geol. Surv. S. Afr., 3, 75-86.

VAN NIEKERK, C.B., and BURGER, A.J. (1969). Lead Isotopic Data relating to the Age of the Dominion Reef Lava. Trans. geol. Soc. S. Afr., 72, 37-45.

VAN NIEKERK, C.B., and BURGER, A.J. (1978). A New Age for the Ventersdorp Acidic Lavas. Trans. geol. Soc. S. Afr., 81, 155-163.

WALKER, D., SHIBATA, T., and DE LONG, S.E. (1979). Abyssal Tholeiites from the Oceanographer Fracture Zone: II. Phase Equilibria and Mixing. Contr. Miner. Petrol., 70, 111-125.

WATCHORN, M.B. (1980). Continental Sedimentation and Vulcanism in the Dominion Group of the Western Transvaal: A Review. Inform. Circ. econ. Geol. Res. Unit, Univ. Witwatersrand, Johannesburg, 146, 8pp.

WATKINS, N.D., GUNN, B.M., and COY-YLL, R. (1970). Major and Trace Element Variations during the Initial Cooling of an Icelandic Lava. Am. J. Sc., 268, 24-49.

WATSON, E.B. (1980). Apatite and Phosphorus in Mantle Source Regions: An Experimental Study of Apatite/Melt Equilibria at Pressures to 25 kbar. Earth Planet. Sc. Lett., 51, 322-335.

WHITESIDE, H.C.M. (1970). Volcanic rocks of the Witwatersrand Triad. In: Clifford, T.N. and Gass, I.G. (Eds.) African Magmatism and Tectonics. Oliver and Boyd, Edinburgh, 461pp.

WILKINSON, J.F.G., and BINNS, R.A. (1977). Relatively Iron-Rich Lherzolite Xenoliths of the Cr-Diopside Suite: A Guide to the Primary Nature of Anorogenic Tholeiitic Andesite Magmas. Contr. Miner. Petrol., 65, 199-212.

WILLIAMS, H., TURNER, F.J., and GILBERT, C.M. (1958). Petrography: An Introduction to the Study of Rocks in Thin Sections. W.H. Freeman and Co., San Francisco, 406pp.

WINCHESTER, T.A., and FLOYD, P.A. (1977). Geochemical Discrimination of Different Magma Series and their Differentiation Products using Immobile Elements. Chem. Geol., 20, 325-347.

WINTER, H. de la R. (1965). The Stratigraphy of the Ventersdorp System in the Bothaville District and Adjoining Areas. Ph.D. thesis, (unpubl.), Univ. Witwatersrand, 131pp.

WINTER, H de la R. (1976). A Lithostratigraphic Classification of the Ventersdorp Succession. Trans. geol. Soc. S. Afr., 79(1), 31-48.

WYATT, B.A. (1976). The Geology and Geochemistry of the Klipriviersberg Volcanics, Ventersdorp Supergroup, South of Johannesburg. M.Sc. thesis (unpubl.), Univ. Witwatersrand, 178pp.

XIII APPENDICES

APPENDIX I

ANALYTICAL PROCEDURES

A. Sample Preparation

Core samples were broken into discs using a rock splitter. The weathered outer surface of the core was ground off on a diamond-impregnated cup-wheel. Extraneous material such as veins and amygdales was removed at the same time. Samples were then crushed in a jaw-crusher and ground in a Hertzog swing mill to approximately 200 mesh using a Mn-steel vessel. The final crush was quartered and seven grams were fine- ground in an agate mortar and pestle.

Of the seven grams, five grams were used for making briquettes in a boric acid/bakelite casing by compression of 15 tons/sq. in. in a steel barrel and plunger apparatus. The briquettes were used for the analysis of trace elements and Na_2O.

The remaining 2 grams were ashed at 1000°C in silica crucibles. .28g of the ashed sample was then used for the preparation of Norrish fusion discs, according to the method of Norrish and Hutton (1969). These were used for the major element analyses, excluding Na_2O.

B. Analytical Methods

All elements were determined by X-ray fluorescence, using a Philips PW-1410 spectrometer. Both international and locally calibrated standards were used for calibration. International standards used include the following: AGV-1, BCR-1, G-2, GSP-1, JG-1 and PCC-1. Rhodes University in-house standards used are CAR-08, KRF-13 and PRO-1. Standards calibrated at N.I.M. (now Mintek) were also used viz. NIM-G, NIM-N, NIM-P, S-9, S-10, S-12 and S-15. Element concentrations of the standards are shown in Table A1.

Analytical conditions for individual elements are summarized in Table A2. Data reduction was performed on the Rhodes ICL 1904 S computer,

using programs compiled at the Geochemistry Department, University of Cape Town, and modified for use at Rhodes by Dr J S Marsh. Full corrections are made for deadtime, instrumental drift, sample position, absorption, background, spectral and tube line interferences. Mass absorption coefficients were calculated from the major element data using Heinrich's coefficients.

The successful duplication of 45 major element analyses demonstrated the reproducibility of results. Reproducibility of trace element determinations was monitored by including, in each sample batch, samples which had already been analysed in a previous batch. (Samples were analysed in 3 separate batches comprising 40, 48 and 238 samples respectively.) Average lower limits of determination and counting errors for each sample batch are given in Table A3.

Table A1: Major and Trace Element Concentrations of Standards

STD	Ba	Nb	Zr	Y	Sr	Rb	Zn	Cu	Ni	Co	Cr	V	La	Ce	Nd
AGV-1	1208												35.0	65.0	39.0
BCR-1	675												25.0	54.0	29.0
CAR-08	243	18.1	125.0	27.7	296.0	18.6	76.5	64.6	69.5						
G-2													96.0	165	55.0
GSP-1	1300														
JG-1															
KRF-13	205	5.4	100.5	30.7	205.0	10.1	75.0	59.5	51.4	45.5	293.0	259.0			
NIM-G															
NIM-P	40														
PCC-1										112.0	2730.0	30.0			
PRO-1	736									21.7	62.0	100.0			
S-09		8.0	137.0	17.2	54.3	56.7	73.0	43.2	111.0	16.9	114.0	137.0			
S-10							38.0	18.0	128.0						
S-12	29	113.0	406.0	89.0	4.0	11.2	267.0	6.1	15.0	8.5	385.0	427.0			
S-15										70.0	1995.0	17.0			

STANDARD CONCENTRATIONS - Major elements

STD	SiO_2	TiO_2	Al_2O_3	Fe_2O_3	MnO	MgO	CaO	Na_2O	K_2O	P_2O_5	LOI
AGV-1	59.00	1.04	17.25	6.76	0.10	1.53	4.90	4.26	2.89	0.49	1.01
BCR-1	54.50	2.20	13.61	13.40	0.18	3.46	6.92	3.27	1.70	0.36	0.39
G-2	69.11	0.50	15.40	2.65	0.03	0.76	1.94	4.07	4.51	0.14	0.55
GSP-1	67.38	0.66	15.25	4.33	0.04	0.96	2.02	2.80	5.53	0.28	0.63
JG-1	72.24	0.26	14.21	2.21	0.06	0.73	2.18	3.39	3.96	0.10	0.45
NIM-N	52.43	0.19	16.64	9.00	0.17	7.43	11.55	2.44	0.26	0.04	0.07

Table A2: Analytical Conditions

element	kV	mA	counter	vacuum	crystal	collimator	tube	STANDARDS USED					
Mn	50	40	flow	on	LiF200	c	Cr	AGV-1	BCR-1	G-2	GSP-1	JG-1	NIM-N
Fe	"	"	"	"	"	f	"	"	"	"	"	"	"
Ti	"	"	"	"	"	"	"	"	"	"	"	"	"
Ca	"	"	"	"	"	"	"	"	"	"	"	"	"
K	"	"	"	"	"	"	"	"	"	"	"	"	"
Si	"	"	"	"	PET	c	"	"	"	"	"	"	"
Al	"	"	"	"	"	"	"	"	"	"	"	"	"
Mg	"	"	"	"	TLAP	f	"	"	"	"	"	"	"
P	"	"	"	"	Ge	c	"	"	"	"	"	"	"
Ba	55	40	flow	on	LiF220	f	Cr	AGV-1	BCR-1	CAR-08	GSP-1	KRF-13	NIM-P PRO-1 S-12
Nb, Zr, Y, Sr, Rb	"	"	scint	off	"	"	W	AGV-1	CAR-08	G-2	KRF-13	PRO-1	S-9 S-12 S-15
Zn, Cu, Ni	"	"	flow & scint	on	"	"	Mo	CAR-08	KRF-13	S-9	S-10	S-12	S-15
Co, Cr, V	"	"	flow	"	"	"	W	KRF-13	PCC-1	PRO-1	S-9	S-12	S-15
La, Ce, Nd	"	"	flow	"	"	"	"	AGV-1	BCR-1	G-2			
Na	"	"	"	"	TLAP	f	Cr	AGV-1	BCR-1	G-2	GSP-1	JG-1	NIM-N

Full corrections made for background, deadtime, instrumental drift, spectral and tube line interference

USGS standards: AGV-1, BCR-1, G-2, GSP-1, JG-1, PCC-1

NIM secondary reference standards: S-9, S-10, S-12, S-15

NIM primary standards: NIM-N, NIM-P

Rhodes University in-house standards: CAR-08, KRF-13, PRO-1

Table A3: Mean Lower Limits of Determination and Counting Errors for Each Batch of Samples Processed

		Nb		Zr		Y		Sr		Rb	
BATCH	N	LLD	CE	LLD	CE	LLD	CE	LLD	CE	LLD	CE
1	40	2.42	.71	1.81	.76	2.19	.68	1.95	1.08	2.11	.69
2	48	2.42	.72	1.81	.80	2.20	.69	1.96	1.06	2.12	.70
3	238	.76	.23	.57	.25	.69	.22	.61	.36	.65	.22

		Co		Cr		V		Zn		Cu	
BATCH	N	LLD	CE	LLD	CE	LLD	CE	LLD	CE	LLD	CE
1	40	2.52	.83	2.56	1.31	3.34	1.41	2.16	1.10	2.45	1.04
2	48	2.56	.84	2.64	1.31	3.58	1.50	2.45	1.17	2.68	1.06
3	238	2.46	.82	2.54	1.41	3.27	1.45	2.67	1.26	2.80	1.17

		Ni		La		Ce		Nd		Ba	
BATCH	N	LLD	CE	LLD	CE	LLD	CE	LLD	CE	LLD	CE
1	40	3.26	1.59	5.84	1.56	11.58	2.98	6.47	1.65	14.0	6.0
2	48	3.46	1.61	6.55	1.62	12.32	3.11	6.64	1.67	14.7	5.8
3	238	3.38	1.63								

APPENDIX II

SELECTED MINERAL ANALYSES

A. Secondary Minerals from Pseudomorphs after Mafic Phenocryst Phases in the Loraine/Edenville and Goedgenoeg/Rietgat Formations:

Tabulated below are representative electron microprobe analyses of constituent secondary minerals pseudomorphous after mafic phenocryst phases in the Loraine/Edenville and Goedgenoeg/Rietgat formations, which were referred to in Chapter V. The chlorite and clinozoisite analyses are from sample KL-146, Loraine/Edenville formation. The clinozoisite occurs as a tiny, discrete grain enclosed by chlorite within the pseudomorph. The sphene is amorphous and occurs as spindle-shaped lamellae within chlorite pseudomorphs in the Goedgenoeg/Rietgat formations. The analysis below is from sample PR-186:

	Sample KL-146		Sample PR-186
	Chlorite	Clinozoisite	Sphene
SiO_2	28.34	37.84	30.23
TiO_2	0.04	0.02	31.96
Al_2O_3	18.21	28.34	3.60
FeO	19.31	5.59	3.56
MnO	0.26	0.03	0.04
MgO	19.91	0.09	1.36
CaO	0.11	23.84	26.78
Na_2O	0.10	-	0.04
K_2O	-	2.28	0.05
Cr_2O_3	0.60	0.53	0.12
NiO	0.12	0.02	-
TOTAL	87.00	98.58	97.75

B. Whole-Rock and Pyroxene Analyses - Sample NL-789, Loraine/Edenville Formation:

Sample NL-789 is described in Chapter V. Orbicular structures were removed from the matrix and the two components were analysed separately. The actual whole-rock composition thus lies on a mixing

line between the orbicule and matrix compositions presented below. Also given are 4 analyses of the cores and rims of pyroxene microphenocrysts occurring within an orbicule (see Plate VI, Chapter V) and the matrix respectively. The augite composition used for petrogenetic modelling of the Loraine/Edenville lavas is representative of these microphenocrysts.

	Whole rock-sample NL-789		Pyroxene in Orbicule		Pyroxene in Matrix	
	Orbicule	Matrix	Core	Rim	Core	Rim
SiO_2	57.92	42.09	51.86	54.24	53.37	53.40
TiO_2	0.577	0.571	0.33	0.19	0.20	0.20
Al_2O_3	12.62	14.70	3.04	1.40	1.98	2.08
Fe_2O_3	7.64	15.15	-	-	-	-
FeO	-	-	7.26	8.50	6.72	6.63
MnO	0.13	0.22	0.17	0.24	0.18	0.20
MgO	7.78	12.10	17.29	19.32	17.46	18.19
CaO	7.97	14.87	18.43	16.42	19.58	18.68
Na_2O	4.50	0.09	0.32	0.13	0.19	0.29
K_2O	0.75	0.16	-	-	-	-
P_2O_5	0.099	0.049	-	-	-	-
Cr_2O_3	-	-	0.56	0.22	0.99	0.94
NiO	-	-	0.06	0.06	0.06	0.06
TOTAL	99.67	100.39	99.31	100.72	100.72	100.66
L.O.I	1.52	5.18				
TRACE ELEMENTS:						
Ba	201	63				
Nb	2.5	2.8				
Zr	52	53				
Y	9.0	22.8				
Sr	174	32				
Rb	31.2	7.4				
Zn	43	93				
Cu	22	59				
Ni	206	388				
Co	49	91				
Cr	870	868				
V	181	266				

Whole rock analyses by XRF, all elements recalculated volatile free, all Fe as Fe_2O_3. Total = orginal total prior to normalization, L.O.I. = Loss on ignition at 1000°C.

Pyroxene analyses by electron microprobe with all Fe as FeO.

C. Microprobe Analytical Procedures

Electron microprobe analyses were carried out on a Cambridge Microscan V instrument, by the standard techniques employed in the Geology Department, Rhodes University. Polished specimen slides were vacuum-coated to a maximum of 25nM with carbon. Specimen current was monitored at regular intervals by means of a Faraday Cage.

Corrections were applied to nominal concentrations by the Bence-Albee correction routine, using the programme HVE MARK III compiled by Professor H V Eales.